uOttawa

L'Université canadienne
Canada's university

FACULTÉ DES ÉTUDES SUPÉRIEURES ET POSTOCTORALES

uOttawa

L'Université canadienne
Canada's university

FACULTY OF GRADUATE AND POSDOCTORAL STUDIES

Hongbin Xu
AUTEUR DE LA THÈSE / AUTHOR OF THESIS

Ph.D. (Biochemistry)
GRADE / DEGREE

Department of Biochemistry, Microbiology and Immunology
FACULTÉ, ÉCOLE, DÉPARTEMENT / FACULTY, SCHOOL, DEPARTMENT

Significance of Arylsulfatase A in Spermatogenesis and Sperm Fertilizing Ability
TITRE DE LA THÈSE / TITLE OF THESIS

Nongnuj Tanhaichitr
DIRECTEUR (DIRECTRICE) DE LA THÈSE / THESIS SUPERVISOR

CO-DIRECTEUR (CO-DIRECTRICE) DE LA THÈSE / THESIS CO-SUPERVISOR

EXAMINATEURS (EXAMINATRICES) DE LA THÈSE / THESIS EXAMINERS

Andrée Gruslin

Carlos Morales (McGill University)

Alexander Sorisky

Zemin Yao

Gary W. Slater
Le Doyen de la Faculté des études supérieures et postdoctorales / Dean of the Faculty of Graduate and Postdoctoral Studies

SIGNIFICANCE OF ARYLSULFATASE A IN SPERMATOGENESIS AND SPERM FERTILIZING ABILITY

by

Hongbin Xu

Thesis submitted to the Faculty of Graduate and Postdoctoral Studies
in partial fulfillment of the requirements for the degree of
Doctor of Philosophy

Department of Biochemistry, Microbiology and Immunology
Faculty of Medicine
University of Ottawa

Your file Votre référence
ISBN: 978-0-494-61367-2
Our file Notre référence
ISBN: 978-0-494-61367-2

ACKNOWLEDGEMENTS

First and foremost, I would like to thank my advisor for her excellent supervision. Dr. N. Tanphaichitr has made use of her extraordinary knowledge and skills as scientists, professors, editors, and logicians, requiring perfection of me as she supervised my graduate work. Her guidance has helped me develop many skills and abilities that are important for conducting competitive science research. Thank your from the bottom of my heart.

I would also like to thank my thesis advisory committee members (Dr. Z.M. Yao, Dr. B. Tsang, and Dr. E. Carmona) for their guidance, as well as our collaborators (Dr. K.F. Faull, Dr. T. Rupar, Dr. L. Hermo, Dr. W. Weerachatyanukul, Dr. P Sretarugsa and Dr. M. Wade) for their continued support and contributions to my Ph.D. project. In addition, this work would not have been possible if it were not for the paramount help and moral support I received from past and present members of our laboratory. I will always be grateful to Ms. K. Kongmanas, Mr. S. Iamsaard, Ms. A. Saewu, Ms. F. Liu, Mr. M. Schenk, Dr. Bou Khalil, Dr. K. Chakrabandhu, Ms. J. Tantibhedhyangkul, Ms. T. Antunes, Ms. S. da Silva, Dr. A. Anupriwan, and Ms. D. Dacosta Santos. I am also very grateful for the help I received from our administrative assistant Ms. T. van Gulik, and departmental academic assistants Ms. K. Carol Ann and Ms. N Trudel.

I gratefully acknowledge the Strategic Training Initiative in Research in the Reproductive Health Sciences, OGS and University of Ottawa for providing scholarships to support my graduate studies.

Last but not least, I thank my mother and father (Huilan and Yuqi for raising me up and for their support for my career choice and graduate studies), my beloved wife Ping for always being with me, my two lovely children (Kevin and Serena) for being my joy maker and stress reliever, and my sister Jing and her husband Jianguo for accommodating me when I first came to Canada.

ABSTRACT

We have previously shown that arylsulfatase A (ASA), present on the sperm head surface, is involved in sperm-zona pellucida (ZP) binding in vitro. Here, I described how ASA, usually known as an acrosomal enzyme without a transmembrane domain, trafficked to the sperm head surface. In the testis, ASA was localized to the developing acrosomal granules of spermatogenic cells as well as late residual bodies of Sertoli cells. However, the roles of ASA in these entities are unknown. ASA was also secreted by the cauda epididymis and vas deferens, resulting in its localization to the sperm plasma membrane overlying the acrosome, a mechanism dependent on the affinity of ASA to the sperm plasma membrane sulfogalactosylglycerolipid (SGG). Purified sperm ASA bound directly to the ZP3 and ZP2 sulfoglycoproteins, suggesting a role of sperm surface and acrosomal ASA in the primary and secondary sperm-ZP binding, respectively. I further characterized the fecundity of *ASA* null males to verify the roles of sperm ASA in fertilization in vivo and to investigate the functions of ASA in the testis. The *ASA* null mice exhibited normal sperm fertilizing ability and spermatogenesis when they were less than 5 months old. However, when they reached 8 months of age, their sperm fertilizing ability was almost zero. The spermatogenesis was also perturbed with significantly increased number of apoptotic germ cells. Since SGG is expressed in male germ cells, and it can be desulfated by ASA in vitro, accumulation of SGG in the testis and sperm of *ASA* null mice was expected. By using a very sensitive quantitative ESI-MS with a proper internal standard (deuterated SGG), the amount of SGG in sperm of 8-month-old mutant mice was found to be significantly reduced, while no significant changes were detected in 5-month-old KO mice. Although these results were contradictory to what was

expected, they may explain, at least in part, the reduced sperm fertilizing ability of the older mutant mice (since SGG is involved in sperm-egg interaction). As expected, SGG was indeed accumulated in the testis of *ASA* null mice at both ages. Consistent with the SGG quantification data on sperm, the levels of SGG in testicular germ cells, analyzed by flow cytometry using affinity-purified anti-SGG IgG, were found to be reduced only in 8-month-old *ASA* null mice, compared with age-matched WT. These results suggested that SGG was unlikely to be accumulated in testicular germ cells. Rather, the sulfoglycolipid might be accumulated in Sertoli cells owing to their phagocytotic activity toward membrane remnants of apoptotic germ cells and residual bodies, which should contain SGG. Palmitoylsulfatide, a sulfoglycolipid not normally present in WT testis at an appreciable amount, was also found to be accumulated in the mutant testis. The accumulation of SGG and other sulfoglycolipids in the testis (in Sertoli cells by deduction) may impair cellular functions, leading to aberrant sperm SGG levels and disruption of spermatogenesis. In conclusion, ASA is important for keeping the balance of SGG in the testis and sperm, which is important for spermatogenesis and sperm fertilizing ability.

CONTENTS

LIST OF FIGURES

LIST OF FIGURES

LIST OF TABLES

LIST OF ABBREVIATIONS

AAG	1-*O*-alkyl-2-*O*-acyl-*sn*-glycerol
AAT	α-1-antitrypsin
ABP	Androgen bindng protein
ADAM	A disintegrin and A metalloprotease
AI-BP	Apolipoprotein A-I binding protein
AKAPs	A kinase anchoring proteins
APM	Anterior plasma membrane
AR	Acrosome reaction
ASA	Arylsulfatase A
AZF	Azoospermia factor
BSA	Bovine serum albumin
CAD	Collisionally activated dissociation
cAMP	Cyclic adenosine monophosphate
CFTR	Cystic fibrosis transmembrane conductance regulator
CGT	Ceramide galactosyltransferase
COC	Cumulus Oocyte complex
CRISP1	Cysteine-rich secretory protein1
CST	Cerebroside sulfotransferase
DAG	Diacylglycerol
DMSO	Dimethyl-sulfoxide
ECL	Enhanced chemiluminescence
EDTA	Ethylenediaminetetraacetic acid

ELISA	Enzyme-linked immunosorbent assay
ESI	Electrospray ionization
F-actin	Filamentous actin
FRAP	Fluorescence recovery after photobleaching
FSH	Follicle-stimulating hormone
FucT	Fucosyltransferase
$GABA_A$	γ-aminobutyric acid type A
gACE	Ggerminal angiotensin I-converting enzyme
Gal	Galactose
GalNAc	*N*-acetyl galactosamine
GalT	β-1,4-galactosyltransferase
GC	*β*-D-galactopyranosyl-1'-1-*N*-tetracosanoylsphingosine or galactosylceramide
GG	1-*O*-alkyl-2-*O*-acyl[*β*-D-galactopyranosyl(1'-3)]-*sn*-glycerol or galactosylglycerolipid
GlcNAc	*N*-acetyl glucosamine
GnRH	Gonadotropin releasing hormone
GPI	Glycosylphosphatidylinositol
HDL	High-density lipoproteins
HFA-GC	GC containing amide linked α-hydroxylated fatty acids
HIV	Human immunodeficiency virus
HPLC	High performance liquid chromatography
HPTLC	High performance thin layer chromatography

HRP	Horseradish peroxidase
HSP	Heat shock protein
ICSI	Intracytoplasmic sperm injection
IIF	Indirect immunofluorescence
IGF	Insulin-like growth factor
IgG	Immunoglobulin G
IP_3	Inositol 1,4,5-trisphosphate
KRB	Krebs Ringers bicarbonate
KRB-HEPES	HEPES-buffered Krebs Ringers bicarbonate
LH	Luteinizing hormone
Lp	Lipid droplets
LTQ-FTMS	Linear ion trap Fourier transform mass spectrometer
MC540	Merocyanine 540
MLD	Metachromic leukodystrophy
MRM	Multiple reaction monitoring
MS	Mass spectrometry
NCS	*p*-nitrocatechol sulfate
NFA-GC	GC containing amide linked non-hydroxylated fatty acids
NMR	Nuclear magnetic resonance
OPD	*o*-phenylenediamine dihydrochloride
PAP	3'-phosphoadenosine-5'-phosphate
PAPS	3'-phosphoadenosine-5'-phosphosulfate
PAS	Periodic acid-Schiff-hematoxylin

PBS	Phosphate-buffered saline
PGC	Percoll gradient centrifuged
PC	3-*sn*-glycerophosphorylcholine
PE	3-*sn*-glycerophosphorylethanolamine
PI	Propidium iodide
PIP_2	Phosphatidylinositol bisphosphate
PIP3	Phosphatidylinositol-3,4,5-triphosphate
PKA	Protein kinase A
PKC	Protein kinase C
PLA_2	Phospholipase A_2
PLC	Phospholipase C
PPG	Palmitoylpalmitylglycerol
PRS	Preimmune rabbit serum
PS	3-*sn*-glycerophosphorylserine
PTK	Protein tyrosine kinases
PUFA	Polyunsaturated fatty acid
PVP	Polyvinylpyrrolidone
RER	Rough endolasmic reticuli
sAC	Soluble adenylyl cyclase
SAP	Sphingolipid activator protein
SBTI	Soybean trypsin inhbitor
SCF	Stem cell factor
SDS	Sodium dodecyl sulfate

SDS-PAGE	Sodium dodecyl sulfate-polyacrylamide gel electrophoresis
SED1	Secreted protein that contains Notch-like **E**GF repeats and **D**iscoidin/F5/8 types C complement domains
SER	Smooth endoplasmic reticuli
SGC	[β-D-(3'-sulfatoxy)galactopyranosyl]-(1'-1)]-*N*-tetracosanoylsphingosine or sulfogalactosylceramide
SGG	1-*O*-alkyl-2-*O*-acyl [β-D-(3'-sulfatoxy)galactopyranosyl(1'-3)]-*sn*-glycerol or sulfogalactosylglycerolipid or seminolipid
SGP	Sulfated glycoprotein
SLIP	Sulfolipid immobilizing protein
SNARE	Soluble NSF attachment protein receptors
SOC	Store operated Ca^{2+} channel
SPINKL	Secreted serine protease inhibitior Kazal-type-like protein
SR	Scavenger receptors
SR-BI	Class B scavenger receptor type I
TBS	Tris-buffered saline
TESP5	Testicular serine protease 5
TGF	Transforming growth factor
TLC	Thin layer chromatography
TLCK	*N*α-p-tosyl-L-lysine chloromethyl ketone
TP	Transition proteins
Tra1	Endoplasmin
Trp	Transient receptor potential protein channels

TUNEL	Terminal deoxynucleotidyltransferase-mediated dUTP–biotin nick end labeling
UDP	Uridine diphosphate
UDP-Gal	Uridine diphosphate galactose
WGA	Wheat germ agglutinin
ZAG	Zinc-α-2 glycoprotein
ZP	Zona(e) pellucida(e)

CHAPTER ONE

INTRODUCTION

1.1. Preamble to My Research Studies

An estimated of one in seven couples worldwide suffer infertility that is contributed equally by male and female factors. Infertility in males can be caused by many different factors. Severe infertility in humans is rare. It occurs in individuals with genetic abnormalities, such as deletion of the azoospermia factor region (*AZF*) of the Y chromosome, which result in a drastic decrease in spermatogenesis (Reijo et al., 1995; Vogt, 2005), and mutations in the cystic fibrosis transmembrane conductance regulator (*CFTR*) gene which can lead to congenital absence of the vas deferens (CAVD) (Jaffe and Bush, 2001; Dohle et al., 2002; Dohle et al., 1999). It may also be caused by external factors that directly destroy testicular germ cells, such as cancer drug (i.e., alkylating agents) treatment and X-ray irradiation. In addition, unexplained infertility (the inability to impregnate partners after 1 year of regular unprotected intercourse, but results of semen analyses are normal) constitutes about 10 to 15% of infertile couples (Quaas and Dokras, 2008).

Understanding the mechanisms of gamete interaction is the first essential step in the treatment of unexplained infertility as well as development of biomarkers for male fertility. However, despite of advances made in the field of reproductive technology, the perfect solutions to male "infertility" remain elusive. In most cases, males visiting "infertility" clinics are subfertile and their sperm can be biochemically and/or mechanically processed for enhancement of their fertilizing ability. For the past decade,

intracytoplasmic sperm injection (ICSI) is used without verifying the lack of sperm fertilizing ability, and is considered not totally safe (it may result in behavioral problems and congenital malformation in the long run (Georgiou et al., 2006; Bowen et al., 1998; Bonduelle et al., 2005)). The application of ICSI may also lead to offspring with an enhanced risk of unbalanced chromosome complement, male infertility due to transmission of an *AZF* deletion, and cystic fibrosis in the case of related genital abnormalities (Dohle et al., 2002). So, the reversion to the use of normal in vitro fertilization (IVF) is being taken into consideration. For this purpose, reliable biomarkers for the selection of sperm with high fertilizing ability are needed. Currently, clinical male "infertility" is often diagnosed through semen analysis using sperm concentration, motility, and morphology as the identifying criteria. However, these criteria can only provide limited prognostic and diagnostic information. New biomarkers of sperm function are in urgent need, especially those involved in key physiological processes, e.g., spermatogenesis, capacitation and sperm-egg interaction.

Molecules selectively present in spermatogenic cells and sperm with significant function in fertilization should be evaluated for their potentials as biomarkers of sperm fertilizing ability. Based on these criteria, work in our laboratory, which is focused on the physiology and biochemistry of mammalian fertilization and male fertility, has revealed the significance of sperm surface arylsulfatase A (ASA) for sperm-egg interaction (Tanphaichitr et al., 2007b). ASA also exists in the sperm acrosome and lysosomes of Sertoli cells, although the functions of ASA in these entities are unknown. We hypothesize that acrosomal ASA may be involved in secondary binding of acrosome reacting/reacted sperm to the ZP, and ASA in Sertoli cells may be involved in keeping

the balance of its substrate sulfogalactosylglycerolipid (SGG), a sulfoglycolipid present specifically and abundantly in male germ cells, which is essential for spermatogenesis (Fujimoto et al., 2000; Honke et al., 2002). Due to the unique properties and significant roles in male fertility, ASA and SGG may serve as reliable biomarkers of sperm function. However, a comprehensive understanding of the cellular and molecular mechanisms of ASA and SGG in the male reproduction is required; this includes confirmation of in vivo roles of these molecules in male fertility.

1.2. Spermatogenesis

Spermatogenesis is dynamic and highly regulated process by which testicular stem cells (undifferentiated spermatogonia) develop into spermatozoa. In mammals, it takes place in the seminiferous tubules within the testes (Figure 1.1 A). Seminiferous tubules consist of the seminiferous epithelium and a fluid-filled lumen, into which mature spermatozoa are released. The mammalian seminiferous epithelium is composed of two basic cell types, germ cells and the somatic Sertoli cells. The Sertoli cells span the entire height of the epithelium to nurture the germ cells through their development (Dym, 1977). Germ cells appear in layers from the basal membrane to the apical region of the seminiferous epithelium, with those at more advanced developmental stage lying closer to the lumen. Finally, elongated spermatids lodge their heads within the Sertoli cell cytoplasm in the apical region for final development into testicular sperm, which are then released into the lumen (Dym, 1977; Cheng and Mruk, 2002; Mruk and Cheng, 2004). As germ cells divide and differentiate, they move from the basement membrane through tight junctions, formed between adjacent Sertoli cells, untill they reside in the adluminal

A

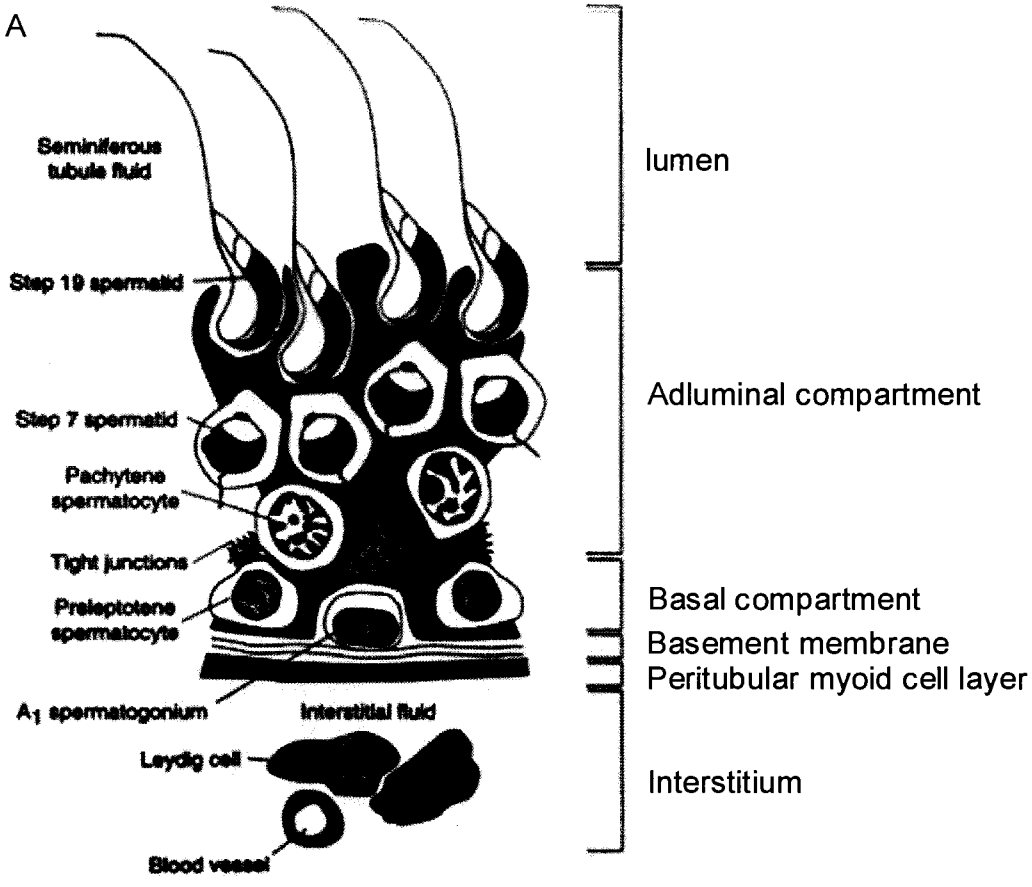
Seminiferous tubule fluid
Step 19 spermatid
Step 7 spermatid
Pachytene spermatocyte
Tight junctions
Preleptotene spermatocyte
A1 spermatogonium
Interstitial fluid
Leydig cell
Blood vessel
lumen
Adluminal compartment
Basal compartment
Basement membrane
Peritubular myoid cell layer
Interstitium

B

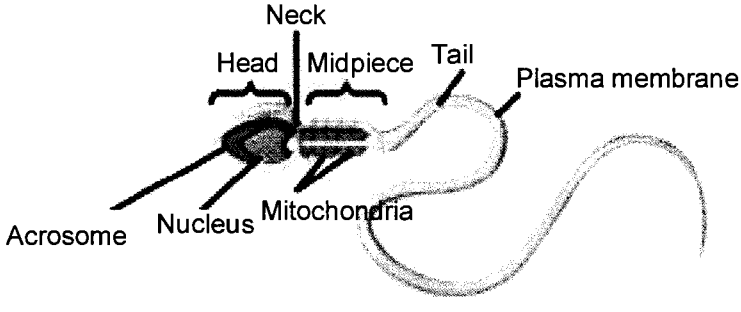
Neck
Head
Midpiece
Tail
Plasma membrane
Acrosome
Nucleus
Mitochondria

Figure 1.1. (A) Schematic drawing of the seminiferous epithelium showing the relation of Sertoli cells and germ cells (Dym, 1977). Each seminiferous tubule is composed of a lumen lined by a specialized epithelium. The seminiferous epithelium contains two cell populations: Sertoli cells and spermatogenic cells (spermatogonia, spermatocytes, and spermatids). Blood-testis barrier is formed between adjacent Sertoli cells. It prevents large molecules including proteins and antibodies from reaching developing spermatogenic cells, and the blood-testis barrier also divides seminiferous epithelium into two compartments: 1) basal compartment, below the junctions, where spermatogonia are located and 2) adluminal compartment, above the junctions, where spermatocytes and spermatids reside. **(B) General structures of mammalian sperm.** The head and midpiece of the flagellum (tail) are joined by the connecting piece. The flagellum is divided into three parts: midpiece, principal piece and end piece. The axoneme, which consists mainly of microtubules (made up mainly from tubulin and dynein) is the major structure throughout the tail. Nine pairs of microtubule doublets are on the tail periphery and there is only one microtubule doublet in the center. In the midpiece, the mitochondrial helical sheath winds around the axoneme. In contrast, the axoneme is covered by the fibrous sheath in both the principal piece and end piece. In the prinicipal piece, outer dense fibers cover the fibrous sheath.

compartment (Dym, 1977). The tight junctions form the blood-testis barrier, which helps to protect the developing germ cells from potentially harmful blood-borne chemicals by restricting the passage of molecules based largely on their molecular weight and chemical nature (Russell and Peterson, 1985; Mruk and Cheng, 2004; Madara, 2000; Dym and Cavicchia, 1977). Spermatogenesis begins with the clonal expansion of spermatogonial stem cells. Through mitosis, diploid spermatogonial type A stem cells divide to reproduce themselves, thus ensuring a constant supply of germ stem cells for spermatogenesis, and to produce differentiating spermatogonia (intermediate (In) and type B spermatogonia). The differentiating cells divide and give rise to the more specialized meiotic spermatocytes. In rodents, type A spermatogonia can be further divided into four subtypes: types A_1, A_2, A_3, and A_4 (Dym, 1977; Dym, 1994). Only the type A_4 spermatogonia differentiate into type B spermatogonia, which in turn are committed to the production of preleptotene and leptotene primary spermatocytes. These primary spermatocytes will then traverse the blood-testis barrier to enter the adluminal compartment to complete meiosis. Following DNA replication in preleptotene spermatocytes, each chromosome of primary spermatocytes appears as a pair of chromatids, having the total DNA content representing twice of that in diploid somatic cells (4C) (de Kretser and Kerr, 1994) (Figure 1.2). These primary spermatocytes range in size from very small preleptotene spermatocytes to very large pachytene spermatocytes with earsily recognizable chromosome characteristics. During the relatively long prophase of the first meiotic division, the chormosomes first unravel as thin filaments in leptotene spermatocytes. Homologous chromosomes become paired in the zygotene stage, forming the synaptonemal complex. At pachytene stage, the nuclei are enlarged as

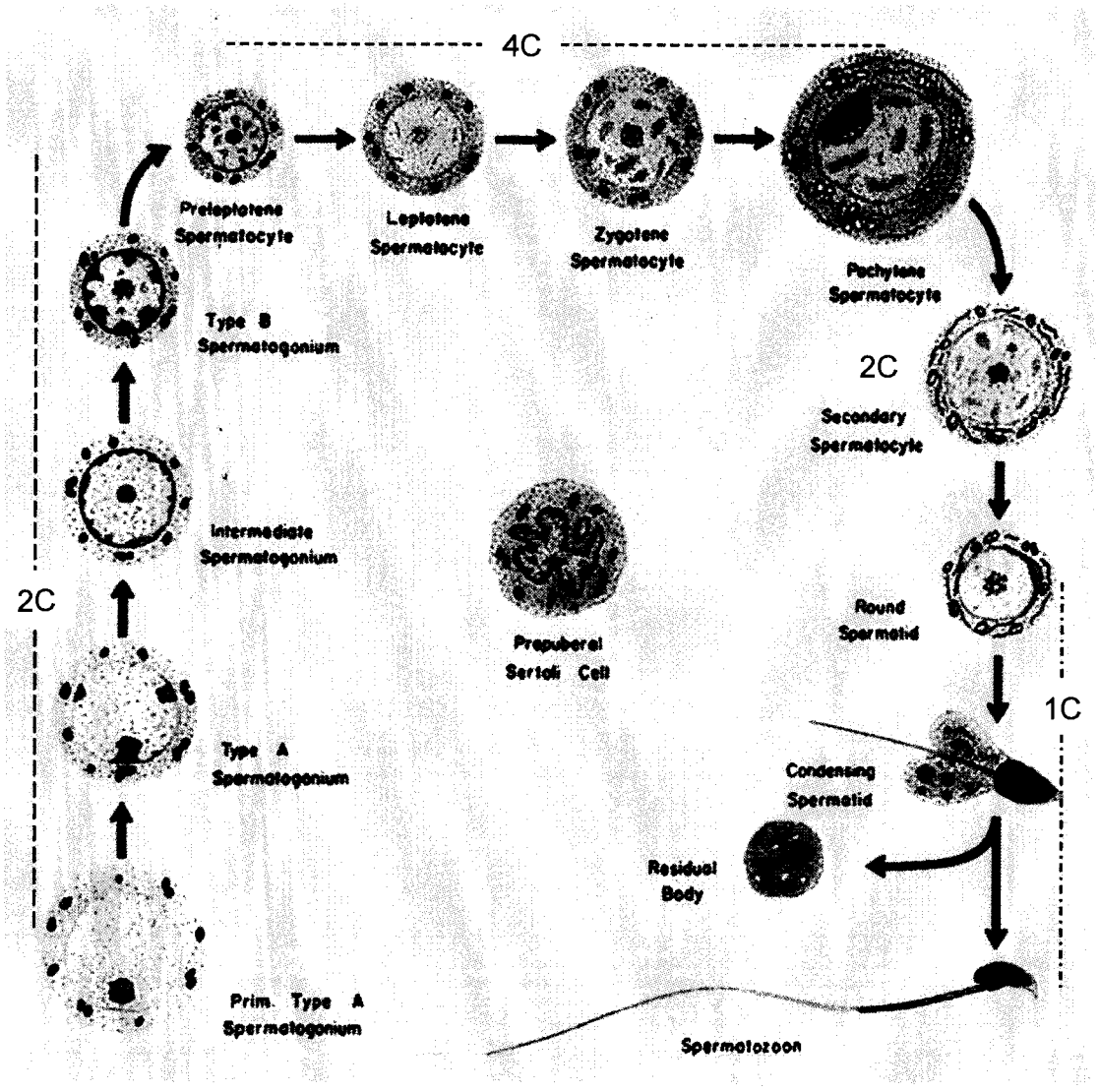
4C
Preleptotene Spermatocyte
Leptotene Spermatocyte
Zygotene Spermatocyte
Pachytene Spermatocyte
2C
Secondary Spermatocyte
Round Spermatid
1C
Condensing Spermatid
Residual Body
Spermatozoon
Type B Spermatogonium
Intermediate Spermatogonium
Type A Spermatogonium
Prim. Type A Spermatogonium
2C
Prepuberal Sertoli Cell

Figure 1.2. Schematic diagram of spermatogenesis in the mouse testis. This complex process occurs in three phases: the mitotic proliferation of spermatogonia (ascending axis); meiosis with its prolonged meiotic prophase (horizontal axis) and two reduction divisions which yield 2 x secondary spermatocytes and then 4x haploid round spermatids. Spermatids undergo differentiation, the so-called spermiogenesis which culminates in the formation of spermatozoa. Spermiogenesis involves changes of the cell shape and the removal of residual bodies via phagocytosis by Sertoli cells. The DNA content associated with each type of spermatogenic cells is indicated, with 2C being somatic amount of DNA (after Bellve et al., 1977).

the chormosomes become condensed, and genetic recombination occurs through cross-over between paired chromosomes at the diplotene stage. There is an increase in RNA and protein synthesis in pachytene spermatocytes to prepare for the next phase of spermatogenesis. The synaptonemal complexes are separated and the chromosomes are spread apart in the nucleus of diplotene spermatocytes. Small secondary spermatocytes (with half the number of chromosomes (1N) but somatic cells equivalent amount of DNA (2C)) are produced by meiosis I which then rapidly divide again by meiosis II to produce haploid spermatids (with haploid number of chromosomes (1N) and half the DNA content of somatic cells (1C)) (Kierszenbaum, 2002) (Figure 1.2). The duration of the secondary spermatocytes is very transient so that they are a minor population in histological preparations. Round spermatids undergo dramatic morphological changes to develop into structurally and biochemically unique spermatozoa, a process referred to as spermiogenesis. The major modifications that occur during spermiogenesis include: (i) The nucleus elongates and chromatin becomes condensed. Round spermatids contain histones (both somatic type and testis specific ones) as their basic nuclear proteins (Brock et al., 1980; Trostle-Weige et al., 1984; Moss et al., 1989; Shires et al., 1975). When spermatids start to elongate, transition proteins (TP) are synthesized and histone displacement from the chromatin initiates (Meistrich et al., 2003; Zhao et al., 2004). Finally, very basic nuclear proteins, protamines, whose syntheses are also de novo, deposit onto elongating/elongated spermatid DNA, replacing almost all histones and TPs. The very basic nature of protamines renders the chromatin of elongated spermatids to be tightly packed, appearing electron dense under an electron microscope. This tightly packed chromatin is generally transcriptionally inactive, (ii) The acrosomal granules

(derived from the Golgi apparatus in round spermmatids) forms a cap-like structure, covering the entire anterior one-half of the nucleus. The acrosomal cap consists of an outer and inner acrosomal membrane enclosing the acrosomal contents (Yanagimachi, 1994; Eddy and O'Brien, 1994; Yoshinaga and Toshimori, 2003); and (iii) Spermatid begins to form a long tail that houses the microtubular structure-based axoneme, which is located at the center of the flagellum throughout its full length and is the motility apparatus. They also develop a thickened mid-piece, where the mitochondria wrap around the axoneme in a helical pattern. As mature elongated spermatids move to the seminiferous tubule lumen, they lodge their heads within the Sertoli cell cytoplasm via the ectoplasmic specialization (Johnson et al., 1978). The residual cytoplasma is then phagocytosed by Sertoli cells as residual bodies once spermiation (release of testicular sperm into the lumen of the seminiferous tubules) has occurred (Figure 1.3) (Dym, 1977; Cheng and Mruk, 2002).

The well developed testicular sperm are terminally differentiated and highly polarized cells, consisting of the sperm head and the flagellum (Figure 1.1 B) (Yanagimachi, 1994; Eddy and O'Brien, 1994; Eddy et al., 2003). The sperm head consists of a highly compact nucleus and the acrosome, with very little cytoplasm (Eddy and O'Brien, 1994) and is the site for sperm-zona pellucida (ZP) interaction. The acrosome is a membrane-bound, cap-like structure located on the anterior portion of the sperm head overlying the nucleus, and contains a battery of hydrolytic enzymes. Along the outer acrosomal membrane and the sperm plasma membrane overlying the acrosome, there is a filamentous F-actin network to stabilize both membranes and to prevent their premature fusion or acrosomal exocytosis (Breitbart and Spungin, 1997). The sperm

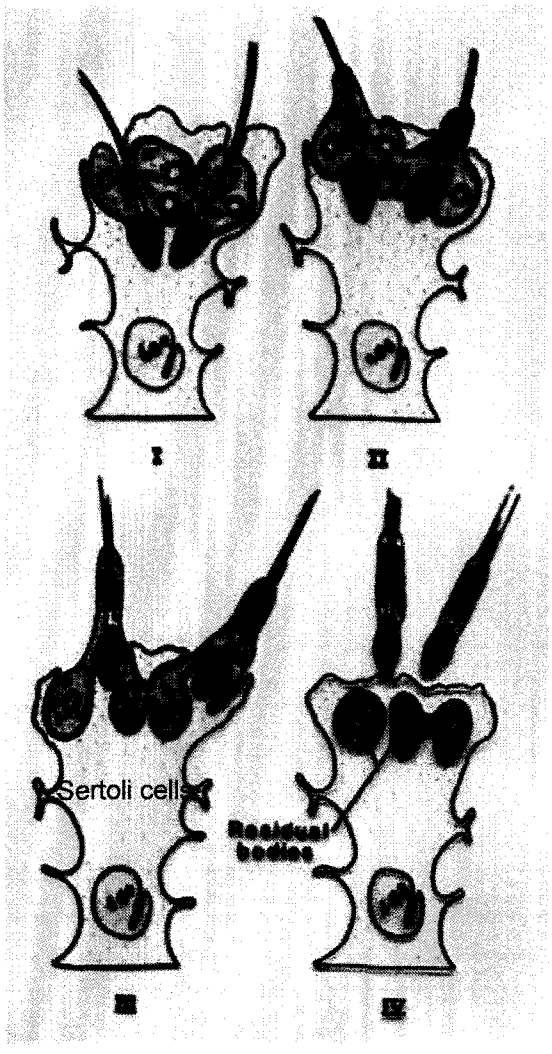
I
II
Sertoli cells
Residual bodies
III
IV

Figure 1.3. The final stages of spermiogenesis. A schematic drawing of the final stages of spermiogenesis (modified from de Kretser and Kerr, 1994) showing that the processes of Sertoli cells cytoplasm essentially "pull off" the residual cytoplasm (residual body) and retain it within their cytoplasm (occurring in the order from image I to IV).

flagellum consists of the connecting piece, the midpiece, the principal piece, and the end piece (Eddy and O'Brien, 1994; Eddy et al., 2003). The midpiece contains the mitochondrial sheath surrounding the microtubular structure of the flagellum and is the energy source of sperm motility. The principal piece is defined by the fibrous sheath, which underlies the plasma membrane, and functions as a scaffold for signaling proteins that might play a role in sperm capacitation and hyperactivated motility (Eddy et al., 2003).

Spermatogenic Stage and Cycle

In all mammals, the spermatogenic cells are organized into well-defined cellular associations within the seminiferous epithelium. The germ cells develop as a syncytium connected to each other by intercellular bridges after cell division. This unique process of incomplete division ensures synchronous development and permits rapid communication between the cells. The synchronized process of spermatogenesis allows germ cells to advance within the seminiferous epithelium. The more advanced germ cells are found away from the basement membrane and are in specific associations with the less developed germ cells that will divide and mature in time. These specific cellular associations occur because: 1) along the basement membrane of the seminiferous tubule, there is more than one spermatogonium that enters spermatogenesis process, but the entry of all spermatogonia into this process is not synchronized, and 2) the duration of spermatogenic cells at each developmental stage is constant. When a cellular association exhibits distinguishing morphological features, it is identified as a specific stage of spermatogenesis. Stages can be recognized by examining cross sections of seminiferous tubules histologically based on the acrosomic system of the spermatids when stained with

periodic acid-Schiff-hematoxylin (PAS) (Clermont, 1972). Fourteen stages have been defined in the rat (Figure 1.4A), 12 stages in the mouse (Figure 1.4B) and 6 stages in the human. Over a set period of time, these cellular associations repeat themselves, thus establishing the spermatogenic cycle.

Sertoli -Germ Cell Interaction during Spermatogenesis

Throughout the course of mammalian spermatogenesis, differentiating spermatogenic cells remain in close contact with somatic Sertoli cells (Russell and Peterson, 1985). This cellular interaction has been considered to be essential for the progression of spermatogenesis as well as for the cyclic function of Sertoli cells (Griswold, 1995; Kierszenbaum, 1994; Cheng and Mruk, 2002; Mruk and Cheng, 2004). The interaction between germ cells and Sertoli cells is established and maintained via development of direct cellular contact as well as indirect paracrine mechanisms by their secreting factors (Jegou, 1993; Cheng and Mruk, 2002; Mruk and Cheng, 2004).

Various adhesion molecules have been implicated in mediating Sertoli-germ cell interaction; for example, *N*-cadherins (existing on both the Sertoli cell and germ cell surface) (Tres and Kierszenbaum, 1983; Newton et al., 1993; Johnson et al., 2000) and β-1,4-galactosyltransferase (present on the germ cell surface that binds a carbohydrate receptor on the Sertoli cell) (Jegou, 1993; Newton et al., 1993; Pratt et al., 1993). In addition, it has recently been reported that glycan structures on spermatogenic cells (*N*-acetylglucosamine (GlcNAc)-terminated tri-antennary and fucosylated *N*-glycans) play important rolls in adhering germ cells to Sertoli cells (Akama et al., 2002). Sertoli cells also secrete paracrine factors (i.e., transforming growth factor β (TGF-β), insulin-like growth factor I (IGF-I), and stem cell factor (SCF)), and provide nutrients (i.e., lactate,

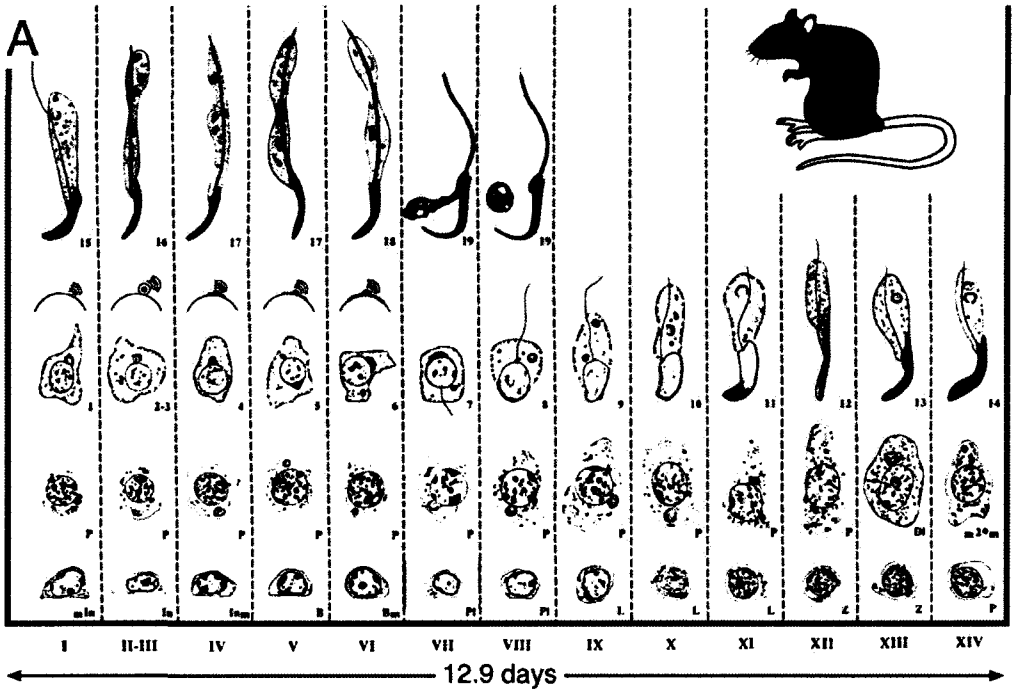

Stages of the Rat Cycle

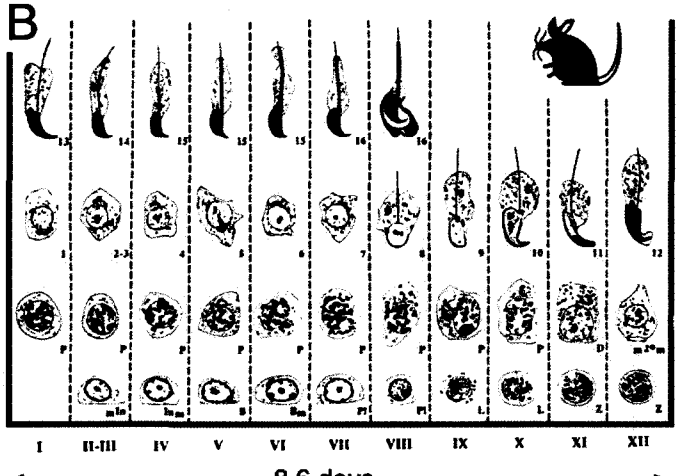

Stages of the Mouse Cycle

- In = Intermediate spermatogonium
- B = Type B spermatogonium
- PI = Preleptotene spermatocyte
- L = Leptotene spermatocyte
- Z = Zygotene spermatcyte
- P = Pachytene spermatocyte
- D/Di/2° = Dliplotene spermatocyte
- m = Cells are dividing in mitotic or meiotic processes
- 1-19 (Fig. A) = Stages 1-19 of rat spermatids
- 1-16 (Fig. B) = Stages 1-16 of mouse spermatids

Figure 1.4. Spermatogenic stages and cycles in rats and mice. The diagrams show the histological relationship of spermatogenic cells in the rat (**A**) and mouse (**B**) seminiferous tubules of the testis during spermatogenesis. In each diagram, the lower row of cells is generally closer to the basement membrane and the upper row of cells is generally closer to the lumen of the seminiferous tubule. In rat, there are 14 stages (indicated by the Roman numerals) that repeat at the same location of the tubule at a 12.9-day interval. In the mouse, there are 12 stages (indicated by the Roman numerals) that repeat at an 8.6-day interval (modified from (Franca et al., 1998)).

the preferred energy source of germ cells) to regulate and support germ cell development (Mruk and Cheng, 2004). Spermatogenesis is regulated by not only Sertoli cell functions but also signals exerted from male germ cells (Jegou, 1991). Some candidates for signals from germ cells include specific growth factors such as basic fibroblast growth factor (Han et al., 1993).

The secretory function of Sertoli cells is under the control of testosterone and follicle-stimulating hormone (FSH). The production and secretion of testosterone by Leydig cells are regulated by pituitary luteinizing hormone (LH). Both LH and FSH are synthesized and secreted by the pituitary under the control of the hypothalamic gonadotropin releasing hormone (GnRH). There is also a negative feedback to the pituitary that occurs via testosterone and inhibin (secreted by Sertoli cells). The role of FSH in spermatogenesis seems to be limited only in prepubertal animals; in adults, its functions are replaced by testosterone (Griswold et al., 1995; Sharpe, 1994).

Testosterone is known to play a key role in the control of spermatogenesis (Sharpe et al., 1994; Singh et al., 1995; McLachlan, 2000); this is evidenced by the germ cell death in hypophysectomized rats, which possess minimal amounts of testosterone (Russell and Clermont, 1977). Testosterone exerts its functions in the initiation and maintenance of spermatogenesis via androgen receptor as demonstrated in androgen receptor knockout male mice (Yeh et al., 2002). Testes of these knockout mice are 80% smaller than those of the wild type (WT), and their seminiferous epithelial area is markedly reduced. Some tubules contain Sertoli cells only while others contain a few germ cells that develop only up to the pachytene stage. No round spermatids, elongated spermatids, or mature spermatozoa are seen in the whole testis, suggesting

spermatogenesis is arrested at the pachytene spermatocyte stage (Yeh et al., 2002). Testosterone action on germ cell development is likely mediated through Sertoli cells, which express androgen receptors and have intimate interactions with germ cells at all stages of spermatogenesis (Griswold, 1995; Jegou and Pineau, 1995). This has been further confirmed in mice whose Sertoli cells were genetically deleted of the androgen receptors (Tsai et al., 2006).

Normal spermatogenesis not only depends on the supporting roles of Sertoli cells, but also requires their phagocytic activity to efficiently remove "dying" spermatogenic cells. During spermatogenesis, more than half of the differentiating spermatogenic cells at various developmental stages become apoptotic before they mature into spermatozoa (Huckins, 1978; Allan DJ, 1987; Billig et al., 1995). It is still unclear why such a large population of spermatogenic cells is discarded. Possible explanations include: (i) the number of spermatogenic cells that Sertoli cells can support is limited, and/or (ii) spermatogenic cells that acquire some defects (e.g., aberrant DNA recombination) need to be removed. In normal testes, apoptotic germ cells are efficiently eliminated by phagocytosis. This is probably why only a limited number of apoptotic spermatogenic cells are detectable when testis sections are examined histochemically. The phagocytic activity of Sertoli cells has been shown to be responsible for the efficient clearance of apoptotic germ cells. One of the "eat me" signals present on apoptotic spermatogenic cells to Sertoli cells is phosphatidylserine (PS) that is externalized during apoptosis (Shiratsuchi et al., 1997). Class B scavenger receptor type I (SR-BI) has been shown to be the Sertoli cells receptor responsible for the recognition of PS-exposing spermatogenic cells (Shiratsuchi et al., 1997; Kawasaki et al., 2002; Nakagawa et al., 2005). The

localization of SR-BI at both the apical and basolateral membranes of Sertoli cells (Shiratsuchi et al., 1997; Nakagawa et al., 2004) corroborates the results showing that Sertoli cells are able to phagocytose apoptotic spermatogenic cells at all differentiation stages (Shiratsuchi et al., 1997; Nakagawa et al., 2005). Most importantly, phagocytic clearance of apoptotic spermatogenic cells is required for the progression of spermatogenesis and efficient production of sperm (Maeda et al., 2002; Nakagawa et al., 2005). Sulfatide (SGC) and its structural analogue, SGG (sulfogalactosylglycerolipid, the male germ cell specific sulfoglycolipid), may also serve as apoptosis markers to be recognized by phagocytes. SGC has been shown to bind directly to scavenger receptors (SRs), suggesting that it could function as a phagocytic ligand on dying cells (Yoshiizumi et al., 2002). Indeed, SGC and SGG, when added exogenously, promotes phagocytosis of apoptotic murine carcinoma cells from the colon and kidney by murine macrophages (Popovic et al., 2007). The phenomenon is principally dependent on the sulfate group of SGC/SGG and their recognition by macrophage SRs (Popovic et al., 2007). These results imply that aberrant amount and organization of SGG within the plasma membrane of spermatogenic cells may likewise be recognized by Sertoli cells as makers of cells that are undergoing apoptosis.

1.3. Epididymal Sperm Maturation

Mammalian sperm just released from the testis lack fertilizing competence; they possess neither the progressive forward motility nor the ability to bind to the zona pellucida (ZP), the extracellular matrix that surrounds the egg (Yanagimachi, 1994; Tulsiani and Abou-Haila, 2001). These physiological attributes are acquired by sperm

during their passage through the epididymis (Turner, 1979; Cooper, 1995; Yoshinaga and Toshimori, 2003). Since mammalian sperm are highly differentiated haploid cells with very condensed DNA, possessing no or only limited capacity to synthesize proteins de novo, sperm maturation is primarily regulated by extracellular environment - the epididymal fluid (Cooper, 1998; Dacheux et al., 2003; Toshimori, 1998; Srivastav, 2000). Therefore, the epididymis plays an important role in the development of fertilization-competent sperm through its secretory products in the luminal fluid (Orgebin-Crist et al., 1987; Yanagimachi, 1994; Toshimori, 1998; Yoshinaga and Toshimori, 2003). In fact, most proteins found in epididymal fluid are secreted from the epididymal epithelia (Gatti et al., 2004). The epididymis is generally divided into several anatomically distinct regions: the initial segment, caput, corpus and cauda. The epididymal epithelium is composed of four distinct cell types: principal, narrow, clear and basal cells (Figure 1.5). Principal cells are the major cell type in the epididymal epithelium and are recognized for their secretory activities (Hermo and Robaire, 2002; Hermo et al., 2002). Basal cells have recently been recognized for their property of sending narrow body projections that can "sense" the luminal side of the epithelium, thus contributing to the acidification of the luminal environment (Shum et al., 2009). Both of these cell types are present along the entire length of the epididymal tubule. Narrow cells are relatively low in number and are located exclusively in the initial segments (Hermo and Robaire, 2002). Clear cells are present in the caput, corpus and cauda epididymidis, as well as in the proximal vas deferens, but are absent from the initial segments. These cells are responsible for absorption of excess secreted materials, and are identified by their possession of numerous vacuoles (Hermo and Robaire, 2002). Note that principal cells are the ones

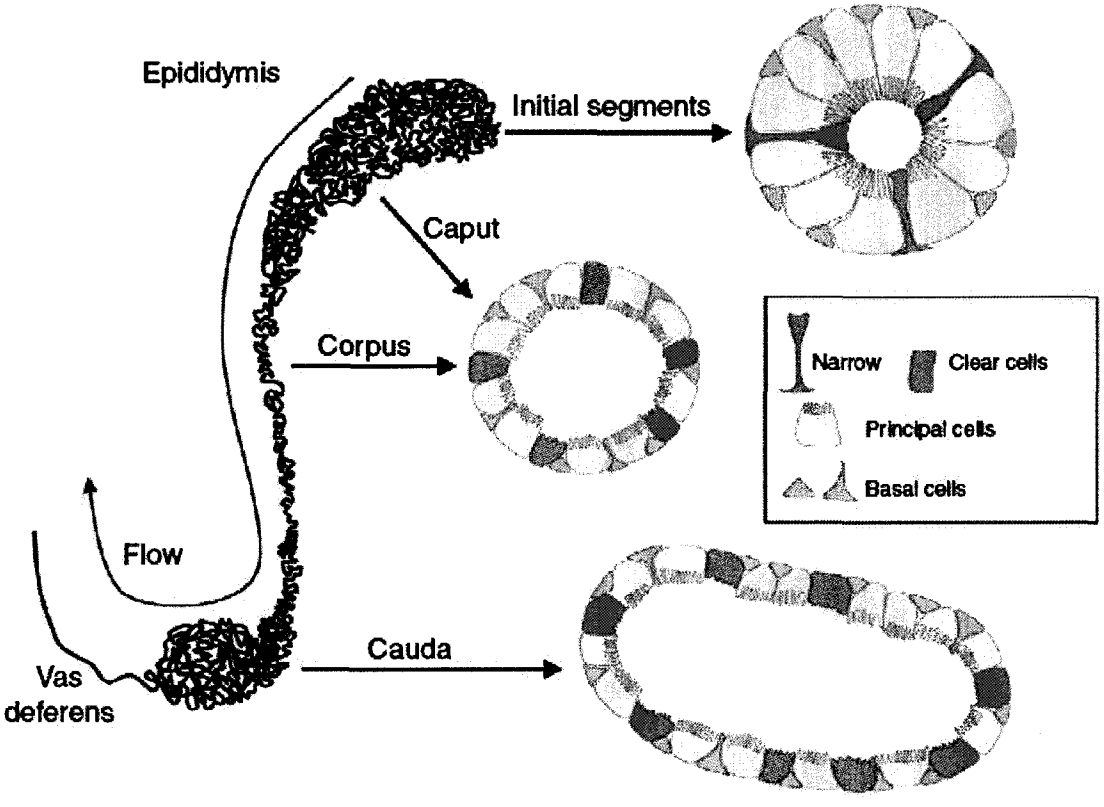
Epididymis
Initial segments
Caput
Corpus
Narrow
Clear cells
Principal cells
Basal cells
Flow
Cauda
Vas
deferens

Figure 1.5. Schematic view of the epididymis. The epididymal epithelium is composed of four distinct cell types: principal, narrow, clear and basal cells. Principal and basal cells are present along the entire length of the epididymal tubule. Principal cells are the major cell type in the epididymal epithelium and are recognized for their secretory activities (Hermo and Robaire, 2002; Hermo et al., 2002). Basal cells have the previously unrecognized property of sending narrow body projections that can contact the luminal side of the epithelium. Narrow cells are relatively low in number and are located exclusively in the initial segments (Hermo and Robaire, 2002). Clear cells are present in the caput, corpus and cauda epididymidis, as well as in the proximal vas deferens, but are absent from the initial segments. These cells are responsible for absorption of excess secreted materials, and are identified by their possession of numerous vacuoles (Hermo and Robaire, 2002) (after Shum et al., 2009).

that secrete molecules essential for sperm maturation, and their secretory activity is the highest in the caput and corpus regions. Sperm become gradually maturing while migrating through the caput and corpus regions, and complete their maturation process during their storage time in the caudal region (Dacheux et al., 2003; Fouchecourt et al., 2000).

Epididymal gene expression (Henderson et al., 2006) and the secretory activity of the epididymal epithelium (Robaire and Viger, 1995; Holland and Nixon, 1998) are primarily under androgen control. They also seem to be influenced by the presence of sperm. It has recently been shown that the presence of sperm in primary cultures of epididymal epithelial cells from different regions of the epididymis not only regulates the secretion rate but also changes the pattern of secreted proteins of the cultured epididymal cells (Reyes-Moreno et al., 2008). Some of the secreted molecules are ZP binding proteins, which deposit onto the head surface of transiting sperm (e.g., P31m (Lamontagne et al., 2001), SED-1 (Ensslin and Shur, 2003), PH-20 (Cherr et al., 2001). In this thesis, I have provided evidence that sperm also acquire ASA (Weerachatyanukul et al., 2003), onto the head surface during their epididymal transit. A number of other changes in membrane structure and composition are also associated with sperm maturation. One of such changes is proteolytic processing of membrane proteins. The processed forms of these proteins are presumably those required for physiological functions of sperm along their path from the epididymis to the site of fertilization, the oviduct, and during sperm-egg interaction. An incomplete list of proteins that are processed in the epididymis include ADAM1b (aka fertilin-α) (Yamaguchi et al., 2006), ADAM2 (aka fertilin-β or PH-30) (Stein et al., 2005; Kim et al., 2006), ADAM3 (aka

cyritestin) (Stein et al., 2005; Kim et al., 2006), ADAM5, 27, 32 (Kim et al., 2006), ADAM24 (aka testase) (Zhu et al., 2001), α-D-mannosidase (Tulsiani et al., 1995b), HE2β1 peptide (von Horsten et al., 2002), cysteine-rich secretory protein1 (CRISP1, aka protein D and E) (Roberts et al., 2008; Roberts et al., 2007) and germinal angiotensin I-converting enzyme (gACE) (Thimon et al., 2005). The processing of ADAM proteins is better studied; their cleavages may allow a better exposure of their disintegrin domain to interact with integrins existing in the epididymis and the oviduct (Breuss et al., 1993; Voigt et al., 1995) or on the egg plasma membrane (Waters and White, 1997; Bigler et al., 1997; Takahashi et al., 2001). As candidate cleavage enzymes, the presence of serine proteases, metalloproteases and an aspartyl protease (cathepsin D) in the epididymis has been documented (Gatti et al., 2004; Metayer et al., 2002a; Thimon et al., 2006; Thimon et al., 2006; Hermo and Andonian, 2003). Interestingly, inhibitors of these proteases are also present in the epdidymal lumen (Metayer et al., 2002b; Gatti et al., 2004; Cornwall et al., 2003; Thimon et al., 2008; Yenugu et al., 2004; Thimon et al., 2006; Zhou et al., 2008). The action of these proteases and their inhibitors must be kept in balance to maintain normal sperm physiology.

Additional changes that occur to the sperm plasma membrane during epididymal maturation include glycosylation of sperm surface proteins (Tulsiani et al., 1998a; Tulsiani, 2003), as well as enrichment of polyunsaturated fatty acid (PUFA) containing phospholipids in caudal sperm. PUFA phospholipids equip sperm with fusogenic ability required during acrosome reaction and sperm-egg plasma membrane fusion (Flesch and Gadella, 2000; Nikolopoulou et al., 1985; Tanphaichitr et al., 2003; Cooper and Yeung, 1997). Several fatty acid desaturases have been identified in the rat testis and epididymis,

including stearoyl-CoA desaturase (SCD) 1 and 2, and Δ^5 - and Δ^6-desaturases (Saether et al., 2003). The testicular desaturases are mainly localized to the Sertoli cells where PUFAs are probably synthesized and then transported to germ cells. The epididymal desaturases may be responsible for further desaturation of existing PUFAs on sperm or de novo synthesis of PUFAs with higher degrees of desaturation as a step in the epididmal maturation process of sperm. In addition, extensive cross-linking of nuclear protamines by disulfide bonds occurs during sperm maturation to protect sperm genome (Dias et al., 2006). Sperm also acquire forward motility during epididymal maturation. A forward motility protein (37.5 kDa), secreted by epididymal epithelial cells, has been shown to induce sperm motility (Acott and Hoskins, 1978). In addition, a rat epididymis-specific gene product Bin1b (SPAG11E), belonging to the β-defensin family with antimicrobial activity (Li et al., 2001), has been shown to be capable of initiating progressive sperm motility via induction of Ca^{2+} uptake (Zhou et al., 2004). Another antimicrobial peptide, HE2β1 (SPAG11D), highly expressed in principal cells of the initial segment and caput epididymis, has also been shown to be secreted into the lumen. Its androgen-dependent expression and binding to the sperm surface suggest that HE2β1 may have a role in sperm maturation (Hamil et al., 2000). Besides their role in initiating sperm motility, these antimicrobial peptides may protect sperm from microbial attacks. Furthermore, a 47 kDa α-1-antitrypsin (AAT) like protein and a 33.8 kDa zinc-α-2 glycoprotein (ZAG)-like protein have recently been reported to be involved in the induction of sperm motility (Ding et al., 2007). Despite all these changes, the fertilizing ability of epididymal sperm is suppressed due to existence of decapacitation factors and the masking of the ZP binding ligands, and probably also due to the overall rigidity of their plasma membrane

owing to the high cholesterol to phospholipid molar ratio (Yanagimachi, 1994; Jones, 1998).

1.4. Capacitation

Sperm are incapable of fertilizing eggs following immediate ejaculation into the female reproductive tract due in part to the maksing of their ZP binding molecules by "decapacitation factors". They need to undergo further maturation in order to gain full fertilizing competence. In vivo, this occurs during sperm transit in the female genital tract where a series of biochemical and biophysical changes occur to sperm both on the surface as well as intracellularly, a process collectively known as capacitation (Yanagimachi, 1994). In vitro, this phenomenon can be reproduced in defined media containing capacitation factors such as cholesterol-releasing agents (e.g., serum albumin and methyl-beta-cyclodextrin (MBCD)), bicarbonate, Ca^{2+} and energy sources such as glucose, pyruvate or lactate (Flesch and Gadella, 2000; Yanagimachi, 1994; Aitken, 1997; De Lamirande et al., 1997; Visconti and Kopf, 1998; Visconti et al., 2002; Harrison, 1997). Following capacitation, sperm acquire hyperactivated motility, a distinct motility pattern characterised by pronounced flagellar movements, marked lateral excursion of the sperm head and a non-linear trajectory (Suarez et al., 1993), which is required for sperm ascent through the oviduct and in part penetration of the ZP (see below). Capacitation also exposes ZP binding molecules on the sperm surface. The ability of sperm to bind to the ZP, and undergo subsequent acrosomal reaction is considered as an endpoint of capacitation (Visconti and Kopf, 1998; Visconti et al., 2002).

It has been shown, in vitro, that bicarbonate, Ca^{2+} and albumin in the external medium are essential to promote capacitation. The entry of bicarbonate into the sperm cell via a HCO_3^-/Na^+ co-transporter (Demarco et al., 2003) activates soluble adenylyl cyclase (sAC) (Okamura et al., 1985; Chen et al., 2000; Esposito et al., 2004; Xie et al., 2006; Hess et al., 2005), which results in an increase of intracellular cAMP concentration (Visconti et al., 1995b; Parrish et al., 1994; Leclerc et al., 1996) and the subsequent activation of protein kinase A (PKA) (Visconti et al., 1995b). As a result of PKA activation, a number of proteins become phosphorylated (at serine and threonine residues) (Salicioni et al., 2007; Visconti and Kopf, 1998; Ficarro et al., 2003; Platt et al., 2009; Gadella and Van Gestel, 2004). One of the end targets of this signaling pathway is the activation of a sperm-specific phospholipid scramblase, localized to the sperm head plasma membrane (Gadella and Harrison, 2000; Harrison and Miller, 2000), that causes asymmetric distribution of plasma membrane phospholipids, resulting in increased membrane fluidity (Gadella et al., 1999b; Gadella and Harrison, 2000; Gadella and Harrison, 2002; de Vries et al., 2003; Rathi et al., 2001). In the presence of Ca^{2+}, this bicarbonate-induced phospholipid scrambling is followed immediately by cholesterol efflux from the sperm plasma membrane induced by albumin/HDL (Flesch et al., 2001), which serves as a sink to remove cholesterol (Cross, 1998; Visconti et al., 2002). Note that both albumin and HDL are present in the female reproductive tract (Ehrenwald et al., 1990; Davis, 1982; Langlais et al., 1988). PKA activation also phosphorylates apolipoprotein A-I binding protein (AI-BP) that is localized to both sperm head and tail domains (Jha et al., 2008). It was released from sperm into medium during in vitro capacitation (Jha et al., 2008), presumably through the interaction with apolipoprotein A-

I, the component of HDL used in this study as a cholesterol transporter (Ritter et al., 2002; Rudolph et al., 2007). This result thus provided a link between cholesterol efflux and PKA-dependent protein phosphorylation. The cholesterol efflux from the sperm membrane causes additional and sustained activation of PKA (Boerke et al., 2008), and as a result, the overall sperm protein tyrosine phosphorylation is enhanced (Osheroff et al., 1999; Visconti et al., 1995a; Visconti et al., 1995c; Osheroff et al., 1999; Asquith et al., 2004). PKA can only phosphorylate serine and threonine residues, and at present, the link between PKA activation and protein tyrosine phosphorylation is still missing. Nevertheless, some of the tyrosine phosphorylated sperm proteins have been suggested to play important roles in rendering sperm fertilizing competence. For example, tyrosine phosphorylation of an A-Kinase Anchor Protein, AKAP3, whose expression is restricted to the tail region, has been suggested to be involved in the development of hyperactivated motility (Moss and George, 2001).

During capacitation, the activation of sperm cells by bicarbonate, Ca^{2+} and albumin also causes sperm surface changes (Yanagimachi, 1994). One of such surface modifications is the exposure of ZP binding molecules on the sperm head surface. It is generally believed that these ZP binding molecules are not yet optimally exposed for ZP interaction until capacitation (Yanagimachi, 1994; Florman and Ducibella, 2006). They are masked by "decapacitation factors" that are present in the seminal plasma and male reproductive tract. The decapacitation factors are removed from sperm during capacitation through yet an unknown mechanism, thus allowing the ZP binding molecules to become exposed for ZP interaction. With regard to decapacitation factors, polylactosaminylglycans that mask galactosyltransferase (a well studied ZP binding

protein) have been shown to be removed from the sperm surface during capacitation (Shur et al., 1998). Other decapacitation factors may include cholesterol containing membrane vesicles (Davis and Davis, 1983) and phosphoethanolamine binding protein 1 (Gibbons et al., 2005; Nixon et al., 2006; Frayne et al., 1998). Recently, a number of serine protease inhibitors including HongrES1 (Zhou et al., 2008) and SPINKL (secreted serine protease inhibitior Kazal-type-like protein) (Lin et al., 2008) have been identified as decapacitation factors. Removal of the protease inhibitors from the sperm surface during capacitation may expose sperm surface serine proteases to interact with the ZP (Boettger-Tong et al., 1992; Baba et al., 1994b; Howes and Jones, 2002; Gyamera-Acheampong et al., 2006) (see the section below). In addition, these proteases may process other sperm surface proteins into mature forms that are important for egg interaction. A novel mechanism has been described for SVS2 (seminal vesicle protein secretion 2), another decapacitation factor, that exists in the mouse seminal vesicle (Kawano and Yoshida, 2007; Kawano et al., 2008). SVS2 prevent sperm capacitation by binding to GM1 gangliosides thereby preventing lipid compositional change and reorganization (Kawano et al., 2008).

Changes in the distribution and composition of plasma membrane lipids are another important feature of sperm capacitation. These changes lead to an increase in the membrane fluidity, and to changes in the architecture and composition of the plasma membrane, which can be monitored by labeling sperm with specific surface dyes such as chlortetracycline (Ward and Storey, 1984), merocyanin (Harrison et al., 1996) and filipin (Flesch et al., 2001). Interestingly, changes of sperm plasma membrane fluidity during capacitation detected by using the membrane stains corresponded to sperm cells with

hyperactivated motility showing increased levels of tyrosine phosphorylation in the tails (de Vries et al., 2003). Using fluorescence recovery after photobleaching (FRAP) technique plasma membrane fluidity has also been shown to increase in the head of hamster sperm capacitated in vivo and in vitro (Smith et al., 1998). Thus, these results suggested that the same signaling events dictate both the sperm surface changes and the induction of hyperactivated motility during capacitation. Cholesterol efflux may also affect the organization of sperm lipid rafts (cholesterol-containing liquid-ordered microdomains (see below for more details)), which serve as platforms for sperm ZP-binding and signaling molecules (Bou Khalil et al., 2006; Nixon et al., 2007; Tanphaichitr et al., 2007b; Thaler et al., 2006). Indeed, we have recently shown that capacitation results in increased levels of sperm lipid rafts with high ZP affinity despite of a global cholesterol efflux from the sperm plasma membrane (Bou Khalil et al., 2006). Our studies have verified the novel concept that lipid rafts are important for cell adhesion and signaling (Tanphaichitr et al., 2007b; Tanphaichitr et al., 2007c; Rajendran and Simons, 2005; Simons and Ehehalt, 2002). Corroborating out results, recent studies from Aitken's laboratory have revealed that tyrosine phosphorylation of a number of sperm head surface molecular chaperones (heat shock protein 90 (HSP90), heat shock protein 60 (Hspd1), endoplasmin (Tra1), and chaperonin 10 (HSP10)) are tightly associated with sperm ZP binding ability (Asquith et al., 2004; Walsh et al., 2008; Ecroyd et al., 2003). The authors have proposed that the activation of sperm-surface chaperones by tyrosine phosphorylation during capacitation may trigger conformational changes facilitating the formation of a functional zona pellucida receptor complex on the surface of mammalian spermatozoa. The capacitation-associated lipid rafts aggregation not only regulates the

sperm ZP binding ability, but also prepares sperm for subsequent ZP-induced acrosome reaction by recruiting matching v- and t-SNAREs to the outer acrosomal membrane and the overlying plasma membrane, respectively (Tsai et al., 2007; Hutt et al., 2005).

Modification of intracellular concentration of Ca^{2+} is the most fully characterized biochemical event during capacitation. An increase in the concentration of Ca^{2+} during capacitation has been demonstrated in several mammalian species, including human (DasGupta et al., 1993; Visconti et al., 1995b). A rise in intracellular pH has also been reported during capacitation of sperm of different species (Baldi et al., 2002). Capacitation also results in hyperpolarization of the sperm plasma membrane potential that is thought to be important for ZP-induced membrane depolarization and the subsequent initiation of acrosome reaction (AR) (Visconti et al., 2002). Several candidates have been proposed to participate in the capacitation-induced hyperpolarization, including a K^+ channels (Munoz-Garay et al., 2001b; Acevedo et al., 2006), a Na^+/HCO_3^- co-transporter (Demarco et al., 2003), an amiloride-sensitive epithelial Na^+ channels (Hernandez-Gonzalez et al., 2006), the cystic fibrosis transmembrane regulator (Hernandez-Gonzalez et al., 2007) and a $Na^+/K^+/Cl^-$ contransporter (Wertheimer et al., 2008).

1.5. The Zona Pellucida (ZP)

Mammalian eggs are surrounded by a thick extracellular matrix (~6.2 μm), the zona pellucida (ZP), which is secreted by growing oocytes (Yanagimachi, 1994; Wassarman, 1990; Wassarman and Litscher, 2008; McLeskey et al., 1998; Prasad et al., 2000; Topfer-Petersen et al., 2008). In most mammals, the ZP consists of a few

sulfoglycoproteins (Dunbar et al., 2001; Wassarman et al., 2004; Takasaki et al., 1999; Noguchi et al., 1992; Topfer-Petersen et al., 2008; Nixon et al., 2007). All zona sulfoglycoproteins have a characteristic ZP domain (an ~260-amino acid sequence containing 8 conserved Cys residues present as intramolecular disulfides) that is important for protein polymerization and the ZP matrix formation (Jovine et al., 2002; Wassarman, 2008). While the C-terminal fragment of the ZP domain (ZP-C) of mouse ZP3 glycoprotein has been implicated in sperm binding, the conserved amino terminal ZP-N domain is involved in zona pellucida filament formation (Jovine et al., 2006; Wassarman, 2008). Crystallographic studies of the ZP-N domain of the mouse ZP3 (at 2.3 angstrom resolution) have revealed that it adopts an immunoglobulin-like antiparallel β-sandwich structure (Monne et al., 2008). Such domains also exist in ZP2 as predicted by structure-based in silico analysis. In addition to the ZP-N domain located within the ZP domain of ZP2, three more isolated ZP-N domains have been identified in the N-terminal region of ZP2 (Monne et al., 2008). In mice, three sulfogylcoproteins (mZP1, mZP2, and mZP3) assemble non-covalently, as driven by the interactions between their ZP domains, into the three-dimensional ZP matrix (Wassarman, 1988; Wassarman, 2008). ZP2/ZP3 heterodimers form long filaments that are crosslinked by ZP1 (Greve and Wassarman, 1985). In addition to being structural components of the ZP, both ZP2 and ZP3 possess specific receptor functions in sperm interaction. Mouse ZP3 is known to serve as the primary sperm receptor (binding capacitated acrosome-intact sperm) and as the acrosome reaction inducer (Yanagimachi, 1994; Florman and Ducibella, 2006; Bleil and Wassarman, 1980a; Bleil and Wassarman, 1986; Vazquez et al., 1989), whereas mZP2 serves as the secondary sperm receptor (binding acrosome-reacted sperm) (Bleil et

al., 1988). In addition to the ZP glycoproteins, newly ovulated oocytes are coated with a glycoprotein that is originated from the oviductal secretion (Rodeheffer and Shur, 2004). It behaves as a ~ 250 kDa, wheat germ agglutinin (WGA)-reactive glycoprotein with a basic isoelectric point that is distinct from the acidic ZP glycoproteins (Rodeheffer and Shur, 2004). Oviductins, another family of highly glycosylated high molecular weight glycoproteins of the oviduct origin, have also been reported to become intimately associated with the ZP of postovulatory oocytes (Kan et al., 1990; Kan et al., 1994; Buhi, 2002).

All three ZP polypeptides are heterogeneously glycosylated with both *O*-linked and *N*-linked oligosaccharides that are further modified by sulfation (Topfer-Petersen et al., 2008). Sulfation occurs at the C-6 position of the *N*-acetylglucosamine (GlcNAc) within the *N*-acetyllactosamine repeating units which can be released by endo-β-galactosidase (Takasaki et al., 1999; Topfer-Petersen et al., 2008). Sulfation at the non-repeated antennae at C-6 position and to a small but significant extent at the C-3 position of the reducing terminal and the innermost *N*-acetylglucosamine residues has also been described (Noguchi and Nakano, 1992; Noguchi et al., 1992; Hokke e tal., 1994; Mori et al., 1998). The carbohydrate moieties of the ZP have been shown to play a very important role in mediating the cellular interaction. A number of terminal glycosides of *O*-linked glycans have been suggested to mediate sperm binding, including α-galactose (Florman and Wassarman, 1985; Litscher et al., 1995; Bleil and Wassarman, 1988), *N*-acetylglucosamine (Miller et al., 1992), mannose (Tulsiani et al., 1992), *N*-acetylgalactosamine and fucose (Benoff, 1997; Johnston et al., 1998), *N*-acetyllactosamine (Galβ1,4GlcNAc) (Clark and Dell, 2006) and the Lewis X epitope (Gal

β 4[Fuc α 3]GlcNAc) (Kerr et al., 2004). *N*-linked oligosaccharides have also been shown to be involved in sperm binding (Yamagata, 1985; Yonezawa et al., 1995). In addition, the ZP polypeptides have also been implicated in sperm binding (Prasad et al., 2000; Florman et al., 1984; Chapman et al., 1998; Hinsch et al., 2005). However, it is unlikely that species specificity of sperm-egg interactions is governed by the ZP polypeptides due to their sequence similarities across species. Rather, species specific sperm-ZP binding is thought to be determined by the ZP glycans since their overall structures differ across animal species (Dell et al., 1999; Oehninger, 2001; Wassarman and Litscher, 2001; Chalabi et al., 2006; Topfer-Petersen et al., 2008). Recent studies from Dr. Jurrien Dean's lab (NIH, Bethesda, Maryland) using ZP transgenic mice suggested that the three-dimensional structure of the ZP rather than a single molecule (protein or carbohydrate) is important for "taxon-specific" sperm binding (Rankin et al., 2003; Hoodbhoy and Dean, 2004).

1.6. Sperm-ZP Interaction and Acrosome Reaction

Sperm bind to the ZP at the head anterior (Yanagimachi, 1994) and isolated sperm head anterior plasma membrane (APM) vesicles have been shown to have ZP affinity (Yurewicz et al., 1993; Peterson et al., 1981; Bou Khalil et al., 2006). A large number of sperm molecules have been shown to have affinity for the ZP and to be involved in sperm-ZP binding. Some of them are synthesized by developing germ cells and targeted to the plasma membrane (such as β-1,4-galactosyltransferase (GalT) (Shur and Hall, 1982; Lopez et al., 1985; Scully et al., 1987), mannosidase (Pereira et al., 1998), P26h (Gaudreault et al., 2001), basigin (Wakayama et al., 2000) and

sulfogalactosylglycerolipid (SGG) (White et al., 2000; Weerachatyanukul et al., 2001), while others are acquired onto the sperm surface during epididymal transit (such as SED1 (Ensslin and Shur, 2003), PH-20 (Deng et al., 2000; Zhang and Martin-Deleon, 2003), spermadhesins (Topfer-Petersen et al., 1998; Sanz et al., 1992; Ekhlasi-Hundrieser et al., 2002) and glutathione S-transferases (GSTs) (Hemachand et al., 2002). In this thesis investigation, it was demonstrated that sperm also acquire ASA from the epididymal fluid onto their surface as part of their epididymal maturation process. Generally, sperm interaction with the ZP involves sperm initial adhesion and binding to the ZP, ZP-induced acrosome reaction, and sperm penetration through the ZP matrix.

The initial adhesion of sperm to the egg extracellular matrix is apparently not particularly species- or order-specific(Hartmann et al., 1972; Bedford, 1977). At least two gamete proteins have been shown to contribute to the initial sperm-ZP adhesion: sperm SED1 and a ZP3-independent oviductal glycoprotein (Ensslin and Shur, 2003; Rodeheffer and Shur, 2004). SED1, a secreted protein that contains Notch-like **E**GF repeats and **D**iscoidin/F5/8 types C complement domains, was originally identified as p47 in the pig sperm plasma membrane through affinity chromatography using immobilized homologous ZP glycoproteins (Ensslin et al., 1998). In mice, sperm SED1 is derived from two independent sources, the de novo synthesis in spermatogenic cells and adsorption from the epididymal epithelium secretion (Ensslin and Shur, 2003). In the epididymis, SED1 is expressed mainly in epithelial cells of the initial segment of the caput epididymis, from where it is secreted and adsorbed onto transit sperm head surface (Ensslin and Shur, 2003). Since the hypervariable loops of the discoidin domain can interact with negatively charged phospholipids and carbohydrate (Fuentes-Prior et al.,

2002), SED1 likely deposits onto the sperm plasma membrane phospholipid bilayers through this domain. This may also be the mechanism how SED1 interacts with the ZP glycans. SED1 binds to the ZP of unfertilized eggs, due to its affinity for both ZP3 and ZP2 glycoproteins; however, it does not bind to fertilized egg ZP (Ensslin and Shur, 2003). In vitro gamete assays demonstrated that recombinant SED1 and anti-SED1 antibodies competitively inhibited sperm-ZP binding (Ensslin and Shur, 2003). In addition, SED1-null sperm showed almost complete inability to bind to the ZP (Ensslin and Shur, 2003). However, SED1-null sperm undergo acrosome reaction normally upon induction with solubilized ZP. Since sperm GalT is known to be a "true" receptor of the ZP (see more below), these data suggested that SED1 is involved in initial sperm-egg adhesion, preceding the specific binding between GalT and ZP3 (Ensslin and Shur, 2003). The initial sperm adhesion to the egg is also facilitated by a high molecular weight oviductal glycoprotein that coats the ZP of ovulated oocytes (Rodeheffer and Shur, 2004). At present, the sperm surface receptor for this oviductal glycoprotein is unknown. In addition, studies in various mammalian species have demonstrated that oviductins, another set of oviductal proteins which are highly glycosylated, also facilitate sperm capacitation and sperm-egg interaction (Buhi, 2002; Kan and Esperanzate, 2006).

Besides SED1, a wide variety of sperm surface molecules have been implicated in binding to the ZP, but only a few have been suggested to function as "true" receptors for ZP3. Of these, GalT appears to be the best candidate that is involved in sperm-ZP3 interactions (Shur et al., 2006). It binds specifically to *N*-acetylglucosamine (GlcNAc) at the non-reducing end of ZP3 glycans (Shur and Hall, 1982; Miller et al., 1992). A number of other ZP-binding proteins are also glycoenzymes (e.g., α-mannosidase

(Tulsiani et al., 1989; Cornwall et al., 1991) and fucosyltransferase (FucT) (Cardullo et al., 1989; Chiu et al., 2007). This is consistent with the observation that ZP glycans are important for sperm binding via carbohydrate-protein and/or carbohydrate-carbohydrate interaction. These glycoenzymes utilize the binding to their substrates - sugar residues of the ZP glycans as the basis of sperm interaction with the ZP. It is conceivable that hydrolysis rate of the substrate must be low or nil, thus allowing the sperm to bind to the ZP at least momentarily. In addition, ZP glycoproteins contain sulfated sugar residues, which may likewise serve as binding ligands for desulfating enzymes such as ASA. The ability of sperm ASA to bind to individual zona sulfoglycoproteins and whether the binding is dependent on the sulfated glycans have been investigated as part of my thesis reported herein.

After mammalian sperm bind to the ZP, they undergo the acrosome reaction, a prerequisite for sperm penetration through the ZP and fusion with the egg (Yanagimachi, 1994). Acrosome reaction is a regulated exocytotic event in which the outer acrosomal membrane fuses at multiple points with the overlying plasma membrane (Yanagimachi, 1994). In mice, only capacitated acrosome-intact sperm are capable of binding to the ZP (Bleil and Wassarman, 1983; Wassarman, 1999) and aggregation of GalT on the sperm surface by the multivalent ZP3 oligosaccharides results in the acrosome reaction (Gong et al., 1995; Leyton and Saling, 1989; Macek et al., 1991). Interestingly, the GalT knockout males are not sterile, despite that the GalT null sperm fail to bind to ZP3 and undergo ZP3-induced acrosome reaction (Lu and Shur, 1997). The ability of the GalT null sperm to undergo spontaneous acrosome reaction was thought to account for the knockout male fertility. Therefore, spontaneous acrosome reaction may have a physiological role if it

occurs after sperm binding to the ZP, even though a high rate of spontaneous acrosome reaction prior to ZP binging would be disadvantageous for sperm to fertilize.

A number of sperm signaling events have been described for the ZP-induced acrosomal exocytosis, with Ca^{2+} influx denoted as a prerequisite. ZP3 induces a two-phase intracellular calcium $[Ca^{2+}]_i$ increase. The first transient $[Ca^{2+}]_i$ increase is through the opening of voltage-sensitive calcium channels, which in turn leads to activation of a pertussis toxin–sensitive heterotrimeric guanine nucleotide-binding protein (G_i protein)–coupled phospholipase C (PLC) (Patrat et al., 2000; Munoz-Garay et al., 2001a; Jimenez-Gonzalez et al., 2006; Darszon et al., 2006). In mice, $PLC_{\delta}4$ has been shown to be required for intracellular Ca^{2+} mobilization and for a sustained increase in $[Ca^{2+}]_i$ through store-operated channel (SOC), essential for ZP and progesterone-induced acrosome reaction (Fukami et al., 2001; Sato et al., 2003). Several other sperm PLCs may also be involved in acrosome reaction: (1) A tyrosine kinase–regulated PLCγ, which may be activated during ZP3 binding (Patrat et al., 2000); (2) PLCβ1 (Walensky and Snyder, 1995); and (3) PLCγ (Spungin et al., 1995; Spungin and Breitbart, 1996). The activated PLCs hydrolyze phosphatidylinositol-4,5-disphosphate (PIP2) to generate two second messengers, inositol 1,4,5-trisphosphate (IP3) and diacylglycerol (DAG). DAG activates phospholipase A_2 (PLA_2), which hydrolyzes membrane phospholipids (mainly PC) to produce arachidonic acid and lysophopholipids (fusogenic lipids) (Yuan et al., 2003). IP3 releases Ca^{2+} from intracellular stores, which in the sperm is likely the acrosome (De Blas et al., 2002; Herrick et al., 2005; Rossato et al., 2001), via binding to IP3 receptor on the outer acrosome membrane (Kuroda et al., 1999; Walensky and Snyder, 1995; Naaby-Hansen et al., 2001). Calcium depletion in the acrosomal store stimulates a subsequent

sustained Ca^{2+} influx via SOCs (Florman, 1994; O'Toole et al., 2000; Breitbart, 2002b). The expression of three Drosophila transient receptor potential protein channels (Trp1, Trp3, and Trp6) in mouse sperm has also been described (Trevino et al., 2001), and Trp2 has been shown to play a role in the ZP3-induced acrosome reaction in mouse sperm (Jungnickel et al., 2001). As a result, intracellular Ca^{2+} concentration is elevated to supramicromolar level, thus inducing F-actin depolymerization and culminating in acrosomal exocytosis (Breitbart and Spungin, 1997; Breitbart, 2002a; Breitbart, 2002b). Another phosphoinositide-dependent signalling pathway is also involved in the ZP3-induced AR (Jungnickel et al., 2007). ZP3 stimulation of capacitated mouse sperm leads to the production of phosphatidylinositol-3,4,5-triphosphate (PIP3) in sperm via phosphorylation of PIP2 by PI3 kinase. In combination with down regulated phosphoinositide D_3-phosphatase activity, PIP3 is accumulated in sperm, resulting in the activation of the downstream effectors, Akt and PKCζ (Jungnickel et al., 2007). The production of PIP3 also appeared to be a sufficient step in sperm signalling leading to acrosome reaction, since the exocytosis could be triggered by direct stimulation of PI3 kinase along in the absence of ZP3 (Jungnickel et al., 2007).

In addition to the ZP, progesterone, a hormone present in the cumulus matrix, may also play a physiological role in the induction of acrosome reaction (Roldan et al., 1994; Meizel, 1997; Forti et al., 1999; Blackmore, 1999; Patrat et al., 2000; Kirkman-Brown et al., 2002). Progesterone has been suggested to have a priming effect on sperm to respond to the ZP (Murase and Roldan, 1996; Roldan et al., 1994; Aitken and McLaughlin, 2007), enhancing both sperm ZP binding as well as ZP mediated induction of the acrosome reaction (Neild et al., 2005). Steroid hormones receptors are generally

known as nuclear receptors, but the sperm progesterone receptor functions as a non-genomic receptor (Contreras and Llanos, 2001). In fact, it is localized on the sperm head plasma membrane (Wu et al., 2006) and upon progesterone binding, it transduces the sperm signaling events leading to acrosomal exocytosis (Rathi et al., 2003). Progesterone-mediated induction of the acrosome reaction has been shown to involve a species-specific protein kinase-dependant signaling pathway (Harrison, 1996; Harrison et al., 2000; Rathi et al., 2003; O'Toole et al., 1996; Murase and Roldan, 1996), possibly through a γ-aminobutyric acid type A ($GABA_A$)-like receptor with Cl^- channel activity (Roldan et al., 1994; Shi and Roldan, 1995; Meizel, 1997). Both ZP and progesterone induced acrosome reaction are initiated through aggregation of their corresponding receptors on sperm (Baldi et al., 2000). However, the fundamental difference between progesterone- and ZP-induced acrosome reaction consists of the nature of their receptors, because the ZP-induced acrosome reaction is mediated by a G_i-protein, which does not exist in the progesterone-mediated pathway (Murase and Roldan, 1996). Despite the differences, cross talk between these pathways is possible (Aitken and McLaughlin, 2007).

The involvement of ligand-receptor signal transduction in acrosome reaction has recently been challenged by the finding that binding of sperm to the ZP was not sufficient to induce acrosome reaction (Baibakov et al., 2007). The authors proposed a mechanosensory signaling model in which initial penetration of sperm into the zona matrix transduces a mechanosensory signal leading to mobilization of acrosomal Ca^{2+} stores (Herrick et al., 2005) and the induction of acrosome reaction (Baibakov et al., 2007).

Regardless of the mechanisms, acrosome reaction results in the release of the acrosomal content and the exposure of acrosomal and/or inner acrosomal membrane molecules. It is important to note that the acrosome reaction is not an all or none event where the acrosome is either "intact" or "reacted" (Kim and Gerton, 2003). In the mouse, there are at least four recognizable successive transitional stages of acrosome reaction, which include (i) plasma membrane intact over the acrosome, (ii) plasma membrane initiating fusion with outer acrosomal membrane with soluble components retained within the acrosome, (iii) soluble acrosomal components lost but acrosomal matrix materials still present, and (iv) most acrosomal components lost (Kim and Gerton, 2003). The acrosomal content containing hydrolytic enzymes may be important for sperm penetration through the ZP matrix, while the newly exposed molecules on the sperm head during and after acrosome reaction are involved in securing acrosome reacting/reacted sperm on the ZP by binding to the ZP2 sulfoglycoprotein. Several ZP binding molecules (proacrosin, sp56, zonadhesin, PH-20, Sp17 and Sp38) have been suggested to be involved in this secondary sperm-ZP binding. Acrosome reacted sperm will then need to penetrate the ZP matrix to reach the egg plasma membrane. Although the mechanism is still a matter of debate, it has been hypothesized that sperm penetration through the ZP is dependent on the mechanical force provided by sperm hyperactivated motility, or on the action of hydrolases (including proteases) released in the acrosomal content or present on the sperm membranes, or the combination of both (Yanagimachi, 1994; Florman and Ducibella, 2006). Three candidate enzymes or enzyme systems have been implicated in sperm penetration through the ZP: acrosomal serine protease acrosin (Baba et al., 1989), GPI-anchored serine protease TESP5 on the sperm membrane (Honda et al., 2002;

Yamashita et al., 2008), and the acrosomal proteasome (Sawada et al., 2002; Sutovsky et al., 2004). Since acrosin-deficient male mice were fertile and their sperm were still able to penetrate ZP (Baba et al., 1994a), acrosin may not be essential in this respect. It may play an alternative role in dispersal of acrosomal content (Yamagata et al., 1998) or activating other proteases such as TESP5 (Yamashita et al., 2008). In this regard, it would be interesting to see whether sperm form mice deficient in both acrosin and TESP5 are incapable of penetrating the ZP matrix. Eventually, acrosome reacted sperm enter the perivitelline space, bind to and fuse with the egg plasma membrane. Finally one sperm is incorporated into the egg proper, signifying that fertilization has occurred (Yanagimachi, 1994).

1.7. SGG

Sulfogalactosylglycerolipid (SGG), also known as seminolipid, is the major glycolipid of testes and sperm of all mammalian species examined (Kornblatt et al., 1972; Ishizuka et al., 1973; Tanphaichitr et al., 2003; Tanphaichitr et al., 2007c). It has a structure of 1-*O*-alkyl-2-*O*-acyl [β-D-(3'-sulfatoxy)galactopyranosyl(1'-3)]-*sn*-glycerol, with both alkyl and acyl chains being mainly C16:0 (Figure 1.6 A) (Ishizuka et al., 1973; Kornblatt et al., 1974; Alvarez et al., 1990; Tupper et al., 1994; Attar et al., 2000). SGG constitutes ~10 mol% total sperm lipids (Ishizuka, 1997; Furimsky et al., 2005; Murray and Narasimhan, 1990; Tanphaichitr et al., 2003). It is a structural analogue of sulfogalactosylceramide (SGC, [β-D-(3'-sulfatoxy)galactopyranosyl]-(1'-1)]-*N*-tetracosanoylsphingosine) (Figure 1.6 A), which is the major sulfoglycolipid in the myelin sheath or membrane in the peripheral nervous system (PNS) and the white matter

A

Sulfogalactosylglycerolipid (SGG)

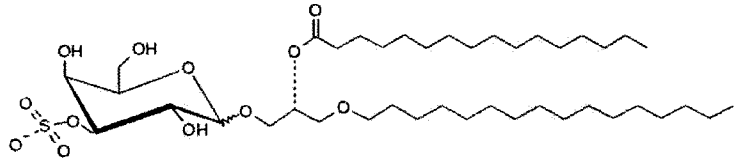

Sulfogalactosylceramide (SGC)

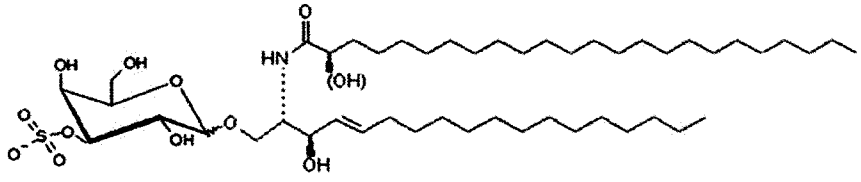

B

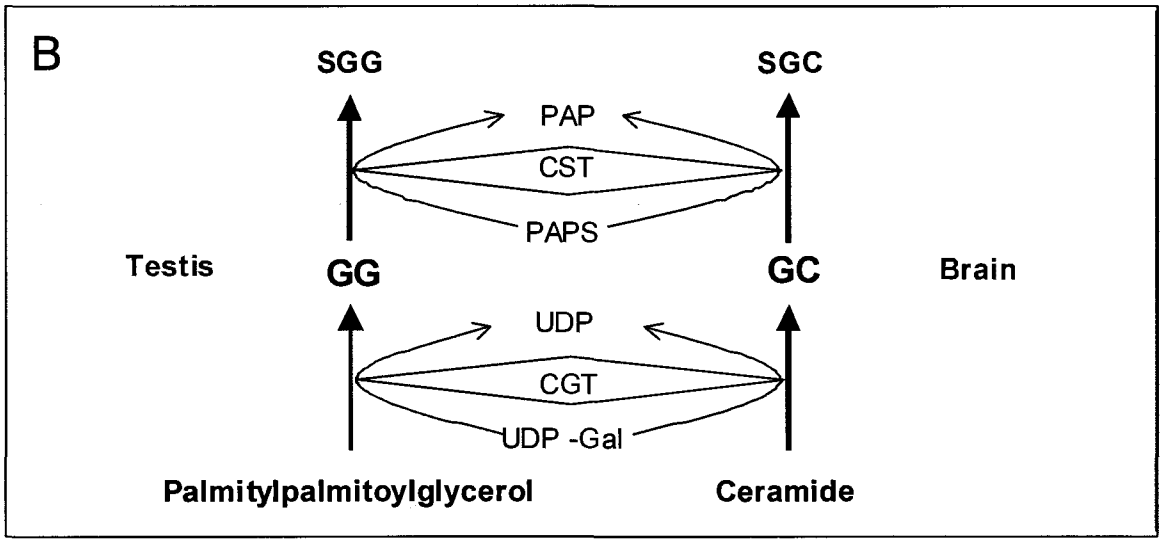

Figure 1.6. Chemical structures and biosynthetic pathway of SGG and SGC. (**A**) Structures of SGG and SGC. The acyl and alkyl chains of SGG are mainly 16:0. SGC exists as hydroxylated and non-hydroxylated forms. The acyl chain is mainly 24:0 for hydroxylated SGC, and mainly 24:1 for non-hydroxylated form. (**B**) SGG and SGC share the same biosynthetic pathway. *Abbreviations:* SGC, [*β*-D-(3'-sulfatoxy)galactopyranosyl]-1'-1-*N*-tetracosanoylsphingosine; SGG, 1-*O*-hexadecyl-2-*O*-hexadecanoyl-*β*-D-(3'-sulfatoxy)galacto-pyranosyl(1'-3)]-*sn*-glycerol; CST, cerebroside sulfotransferase; CGT, ceramide galactosyltransferase; GC, galactosylceramide; GG, galactosylglycerolipid; PAP, 3'-phosphoadenosine-5'-phosphate; PAPS, 3'-phosphoadenosine-5'-phosphosulfate; SGC, sulfogalactosylceramide; SGG, sulfogalactosylglycerolipid; UDP, uridine diphosphate; UDP-Gal, uridine diphosphate galactose.

of the brain (Ishizuka, 1997; Murray and Narasimhan, 1990). SGC is also expressed in the cytoplasm and nuclear membrane of neurons and astrocytes of the adult rat brain gray and white matter (Pernber et al., 2002; Murray and Narasimhan, 1990; Han et al., 2003). SGC is also found in epithelial cells of the kidney, digestive tract and the cervix and vagina (Ishizuka, 1997), as well as in male germ cells of lower vertebrates and invertebrates (Murray and Narasimhan, 1990; Ishizuka, 1997; Vos et al., 1994). Due to structural similarity between SGG and SGC, antibodies generated against either SGC or SGG cross-react with both sulfoglycolipids (Lingwood et al., 1980; Eddy et al., 1985; Crook et al., 1987; Fredman et al., 1988; Gadella et al., 1994; White et al., 2000). SGC and its desulfated analog, galactosylceramide (GC, β-D-galactopyranosyl-1'-1-*N*-tetracosanoylsphingosine, (Figure 1.6)), occur naturally as non-hydroxylated and α-hydroxylated species (Vos et al., 1994; Norton and Cammer, 1984). The hydroxyl group may increase the hydrogen bonding potential of SGC (Boggs et al., 1988) and GC (Pascher and Sundell, 1977; Lee et al., 1986), thus providing stability to biological membranes.

1.7.1. Biosynthesis and Degradation of SGG/SGC

SGG and SGC share the same biosynthetic pathway (Figure 1.6 B). UDP-galactose: ceramide galactosyltransferase (**CGT**; EC 2.4.1.62) first catalyzes the formation of 1-*O*-alkyl-2-*O*-acyl[β-D-galactopyranosyl(1'-3)]-*sn*-glycerol (aka, galactosylglycerol or GG) and galactosylceramide (aka cerebroside, GC) by transferring galactose from UDP-galactose to alkylacylglycerol (AAG) and ceramide, respectively (Hsu et al., 1983; Coetzee et al., 1996; Fujimoto et al., 2000). Cerebroside sulfotransferase (**CST**; EC 2.8.2.11) then sulfates the galactose residues using 3'-

phosphoadenosine -5'-phosphosulfate (PAPS) as a sulfate donor (Knapp et al., 1973; Sakac et al., 1992; Honke et al., 2002).

The galactosylation reaction is likely to occur in the endoplasmic reticulum (ER) of early primary spermatocytes (Fujimoto et al., 2000) where the enzyme CGT is localized (Sprong et al., 1998). Subsequent sulfation occurs in the Golgi apparatus of primary spermatocytes (Kornblatt et al., 1974; Letts et al., 1978; Kornblatt, 1979; Lingwood and Taylor, 1985), and the final product SGG is targeted to the outer leaflet of the germ cell plasma membrane, presumably via vesicular transport (Vos et al., 1994; Ishizuka, 1997). The sulfotransferase activity has been shown to be developmentally regulated by the appearance of an inhibitor, a phosphoinositol glycerolipid, at the mid-pachytene stage (Lingwood, 1985a; Lingwood et al., 1994). The same sulfotransferase is also responsible for the synthesis of SGC in the brain and kidney (Honke et al., 2002). An old study (Kornblatt, 1979) using mice radiolabeled in vivo with [^{35}S] sulfate suggests that SGG is metabolically stable during spermatogenesis and epididymal sperm transit. However, inaccuracy of these results may arise from cell death and cell shape changes, which take place during these processes. Precise quantification of SGG in testicular germ cells and sperm at different development stages is needed. Nonetheless, SGG is the only sulfoglycolipid in sperm (Gadella et al., 1993; Tanphaichitr et al., 1990), and the sulfoglycolipid is stable during the initial phase of in vitro capacitation of epididymal mouse sperm (Tanphaichitr et al., 1990).

The major SGC and SGG degradation pathway starts with desulfation of these sulfoglycolipids in the lysosome (Figure 1.7 I). The lysosomal enzyme responsible for cleavage of the sulfate ester is ASA (EC 3.1.6.8). Usually, ASA requires a lysosomal

I

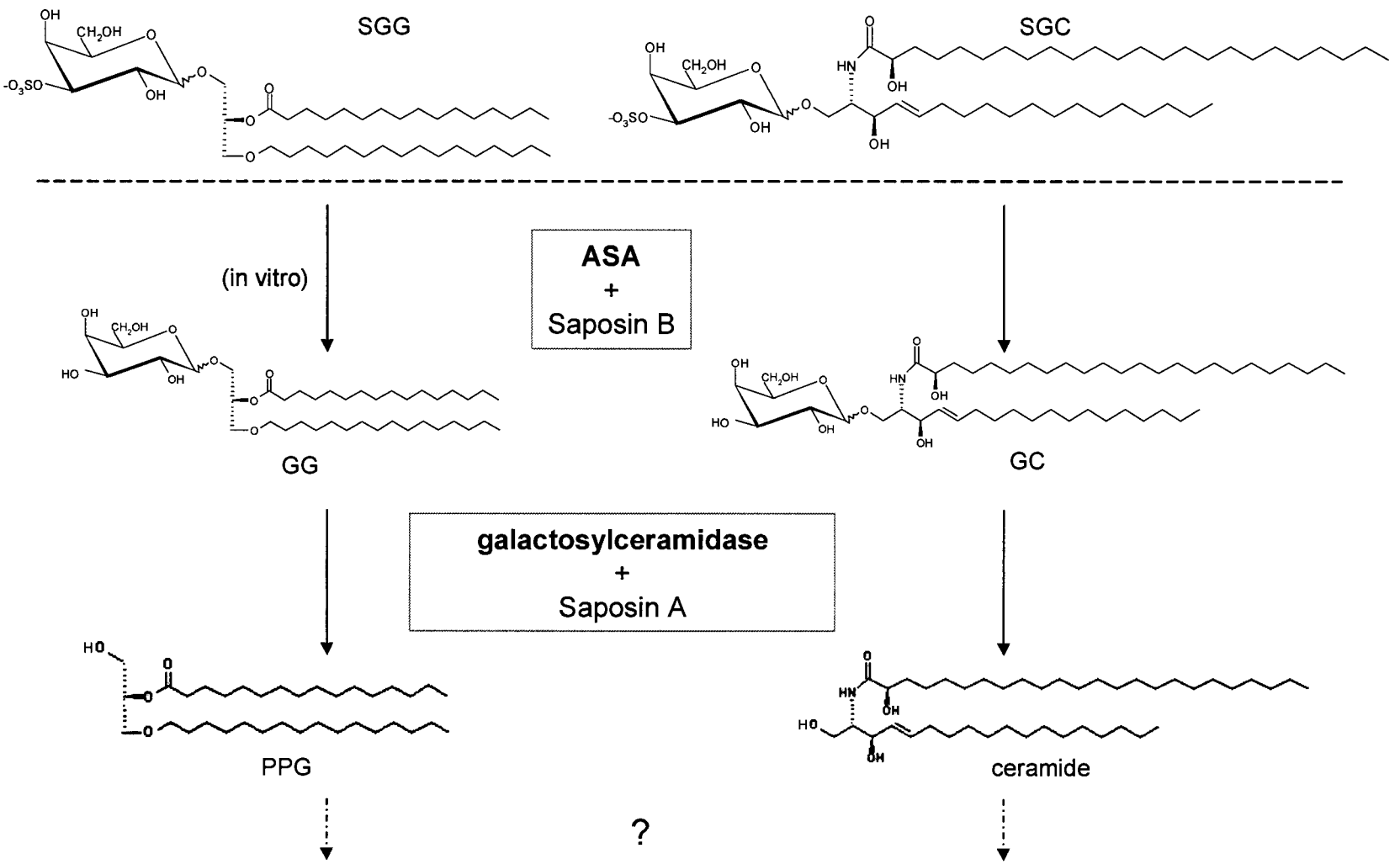
SGG
SGC
(in vitro)
ASA
+
Saposin B
GG
GC
galactosylceramidase
+
Saposin A
PPG
ceramide
?

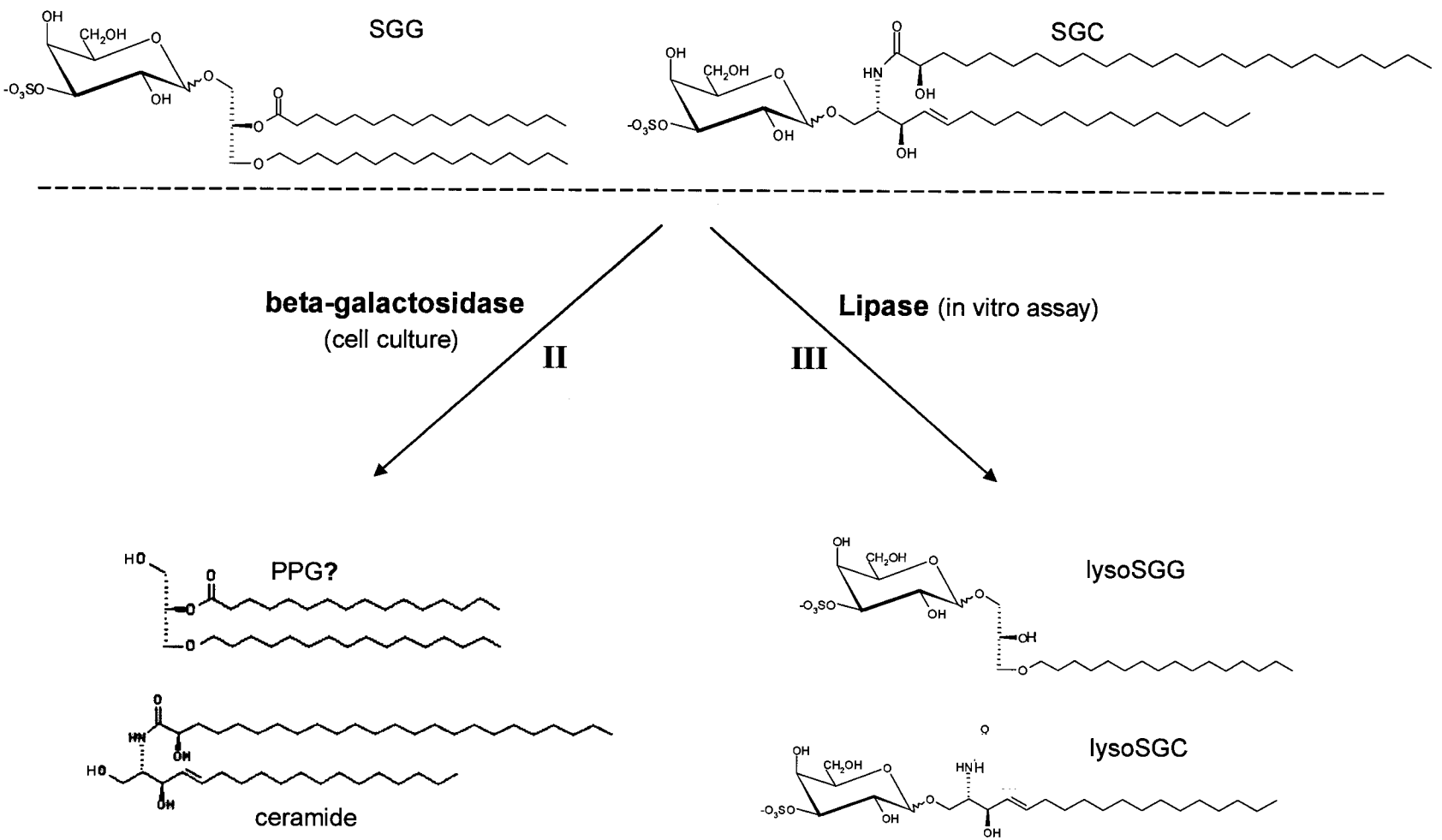
SGG
SGC
beta-galactosidase
(cell culture)
II
Lipase (in vitro assay)
III
PPG?
ceramide
lysoSGG
lysoSGC

Figure 1.7. Degradation pathways of SGC/SGG. Three degradation pathways have been described for SGC and SGG. The major degradation pathway for SGC starts with desulfation of the sulfoglycolipids in the lysosome catalyzed by ASA, provided that these lipids are presolubilized by saposin B (**I**). SGC has been shown as a natural substrate of ASA both in vitro and in vivo, whereas desulfation of SGG by ASA has only been demonstrated in vitro, and it is presumptive that it also occurs in the lysosomes. The desulfated products, GC can be further degraded by galatosylceramidase to become ceramide. This reaction requires saposin A as a co-factor. SGG is likely degraded through the same pathway, based on the in vitro results. SGC can also be degraded by β-galactosidase in the endosome to become ceramide without prior desulfation step. It is not clear whether a similar degradation pathway exists for SGG (**II**) (Zeng et al., 2008). It is likely that ceramide and PPG, generated from pathways I and II, can be either further degraded or reused for synthesis. A lipase purified from rat liver has been shown to deacylate SGC and SGG to become lysoSGC and lysoSGG, respectively (**III**) (Reiter et al., 1976). SGC, sulfogalactosylceramide; SGG, sulfogalactosylglycerolipid; GC, galactosylceramide; GG, galactosylglycerolipid; PPG, palmitoylpalmitylglycerol.

sphingolipid activator protein (SAP), saposin B, to desulfate sulfogalactolipids (Louis and Fluharty, 1991; Ahn et al., 2003; Norris et al., 2005; Matzner et al., 2009; Furst and Sandhoff, 1992; Kishimoto et al., 1992). Saposin B, a homodimeric glycoprotein, behaves as a physiological detergent; it extracts a single SGC or SGG molecule from micelles or membranes as a water-soluble 1:1 complex (Furst and Sandhoff, 1992; Ahn et al., 2003). The soluble sulfogalactolipid-saposin B complex can then be recognized by ASA and access its active site pocket (Kolter and Sandhoff, 2005; Von Bulow et al., 2001). Saposin B is derived from its precursor protein, prosaposin, through proteolytic processing (O'Brien and Kishimoto, 1991). Direct evidence of SGC being ASA's natural substrate came from studies of humans with metachromatic leukodystrophy (MLD) disease. MLD is caused by the deficiency of either ASA or its activator protein, saposin B (Ohashi et al., 1995; Henseler et al., 1996). In MLD patients, SGC is accumulated intralysosomally in oligodendrocytes (cells that form the myelin sheath for the axon insulation), thus causing a progressive loss of the myelin leading to various neurological symptoms (Kolodny and Fluharty, 1995). ASA null mice were created as an animal model of human MLD, and accumulation of SGC in the brain of these mice was observed, although the MLD phenotype is very mild (Hess et al., 1996; Ramakrishnan et al., 2007; Eckhardt et al., 2007). In vitro, both SGC and SGG can be desulfated by ASA, provided that the sulfoglycolipids are presolubilized by saposin B (a "physiological detergent") or other compatible detergents to become micelles (Ahn et al., 2003; Fluharty and Edmond, 1978; Louis and Fluharty, 1991; Schenk et al., 2009). However, direct evidence is lacking in terms of whether SGG is accumulated in the ASA null testes. Accumulation of SGG was observed in testes of mice deficient in prosaposin, the

precursor of saposin B (Tadano-Aritomi et al., 2003). Histochemical staining of ASA null testis sections with alcian blue (which stains polysulfated materials) and OsO_4 (which stains lipids) have revealed osmiophilic inclusions and occasionally alcianophilic inclusions in Sertoli cells, suggesting that SGG might be accumulated in these cells (Schott et al., 2001). Supporting to this speculation is the presence of ASA and prosaposin (aka SGP1, the precursor of saposin B) in Sertoli cells, as shown in immunolocalization studies on testis sections. Specifically, both ASA and prosaposin are present in the lysosomes of Sertoli cells (Moviglia et al., 1982; Morales et al., 1998; Weerachatyanukul et al., 2003). After fusion of lysosomes with residual bodies to form late residual bodies (Weerachatyanukul et al., 2003), ASA may be involved in the degradation of membrane SGG from residual bodies, which are phagocytosed by Sertoli cells from differentiating spermatids.

An alternative degradation pathway for SGG was also described (Reiter et al., 1976) (Figure 1.7 III). In this case, SGG can be degraded by a lipase isolated from the secondary lysosomes of rat liver, resulting in deacylation to form lyso-SGG (Reiter et al., 1976). Presumably, lyso-SGG can be further desulfated by ASA. If this is the case, lyso-SGG is expected to be accumulated in testes of mice deficient for ASA. However, we have never observed lyso-SGG in lipid samples prepared from ASA null testes by high performance thin layer chromatography (HPTLC) or electrospray-ionization mass spectrometry (ESI-MS). Presumably, this pathway does not exist in male germ cells.

Recently, Zeng et al. (Zeng et al., 2008) explored the biochemical changes in cultured neuroblastoma cells and primary neurons upon administration of exogenous SGC. They found that SGC and its break-down products, ceramide and sphingosine

were accumulated in these cells in a time- and dose-dependent manner. SGC was predominantly accumulated in lysosomes, whereas most of ceramide was accumulated in the endosomal compartment. A beta-galactosidase activity, which can directly hydrolyse sulfatide to ceramide without a prior desulfation step, was found to be responsible for the ceramide generation (Figure 1.7 II). The accumulation of these molecules was accompanied by substantial cell apoptosis. These results not only provided yet another novel SGC degradation pathway, but also demonstrated that abnormal sulfatide metabolism can induce cell apoptosis due to endosome-mediated ceramide generation and the accumulation of cytotoxic levels of sulfatides in lysosomes (Zeng et al., 2008). It still remains to be examined whether or not the same degradation pathway for SGG exists in the testis, and whether the parallel breakdown product of SGG, palmitylpalmitoylglycerol, would have similar proapoptotic effect as ceramide.

1.7.2. Cellular Localization of SGG in Mammalian Male Germ Cells

Indirect immunofluorescence (IIF) of frozen rat testis sections and loose spermatogenic cells reveals SGG presence in pachytene spermatocytes and spermatids, but not in spermatogonia and Sertoli cells (Lingwood, 1981). Zhang et al., (2005) has recently demonstrated by immunofluorescence that SGG synthesis in the mouse testis starts as early as on postnatal day 8 when Type B spermatogonia emerge. SGG is also localized to the rat epididymal sperm head (Lingwood, 1986), to the convex ridge of mature mouse sperm head surface (White et al., 2000), and to the anterior plasma membrane of ejaculated human sperm (Weerachatyanukul et al., 2001) and pig sperm (Bou et al., 2006). All of these sites on sperm are involved in sperm binding to the ZP (Yanagimachi, 1994; Chen and Cardullo, 1994; Kerr et al., 2002). Corroborating results

from these imaging studies, biochemical studies also demonstrate the presence of SGG in isolated head anterior plasma membranes of pig, bull, stallion, and rooster sperm (Parks and Lynch, 1992). Furthermore, SGG has been shown to be enriched in isolated lipid rafts from capacitated pig sperm, which have ZP affinity (Bou et al., 2006). Since the last step of SGG biosynthesis is believed to take place in Golgi bodies (Kornblatt et al., 1974; Letts et al., 1978; Kornblatt, 1979; Lingwood and Taylor, 1985), from which the acrosome is originated, it is possible that SGG may also be localized in the acrosome.

1.7.3. Role of SGG in Spermatogenesis

The significance of SGG in spermatogenesis is evidenced by spermatogenesis arrest in SGG-depleted mice, genetically null in either of the two enzymes in the SGG biosynthetic pathway (Figure 1.6 B), i.e., ceramide galactosyltransferase (*Cgt)* (Fujimoto et al., 2000) and cerebroside sulfotransferase (*Cst*) (Honke et al., 2002). These mice do not produce sperm and are thus infertile. Spermatogenesis in *Cst* $^{-/-}$ mice is blocked at the end of the meiotic prophase (Honke et al., 2002), somewhat later than that in *Cgt* $^{-/-}$ mice, in which spermatogenesis is arrested at the late pachytene stage (Fujimoto et al., 2000). These results suggest that GG and SGG are successively involved in spermatogenesis in the same sequence as their involvement in SGG biosynthesis. However, despite the fact that GG is accumulated in the testes of the *Cst* $^{-/-}$ mice, this GG cannot rescue spermatogenesis. In fact, the arrested primary spermatocytes undergo apoptosis (Fujimoto et al., 2000; Honke et al., 2002). These findings implicate an important role for SGG in spermatogenesis and cell survival. However, spermatogonia and Sertoli cells (the cells that do not contain SGG on their surface) in these mutant mice are not affected (Fujimoto et al., 2000; Honke et al., 2002). When wild-type

spermatogonia were introduced into the seminiferous tubules of *Cst* $^{-/-}$ testes, spermatogenesis could proceed at a normal rate (Zhang et al., 2005). How SGG is involved in this process still remains to be determined. It is known that interactions between layers of developing germ cells, and those of germ cells with Sertoli cells in the seminiferous tubules are important for the progress of spermatogenesis (Sharpe, 1994; Jegou, 1993). Since SGG is expressed on the cell surface of male germs cells throughout various developmental stages, starting from the end of the leptotene or zygotene stage of primary spermatocytes (Ishizuka, 1997; Vos et al., 1994; Fujimoto et al., 2000), and since L-selectin with affinity for sulfoglycolipids (Suzuki et al., 1993; Brockhausen and Kuhns, 1997) is present on the Sertoli cell surface (Freeman et al., 2002), the interaction between L-selectin and SGG may serve as a basis of how Sertoli cells and spermatocytes associate with each other. This communication in turn is important for the progress of spermatogenesis (Jegou, 1993).

1.7.4. Role of SGG in Sperm-Egg Interaction

In vitro gamete binding assays revealed that sperm surface SGG was involved in sperm-ZP (White et al., 2000; Weerachatyanukul et al., 2001) and sperm-egg plasma membrane binding events (Ahnonkitpanit et al., 1999). Corroborating these results is the enrichment of SGG in Percoll-gradient centrifuged (PGC) sperm, having high ZP affinity (Furimsky et al., 2005). Furthermore, lipid rafts isolated from capacitated pig sperm bound to pig ZP with higher affinity and capacity (Bou Khalil et al., 2006). SGG was enriched in the isolated sperm lipid rafts and contributed not only to the ZP binding but also to lipid raft formation (Bou Khalil et al., 2006). The significance of SGG in human

fertility is further evidenced by the observation that a subset of infertile women has high titers of anti-SGG antibodies in their serum (Tsuji et al., 1992).

Our findings are in concert with observations that SGG and SGC are engaged in other cell-cell/extracellular protein adhesion (Brockhausen and Kuhns, 1997; Flesch and Gadella, 2000), including their binding to laminin, L-selectin, gp120, mycoplasmas and HIV-1 (Flesch and Gadella, 2000; Ishizuka, 1997; Brockhausen and Kuhns, 1997). Carbohydrate-carbohydrate interaction is known to be a mechanism through which glycosphingolipids participate in cell adhesion including trout sperm-egg interaction (Hakomori, 2000; Iwabuchi et al., 1998; Song et al., 1998; Wang et al., 2001; Yu et al., 2002; Zheng and Hakomori, 2000) and through which galactosylceramide and SGC interact with each other (Boggs et al., 2000; Koshy et al., 1999). The galactosyl sulfate moiety of SGG may likewise interact with the ZP glycans. This type of interaction, although weaker than protein-protein/carbohydrate interaction, can be stabilized by the multiplicity of SGG molecules on the sperm plasma membrane.

SGG also contributes to the conformational property of the sperm plasma membrane. Our infrared spectroscopy studies indicate that SGG and SGC are ordered lipids (Tanphaichitr et al., 2003). Their saturated hydrocarbon chains allow them to pack tightly into membrane lipid bilayers. This orderedness is further enhanced by intermolecular hydrogen bonding networks between the hydroxyl groups of their galactose and ester or amide C=O groups of the adjacent molecules (Attar et al., 1998; Attar et al., 2000; Bou Khalil et al., 2001; Tupper et al., 1992, Tupper et al., 1994). SGG/SGC also interacts with other ordered lipids, i.e., saturated phospholipids (Attar et al., 1998), (Attar et al., 2000) and cholesterol (Bou Khalil et al., 2006). The interaction of

SGG with cholesterol renders the lipid complex insoluble in Triton X-100, a property in common with lipid rafts (see below).

1.7.5. Sperm Lipid Rafts in Mediating Gamete Interaction

With the large number of ZP binding molecules identified on sperm, it is apparent now that sperm-egg binding is mediated by multiple receptors and their corresponding ligands. However, the molecular mechanism for this interaction is still elusive. It has been postulated that these sperm molecules may act cooperatively or in sequence to achieve optimal binding to the ZP. Emerging evidence has point to the role of sperm lipid rafts in orchestrating these sperm proteins for optimal ZP binding.

The biological membranes were originally envisioned by Singer and Nicholson (1972) as a homogenous sea of lipids with proteins freely diffusing in it. This concept has been challenged by recent evidence suggesting the existence of discrete lipid microdomains known as lipid rafts. Lipid rafts are liquid ordered membrane domains enriched in cholesterol, glycolipids, sphingolipids, and saturated phospholipids (Rajendran and Simons, 2005; Simons and Ehehalt, 2002). The lipid composition of rafts renders the liquid-ordered property to the raft membranes. The hydrophobic interaction between saturated hydrocarbon chains of these lipids and with the planar rings and side chains of cholesterol are the driving force for the raft formation. Hydrogen bonding between cholesterol and glycolipids (such as GM1) further stabilizes the lipid rafts. In addition, F-actin may stabilize lipid rafts on the cytoplasmic side, and organize an architecture allowing different components of the signaling machinery to interact with each other (Harder and Simons, 1999). This results in the resistance of lipid rafts to solubilization by a number of non-ionic detergents (London and Brown, 2000; Schuck et

al., 2003; Shogomori and Brown, 2003) and they are referred to as detergent resistant membranes (DRM). Due to high lipids to proteins ratio, lipid rafts have low buoyant density, allowing them to float up on density gradients.

In addition to their characteristic lipid composition, lipid rafts are also enriched in cell adhesion, signaling and trafficking molecules (Foster et al., 2003; Iwabuchi et al., 1998; Nguyen et al., 2006; Delacour et al., 2005; Iwabuchi et al., 1998; Galbiati et al., 2001; Hakomori and Handa, 2003), suggesting that they may be involved in cell-cell/matrix adhesion, cell signaling as well as intracellular sorting and trafficking of lipid-protein assembly (Rajendran and Simons, 2005; Simons and Ehehalt, 2002). Recently, SGC and SGG have been shown to exist in isolated sea urchin and pig sperm lipid rafts, respectively (Ohta et al., 2000b; Ohta et al., 2000a; Bou Khalil et al., 2006). Sea urchin sperm lipid rafts have been shown to have affinity for a sperm binding protein present in egg vitelline layer (Maehashi et al., 2003). SGC and highly acidic sulfated and non-sulfated poly-sialic acid containing glycolipids in the isolated lipid rafts are involved in the interaction (Maehashi et al., 2003). Significantly, we have shown that isolated pig sperm lipid rafts bound to solubilized pig ZP with mechanisms similar to those used by intact pig sperm or isolated sperm anterior head plasma membranes (Bou Khalil et al., 2006). Notably, capacitated sperm lipid rafts have higher affinity and capacity to bind to the ZP, compared with those of control sperm (Bou Khalil et al., 2006). Interestingly, the majority of SGG (70% of the total amount) exists in capacitated sperm lipid raft microdomains, along with cholesterol and saturated phospholipids with which SGG interacts (Bou et al., 2006). Besides SGG, its binding protein arylsulfatase A also exists in sperm rafts (Tanphaichitr et al., 2007a; Tanphaichitr et al., 2007c; Nixon et al., 2009).

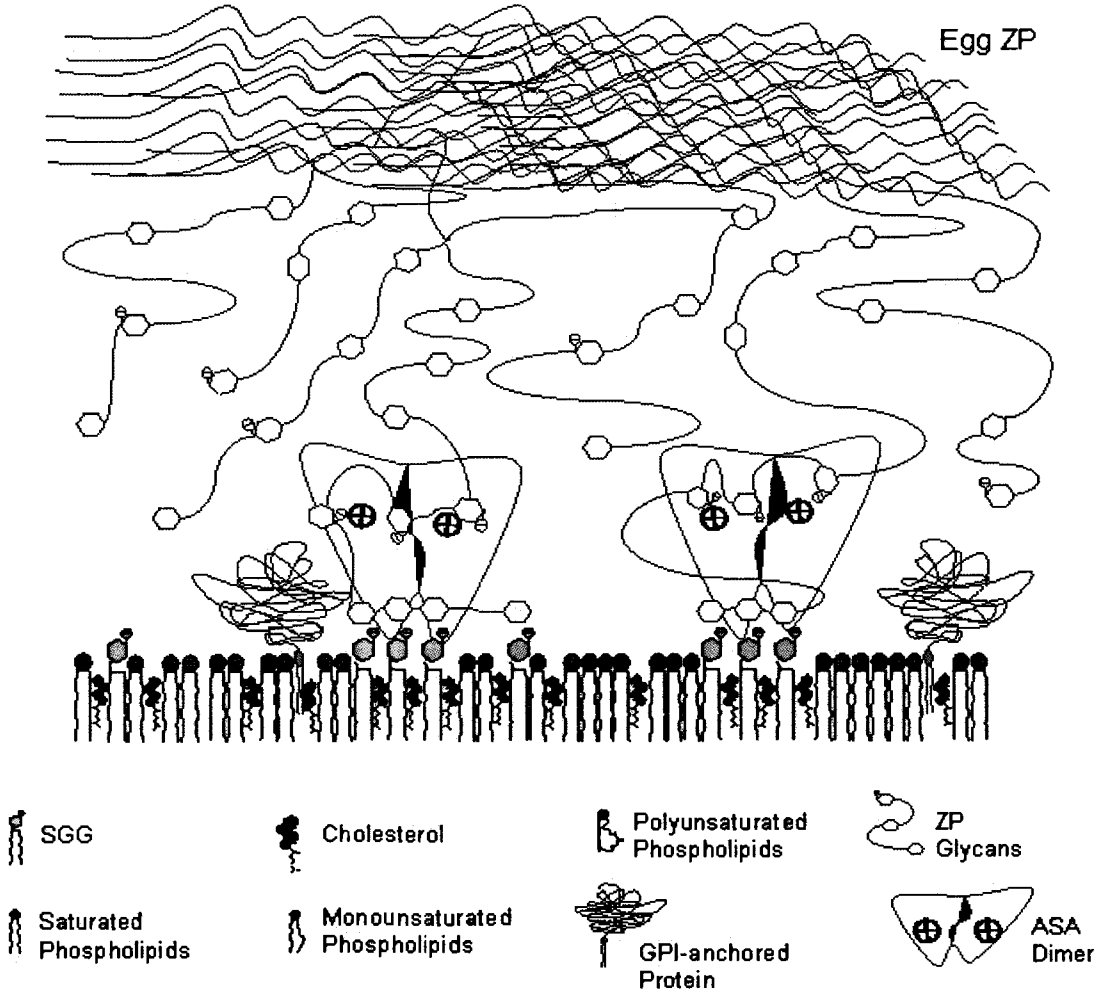
Egg ZP
SGG
Cholesterol
Polyunsaturated Phospholipids
ZP Glycans
Saturated Phospholipids
Monounsaturated Phospholipids
GPI-anchored Protein
ASA Dimer

Figure 1.8. Hypothetical model of how sperm surface ASA and SGG cooperate in binding to the ZP glycans. The ZP glycans likely interact with the galactosyl sulfate moiety of SGG. However, since this monosaccharide head group would rise only a short distance above the sperm membrane bilayer, it would be difficult for the ZP glycans to reach this head group without additional anchoring force. ASA, a peripheral plasma membrane protein which exists as a dimeric at physiological pH, has affinity for both SGG and the ZP. ASA may first bind to the ZP glycans (possibly via interaction between positively charged amino acids of ASA and sulfated sugar residues of the glycans) and attract them to the sperm plasma membrane for the interaction with the galactosyl sulfate lawn of SGG molecules. Although the carbohydrate–carbohydrate interactions between the galactosyl sulfate groups of SGG and ZP glycans are not strong, they may be stabilized by the multiplicity of SGG molecules on the sperm surface (in the lipid raft microdomains).

All of these results strongly suggest that sperm lipid rafts are ZP binding microdomains and SGG may contribute to sperm raft formation as well as to the raft function in ZP binding (Bou Khalil et al., 2006).

SGG is thought to interact with the sugar moieties of the ZP glycoproteins through its sulfated galactose residue via electrostatic interactions. However, since the sulfated galactosyl group of SGG molecules rise only a short distance above the sperm plasma membrane, its role in ZP binding is likely facilitated by one of its binding proteins ASA, also a raft-associated protein with affinity for the ZP (Carmona et al., 2002a; Carmona et al., 2002b; Tantibhedhyangkul et al., 2002). We propose that ASA is engaged in capturing the ZP glycans via interactions between its positively charged amino acid residues and sulfated sugar residues of the ZP glycans, thus allowing subsequent carbohydrate-carbohydrate interactions with SGG head groups (Bou Khalil et al., 2006) (Figure 1.8).

In addition to ASA and SGG (Bou Khalil et al., 2006; Nixon et al., 2009), a number of other ZP binding molecules have been found in isolated sperm lipid rafts, including PH-20 (Nixon et al., 2009), basigin, IZUMO, CRISP1 (Sleight et al., 2005; Nixon et al., 2009), TESP1 (Sleight et al., 2005), GalT, Adam1b, Sp56, SED1, mannosidase 2, and Ace (Angiotensin converting enzyme) (Nixon et al., 2009). Interestingly, several molecular chaperone proteins, including Hsp90b1 (aka, endoplasmin) and Hspd 1 (aka, Hsp60), have also been identified in lipid rafts isolated from capacitated sperm (Nixon et al., 2009). It is likely that these chaperone proteins are recruited to the lipid rafts during sperm capacitation (Asquith et al., 2004; Asquith et al.,

2005) to serve as a scaffold to further recruit other ZP binding proteins and to properly organize them into a functional ZP binding complex.

Taken together, the capacitation-dependent changes in the sperm lipid raft composition and the acquisition of higher ZP affinity provide compelling evidence that lipid rafts are platforms of sperm functional ZP binding complexes.

1.8. Properties of Arylsulfatase A and its Roles in Sperm-Egg Interactions

SGG binding protein(s) was first described by Cliff Lingwood (Hosptial for Sick Children, Toronto, Canada) and named sulfolipid immobilizing protein 1 (SLIP1) (Lingwood, 1985b). It was first isolated from a rat testis homogenate and was one of the fractions that remained bound to the SGG matrix following SGG affinity column chromatography (Lingwood, 1985b). This purified SLIP1 had an apparent molecular mass of 68 kDa on SDS-PAGE and it was used to generate a rabbit polyclonal antibody (Lingwood, 1986). Using this antibody in indirect immunofluorescence, SLIP1 was colocalized with SGG in spermatogenic cells and sperm (Lingwood, 1986; Tanphaichitr et al., 1993). Purified SLIP1 exhibits affinity to SGG (Law et al., 1988; Lingwood and Nutikka, 1991) and to the ZP of intact eggs (Tanphaichitr et al., 1993). Further characterization of purified SLIP1 reveals that it consists of three proteins, a ZP binding component, heat shock protein 70 (Hsp70), and albumin (Tanphaichitr et al., 1998a; Tanphaichitr et al., 1998b; Tanphaichitr et al., 1999; Carmona et al., 2002a; Boulanger et al., 1995). The ZP binding component of SLIP1 was initially termed P68, and it was further identified as ASA by molecular cloning approach (Carmona et al., 2002a).

Arylsulfatase A (ASA; EC 3.1.6.8) is known as a lysosomal/acrosomal enzyme, belonging to a highly conserved sulfatase family of enzymes that cleave sulfate esters from a wide variety of substrates, including sulfolipids, sulfated sugar, tyrosine sulfate and ascorbic sulfate (Mehl and Jatzkewitz, 1968; Waheed and Van Etten, 1980; Rahi and Srivastava, 1983; Fluharty et al., 1979; Stevens et al., 1976). ASA is required to catalyze the first step in the degradation pathway of the sphingolipid sulfatide (SGC; galactosyl-3-sulfate cerebroside) in myelin, as well as the male germ cell specific seminolipid (SGG; galactosyl-3-sulfate glycerol) in the testis (Figure 1.7 I), and its physiological significance in the brain has been well documented (Kolodny and Fluharty, 1995; Hess et al., 1996; Ramakrishnan et al., 2007; Eckhardt et al., 2007; Gieselmann, 2003; Hanson et al., 2004). The activity of ASA requires the posttranslational modification of the active site pocket amino acid residue Cys into 2-amino-3-oxopropanoic acid [α-formylglycine (FGly)] (Dierks et al., 1997; Schmidt et al., 1995).

In an acidic environment at ~pH 5, ASA shows optimal catalytic activity and human ASA occurs as homo-octamer, whereas at neutral and alkaline pH it exists as a homodimer (Nichol and Roy, 1965). Octomerization from dimers depend on hydrophobic interaction and hydrogen bonding between dimers, as well as 2 x 7 water molecules in the interaction areas (Lukatela et al., 1998).

From the crystal structure of ASA (Von Bulow et al., 2001; Lukatela et al., 1998) and our structural modeling studies (Schenk et al., 2009), the active site pocket of ASA allows the fitting of only one molecule of SGC or SGG (Figure 1.9 B). Hence, a small aqueous soluble sulfated molecule, *p*-nitrocatechol sulfate (NCS), that can freely enter ASA's active site pocket is routinely used as an artificial substrate of ASA for

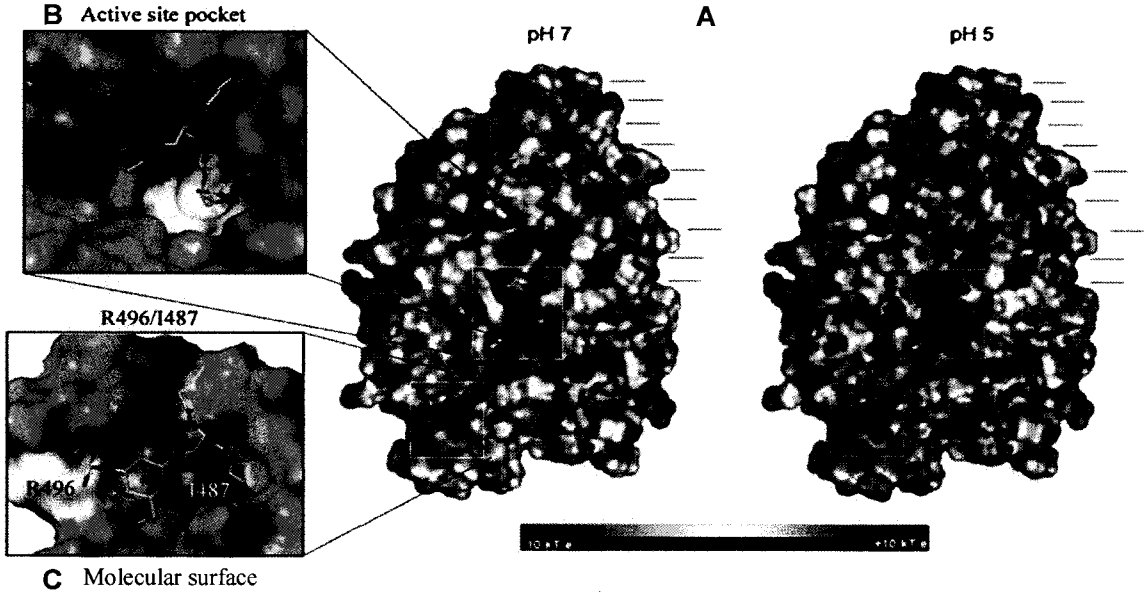
B Active site pocket
A
pH 7
pH 5
R496/I487
R496
I487
C Molecular surface

Figure 1.9. Electrostatic surface of ASA at pH 7 and pH 5 (A) and computational docking of SGG to the active site (B) and molecular surface (C) of ASA. (**A**) The electrostatic potential of ASA was calculated at pH 7 and 5 based on the pK_a values of individual amino acids in the area; however, these pK_a values were calculated with the consideration of the influence of neighboring residues (Schenk et al., 2009). The surfaces are displayed with negative and positive potential values in red (negative) and blue (positive), respectively (in energy units of kT/e). ASA is more positively charged at pH 5, as expected. In particular, the active site (surrounded by a big white box) is significantly more positive at pH 5. At pH 7, the active site pocket is less positively charged. These results suggest that electrostatic interactions play a crucial role in substrate binding. At both pH values, there is a molecular surface (indicated with a small box) with the second highest positive charge. (**B**) SGG docked into the ASA active site with the lowest energy. (**C**) SGG also docked, with the second lowest energy, at the molecular surface of ASA, interacting with amino acid residues Arg496 & Ile487.

activity assay (Schenk et al., 2009). In the active site pocket, C69 is the active site amino acid and K302 and K123 are important for capturing the sulfate group of the substrate for the hydrolysis, which occurs at the optimum pH of 5 (Schenk et al., 2009; Von Bulow et al., 2001). The electrostatic potential of the molecular surface of ASA at pH 7 and 5 has recently been illustrated by us through computation biology using pK_a values of amino acids, calculated with consideration of influences of surrounding amino acid residues (Schenk et al., 2009). ASA is more positively charged at pH 5 than at pH 7, especially the active site (Figure 1.9 A), suggesting that electrostatic interaction plays a crucial role in substrate binding. At both pH values, there exists a surface cleft area, formed around Arg 496 and Ile 487, with positive electrical potential second to the active site pocket; SGG's sulfated galactose head group docks with low energy into this ASA cleft (Figure 1.9 C). This suggests that the surface cleft of ASA may be involved in electrostatic interaction with negatively charged molecules (e.g., SGG and sulfated ZP glycans).

In mammalian sperm, ASA is localized in the acrosome, which is de novo synthesized in primary spermatocytes (Kreysing et al., 1994b). As part of this thesis, ASA is also shown to be present on the sperm head surface, the site involved in ZP binding (Carmona et al., 2002a; Tantibhedhyangkul et al., 2002; Weerachatyanukul et al., 2003). Indeed, sperm surface ASA has direct affinity for both mouse and pig ZP, and treatment of mouse and pig sperm with anti-ASA IgG specifically inhibits homologous sperm-ZP binding (Carmona et al., 2002a; Tantibhedhyangkul et al., 2002). These results suggest that the sperm surface ASA is involved in the primary sperm-ZP binding. Unlike sperm surface ASA, functions of the acrosomal ASA are largely unexplored. We propose that it may be involved in the secondary binding of acrosome-reacting/reacted

sperm to the ZP. The acrosomal ASA may also desulfate ZP glycans, thus the secondary sperm-ZP adhesion could depend on repetitive binding and hydrolysis of the sulfated ZP glycans. Such a mechanism would allow acrosome-reacted sperm remain attached to the ZP, and at the same time releases focal adhesion and facilitates sperm penetration through the ZP matrix. In support of this hypothesis, prosaposin is present in the male and female reproductive tracts and seminal plasma (Hermo et al., 1992a; Hiraiwa et al., 1993). Saposin B can be generated from prosaposin by treatment with purified cathepsin D (Hiraiwa et al., 1997), the enzyme known to be present in the acrosome (Tulsiani et al., 1998b). Therefore, it is possible that cathepsin D released from the acrosome during the acrosome reaction may be able to process prosaposin to saposin B, which in turn activates the desulfation activity of ASA.

One interesting aspect of the roles of sperm ASA in fertilization is that it is not only a ZP adhesion molecule, but also an active enzyme. Much is known about ASA being an adhesion molecules, but little has been learned about the involvement of its enzymatic activity in fertilization. In this regard, several sperm enzymes have been described as ZP adhesion molecules. Some of the sperm enzymes use the active site pocket to bind to the substrates present on the ZP glycans, and the completion of the reaction is at a slow rate so that sperm are transiently anchored to the ZP. Such enzymes may include *N*-acetylglucosaminidase (Zitta et al., 2006), β-1,4-galactosyltransferase (Miller et al., 1992), α-D-mannosidase (Cornwall et al., 1991) and P26h (Montfort et al., 2002). Other sperm enzymes use domains distinctive from their active site pocket to bind to the ZP glycans. PH-20 (Hunnicutt et al., 1996), proacrosin/acrosin (Francavilla et al., 1994; Howes and Jones, 2002) and gluthathione S-transferase (GST) (Hemachand et al.,

2002; Aravinda et al., 1995; Gopalakrishnan et al., 1998) may belong to the second category. In the case of ASA, the physiological pH of 7 is distinctively different from the optimum pH of the enzymatic activity (Hanson et al., 2004). However, once sperm bind to the ZP, the ZP sulfoglycans can provide an acidic microenvironment, and this may allow the enzyme to exert its catalytic activity. The digestion of the sulfate group from the sulfated sugar residues of the ZP glycans would allow sperm to topically disengage from the ZP matrix and move forward to the next site for the subsequent round of the binding. The ability of the cells to make multifunctional proteins is of fundamental importance to the course of evolution. As sperm are terminally differentiated and transcriptionally inactive, the ability of sperm enzymes to also serve as adhesion molecules might reflect the unusual demands sperm meet in different parts of the reproductive tract *en route* to the egg. It is possible that the two functions of these enzymes – as an adhesion molecule and as a hydrolytic enzyme are separated by the window of time, or under different environment/condidtions. The elucidation of dual functions of enzymes in sperm may open interesting prospects for future studies into the mechanisms of infertility. Defects in either ZP-binding capacity or the catalytic function of these molecules may be responsible for certain forms of infertility.

1.9. Research Hypotheses and Objectives

The following specific aims were undertaken to verify our hypothesis.

(**a**) To determine the direct binding of purified sperm ASA to purified individual mouse ZP sulfoglycoproteins by immuno-dot blotting (hypothesis and rationale: ASA is involved in both primary and secondary ZP binding; the identity of the mouse ZP

glycoprotein for which ASA has affinity would implicate in which ZP binding step ASA is engaged).

(**b**) To determine the ability of recombinant mutant ASA (with active site mutated or both active site and substrate binding site mutated) to bind to individual mouse ZP sulfoglycoproteins using the same technique (hypothesis and rationale: the active site pocket of ASA is involved in binding to the ZP sulfoglycoproteins; sperm surface ASA is enzymatically active)

(**c**) To determine whether ASA-ZP sulfoglycoprotein binding is dependent on the ZP sulfated sugar moieties (hypothesis and rationale: ASA utilizes its active site pocket or positively charged molecular surface to interact with sulfated sugar residues of the ZP glycans; sulfated sugars have been shown to be ASA's substrates, and sulfated glycans (e.g., fucoidan) exhibit inhibitory effects on sperm-egg interaction).

(**d**) To characterize the mechanism of how ASA is transferred to the sperm plasma membrane (hypothesis and rationale: ASA is present in the epididymal fluid and is adsorbed onto the sperm surface during epididymal transit; ASA has high affinity for SGG).

(**e**) To examine the fertility and spermatogenesis status in *ASA* null male mice (hypothesis and rationale: sperm ASA is important for male fecundity; ASA has been previously shown to play roles in sperm-egg interaction in vitro.

(**f**) To determine the SGG amounts as well as the lipid profiles of *ASA* null mouse sperm and testes in relation to the fertility and spermatogenesis status of the mutant mice (hypothesis and rationale: testicular and sperm SGG is a substrate of ASA in vivo and the

SGG level is integratively well controlled; deficiency of ASA may lead to changes of SGG in vivo).

CHAPTER TWO

MATERIALS AND METHODS

2.1. Materials

DRAQ5 was purchased from Biostatus ltd. (Shepshed, Leicestershire, UK). Bovine testicular hyanuronidase was purchase from ICN Biochemicals (Costa mesa, CA, USA). Collagenase was from Worthington biochemical company (Lakewood, NJ, USA). Trypsin, Gibco OptiMEM-I medium, Dulbecco's Modified Eagle Medium (D-MEM) and lipofectamine reagent were from Invitrogen (Burlington, ON, Canada). DNase I was from Boehrinnger Mannheim (Burlington, ON, Canada). Trizol reagent was purchase from Gibco BRL (Burlington, ON, Canada). RETROscript First-Strand Synthesis Kit was from Ambion (Austin, TX, USA). The enhanced chemiluminescence (ECL) Western blotting detection kit was obtained from Amersham Pharmacia Biotech (Piscataway, NJ, USA). Mouse monoclonal anti-SGC IgM (O4) antibody was purchased from Neuromics (Edina, MN, U.S.A.). Sodium chloride, acetic acid, acetone, $CHCl_3$, MeOH, and heptane were purchased from BDH (Toronto, ON, Canada). Acetone, $CHCl_3$, and MeOH were glass distilled before use (Kates, 1986). Paraformaldehyde was purchased from Polysciences Inc. (Warrington, PA, USA). Quick-Seal centrifuge tubes (16 x 76 mm) and Ultra-clear™ ultracentrifuge tubes (14 x 95 mm) were obtained from Beckman (Palo Alto, CA, USA). Bio-Rad protein assay dye reagent concentrate, Coomassie brilliant blue G-250, goat anti-rabbit IgG conjugated with horseradish peroxidase (HRP), nitrocellulose membranes (0.45 μm), sodium dodecyl sulfate (SDS), tris(hydroxymethyl)-aminomethane (Tris) and Triton X-100 were purchased from Bio-

Rad Laboratories (Hercules, CA, USA). Pig ovarian ZP was purchased from Calbiochem (San Diego, CA, USA). Anhydrous EtOH was bought from Commercial Alcohols (Brampton, ON, Canada). Polystyrene 96-well flat-bottom black (CS003915) and clear (CS003370) microtiter plates were obtained from Corning (New York, NY, USA). Palmitoylsulfatide (C16) was purchased from Avanti Polar Lipids (Alabaster, AL, USA). Phospholipid and neutral lipid standards (PC, PE, sphingomyelin, cholesterol, and DAG) were purchased from Doosan Serdary Research Laboratories (Englewood Cliffs, NJ, USA). Microcons were purchased from Millipore (Bedford, MA, USA). Merocyanine (MC540), calcein-AM, Amplex™ Red, Alexa-488 goat anti-rabbit IgG, Alexa-488 goat anti-mouse IgM, Alexa-595 goat anti-rabbit IgG and propidium iodide (PI) were purchased from Molecular Probes (Eugene, OR, USA). Immuno Pure Immobilized Protein A Affinity Pak Column and Aminolink beads were purchased from Pierce (Rockford, IL, USA). Bouin's solution, bovine brain SGC (containing both α-hydroxylated and non-hydroxylated fatty acids; major cations were 1.72% Na^+, 1.07% Ca^{2+}), and GC (HFA-GC and NFA-GC containing 98% α-hydroxylated and non-hydroxylated fatty acids, respectively), bovine serum albumin (BSA, essentially fatty acid free), BSA (cold ethanol precipitated, fraction V), calcium chloride, cholesterol, cholesterol oxidase, dihydrostreptomycin, dimethyl-sulfoxide (DMSO), ethylenediaminetetracetic acid (EDTA), glucose, Hepes, H_2O_2, (horseradish peroxidase) HRP, ovalbumin, potassium chloride, magnesium chloride, Nα-p-tosyl-L-lysine chloromethyl ketone (TLCK), *o*-phenylenediamine dihydrochloride (OPD), orcinol, potassium phosphate, pyruvic acid, sodium bicarbonate, sodium carbonate, sodium citrate, sodium hydroxyde, sodium phosphate, soybean trypsin inhbitor (SBTI),

triethanolamine, deoxycholate, sucrose, and Pregnant mare's serum gonadotropin (PMSG) and human chorionic gonadotropin (hCG) were purchased from Sigma (St. Louis, MO, USA). HPK silica gel high performance thin layer chromatography (HPTLC) plates (60 Å, 10 μm pore size, 200 μm thickness, 10 x 10 cm), and K6 silica gel TLC plates (60 Å, 10 μm pore size, 250 μm thickness, 20 x 20 cm) were obtained from Whatman (Clifton, NJ, USA). Percoll was purchased from GE Healthcare (Uppsala, Sweden). Vectastain ABC Elite kit was purchased from Vector Laboratories (Burlingame, CA). TUNEL Enzyme and TUNEL Label Mix and protease inhibitors cocktail were purchased from Roche (Roche Diagnostics, Mannheim, Germany).

2.2. Animals

Sexually mature CF-1 female mice (6 – 8 weeks of age) and CD-1 male mice (~10 weeks of age) were purchased from Charles Rivers (Montreal, Quebec). C57BL/6J (B6) male and female mice, either WT (+/+) or null congenics (-/-) for the *Asa* allele were given to us by Dr. T. Tupar (University of Western Ontario), and the colonies were maintained in our institutional animal facility. They were housed in temperature and humidity controlled rooms with 14L:10D cycles and were provided with food and drink ad libitum. Mice were handled according to the guidelines of the Canadian Council on Animal Care.

2.3. Gamete and Reproductive Tract Fluid Preparation

2.3.1 Cauda Epididymal and Vas Deferens Sperm Preparation

The cauda epididymides were longitudinally scored once with a surgical blade and the dense sperm masses squeezed out from this incision and that from the vas deferens were placed at the bottom of a 1.5-ml micro centrifuge tube containing 500 µl of Krebs Ringers bicarbonate (KRB) supplemented with 0.3% BSA (KRB-BSA) (KRB: 119.4 mM NaCl, 4.8 mM KCl, 1.7 mM $CaCl_2$, 1.2 mM KH_2PO_4, 1.2 mM Mg_2SO_4, 25 mM $NaHCO_3$, 25 mM sodium lactate, 1 mM sodium pyruvate, 5.6 mM glucose, 2.8 µM phenol red, pH 7.4). The tube was then filled up to 1 ml slowly with the same medium and the sperm were allowed to swim up into the medium for 30 min at 37°C. The supernatant containing actively motile sperm (600 – 800 µl) was then transferred to pre-warmed new tubes. An aliquot of appropriately diluted (10-20 X) sperm suspension was placed onto a hemocytometer, and the numbers of total sperm and motile sperm were immediately counted under a Nikon inverted microscope (DIAPHOT-TMD, Nikon Canada, Mississauga, ON) at 200 X magnification. The number of sperm (mostly immotile) in the leftover medium (200-400 µl) was also counted in order to calculate the total number of sperm and the percentage of motile sperm.

To prepare Percoll-gradient centrifuged (PGC) capacitated sperm, the sperm suspension, collected as described above, was diluted to 2 ml with HEPES-buffered Krebs Ringers bicarbonate (KRB-HEPES) medium (KRB-HEPES: 119.4 mM NaCl, 4.8 mM KCl, 1.7 mM $CaCl_2$, 1.2 mM KH_2PO_4, 1.2 mM Mg_2SO_4, 21 mM HEPES, 5 mM $NaHCO_3$, 25 mM sodium lactate, 1 mM sodium pyruvate, 5.6 mM glucose, 2.8 µM phenol red, pH 7.4), and loaded onto a two-step Percoll gradient (45% and 90% Percoll (Amersham Biosciences, Uppsala, Sweden) in KRB-HEPES) (Tanphaichitr et al., 1990). The gradient was centrifuged (650 x *g*, 25°C for 30 min), allowing motile sperm to

sediment as a pellet and immotile sperm to interface between the two Percoll layers. After removing the interfaced immotile sperm and most of the Percoll solution, the pelleted motile sperm was washed once in KRB-0.3% BSA (350 x *g*, 28°C for 10 min), and then allowed to capacitate in the same medium (37°C, 5% CO_2 for 30 min) at a concentration of approximately 10 x 10^6 sperm/ml.

2.3.2. Collection of Sperm from the Testis, Caput and Corpus Epididymis

To collect testicular sperm, decapsulated testes were first minced into 1- to 2-mm pieces in KRB-HEPES-BSA containing 1 mg/ml DNaseI (Sigma, St. Louis, MO) and protease inhibitor cocktail (PIC; Roche Diagnostics, Mannheim, Germany). Large fragments and clumps of Leydig and Sertoli cells were pelleted (30 x *g*, 25°C, 5 min). The supernatant (2 ml), containing loose testicular cells, testicular sperm, and red blood cells, was layered on top of a 2-ml 45% Percoll solution in KRB-HEPES. The tube was centrifuged (600 x *g*, 25°C, 5 min) to pellet red blood cells, which were then carefully removed using a Prot/Elec Pipet Tip (BioRad Laboratories, Hercules, CA) without disturbing the testicular cells and testicular sperm that were sedimented at the interface between the loaded medium and the 45% Percoll solution. The tube was further centrifuged (1000 x *g*, 25°C, 30 min) to selectively pellet testicular sperm. After removing the top fluid layers, the pelleted testicular sperm were washed (350 x *g*, 25°C, 10 min) once in KRB-HEPES and resuspended in KRB-HEPES-BSA for IIF and flow cytometry analysis.

To collect caput and corpus epididymal sperm, the caput and corpus epididymis was cut once longitudinally and then immersed in KRB-BSA. Caput and corpus epididymal sperm were allowed to swim out into the medium by incubating the tissue at

37°C with gentle shaking for 15 min. At the end of the incubation, the tissue was removed from the tube, and the cell suspension was centrifuged at 45 x *g* to pellet red blood cells, tissue debris, and cell aggregates. The supernatant containing mainly caput and corpus epididymal sperm was transferred into a new tube and centrifuged at 350 x *g* for 10 min. The pelleted caput and corpus epididymal sperm were washed once in KRB-BSA by centrifugation (350 x *g*, 10 min) and subject to indirect immunofluorescence (IIF) and flow cytometry.

2.3.3. Preparation of Testicular Germ Cell Mixture

Testicular germ cell mixture was prepared by sequential enzymatic digestion of seminiferous tubules with collagenase and trypsin. Decapsulated testes were first digested with 0.5 mg/ml collagenase in Dulbecco's Modified Eagle Medium (D-MEM, Invitrogen) at 33°C for 15 min with constant shaking at 100 cycles per minute. At the end of the incubation, the dissociated tubules were allowed to sediment by gravity and washed 3 times with D-MEM. During each of the washing steps, the tubules were allowed to settle by gravity and supernatant was decanted. The tubules were further digested with 0.5 mg/ml trypsin in D-MEM supplemented with 1 μg/ml of DNase I at 33°C for 15 min with constant shaking at 130 cycles per minute. During the collagenase and trypsin treatments, 5% CO_2 was directed into the tubes via a large (18 G) needle. At the conclusion of trypsin digestion, trypsin soybean inhibitor was added to the suspension to a final concentration of 0.5 mg/ml. The suspension was gently pipetted with a large bore plastic transfer pipet to break up small cell clumps and filtered through a 70 μm nylon screen. The filtered cell suspension was centrifuged at 450 x g for 8 min to collect the testicular germ cell mixture and the cells were washed 3 times with washing buffer

(0.5% BSA, 0.25 mg/ml SBTI, 0.5 μg/ml DNase I in D-MEM) by centrifugation (450 x g, 5 min).

2.3.4. Collection of Fluid from the Cauda Epididymis and Vas Deferens

Collection was made at the vas deferens by inserting PE10 polyethylene tubing sleeved over a 25-ga needle, which was attached to a 1-ml tuberculin syringe, into the tubule. Following fluid aspiration, the vas deferens tubule was washed twice with KRB-HEPES supplemented with protease inhibitors cocktail (PIC; Roche Diagnostics, Mannheim, Germany) at a dose recommended by the manufacturer (i.e., 1 tablet per 10 ml of the medium), and all washes were combined with the original fluid. To collect fluid from the cauda epididymis, the organ was longitudinally cut once with a sharp razor blade and gently squeezed with flat-end tweezers. The thick fluid that oozed from the organ was collected and mixed with KRB-HEPES-PIC. Fluid from both the vas deferens and cauda epididymis was combined and centrifuged (500 x *g*, 25°C, 10 min) to pellet sperm. The collected supernatant was further centrifuged in a Microfuge 18 (Beckman Coulter, Palo Alto, CA) (18,000 x *g*, 4°C, 10 min) to remove all sperm and particulates. The sperm-free fluid was then used for subsequent experiments.

2.3.5. Preparation of Mouse Oocytes

Female CF-1 mice, 8 weeks of age, were superovulated by intraperitoneal (IP) injection of 7.5 units of Pregnant mare's serum gonadotropin (PMSG) followed 48 h later by IP injection of 7.5 units of human chorionic gonadotropin (hCG). Cumulus masses containing mature eggs were collected 14–15 h after hCG injection from the superovulated female mice into KRB-HEPES-0.3% BSA using established procedures (Hogan et al., 1994). ZP–intact eggs were freed from the cumulus cells by treatment with

0.1% (wt/vol) (~1-2 min) bovine testicular hyaluronidase (300 USP units/mg; ICN) in KRB-HEPES. The cumulus-free oocytes were thoroughly rinsed with KRB-HEPES-0.3% BSA medium and kept in KRB-0.3% BSA in an incubator (37°C, 5% CO_2) before use. The eggs were usually used within one hour. Only the oocytes with disintegrated first polar bodies and good morphology were used for gamete binding assays and IVF experiments.

2.4. Gamete Functional Assays

2.41. In vitro Sperm–Egg Binding

Sperm–egg binding was determined using procedures described previously (Tanphaichitr et al., 1993). Briefly, ZP-intact eggs (n = 20–30) were incubated with 60 x 10^3 motile swim-up sperm from wild type and ASA null mice in 60 µl droplets of KRB-0.3% BSA (37°C, 5% CO_2) for 30 min. Loosely attached sperm on the ZP were removed by transferring the sperm–egg complexes through 4 drops of 60 µl of KRB-0.3% BSA using a drawn glass Pasteur pipette with an inner diameter of ~200 µm. The sperm-egg complexes were then placed into wells of a sera culture slide in groups of ~5, and overlayered with mineral oil. The number of sperm bound to the ZP of each egg was counted under a Nikon Diaphot inverted microscope. Because numerous sperm bound to the ZP, only those in the focal plane of the zona diameter were counted. The nonspecific binding level of sperm to the egg ZP was determined by incubating sperm with fertilized eggs (Hogan et al., 1994). Under our experimental conditions, this nonspecific binding level was always within 5–10% of the positive control value (i.e., when mature eggs were incubated with capacitated sperm) (Tanphaichitr et al., 1993).

To test for the role of sperm-surface ASA, PGC sperm, resuspended in KRB-BSA, were preincubated (30 min, 37°C, 5% CO_2) with various concentrations of anti-ASA IgG/Fab or affinity-purified anti-ASA IgG. Sperm pretreated with PRS IgG or PRS Fab served as corresponding negative controls for sperm preincubated with anti-ASA IgG or anti-ASA Fab, respectively. The number of sperm bound to the egg ZP was counted using our method as above.

2.4.2. In Vitro Fertilization (IVF)

Approximately 5 x 10^5 motile capacitated PGC sperm from CD-1 mice or swim-up sperm from wild type and ASA null mice were incubated (37°C, 5% CO_2) with 20–25 cumulus-free, ZP-intact mature eggs in 500 µl of KSOM medium supplemented with 0.3% BSA (KSOM: 95.0 mM NaCl, 2.5 mM KCl, 1.7 mM $CaCl_2$, 0.35 mM KH_2PO_4, 0.2 mM Mg_2SO_4, 25 mM $NaHCO_3$, 0.2 mM sodium pyruvate, 10 mM sodium lactate, 0.2 mM glucose, 0.01 mM sodium EDTA, 1.0 mM L-glutamine, 1 U/ml of penicillin G, 1 µg/ml of streptomycin sulfate, and 28 µM phenol red at pH 7.40). After 6 h of gamete coincubation, eggs were assessed for their fertilization status under a Nikon Diaphot inverted phase-contrast microscope at 400 X magnification. Fertilized eggs were identified by the presence of two pronuclei. To assess the level of parthenogenesis, eggs were incubated under the same conditions but without sperm addition. This level was consistently 0%.

2.4.3. Artificial Insemination and Assessment of In Vivo Fertilization

Artificial insemination was performed with superovulated CF-1 mice (Tanphaichitr et al., 1992). Briefly, sperm-containing fluid, collected from both cauda epididymis and vas deferens of a CD-1 mouse into 400 µl KRB-HEPES-BSA

(concentration ~5 x 10^7 sperm/ml), was aliquoted into 2 fractions, 1 of which was treated (30 min, 37°C, 5% CO_2) with anti-ASA IgG (200 μg/ml) and the other with PRS IgG (200 μg/ml). A 50-μl aliquot of the antibody-treated sperm suspension was used for transcervical injection into each superovulated female approximately 2 h before the expected ovulation time (10 h post-hCG injection (Hogan et al., 1994). Insemination was done in a paired sequence with sperm collected from the same male. The first female was inseminated with PRS-IgG-treated sperm and the second with anti-ASA-IgG-treated sperm. Females were killed 22–24 h post-hCG injection, and the eggs were retrieved from the oviduct for microscopic assessment of the fertilization occurrence, i.e., presence of 2 pronuclei.

2.4.4. Evaluation of Sperm Acrosomal Status

Cauda epididymal and vas deferens sperm were collected from WT and ASA null mice and one aliquote of the sperm suspension from each genotype were taken immediately and evaluated for basal level acrosome reaction. The rest of samples were subject to swim-up sperm preparation as described above except that the incubation was carried out for 60 min. The swim-up sperm were then divided into two halves. One half was evaluated for spontaneous acrosome reaction, and the other was treated with solubilized mouse ZP at a final concentration of 8 ZP/μl (37°C, 5% CO_2 for 30 min) to assess ZP-induced acrosomal exocytosis. Sperm samples were fixed with 4% paraformaldehyde and stained with Coomassie Blue following the method described (Bleil and Wassarman, 1990) to assess the acrosomal status. Specifically, aldehyde-fixed acrosome intact sperm were stained with Coomassie Blue at their head convex ridge (the site of the acrosome), whereas acrosome-reacted sperm lost this staining. At least two-

hundred sperm from each sample were evaluated using a Zeiss Axioskop light microscope at x400 magnification. Three replicate slides were made for each sperm sample. The average percentage of acrosome-reacted sperm from the three slides in each experiment was recorded. The experiment was repeated 3 times using 3 different animals, and the final percentage of acrosome-reacted sperm for each sample was expressed as a mean ± SD of the mean values from the 3 experiments.

To assess the effects of anti-ASA antibody treatment on sperm acrosome reaction, caudal epididymal and vas deferens sperm treated with 100 μg/ml anti-ASA IgG or PRS IgG were stained with Coomassie Blue to reveal their acrosomal status following the described method as describe above. The antibody-treated sperm were evaluated for both spontaneous acrosome reaction and the acrosome reaction induced by heat solubilized mouse ovarian ZP using 10 zonae/μl of the sperm suspension.

2.5. Mating Study

The mating study was designed to evaluate the fecundity of ASA null male mice as a function of their age. Four WT and eight ASA null male mice were used for the mating study over a period of 6 months starting when the males were ~2 to 3 months old. Each of these males was individually caged with an 8-week-old wild type female (C57BL/6J) for a duration that the female could give birth to 2 litters (approximately 2 months). Afterwards the female was replaced with another 8-week-old WT female. The old females were kept individually for an additional month to make sure no live births were missed. All the females used were proven fertile by their ability to diliver pups following mating with WT males after this 1-month waiting period. At the beginning of

the mating study and each time the females were replaced, the females were checked for vaginal copulation on the following morning as an indication of the males' mating behavior.

2.6. Antibodies

2.6.1. Production of anti-ASA Antibody

Two anti-ASA antibodies were produced. The first rabbit polyclonal IgG antibody was produced against highly purified human liver ASA (a generous gift from Dr. Arvan Fluharty, University of California, Los Angeles, (Sarafian et al., 1982) following standard protocols (Harlow and Lane, 1988). The second one was raised against purified pig sperm ASA (see below for ASA purification). Briefly, purified pig sperm ASA was electrophoresed into three lanes (~16 μg per lane) of SDS-PAGE and transferred to nitrocellulose membrane (Towbin and Gordon, 1984). The ASA bands were cut into small pieces, frozen in liquid nitrogen, and crushed using a mortar and pestle into powder. The ASA containing nitrocellulose membrane powder was resuspended in PBS and used for immunizing a female New Zealand white rabbit. Seven days before the antigen injection, serum was collected from this rabbit and termed preimmune rabbit serum (PRS). Immunization was repeated three times with the same amount of ASA, 21, 30, and 42 days after the first injection. Suspension of ASA antigen mixed with an equal volume of incomplete Freund's adjuvant was used for all injections. The interim and final antiserum titers were determined by ELISA. Briefly, purified sperm ASA (20 ng) was attached to the wells of a 96-well plate in 100 mM sodium carbonate, pH 9.6 (4°C, overnight). Following three washings with TBS-0.05% Tween-

20 (TBST), the wells were blocked for non-specific binding with TBS containing 1% fatty-acid free bovine serum albumin (BSA) (1 h, room temperature), washed three times with TBST, and then incubated with anti-ASA antiserum of various dilutions in TBST (1 h, room temperature). After washing three times with TBST, the wells were incubated (30 min, room temperature) with horseradish peroxidase (HRP) conjugated goat anti-rabbit IgG (H + L) (1:3,000 dilution in TBS, Bio-Rad Laboratories, Hercules, CA) and washed three times in TBST. Bound antibody was then detected using an *o*-phenylenediamine hydrochloride (OPD) colorimetric assay according to the manufacturer's protocol (Sigma, St. Louis, MO). Fifty three days after the first ASA injection, ELISA revealed 1:10,000 titer of the antiserum and the animal was sacrificed for the final bleed. Immunoblotting revealed that this antibody recognized purified human liver ASA (prepared as previously described (Sarafian et al., 1982), and provided by Dr. Arvan Fluharty, University of California at Los Angeles, Los Angeles, CA, U.S.A.) and a ~68 kDa band of pig and mouse sperm proteins (Carmona et al., 2002a; Tantibhedhyangkul et al., 2002). IgG was isolated from anti-ASA antiserum and PRS using an ImmunoPure Immobilized Protein A AffinityPak Column (Pierce) and quantified by Bio-Rad Protein Assay.

2.6.2. Affinity Purification of anti-SGG IgG

Rabbit polyclonal antiSGG/SGC IgG was prepared and affinity-purified according to our previously described method (White et al., 2000) except that SGC multilamellar liposomes were used for the affinity purification instead of the SGC BioSil matrix, since this antibody reacts with both SGG and SGC (White et al., 2000). To prepare multilamellar SGC liposomes, dried SGC was resuspended in PBS (1 mg/ml) and

vortexed. The obtained dispersion was then subjected to four freeze-thaw cycles to obtain homogeneous bilayers (Mayer et al., 1985; Kulkarni and Brown, 1998). During each cycle, the lipids were brought to 90°C (20 s) and vortex-mixed for complete dispersion. The lipid dispersions were then immediately frozen by plunging the glass vial into liquid nitrogen (-215°C, 20 s). After the final thawing, the dispersion was left to equilibrate to room temperature (23°C) for 1 h before use. For affinity purification, 100 µl of anti-SGG/SGC IgG (0.007 µmoles) were co-incubated (room temperature, 1h) with 100-fold mole concentration of multilamellar SGC liposomes (0.7 µmoles, prepared in PBS, 10 mM sodium phosphate, 150 mM NaCl, pH 7), followed by ultracentrifugation (200,000 g, 4°C, 1 h) using a Beckman (Chaska, MN, USA) TLA 120.2 rotor. The pellet was then resuspended in 400 µl 1 M potassium iodide (Boulanger et al., 1994), and left at 4°C for 1 h with gentle agitation to dissociate the bound anti-SGG/SGC IgG from the SGC liposomes. Subsequently, the mixture was diluted with 1 ml PBS, and ultracentrifuged as described in the previous step. The supernatant, containing the affinity-purified anti-SGG/SGC IgG, was washed free of KI with PBS (0.5-1 ml) by centrifugation (4,000 g, 4°C) using Microcon YM-30. This Microcon YM-30 was pretreated with 1% BSA to block non-specific binding sites on the membrane. The affinity purified anti-SGG/SGC IgG was resuspended in PBS (10 µg/µl).

2.7. Immunolocalization of ASA and SGG

2.7.1. Indirect Immunofluorescence (IIF) of ASA on Capacitated and Noncapacitated Mouse Sperm

Live PGC caudal epididymal and vas deferens sperm, prepared as described above, were incubated (37°C, 30 min) with 10 μg/ml anti-ASA IgG or affinity-purified anti-ASA IgG in KRB-HEPES-BSA. They were then washed in the same medium and incubated (37°C, 30 min) with 25 μg/ml Alexa-488-conjugated goat anti-rabbit IgG (Molecular Probes). Sperm treated with 10 μg/ml PRS IgG served as controls. In order to confirm that sperm were viable during this treatment, propidium iodide was added to the sperm suspension at a final concentration of 1 μg/ml, 5 min before the incubation time of the secondary antibody ended. Sperm were then washed twice in KRB-HEPES-BSA, resuspended in the same medium, mounted onto a slide in 50% PBS/50%glycerol, and topped with a cover slip. The slide was viewed under a Zeiss IM35 epifluorescent microscope (Carl Zeiss Canada, Toronto, ON, Canada). Phase contrast and fluorescent images of sperm were recorded by a Spot Junior CCD camera (Carl Zeiss Canada) and processed through Corel PhotoPaint software.

IIF was also performed with live oviductal/uterine sperm collected as described previously (Tanphaichitr et al., 1992). Briefly, uterine horns and oviducts were dissected from a superovulated female CF-1 mouse mated with a fertile CD-1 male. The organs were cut open and incubated (30 min, 37°C, 5% CO_2) in 2 ml KRB-BSA. At the end of the incubation, sperm were flushed from the organs with the same medium and then subjected to PGC using the same procedure applied to epididymal and vas deferens sperm. This procedure removed the surrounding viscous material from the oviductal/uterine sperm, which sedimented as a pellet. Following resuspension in KRB-HEPES-BSA, the isolated oviductal/uterine sperm were subjected to IIF as described above for epididymal and vas deferens PGC sperm.

Intracellular localization of ASA was performed with aldehyde-fixed sperm on slides. Briefly, caudal epididymal and vas deferens sperm resuspended in KRB-HEPES-BSA were plated onto slides precoated with 1 mg/ml poly-l-lysine (molecular weight ~75,000 to 150,000; Sigma Chemical Co., St. Louis, MO) in a moist chamber. Sperm loosely adhered to the slide were washed away by flushing the slide gently with PBS. The attached sperm were fixed with 4% paraformaldehyde in 0.1 M phosphate buffer, pH 7.4. Following 2 washes in PBS, sperm were treated with cold methanol for 3–5 min, washed with PBS, and then incubated (1 h, room temperature) with PBS-2% BSA to prevent nonspecific binding of antibodies. The sperm were then incubated (30 min, room temperature) with 10 μg/ml anti-ASA IgG or with 10 μg/ml PRS IgG (controls), followed by washing with PBS and incubation (30 min, room temperature) with 25 μg/ml Alexa 488-conjugated goat anti-rabbit IgG. The slide mounting and viewing and the recording and processing of sperm images were the same as those described above for live sperm.

IIF of ASA was also performed with live and aldehyde/methanol-fixed noncapacitated sperm (collected from the caudal epididymal and vas deferens sperm and resuspended in PBS) as well as with aldehyde/methanol-fixed PGC caudal epididymal and vas deferens sperm that were treated with Triton X-100 (described above). The same immunofluorescent procedures as described above were used for localizing ASA in these sperm.

2.7.2. IIF for SGG on live testicular sperm, and caudal epididymal and vas deferens sperm

Live testicular sperm, and caudal epididymal and vas deferens sperm were separately incubated (5% CO_2, 37°C, 30 min) with 10 μg/ml affinity-purified anti-SGG

IgG in KRB-HEPES-BSA. The remaining procedures were essentially the same as described for the IIF of ASA.

2.7.3. IIF for ASA on Acrosome-Reacted Sperm

PGC caudal epididymal and vas deferens sperm were capacitated in KRB-0.3% BSA for 30 min (5% CO_2, 37°C) and then induced to undergo acrosome reaction with 10 μM calcium ionophore (A23187, final concentration) for 10 min under the same condition. The sperm were washed twice with PBS by centrifugation (350 x g, 10 min, 28°C) and blocked with 5% decomplemented normal goat serum (prepared in PBS) for 15 min at room temperature (RT). After washing with PBS by centrifugation (350 x g, 10 min, 25°C), sperm were incubated with 10 μg/ml anti-ASA IgG, plus 0.5 μg/ml monoclonal antibody OBF13 (mouse IgM) in PBS for 30 min (RT). Following washing with PBS by centrifugation, the sperm were incubated with secondary antibodies, 25 μg/ml Alexa 594-conjugated goat anti-rabbit IgG and 5 μg/ml Alexa 488-conjugate goat anti mouse IgM (Molecular Probes, Eugene, OR) (30 min, RT). Sperm treated with PRS IgG in place of the primary antibody served as controls. To assess cell viability during the staining process, propidium iodide (Molecular Probes, Eugene, OR, USA) was added to the cell suspension at a final concentration of 1 μg/ml 5 min before the secondary antibody incubation period ended. Sperm were then washed twice in PBS, mounted onto a slide in 50% PBS/ 50% glycerol, topped with a cover slip, and viewed under a Zeiss IM35 epifluorescence microscope (Carl Zeiss Canada, Toronto, ON, Canada). Fluorescent images of sperm were recorded by a Spot Junior CCD camera (Carl Zeiss Canada).

2.7.4. Electron Microscopic Immunoprotein-A Gold Labeling

Live caudal epididymal and vas deferens sperm were treated with anti-ASA IgG as described for IIF. At the transmission electron microscopy level, antibody-antigen complexes were detected by incubating anti-ASA-treated sperm (1 h, room temperature) with protein A-gold (8 nm) solution (Slot and Geuze, 1985) (provided by Dr. F. Kan, Queen's University, Kingston, ON, Canada). The sperm were then washed twice in PBS, and the sperm pellet was fixed (1 h, room temperature) with a mixture of 4% paraformaldehyde and 0.5% glutaraldehyde in 0.1 M phosphate buffer, pH 7.4, containing 0.2 M sucrose. The fixed sperm were then serially dehydrated in ethanol and embedded in LR white (London Resin Co., Berkshire, UK). Thin sections of these sperm were stained with saturated uranyl acetate and Reynold lead citrate and viewed using a Hitachi 7100 transmission electron microscope (Hitachi, Ltd, Tokyo, Japan) at 75 kV.

2.8. Flow Cytometry

2.8.1. Flow Cytometric Analysis of ASA on Live Testicular Sperm, Caput and Corpus Epididymal Sperm, and Caudal Epididymal and Vas Deferens Sperm

Live testicular sperm, caput and corpus epididymal sperm, and caudal epididymal and vas deferens sperm were separately subject to IIF staining procedures as described above. Caudal epididymal and vas deferens sperm incbated with PRS IgG in place of anti-ASA IgG served as controls. After extensive washes to remove unbound fluorescent secondary antibody, the sperm were filtered through a 70-μm mesh (Tube-top Filicon; DAKO Diagnostics Canada, Mississauga, ON, Canada) immediately before analysis on a Coulter Epics Profile II Flow Cytometer (Beckman Coulter, Fullerton, CA). Samples were excited by an argon ion laser at 488 nm, and the emission fluorescence was

monitored at 525 ± 20 nm band pass. Sperm cells were gated from debris using their unique properties of forward and side light scattering. Data from at least 5000 events were collected, and relative ASA staining intensity was determined using FCS Express Software (De Novo Software, Orangeville, ON, Canada).

2.8.2. Flow Cytometry Analysis of Sperm Membrane Fluidity

WT and ASA null sperm plasma membrane fluidity were assessed by flow cytometry using merocyanine 540 (MC540, Molecular Probes) (Harrison et al., 1996). To avoid interference from BSA on the fluorescence of merocyanine (Harrison et al., 1996), swim-up sperm samples were washed once with PBS-0.1% PVA by centrifugation (500 x *g*, 5 min, 37°C) and incubated in PBS-0.1% PVA containing 2.7 μM MC540 and 1 μM calcein AM (Molecular Probes) in the dark for 15 min at 37 °C. The cells were washed once with PBS-0.1% PVA before flow cytometric analysis on a Coulter EPICS XL flow cytometer (Beckman Coulter Ltd., Miami, Florida) equipped with a 15 mW argon laser with excitation at 488 nm. Light-scatter data were collected in linear mode, while fluorescence data were collected in logarithmic mode. Side- and forward-light scatter parameters were used to identify the sperm events and 10,000 sperm cells per sample were collected at a flow rate of 200-500 sperm/second. Calcein fluorescence in the sperm population were detected using a 525 ± 20 nm BP filter (FL1), and MC540 fluorescence was detected using a 575 ± 15 nm BP filter (FL2). Unstained samples were used as negative fluorescence controls in initial protocol set-up.

2.8.3. Flow Cytometric Analysis of SGG on Testicular Germ Cells

The SGG levels on spermatogenic cell populations were analyzed in fixed cells using a flow cytometric method. Approximately 2 x 10^6 of testicular germ cells in 1 ml

of D-MEM were incubated with DRAQ5 (Biostatus ltd., UK) at a final concentration of 20 μM in the dark for 15 min at room temperature. The cells were washed once with PBS by centrifugation (450 x g, 5 min) and then fixed with 4% paraformaldehyde in PBS for 15 min at RT. After two washes with PBS supplemented with 0.3% BSA (PBS-BSA), the cells were blocked with 5% normal goat serum (diluted in PBS) at RT for 15 min. After centrifugation (450 x g, 5 min), the pelleted cells were incubated (45 min, RT) with 5 μg/ml O4 monoclonal antibody or normal mouse IgM diluted in PBS-BSA. The cells were then washed in the same medium and incubated (30 min, RT) with 20 μg/ml goat anti-rabbit IgG conjugated with the Alexa 488 fluorochrome (Molecular Probes, Eugene, OR). The cells were then washed twice with PBS-BSA, resuspended in 1 ml of the same buffer and analyzed on a Coulter EPICS XL flow cytometer (Beckman Coulter Ltd., Miami, Florida) equipped with a 15 mW argon laser with excitation at 488 nm. Cell doublets were eliminated on the basis of the cytogram DNA peak vs. DNA area. Ten thousand cells from each sample were analyzed at a flow rate of 200 – 400 cells/second. Fluorescence emission of DRAQ5 (emission λ_{max} 681 nm / 697 nm) was quantified in FL4 after passage through a 675 nm bandpass filter (660 – 700 nm), while SGG fluorescence was reflected by a 550 nm dichroic longpass filter and quantified after passage through a 525 ± 20 nm bandpass filter.

2.9. Light Microscopic Immunocytochemistry of ASA on Mouse Testis, Epididymis, and Vas Deferens Sections

CD-1 male mice (~10 week old) were used for all studies. Mice (n = 5) were perfused with Bouin's solution in situ through the left ventricle. The testis, epididymis,

and vas deferens were removed in one piece and further fixed in Bouin's solution for an additional 2 h. Tissues were then embedded in paraffin for sectioning according to standard procedures. Sections (4 μm thick) were deparaffinized and rehydrated through decreasing concentrations of ethanol (100% to 70%). The tissues were treated with 1% hydrogen peroxide in 70% ethanol and subsequently with 1% lithium carbonate in 70% ethanol to quench endogenous peroxidase and to remove residual picric acid, respectively. The tissues were then treated with 300 mM glycine to neutralize residual formaldehyde. The antigen was retrieved by microwaving the tissues (which were immersed in 0.01 M citrate buffer, pH 6.0) for 3 min at the highest power and an additional 7 min at low power. To block nonspecific binding, the tissues were incubated for 15 min at room temperature with 10% normal goat serum in Tris-buffered saline (TBS). The tissues were then incubated (90 min, 25°C) with affinity-purified anti-ASA IgG. Following successive washing with 0.1% Tween in TBS, the slide was examined for antigen-antibody interaction using the Vectastain ABC Elite kit (Vector Laboratories, Burlingame, CA). This process involved treatment of the slide with biotinylated secondary antibody (goat anti-rabbit IgG, 30 min, room temperature), followed by incubation with avidin-biotin-horseradish peroxidase complex and detection by a reaction with a peroxidase substrate, diaminobenzidine. Concentrations of chemicals and conditions for these treatments were as described by their manufacturers. The brown product of the peroxidase reaction signified ASA localization. Tissues treated with 10 μg/ml PRS IgG served as negative controls.

2.10. Histological Analyses of Testes and Epididymides

Testes were fixed in Bouin's solution (Sigma Chemical Co, St. Louis, MO) at room temperature overnight, washed several times with 70% ethanol and stored in 70% ethanol. The fixed testes were sent to the Centre for Bone and Periodontal Research (Mcgill University, Montreal) for sectioning. Briefly, the testes were serially dehydrated in increasing concentrations of ethanol and embedded in paraffin. The testis paraffin blocks were cut into 6-μm-thick sections and the sections were mounted onto glass slides. At the time of experiment, the sections were heated at 60°C in an oven for 30 min, and deparaffinized in Xylene (3 x 5 min). The sections were then rehydrated through a graded series of ethanol (100%, 95% and 70%, 5 min each) and milliQ water (5 min), respectively, and stained with hematoxylin (nuclear staining) and eosin (cytoplasmic staining) (Fisher scientific company, Ottawa, Ontario, Canada). The sections were topped with Permount (Fisher scientific company, Ottawa, Ontario, Canada) and coverslips and viewed in bright field under a Zeiss IM35 epifluorescent microscope and the images were captured at 100 x and 400 x magnification. Testes collected from three animals of each genotype were sectioned and fifty seminiferous tubules were viewed for each animal sample.

2.11. TUNEL Immunohistochemistry

Paraffin sections of mouse testes (6-μm thick) were deparaffinized and rehydrated as described above. The sections were then permeabilized in freshly prepared 0.1% sodium citrate containing 0.1% Triton X-100 for 8 min at room temperature. After two rinses with PBS, the slides were treated with 1% hydrogen peroxide in 70% ethanol for 10 min to quench endogenous peroxidase. This was followed by two washes in PBS and

subsequent steps for TUNEL staining were carried out using the TUNEL Enzyme and TUNEL Label Mix (Roche Applies Science, Penzberg, Germany) according to the supplier's instructions. Following incubation of the sections with the TUNEL reaction mixture in a humidified chamber at 37°C for 1 h, the sections were washed 3 times with PBS and viewed under a Zeiss IM35 epifluorescence microscope (Carl Zeiss Canada Ltd., Toronto, ON, Canada) and photographed. The fluorescent signals were subsequently converted into colorimetric signals by incubating the sections with anti-fluorescein Fab - peroxidase (POD) complex (Roche Applies Science, Penzberg, Germany) for 30 min at 37°C. TUNEL-positive cells were finally detected by incubating the sections for 2-10 min with 3,3'-diaminobenzidine (DAB) substrate kit (Vectorlabs, Burlingame, CA) that stained positive cells brown. Sections were washed 3 times with PBS, mounted with 50% glycerol in PBS under glass coverslips and analyzed under light microscope (Zeiss, West Germany).

2.12. Protein and Enzyme Biochemistry

2.12.1. Purification of Pig Sperm ASA

ASA was purified from ejaculated boar sperm according to the modified method of Carmona et al. (Carmona et al., 2002a). Briefly, a sperm homogenate was prepared in 20 mM Tris-maleate, 50 mM $MgCl_2$, 1 mM EDTA, pH 6.1, supplemented with protease inhibitor cocktail (Roche Diagnostics GmbH, Mannheim, Germany, used as per the manufacturer's instruction). Following removal of the sperm particulate by low speed centrifugation, ASA in the supernatant was purified by a series of column chromatography, first through a Mono-Q Sepharose column equilibrated with 20 mM

Tris-maleate, pH 6.1, and then through a Sephacryl S-200 column (Amersham Pharmacia Biotech, Piscataway, NJ), as previously described (Carmona et al., 2002a). The partially purified ASA was subject to a third chromatography step using the same Sephacryl S-200 column but equilibrated and eluted with 50 mM sodium acetate, 150 mM NaCl, pH 5. In the acidic pH, ASA exists as an octamer (Lukatela et al., 1998) and it was eluted in the void volume from the Sephacryl S-200 column. All column eluted fractions were assayed for protein content by A280 and for ASA activity using an artificial substrate, *p*-nitrocatechol sulfate (NCS), as previously described (Carmona et al., 2002a). These purification steps yielded ASA with a specific activity of ~60 U/mg and the purified ASA appeared as a single band on a 12% polyacrylamide gel following silver stained SDS-PAGE (Laemmli, 1970).

2.12.2. Quantification of ASA in the Caudal Epididymal and Vas Deferens Fluid

ASA purified from the pig sperm surface extract to a single band on SDS-polyacrylamide gels (Carmona et al., 2002a) was used as a standard. Caudal epididymal and vas deferens fluid containing 6 μg of total proteins or ASA standard (1–15 ng, as quantified using Protein Assay Solution; Bio-Rad) in 100 μl of 100 mM sodium carbonate, pH 9.6, was allowed to attach to the bottom surface of the wells of a Limbro/Titerteck 96-well polystyrene plate (ICN Biomedical, Aurora, OH) overnight at 4°C. Wells containg only the buffer served as a blank. The wells were blocked with 1% BSA in TBS at 25°C for 1 h followed by three washes in TBS containing 0.05% Tween 20 (TBST). The protein wells were then incubated with 100 μl of anti-ASA antiserum (1:1600 dilution in TBS) at 25°C for 1 h. Following successive washing in TBST, 100 μl of HRP-goat anti-rabbit IgG (1:3000 dilution in TBS) was added to the wells for

incubation at 25°C for 30 min. After washing thoroughly with TBST, 100 µl of an HRP substrate, *o*-phenylenediamine dihydrochloride (0.05% in 100 mM sodium citrate, pH 5.0), and H_2O_2 (1.5 µl/ ml of the substrate solution) were added to the wells, which were then incubated at 25°C until the yellow color developed. The reaction was then stopped with 50 µl of 30% H_2SO_4, and the color intensity was measured at A_{490}. After subtracting blank reading, a standard curve was constructed of readings obtained from wells containing different amount of the ASA standard (1-15 ng), and the amount of ASA in the samples were calculated from the curve.

2.12.3. ASA Enzymatic Activity Assay

ASA activity was assayed using the artificial substrate *p*-nitrocatechol sulfate (NCS). The reaction mixture, consisting of 5 mM NCS, 0.25 mM $Na_4P_2O_7$, 0.85 M NaCl, 1 mg/ml of BSA, 0.25 M sodium acetate, pH 5, and the sample homogenate containing 0.1-0.3 mg of total proteins in a total volume of 200 µl, was incubated at 37°C for 1 h. At completion of the incubation, 800 µl of 1 M NaOH was added to the reaction for brown color development of *p*-nitrocatechol, the desulfated product of NCS, which was then measured spectrophotometrically at 515 nm and quantified using its molar extinction coefficient (i.e., 1 M of nitrocatechol has A_{515} of 12400) (Baum et al., 1959). One unit of ASA activity was defined as 1 µmole of nitrocatechol released in 1 h at 37°C.

To assay for sperm surface ASA desulfation activity, caudal epididymal and vas deferens sperm (10×10^6 sperm/ml), washed free from the bathing fluid, were incubated (30 min, 37°C) at pH 5.0 in an isotonic reaction solution (0.1 M sodium acetate buffer, pH 5.0, 0.5 mM $Na_4P_2O_7$ and 0.6% NaCl) (Chang and Moudgil, 1984) containing 10 mM NCS. Following centrifugation (350 x *g*, 10 min, 28°C) to remove sperm, 1 M NaOH

was added to the supernatant and the product was measured spectrophotometrically as described above. The viability of sperm exposed to the reaction solution at pH 5.0 was assessed by exclusion of propidium iodide (Molecular Probes, Eugene, OR) used at 1 μg/ml following manufacturer's instruction. The ASA activity was also measured in sonicated mouse sperm, resuspended in 250 mM sodium acetate buffer, pH 5.0. Sonication was performed using a Branson B220 water bath sonicator (Branson Cleanings Equipment Company, Shelton, CT) for three 30-sec cycles, followed by vigorous vortexing for 30 sec. One unit of activity was defined as 1 μmole of NCS hydrolyzed in 1 h.

2.12.4 Extraction of ASA from mouse caudal epididymal and vas deferens sperm

Cauda epididymis and vas deferens sperm of CD-1 mice were washed free from the bathing fluid in TBS by centrifugation (350 x *g*, 10 min, 28°C). The plasma membranes and soluble components of the acrosome were then extracted from the sperm pellet following the described method (Kim et al., 2001). Briefly, sperm were resuspended at a concentration of 20 x 10^6/ml in 0.625% Triton X-100 and 0.15 M NaCl, 5% sucrose, protease inhibitor cocktail (concentration used as instructed by the manufacturer; Roche Diagnostics, Mannheim, Germany) and 20 mM sodium acetate, pH 5.2 (5 min, 4°C). The sperm suspension was further homogenized by passing through a 26-gauge syringe needle twice. The soluble and insoluble fractions of the Triton X-100-treated sperm were obtained by centrifugation (10,000 x *g*, 10 min, 4°C) of the sperm suspension and were then subjected to protein quantification using a BioRad Protein Assay Solution (Bio-Rad Laboratories, Hercules, CA) and to SDS-PAGE/immunoblotting. The treated sperm were also subject to IIF.

Caudal epididymal and vas deferens sperm collected and washed in TBS as described above were also subjected to treatment with a sucrose solution (320 mM) containing 1 mM ATP, 1 mM EDTA, and 0.2 mM *N*-$_{\alpha}$-*p*-tosyl-l-lysine chloromethylketone hydrochloride (AES), which had been used to extract peripheral plasma membrane proteins from intact cells (Carter and Hakomori, 1977), including SLIP1 and P68 from mouse and pig sperm, respectively (Tanphaichitr et al., 1993; Tanphaichitr et al., 1998a). Approximately 70 x 10^6 mouse sperm were incubated in 0.5 ml of AES for 20 min at 4°C. Sperm were then centrifuged (600 x *g*, 10 min, 4°C), and the collected AES supernatant was concentrated for immunoblotting using a Microcon 30.

2.12.5. SDS-PAGE, Silver Staining, Western Blotting and Dot-Immunoblotting

Proteins were resolved by SDS-PAGE using 7.5% to 12% polyacrylamide depending on experimental needs, and transferred electrophoretically (250 mA, 1 hr) onto nitrocellulose membranes (0.45 μm) (Laemmli, 1970; Towbin and Gordon, 1984). No-reducing condition was used for electrophoration of ZP glycoproteins. Non-specific binding sites on the membrane were blocked (1 h, room temperature) with 5% non-fat milk in Tris-buffered saline (TBS: 137 mM NaCl in 20 mM Tris-HCl, pH 7.6) containing 0.05% Tween 20 (TBST). The membranes were then incubated with primary antibody (1 hr at RT or 4°C overnight), washed 3 x 5 min with TBST and then incubated with appropriate secondary antibody conjugated with HRP (1 hr at RT). Both primary and secondary antibodies were prepared in the blocking buffer. After washing the membrane (3 x 10 min) with TBST to remove unreacted secondary antibody, the protein-antibody recognition was detected using an enhanced chemiluminescence ECL Western blotting

detection kit, according to the manufacturer's instructions (Pierce, Rockford, IL). The emitted chemiluminescence was captured by Hyperfilm^{TM} ECL^{TM} film by exposing the film to the membrane in the dark, and the films were developed on a Kodak M35A X-OMAT processor (Kodak, Canada).

For dot-immunoblotting, solubilized mouse ZP and individual ZP glycoproteins were spotted onto nitrocellulose membrane and air dried. Ovalbumin (1 μg) and solubilized pig ZP (CalBioChem, 1 μg) were also spotted onto the membrane strips as a negative and positive control for ASA binding, respectively (Carmona et al., 2002). The membrane was blocked in 5% non-fat milk in TBST (1 h, room temperature) and incubated (1 h, room temperature) with 3 μg purified ASA in 1 ml of TBST. Purified ASA of a specific activity of 40 U/mg was used for the binding assay. The membrane was then washed three times (5 min each) with TBST and incubated (1 h, room temperature) with anti-ASA antiserum (1:1,000 dilution in 5% skim milk). After washing three times in TBST, the membrane was incubated (1 h, room temperature) with HRP-conjugated goat anti-rabbit IgG (1:5,000 dilution in TBST containing 5% skim milk), and processed for signal detection as described above.

2.13. Reverse Transcription Polymerase Chain Reaction (RT-PCR) of ASA from Cauda Epididymis + Vas Deferens and from Testes and Nucleotide Sequencing of the Product

Total RNAs from cauda epididymis + vas deferens and from testes were separately extracted using Trizol reagent (Gibco BRL, Burlington, ON, Canada), following the manufacturer's protocol. Using RETROscript First-Strand Synthesis Kit for

reverse transcription polymerase chain reaction (RT-PCR) (Ambion, Austin, TX), total RNAs (1 μg, determined from A_{260}) were reverse-transcribed into first-strand cDNAs in a 20-μl reaction mixture. Subsequently, 2 μl of this reaction mixture containing the first-strand cDNA was used as a template for PCR. The primers for amplification of *ASA* were as follows: F-ASA: 5'-atggggtctttgctgttcgg-3' (nucleotides 566–587; numbering as described for human AS-A sequence (Stein et al., 1989); R-ASA: 5'-ttctggtaaggtggcatcggac-3' (complementary to nucleotides 2412–2434). Amplification reactions were carried out in a Mastercycler (Brinkmann Instruments, Mississauga, ON, Canada). These reactions were initiated with 10-min denaturation at 94°C, followed by 30 cycles of denaturation at 94°C for 30 sec, annealing at 56°C for 45 sec, and extension at 72°C for 45 sec, and ending with further extension at 72°C for 10 min. RT-PCR products were then resolved by electrophoresis in a 2% agarose gel containing ethidium bromide (0.5 μg/ml) followed by visualization under an ultraviolet lamp (UV Transilluminator, Gel Doc 1000; BioRad). RT-PCR experiments were repeated three times using RNA samples prepared on different days from three different animals. Negative controls were performed in all experiments by omitting the RT step.

The RT-PCR product of *ASA* from cauda epididymis and vas deferens was purified by agarose gel electrophoresis. The product band was excised and purified using a Concert Rapid Gel Extraction System (Gibco BRL, Gaithersberg, MD). Approximately 100 ng of the purified RT-PCR product was used for nucleotide sequencing, which was performed by the chain termination method using an automated capillary electrophoresis and fluorometric detection system (ABI Prism 3100 Genetic Analyzer; Applied Bioystems, Foster City, CA).

2.14. Binding Assays

2.14.1. Binding of Alexa-430 ASA onto the Caudal Epididymal Sperm

Alexa-430 ASA and Alexa-430 ovalbumin were prepared by conjugating ASA and ovalbumin, respectively, with the Alexa 430 fluorochrome (Molecular Probes) as instructed by the manufacturer. Caudal epididymal sperm (1.2×10^6) were incubated (37°C, 5% CO_2, 1 h) with various concentrations (0–60 nM) of Alexa-430 ASA or with 60 nM Alexa-430 ovalbumin in 600 µl of KRB-BSA. At the end of the incubation, sperm were washed free from the unbound protein by centrifugation (600 x *g*, 25°C, 10 min) in KRB-BSA. The washed sperm pellet was resuspended in 600 µl of KRB-HEPES, and 100-µl aliquots (2×10^5 sperm) were placed in each well of a Costar black 96-well microtiter plate (Corning, Corning, NY) for measurement of fluorescence intensity using a Spectramax GeminiXS spectrofluorometer (Molecular Devices) at the excitation and emission wavelengths of 425 and 520 nm, respectively. The amount of ASA bound per sperm was then calculated from the Alexa-430 ASA standard curve. The data obtained were analyzed for the K_d value of ASA-sperm by Scatchard plotting using Grafit 4.0 software for Windows (Erithacus Software, Surrey, U.K.). In an alternative experiment, 600 nM ASA was included with 60 nM Alexa-430 ASA for sperm incubation. Measurement of Alexa-430 ASA binding to sperm was then performed as described above.

To investigate the roles of SGG and mannose phosphate receptors on the sperm surface in ASA binding, 2×10^5 caudal epididymal sperm in 150 µl KRB-HEPES were pretreated (37°C, 5% CO_2, 30 min) with various concentrations of anti-SGG Fab (0–10 µM), PRS-Fab (0–10µM), or mannose 6-phosphate (0–5 mM) before incubation with 63

nM Alexa-430 ASA following the procedure described above. Data were expressed as percentages of the control fluorescence intensity values (i.e., from incubations of Alexa-430 ASA with sperm without any competitors) for each of the competitor concentrations.

2.14.2 Isolation of Mouse Ovarian ZP and Purification of Individual ZP Glycoproteins

Large numbers of ZP (5-20 × 10^3) were isolated by Percoll (GE Healthcare, Uppsala, Sweden) gradient centrifugation of ovarian homogenates. Ovaries dissected from 20-30 mice (6-8 weeks old) were homogenized with a Dounce homogenizer on ice in 4 ml of homogenizing buffer (25 mM triethanolamine, pH 8.5, 150 mM NaCl, 1 mM $MgCl_2$, 1 mM $CaCl_2$, and 1% Nonidet P-40) supplemented with protease inhibitors cocktail (1 tablet/10 ml), 0.1 mg/ml DNase (Sigma Chemical Co., St. Louis, MO; Type 1II) and 0.1 mg/ml hyaluronidase (Sigma Chemical Co., Type IV) until they became particulate. The homogenate was then brought to 1% deoxycholate and homogenized on ice until it became opalescent (~ 5 strokes). For ultracentrifugation, 4 ml of 90% Percoll solution (made up in 10 x homogenization buffer) was placed in an ultraclear Quick-Seal (Beckamn) centrifuge tube and ovarian homogenate (4 ml) was layered on top and the tube was then filled up with 50% Percoll (made up in 10 x homogenization buffer). Sealed tube was then centrifuged in a 70.1 Ti Beckman rotor at 81000 x *g* for 45 min at 18°C. An opalescent band containing intact ZP and ZP fragments appeared at ~1/3 of the way down the tube. The band was recovered by puncturing the side of the centrifuge tube with a syringe pre-filled with ~0.5 ml of 50% Percoll. The ultracentrifugation step was repeated by placing the ZP containing Percoll solution on the bottom of a new centrifuge tube and filled up with 50% Percoll. This time, ZP banded at about half way down the tube. Again, the band was recovered as before and the ZP was washed with 25

mM triethanolamine, pH 8.5, 150 mM NaCl, in a 15 ml conical polypropylene tube (Corning) by centrifugation at 1500 x *g* for 10 min at room temperature (RT). The resulting pellet was transferred to a microcentrifuge tube and was washed with phosphate-buffered saline (PBS; 30 mM sodium phosphate, pH 7.4, 150 mM NaCl) by centrifugation at 10000 rpm for 5 min at RT. The final pellet was stored in 50% glycerol in PBS at -20°C.

To solubilize ZP, the isolated ZP were washed in PBS, pH 6.8, by centrifugation at 10,000 rpm for 5 min at RT and then resuspended in 100 µl of 0.2 M sodium phosphate buffer, pH 6.8, containing 0.1% SDS (HPLC buffer) by vortexing. The ZP were solubilized by heating at 65°C for 10 min, cooled to RT, and centrifuged at 14,000 x g for 1min to remove any insoluble material. The supernatant, containing solubilized ZP, was used to purify individual ZP glycoproteins. The solubilized ZP was first resolved by SDS-PAGE under non-reducing condition according to the method of Laemmli (Laemmli, 1970), using 7.5% separating gel (1.5 mm thick). The sample was applied on several lanes, with each lane containing no more than 25 µg of total ZP glycoproteins. One microgram of solubilized ZP was applied to a separate lane on the same gel. Following gel electrophoresis, the lane with 1 µg of solubilized ZP was cut off the gel and stained with silver nitrate using the Bio-Rad Silver Stain kit (Bio-Rad Laboratories, Mississauga, ON, Canada) to reveal the positions of ZP1, ZP2, and ZP3. Corresponding regions of each ZP glycoproteins from lanes with experimental samples were marked by matching with the stained gel. The marked areas were sliced and the gel slices were subjected to electroelution using a Centrilutor® Micro-Electroeluter (Millipore, Billerica, Massachusetts). The electroelution was carried out at a constant voltage (200 volts) for 2

h at RT using degassed SDS-electrophoretic buffer minus SDS. The eluted proteins were washed extensively with PBS, pH 7.4, through 6 cycles of volume reduction-resuspension (more than 10 fold volume reduction each time) in Centricon YM-30 (Millipore, Billerica, Massachusetts). Solubilized ZP and each purified ZP glycoprotein were quantitated by absorbance at 280 nm.

For HPLC purification of ZP glycoproteins, solubilized ZP (in HPLC buffer) was fractionated by HPLC at RT on a size exclusion column (BioRad; BioSil SEC-250) and eluted with HPLC buffer at a flow rate of 0.1 ml/min. Absorbance at 280 nm was monitored continuously and 100 µl fractions were collected. By this procedure, the supernatant was frantionated into three peaks of absorbance that corresponded to mZP1 (~200 kDa), mZP2 (~120 kDa), and mZP3 (~83 kDa). The three peaks were eluted at about 55-60 min (mZP1), about 61-66 min (mZP2), and about 66-73 min (mZP3). The fractions containing mZP1, mZP2, and mZP3 were pooled and the amount of each glycoprotein was determined spectrophotometrically at 280 nm. The individual glycoproteins were then dialyzed extensively (24-48 h) against distilled water at 4°C using precut dislysis tubing with a molecular weight cutoff of 30 kDa. Finally, the samples were lyophilized and stored at -80°C prior to use.

2.14.3. Characterization of Isolated ZP and Purified ZP Glycoproteins

The quality of the isolated ZP was initially examined by light microscopy and the purity of the solubilized ZP was evaluated by silver staining following SDS-PAGE. The purities of the electroeluted ZP glycoproteins were examined by silver staining and their identities were confirmed by Western blot using monoclonal antibodies against mZP2 and mZP3, respectively. The biological activity of total solubilized ZP and the purified

ZP3 as a sperm acrosome reaction inducer was also assessed. Briefly, capacitated PGC sperm were incubated with 6 ZP equivalent amounts (assuming 3.5 ng of protein per ZP, (Wassarman et al., 2004)) of solubilized ZP and each individual ZP glycoprtoeins for 30 min (37°C, 5% CO_2) and the acrosome status of the sperm was determined by Coomassie blue staining (Bleil and Wassarman, 1990). Capacitated sperm untreated or treated with ovalbumin or fetuin served as negative controls (Carmona et al., 2002b) and sperm treated with 10 μM A23187 served as a positive control. Ovalbumin and fetuin used were also subject to the same electroelution purification process and the subsequent washing steps as the ZP glycoproteins.

2.14.4. Binding of ASA to Mouse Zona Pellucida

Binding of ASA to intact unfertilized and fertilized mouse eggs was performed by incubating (37°C, 30 min, 5% CO_2) 0.15 μM ASA (molarity calculated based on the molecular mass of ASA monomer, i.e., 63 kDa) conjugated with Alexa 430 (Molecular Probes; conjugation performed as instructed by the manufacturer) with 20–30 eggs in a 60-μl droplet of KRB-BSA. After successive washes of the eggs in the same medium, they were viewed under a Zeiss IM35 epifluorescent microscope. Unfertilized eggs incubated with 0.15 μM Alexa-430 ovalbumin served as negative controls.

The ability of ASA to bind to solubilized ovarian ZP was also evaluated. Ovarian ZP free from the egg proper and cytoplasm were solubilized with acid Tyrode solution (Hogan et al., 1994) and neutralized and concentrated in TBS by a Microcon 30 microconcentrator to 7 ZP/10 μl TBS. Seventy solubilized ZP, applied to each well of a Limbro/Titerteck 96-well polystyrene plate (ICN Biomedical, Aurora, OH), were allowed to attach to the well bottom surface overnight at 37°C. The attached ZP was blocked (2 h,

37°C) with 100 µl TBS-2% BSA. Following 4 washes with TBS-0.05% Tween20, ZP were incubated (1 h, 37°C) with 100 µl of Alexa-430 ASA (0–0.9 µM). The unbound enzyme was removed by washing the wells with TBS-0.2% BSA, and the fluorescence intensity of ASA bound to ZP in the wells was measured using a Spectramax GeminiXS fluorometer (Molecular Devices, Sunnyvale, CA) with excitation and emission wavelengths of 425 and 520 nm, respectively. The amount of ASA bound to each ZP-coated well was determined from the Alexa-430 ASA standard curve. The data obtained were analyzed for the K_d (dissociation constant) value of ASA-ZP binding by Scatchard plotting using Grafit 4.0 software for Windows (Erithacus Software Ltd., Surrey, U.K.). Alternatively, Alexa-430 ovalbumin was used instead of Alexa-430 ASA as a negative control for incubation with ZP under the same conditions.

2.15. Recombinant ASA Production and Purification

2.15.1. Construction of Wild Type and Mutant ASA Expressing Vectors

Our cloned pig testis ASA cDNA (Gene Bank AF316108.2; GI: 45686370) (Carmona et al., 2002a) was used as template for site directed mutagenesis. Pig testis ASA cDNA originally in a pBluescript II SK(-) plasmid (UniZAP system from Stratagene, La Jolla, CA, U.S.A.) was sub-cloned into pcDNA3.1(+) (Invitrogen, Carlsbad, CA, U.S.A.) for mammalian cell expression. The sequence of the entire inserted ASA cDNA was confirmed by sequencing using an ABI DNA analyzer (Applied Biosystems, Foster City, CA, U.S.A.) at the Ontario Genomics Innovation Centre, Ottawa, Ontario, Canada. Site-directed mutagenesis was performed, according to the manufacture's instructions, using the QuickChange XL kit from Stratagene, which allows

site-specific mutation in a double stranded plasmid. For the single mutant C69A, sense and antisense primers of the following sequence were used to replace the cysteine codon, TGC, by the alanine codon, GCC: 5'CGGTGTCTCTGGCCACACCCTCCCG3'. The obtained C69A plasmid was then used as a template to create the double mutant C69A/K123A. Primers for the sequence 5'GGGATGGCTGGCGCCTGGCACCTTGGG3' were used to replace the lysine codon AAG by the alanine codon GCC. The triple mutant C69A/K123A/K302A (CKK) was finally obtained using this C69A/K123A plasmid as the template with sense and antisense primers for the sequence 5'CCTACGATGCGGAGCCGGAACCACTTTTG3', also replacing the AAG lysine codon by the alanine codon. For all mutations, positive constructs, screened by differential restriction patterns, were re-sequenced to confirm nucleotide replacement.

2.15.2 Expression and Partial Purification of Recombinant WT and Mutant ASA

Chinese hamster ovary-K1 (CHO-K1) cells (American Type Culture Collection, Manassas, VA) were used for the production of recombinant WT and mutant ASA. The cells were grown and maintained in "complete medium", containing Gibco OptiMEM-I medium (Invitrogen, Burlington, ON, Canada), supplemented with 2% fetal bovine serum (FBS), 1% L-glutamine, 0.1% penicillin/ streptomycin and 0.1% gentamycin. Wild type ASA cDNA, and mutants C69A and CKK, inserted into the pcDNA3.1 expression vector (as described above), as well as the control empty pcDNA3.1, were used to transfect CHO-K1 cells. Cells (~70% confluency) were transiently transfected, in 100 mm culture dishes, with 3.5 μg of plasmid DNA and 20 μl lipofectamine reagent (Invitrogen) in OptiMEM-I medium for 5 h (37 ^{o}C, 5% CO_2). At the conclusion of transfection, the

incubation medium was replaced with the complete medium and the cells were allowed to grow for 48 h (37°C, 5% CO_2). In order to induce secretion of ASA (a lysosomal enzyme) into the culture medium, cells were washed with phosphate buffered saline (PBS), cultured in serum-free medium for 6 h and then incubated with fresh serum-free medium containing 10 mM ammonium chloride for 18 h (Chang et al., 1988). The resulting culture medium, containing mainly over-expressed rec ASA (called wild type, C69A, CKK and pcDNA from cells transfected with pcDNA3.1 containing unaltered ASA cDNA, C69A construct, CKK construct and blank pcDNA3.1, respectively), was collected in tubes containing protease inhibitor cocktail, centrifuged at low speed to remove cells and an aliquot was used for assaying the NCS desulfation activity. In the initial set of experiments, transfected cells were scraped from the plate in PBS and solubilized in SDS-PAGE sample buffer (Laemmli, 1970). Both the collected medium and the SDS-solubilized cells were subjected to immunoblotting for ASA detection (see below).

In subsequent experiments, ASA was purified from the spent medium. The medium was first dialyzed against 10 mM ammonium bicarbonate using Spectra/Por tubing (molecular weight cut-off 50 kDa; VWR International, Mississauga, ON) and then lyophilized and stored at -20 °C. To purify ASA, the lyophilized sample was resuspended in 20 mM Tris-maleate, pH 6.1, and then incubated with Q-Sepharose Fast Flow resin (Amersham Bioscience, Uppsala, Sweden) at 4 °C for 1 h with gentle shaking. After washing the resin 4 times with 20 mM Tris-maleate, pH 6.1, bound proteins were eluted with 2 M sodium chloride in 20 mM Tris-maleate, pH 6.1. The sample was concentrated using Microcon filter (molecular weight cut-off 100 kDa; Amicon

Bioseparations, Millipore Corporation, Bedford, MA, U.S.A.). The retentate containing rec ASA was collected from the membrane in 30-50 μl of 0.25 M sodium acetate, pH 5, and an aliquot was quantified for proteins using Bio-Rad Protein Assay Solution (Bio-Rad Laboratories, Hercules, CA, U.S.A.).

The retentate of recombinant ASA was further purified by removing transferrin using Aminolink beads (Pierce) coupled with anti-transferrin IgG, which were prepared following manufacturer's instruction. Briefly, ~100 μg proteins containing retentate was incubated with 30% v/v antibody-coupled Aminolink beads in a total volume of ~600 μl TBS for 2 h at 4°C with gentle shaking. After centrifugation (3000 x *g*, 1 min, RT), the supernatant, containing mainly recombinant ASA, was collected. The pelleted beads were washed 3 times with 0.4 ml of TBS, and all 3 washes were collected and combined with the supernatant. The combined samples were further concentrated with Microcon YM-50 (Millipore). Aliquots of the final product were assayed for NCS desulfation activity and subject to SDS-PAGE.

2.16. Radioimmunoassay for Determination of Serum Testosterone

Blood was withdrawn from males by cardiac puncture. Serum was collected from coagulated blood by centrifugation (100 g, 15 min, 4 C) and stored frozen at –20°C for subsequent testosterone assays, which were done at the Bangkok Pathology Laboratory Co., Ltd. (Bangkok, Thailand), using the Bayer's ACS:180 automated chemiluminescence system (E for L International Ltd., Bangkok, Thailand). All radioimmunoassays were conducted in duplicate in one assay.

2.17. Lipid Analyses

2.17.1. Lipid Extraction

Lipids were extracted from sperm and testis homogenates of wild type and *ASA* null males, using the modified Bligh-Dyer method (Bligh and Dyer, 1959; Kates, 1986). Briefly, sperm suspension or testis homogenates was mixed with chloroform and methanol at the ratio of 1:2:0.8 (v/v/v) to make a one-phased chloroform/methanol/ aqueous mixture. After vigorous vortexing, this mixture was left at room temperature (25°C) for 1 hour to allow the chloroform to extract lipids from the cells or tissue samples. Chloroform and water was then added to the mixture to make the final ratio of chloroform/ methanol/water to be 1:1:0.9 and this would allow phase separation to occur. After centrifugation (500 x g, 5 min, 4°C), total lipids extracted in the chloroform phase stayed in the bottom of the tube, whereas aqueous-soluble materials stayed on top in the methanol/water phase. A protein plaque was formed at the interphase. The chloroform phase containing lipids was then collected with a long glass pipette and dried under a stream of nitrogen. The dried lipids were flushed briefly with nitrogen and stored at -20°C until use.

2.17.2. Cholesterol Quantification

Cholesterol in extracted sperm lipids was quantified fluorometrically by the Amplex Red (Molecular Probes) assay, according to the manufacturer's instructions. The assay is based on an enzyme-coupled reaction that can measure both free cholesterol and cholesteryl esters. Cholesteryl esters are first hydrolyzed by cholesterol esterase into cholesterol, which is then oxidized by cholesterol oxidase to yield H_2O_2 and the corresponding ketone product, 4-cholestene-3-one. In the presence of (horseradish

peroxidase (HRP), the Amplex Red reagent (10-acetyl-3,7-dihydroxyphenoxazine) reacts with H_2O_2 with a 1:1 stoichiometry, resulting in the formation of highly fluorescent resorufin. Lipids extracted in chloroform were dried under a stream of N_2 and then resuspended in an appropriate volume of methanol such that 5 µl is equivalent to the amount of lipids extracted from 0.5 million sperm or 0.5 mg of testis (wet weight of decapsulated testis). The lipid samples were diluted 10 times with 1 X Reaction Buffer (100 mM potassium phosphate, pH 7.4, 50 mM NaCl, 5 mM cholic acid and 0.1% Triton X-100) and 50 µl of the diluted samples was transferred into separate wells of a black 96-well plate (Corning, Inc., Corning, NY). To each well, 50 µl of Working Solution (1 X Reaction Buffer containing 300 µM Amplex Red reagent, 2 U/ml HRP, and 2 U/ml cholesterol oxidase) was added. To measure total cholesterol (free cholesterol + cholesteryl esters), 0.2 U/ml of cholesterol esterase was included in the Working Solution. A cholesterol standard curve was generated using different amount of cholesterol (0 to 1 µg) and the Working Solution with cholesterol esterase. One strength Reaction Buffer + Working Solution with cholesterol esterase was used for the blank. After gentle mixing by hand, the plate was incubated for 30 min at 37°C, protected from light. The fluorescence was measured in a fluorescence microplate reader, SpectraMAX GeminiXS (Molecular Devices, Sunnyvale, CA), using excitation and emission wavelengths of 560 nm and 590 nm, respectively. Background fluorescence measured for the blank reaction was subtracted from each value for data analysis. All samples were assayed for both free cholesterol and cholesteryl esters, and each assayed in triplicate.

2.17.3. High Performance Thin Layer Chromatography (HPTLC)

HPTLC was performed using an HPK silica gel 60 Å plate (200 μm thickness, 10 x 10 cm dimension, Whatman, Kent, U.K.). HPTLC plates were pre-washed in chloroform/methanol 1:1 (v/v), air dried and activated by heating at 100°C for 1 h. Total lipids extracted from sperm (7 million sperm/sample) and testes (10 mg of testis weight/sample) of WT and ASA null mice were used for HPTLC. The lipid samples were dried under a stream of N_2, reconstituted in 20 μl of chloroform/methanol (1:1, v/v) and loaded as a 0.8-cm band onto each HPTLC plate. A 25-μl glass syringe with a 22-gauge needle was used for sample loading (Hamilton, Reno, NV). The plate was developed with the solvent system $CHCl_3$, CH_3OH, 0.2% aqueous $CaCl_2$ = 60:35:8 (v/v/v). At the completion of the chromatography, the plate was briefly air dried and sprayed with 0.2% orcinol in 50% H_2SO_4 and heated at 120°C for 2-3 min. After charring, glycolipid bands became purple, whereas phospholipid bands and cholesterol band became yellow-brown and red, respectively (Kates, 1986). To obtain the total lipid profiles, the orcinol-stained plate was further stained with 0.03% Coomassie Brillliant Blue G-250 in 30% methanol/100 mM NaCl and destained with the destaining solution (30% methanol in 100 mM NaCl) (Iida et al., 1989; Furimsky et al., 2005). To obtain sulfolipid profiles, lipids extracted from 15 mg of testis of 8-month-old WT and ASA null mice were resolved by HPTLC as described above, and the HPTLC plate was sprayed with 0.016% Azure A in 1 mM H_2SO_4 to specifically reveal sulfolipid bands. The excess Azure A dye was washed off the plate with 0.05 M H_2SO_4: methanol (3:1, v/v). Lipid standards, including SGG, galactosylglycerol (GG), phosphatidylethanolamine (PE), phosphatidylcholine (PC), cholesterol (Chol) and

sphingomyelin (SM) were co-chromatographed on separate lanes with the lipid samples to locate these lipids.

For MS identification of extra glycolipid bands present in ASA KO testes, these lipids were purified by preparative thin layer chromatography. An aliquot of total testis lipids corresponding to 5 mg wet testis weight was spotted on one lane (~0.8 cm wide) on a HPTLC plate to serve as a reference. Separated by a lane without sample, the remaining lipid sample from the same animal was applied to the plate as a wide strip (~ 6 cm wide). Plates were developed with the solvent system $CHCl_3$, CH_3OH, 0.2% aqueous $CaCl_2$ = 60:35:8 (v/v/v). The lane with the reference lipids was cut off the plate, and regions of lipids of interest were identified by orcinol charring. Areas of the plate corresponding to the lipid bands of interest were scraped into glass extraction tubes containing chloroform/methanol (2 ml, 1/1, v/v). Tubes were then vortexed and let stand at room temperature for 1 hr. After centrifugation (900×g, 5 min), solvent containing extracted lipids was removed. The extraction was repeated once and the two extracts were combined, dried under N_2, and kept at -20°C until MS analysis.

2.18. Mass Spectrometry

2.18.1. Electrospray ionization mass spectrometry (ESI-MS)

ESI-MS analyses of sperm and testis lipids were performed in collaboration with Dr. Kym Faull (University of California, Los Angeles, CA). Briefly, the extracted lipids were dissolved in methanol/chloroform (4:1, v/v, 20 pmole/μl) and injected (20 μl/injection) into a stream of the same solvent flowing (20 μl/min) into an ESI (Ionspray™) source connected to a triple quadrupole mass spectrometer (API III$^+$, Perkin-

Elmer Sciex, Thornhill, ON, Canada). Negative ion mass spectra were recorded by scanning from m/z 100-1000 (orifice 70 volts, 0.3 Da step size, 5 sec/scan). Fragment ion spectra of Q1 pre-selected parent ions were produced by scanning Q3 (m/z 50-800, 0.3 Da step size, 2 ms dwell time, 5.13 second/scan, orifice 90 volts) under collisionally activated conditions (collision gas: 10% nitrogen in argon, thickness instrumental setting (CGT) of 200, collision energy of 60 eV). Averaging of all the scans accrued from each sample injection was achieved with the MacSpec™ computer program.

2.18.2. ESI-MS Quantification of SGG - Preparation of SGG and $^2H_3$-Labelled SGG Standards

SGG was purified from pig testis total lipid extracts via Biosil-A column chromatography, followed by preparative TLC (Kates, 1986; Tupper et al., 1994; Franchini et al., 2008). When examined by HPTLC using chloroform/methanol/water (65/25/4, v/v/v) as a solvent followed by orcinol and Coomassie Blue staining, the final product revealed a single band positive for both dyes at R_f of 0.33. Negative ion electrospray (ESI) mass spectrometry confirmed the purity and identity of the product with the signature peak at m/z 795.5, corresponding within experimental error to the SGG $(M-H)^-$ anion calculated from the chemical structure (Franchini et al., 2008).

For SGG quantification by mass spectrometry, two forms of $^2H_3$-labelled SGG were prepared for use as internal standards (IS) (Franchini et al., 2008). One form contained the deuterium label on the alkyl chain, and the other form contained the deuterium label on the acyl chain. In the work reported here, the alkyl chain-labeled form was used as the IS. The identity and purity of this product was determined by NMR spectroscopy and negative ion ESI mass spectrometry which revealed an intense ion at

m/z 798.5 corresponding to the $(M-H)^-$ anion, and the MS/MS spectrum revealed an informative product ion at m/z 542 corresponding to the loss of the fatty acyl chain [M-$C_{16}O_2H_{31}]^-$ in addition to the expected strong signal at m/z 97 corresponding to HSO_4^- (Franchini et al., 2008).

2.18.3. Combined Liquid Chromatography Mass Spectrometry (LC-MS)

After centrifugation, aliquots of the lipid extracts (typically 100 µl) were injected onto a reverse phase HPLC column (Supleco Ascentis® Express, C18, 150 x 2.1 mm) equilibrated in buffer A (methanol/water, 95/5, v/v, containing 1 mM ammonium acetate), and eluted (100 µl/min) with an increasing concentration of buffer B (chloroform/water, 500/0.2, v/v, containing 1 mM ammonium acetate; min/%B, 0/0, 5/0, 55/100). The effluent from the column was split, with a portion (about 70%) directed to a fraction collector (1 min fractions) and the remainder (about 30%) passed to an Ionspray® source connected to the triple quadrupole mass spectrometer (PE Sciex API III^+) operating as described above.

For SGG quantification, $^2H_3$-SGG (100 pmol in 20 µl of chloroform/methanol, 1/1, v/v) was added to each sample of testis (from 0.2 mg of testis wet weight) or sperm (from 0.7 million sperm) lipid extracts which had been previously redissolved in acetonitrile/methanol/water/acetic acid (41/23/36/1, v/v/v/v, 180 µl). Aliquots of this solution (typically 100 µl) were subject to HPLC as described above. The effluent from the column was passed to an Ionspray source connected to a triple-quadrupole mass spectrometer (Sciex API III^+ Perkin Elmer-Sciex Instruments, Thornhill, Ontario, Canada). Data were collected using instrument manufacturer-supplied software (TUNE version 2.5-FPU and RAD version 2.6-FPU) in the tandem mass spectrometric (MS/MS)

mode by multiple reaction monitoring (MRM) of transitions selected for SGG (m/z 795.6→ 97.0 and 795.6→ 539.5) and $^{2}H_3$-SGG (m/z 798.6→97.0 and 798.6→ 542.3) under conditions previously optimized for maximal signal production from SGG (orifice 120 volts, collision gas (argon) thickness at an instrumental (CGT) setting of 200). Peak areas and heights for the SGG and $^{2}H_3$-SGG signals were recorded using instrument manufacturer-supplied software (MacSpec version 3.3). Calculations of the amount of SGG in each sample, made from the amount of internal standard added to each sample adjusted by the relative intensity of the two sets of signals, assumed 100% purity of the IS synthesized as the sodium salt.

To prepare sulfated glucosylceramide, total lipid extract from rat kidneys was dissolved in acetonitrile/methanol/water/acetic acid (41/23/36/1, v/v/v/v), and sonicated for 1 min. After centrifugation to remove any insoluble particulates, the supernatant was subject to HPLC as described above. The effluent from the column was passed onto an Ionspray source connected to a triple-quadrupole mass spectrometer (Sciex API III^{+} Perkin Elmer-Sciex Instruments, Thornhill, Ontario, Canada). The fractions containing the ion at m/z 778.5, corresponding to $[M-H]^{-}$ of sulfated glucosylceramide, was monitored negative ion ESI-MS. All fractions that contained the lipid (fractions 26 to 28) were pooled and used for ESI-MS/MS determination of its fragmentation pattern.

2.19. Statistical Analyses

Student *t*-test and ANOVA were used to determine a significant difference between control and treated groups, or between WT and *ASA* KO male mice. Specifically, ANOVA was used to determine significant differences between: (1) the

numbers of sperm bound per egg of the control and anti-ASA-treated samples; (2) the numbers of sperm bound per egg of the WT and *ASA* KO mice; and (3) the levels of ASA binding to sperm in the control incubations and in those with competitors included. The Student *t*-test was used to analyze significant difference in the average data for the percentage of eggs fertilized by control and experimental groups, or by WT and *ASA* KO sperm. Significant differences between the percentages of fertilized eggs retrieved from females inseminated with anti-ASA IgG-treated sperm and from those injected with PRS IgG-treated (control) sperm were also analyzed by Student *t*-test. A *P* value of less than 0.05 was considered to be statistically significant.

CHAPTER THREE

RESULTS

3.1 Roles of Arylsulfatase A (ASA) in Sperm-Egg Interaction

3.1.1. Production of Anti-ASA Antibodies

Two anti-ASA antibodies were generated; one against human liver ASA (produced by Drs. Weerachatyanukul and White; (Tantibhedhyangkul et al., 2002) and the other against pig sperm ASA (produced by Ms. Antunes and Ms. Costa Santos; (Wu et al., 2007b). The rabbit polyclonal antibody, generated against human liver ASA, recognized pig sperm ASA as shown by immunoblotting (Figure 3.1). Since the amino acid sequences derived from the cDNA sequences of human and pig testis ASA have high identity to that of mouse testis ASA (85% and 82%, respectively) (Stein et al., 1989; Carmona et al., 2002a; Kreysing et al., 1994a), the anti-ASA reactive protein band of solubilized mouse sperm on the immunoblot (Figure 3.1, lane 3) should represent ASA in these cells. Note that mouse sperm ASA had a similar molecular mass, i.e., ~68 kDa, as human liver, and pig sperm ASA. The second polyclonal anti-ASA antibodies generated against purified pig sperm ASA recognized pig sperm ASA as well as purified human liver ASA (Sarafian et al., 1982) and mouse sperm ASA, indicating its specificity to ASA. Since both polyclonal anti-ASA antibodies recognized pig and mouse sperm ASA, the two antibodies were used interchangeably in the current studies.

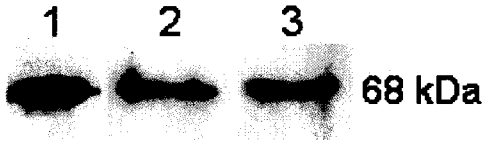
1
2
3
68 kDa

Figure 3.1. Reactivity of anti human liver ASA antiserum with human liver ASA, pig sperm ASA and mouse epididymal sperm ASA. Lane 1: 1.0 μg purified human liver AS-A; lane 2: 1.4 μg purified pig sperm ASA; lane 3: 2 x 10^6 mouse epididymal sperm. Note that the figure is made from previously published results obtained from different experiments. Thus, this figure is used only to show the antibody specificity. It is not for quantitative purpose.

3.1.2. Immunolocalization of ASA in the Male Reproductive System

To elucidate how ASA, generally known as a lysosomal enzyme, targets to the surface of mature sperm (Tantibhedhyangkul et al., 2002; Carmona et al., 2002a), immunocytochemistry of mouse testis and epididymis sections and IIF of live mouse sperm were performed using affinity-purified anti-ASA IgG antibody. All experiments, performed with tissues and sperm collected from five different mice, gave consistent results. The figures shown are representative of three experiments. Drs. Anupriwan and Weerachatyanukul contributed to this work along with me.

3.1.2.1. Testis Localization

Immunocytochemical localization of ASA on the testis sections at the light microscopic levels revealed the presence of ASA in spermatids, with intense immunoreactivity in the developing acrosome of round spermatids and to the acrosome ridge of elongating spermatids (Figure 3.2a and b). No ASA immunoreactivity was detected in the primary spermatocytes or spermatogonia. Nor was it detected in the lumen of seminiferous tubules (Figure 3.2a and b). ASA staining was also present in the cytoplasm of Sertoli cells, appearing from the base of the seminiferous epithelium toward the supranuclear region, which was stained with higher intensity and showed globular patterns. This localization pattern suggested that the enzyme compartmentalized into cytoplasmic organelles, presumably lysosomes (Figure 3.2a). Early residual bodies did not show any immunoreactivity. In contrast, late residual bodies were intensely stained (Figure 3.2b). Preimmune rabbit IgG produced only background levels of staining (Figure 3.2c), suggesting that the immunocytochemical staining observed in the

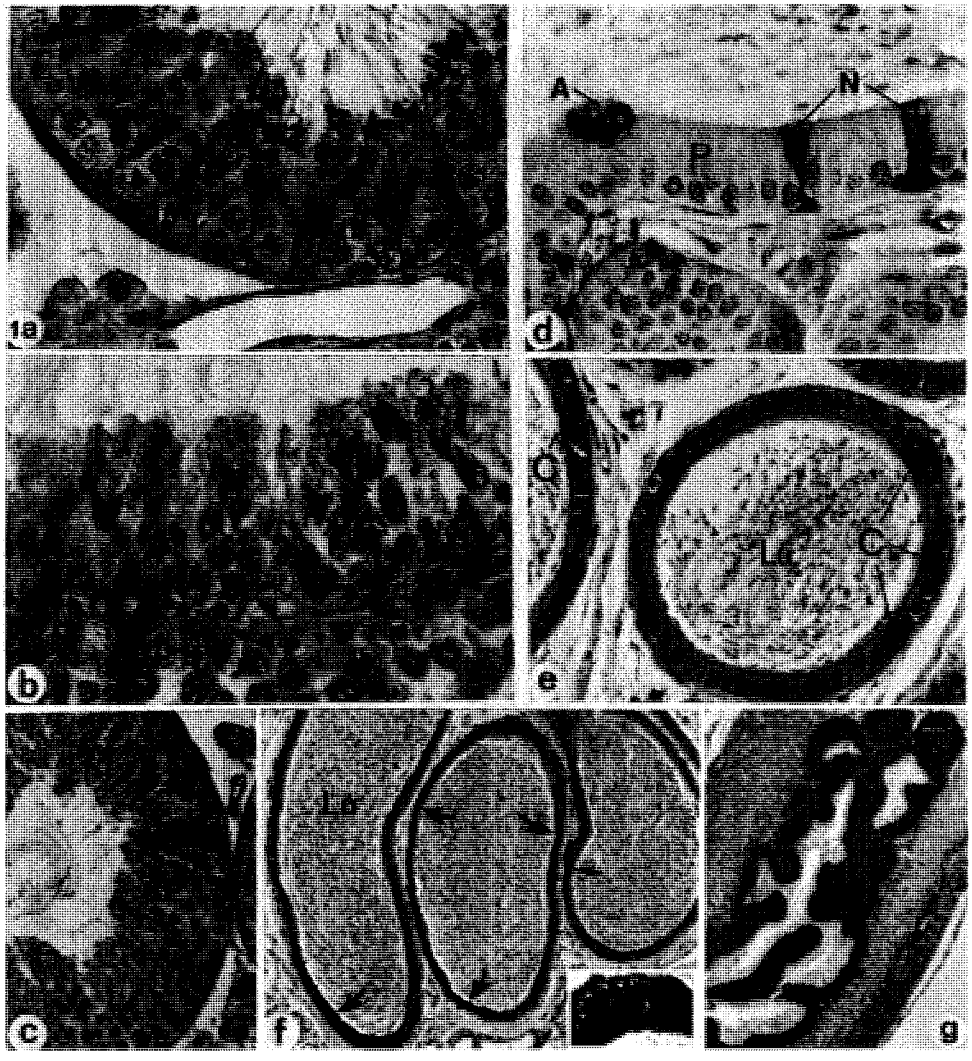
1a
A
N
P
d
b
Q
LC
CV
e
c
1a
f
g

Figure 3.2. Light microscopic immunocytochemistry for ASA in testis and epididymis sections of adult mice. Sections in **a**, **b**, and **d**–**f** were exposed to anti-ASA IgG, whereas the section shown **c** was incubated with PRS IgG. **a**) The seminiferous epithelium of the testis is at stage VII of the cycle. At this stage, the immunoperoxidase reaction product is intense in Sertoli cells and appears as columns extending from the base of the seminiferous epithelium to the lumen, revealing densely stained globular masses along their length (arrows). Also reactive are the acrosomic systems of early round (large arrowheads) and late elongating (small arrowheads) spermatids. x358. **b**) The seminiferous epithelium is at stage X of the cycle. The Sertoli cells are not intensely reactive at this stage of the cycle; however, the acrosomic systems of the step 10 elongating spermatids are intensely reactive (arrowheads). Also intensely reactive at the base of the epithelium are the late residual bodies (open arrows). x358. **c**) Adjacent seminiferous tubules show no reaction product over the entire seminiferous epithelium (SE) when immunostained with PRS IgG. x235. **d**) In the initial segment of the epididymis, narrow (N) and apical (A) cells are the only cells to show intense reaction; principal cells (P) are unreactive. x358. **e**) In the corpus epididymis, clear cells (C) are intensely reactive, and principal cells (P) are unreactive. x358. **f**) In the cauda epididymis, strips of principal cells show intense reaction (curved arrows), alongside adjacent strips of unreactive principal cells. x235. Inset: Higher magnification reveals network patterns of staining within the cytoplasm. Among the principal cells, a few clear cells also show intense reaction (straight, small arrow). x1092. **g**) In the vas deferens, all principal cells react with the antibody, although the intensity of the staining is weaker than that observed in the cauda epididymis. The lumen (Lu) of the epididymis and its contents do not show any significant reaction. x352

organelles of Sertoli cells, presumably lysosomes, and in the acrosomal machinery of spermatid was specific to ASA.

3.1.2.2. Epididymis Localization

Immunocytochemical results also revealed a cell type- and region-specific expression of ASA in the epididymis. Sperm are released from the testis through efferent ductules and enter the initial segment of the caput epididymis. Here, immunoreactivity was restricted to narrow and apical cells (Figure 3.2d). Narrow and apical cells were identified by their shape and location. Narrow cells have a slender shape and apical cells have an apical location (close to the lumen) of their nuclei. Both cell types are only present in the initial segment (Hermo and Robaire, 2002). In the corpus region, ASA immunoreactivity was observed in clear cells (as identified by their possession of numerous vacuoles (Hermo and Robaire, 2002)), which are responsible for absorption of excess secreted materials (Hermo and Robaire, 2002) (Figure 3.2e). In the caudal region, a much greater number of cells reacted with anti-ASA. The majority of reactive cells often were grouped together, appearing as positively stained strips (Figure 3.2f). These cells spanned from the basal membrane to the apical membrane, showed a brush border at a high magnification and were the majority of the epididymal epithelial cells, and therefore they were identified as principal cells (Hermo and Robaire, 2002). The ASA immunoreactivity in principal cells was over the entire cytoplasm, appearing as network patterns (Figure 3.2f, inset). In the vas deferens, most principal cells surrounding the lumen were reactive for ASA, although the intensity of the staining was not as high as for principal cells in the cauda epididymis (Figure 3.2g). Principal cells are recognized for

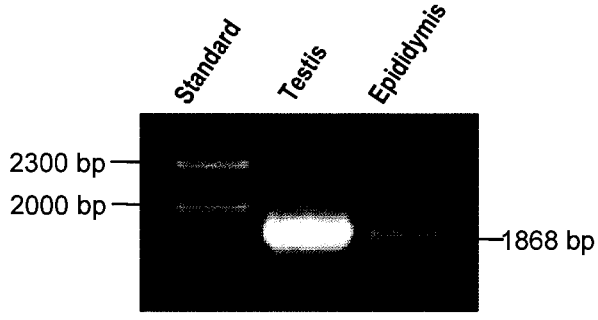
Standard
Testis
Epididymis
2300 bp
2000 bp
1868 bp

Figure 3.3 Long-range RT-PCR products of ASA from mouse testis and cauda epididymis + vas deferens. Total RNA fractions extracted from the testis and from the cauda epididymis and vas deferens were subjected to RT-PCR using ASA primers synthesized based on nucleotides 566–587 and nucleotides 2412–2434 of human testis ASA cDNA sequence. RT-PCR products were then characterized by agarose gel electrophoresis. RNAs from both the testis and the cauda epididymis + vas deferens gave RT-PCR products of the same size (1868 base pairs). DNA size markers are shown in the left lane.

their secretory activities (Hermo and Robaire, 2002; Hermo et al., 2002). The network patterns of ASA staining in principal cells (Figure 3.2f, inset), resembling the endoplasmic reticulum and Golgi apparatus (Robaire and Hermo, 1988), suggest that ASA is synthesized in these cells. However, the staining of ASA in the lumen in both the cauda epididymis and vas deferens was not apparent (see example in Figure 3.2f and g). It is possible that the amount of ASA secreted into lumen may be small and was therefore washed out from the sections during the processing of the tissue sections.

To verify whether ASA is synthesized in the cauda epididymis and vas deferens, the expression of ASA in these tissues was examined by RT-PCR using primers synthesized based on sequences in the 5' and 3' regions of testis ASA cDNA sequence. RT-PCR products of the same size (1868 base pairs) were obtained from both testis and cauda epididymis and vas deferens RNA (Figure 3.3). Since RNA was extracted from the epididymis of 3-week-old mice, when there were no sperm in the epididymis yet, the results implied ASA synthesis in the epididymal epithelium. Nucleotide sequencing revealed 100% identity between these two RT-PCR products, with 100% match to the mouse testis ASA sequence previously described (Kreysing et al., 1994a). These results indicated that the sequence of the ASA transcript synthesized in the epididymal epithelial cells was identical to that from testis.

To further determine whether ASA is secreted into the caudal epididymal and vas deferens lumen, fluid from these reproductive tract regions was collected. Care was taken not to cause much damage to the epithelial cells during collection. Immunoblotting revealed the presence of ASA in the caudal epididymal and vas deferens fluid (Figure 3.4). A single band of ASA was observed, with the same apparent molecular mass of

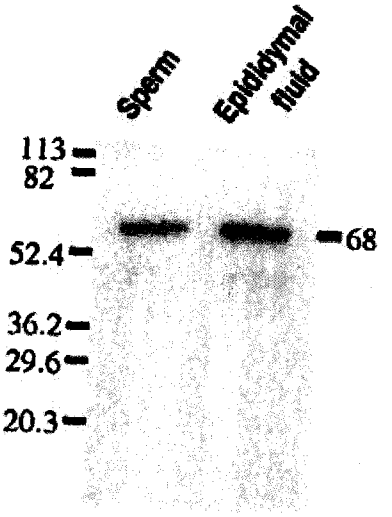
Sperm
Epididymal fluid
113
82
52.4
36.2
29.6
20.3
68

Figure 3.4 Western blot for ASA in epididymal sperm and fluid. ASA in an AES extract of caudal epididymal + vas deferens sperm (left lane) and caudal epididymal + vas deferens fluid (right lane) was detected by Western blot using anti-ASA antiserum. The AES extract prepared from 20×10^6 sperm and 15 μg proteins of epididymal and vas deferens fluid were used.

68 kDa as that of ASA in the mouse sperm surface extract (Figure 3.4). Using ASA purified from the pig sperm surface extract to a single band on SDS-polyacrylamide gels (Carmona et al., 2002a) as a standard, the amount of ASA in the fluid from the cauda epididymis and vas deferens was quantified by ELISA to be 1.28 ng per microgram of total fluid proteins (an average of two analyses with < 4% difference).

3.1.2.3. Localization of ASA in Mouse Sperm

3.1.2.3.1. Immunofluorescence

Indirect immunofluorescence (IIF) revealed the absence of ASA on the surface of live (identified by negative staining for propidium iodide) testicular sperm (Figure 3.5A). A histogram frequency of ASA staining intensity, based on flow cytometry analysis, showed a major peak of testicular sperm (~80% of the total cell analyzed), with background fluorescence intensity similar to that of the negative control cells, i.e., mature sperm (caudal epididymal and vas deferens sperm) that were subjected to PRS IgG and Alexa-488-conjugated secondary antibody (Figure 3.6A). The remaining ~20% of testicular sperm showed ASA immunofluorescence with no consistent patterns. These cells were also stained positive for propidium iodide, indicating that their plasma membrane was compromised (Figure 3.6A). Thus, the fluorescence observed on these cells might reflect nonspecific binding of the primary and/or secondary antibodies to sperm. Taken together, the results suggested that live testicular sperm with intact plasma membranes were devoid of ASA on the surface. Nonetheless, the absence of ASA staining on testicular sperm might be due to the masking of the surface of these cells. To test this possibility, IIF of SGG, a male germ cell surface sulfoglycolipid (White et al.,

2000; Lingwood, 1986; Kornblatt, 1979; Tanphaichitr et al., 1990), was performed with live testicular sperm and mature sperm from the cauda epididymis and vas deferens. Results shown in Figure 3.7 indicated that both testicular and mature sperm exposed to affinity purified anti-SGG IgG possessed specific fluorescent staining patterns, i.e., at the convex ridge of the sperm head and the posterior head region. In contrast, no fluorescence was observed on either sperm types when PRS IgG was used (Figure 3.7C). Therefore, it was apparent that SGG could be detected by IIF on the surface of both testicular sperm and mature sperm, and this argued against the possibility that the testicular sperm surface was masked. The reason why SGG was chosen to determine accessibility of antibodies to the sperm surface was because the sulfated galactose head groups of SGG molecules, the epitopes recognized by anti-SGG antibodies (White et al., 2000), extend only a short distance from the sperm plasma membrane bilayers. Unlike SGG, ASA is a much larger molecule (50 x 100 angstrom), which would be more exposed on the sperm surface, as compared with SGG. The majority of caput and corpus epididymal sperm did not show ASA immunostaining, whereas the remainder only showed staining in the postacrosomal region of the sperm head (Figure 3.5B). On Percoll gradient centrifuged (PGC) and capacitated live caudal epididymal and vas deferens sperm, however, ASA was localized to the plasma membrane overlying the acrosome (the convex ridge) and the postacrosomal region (Figure 3.5C), the areas of the sperm surface involved in binding to the zona pellucida (Ponce et al., 1994; Chen and Cardullo, 1994; Kerr et al., 2002; Primakoff and Myles, 2002; Wassarman and Litscher, 2001). Preimmune IgG produced only background levels of fluorescence (data not shown). The results indicated the presence of ASA on the mouse sperm surface.

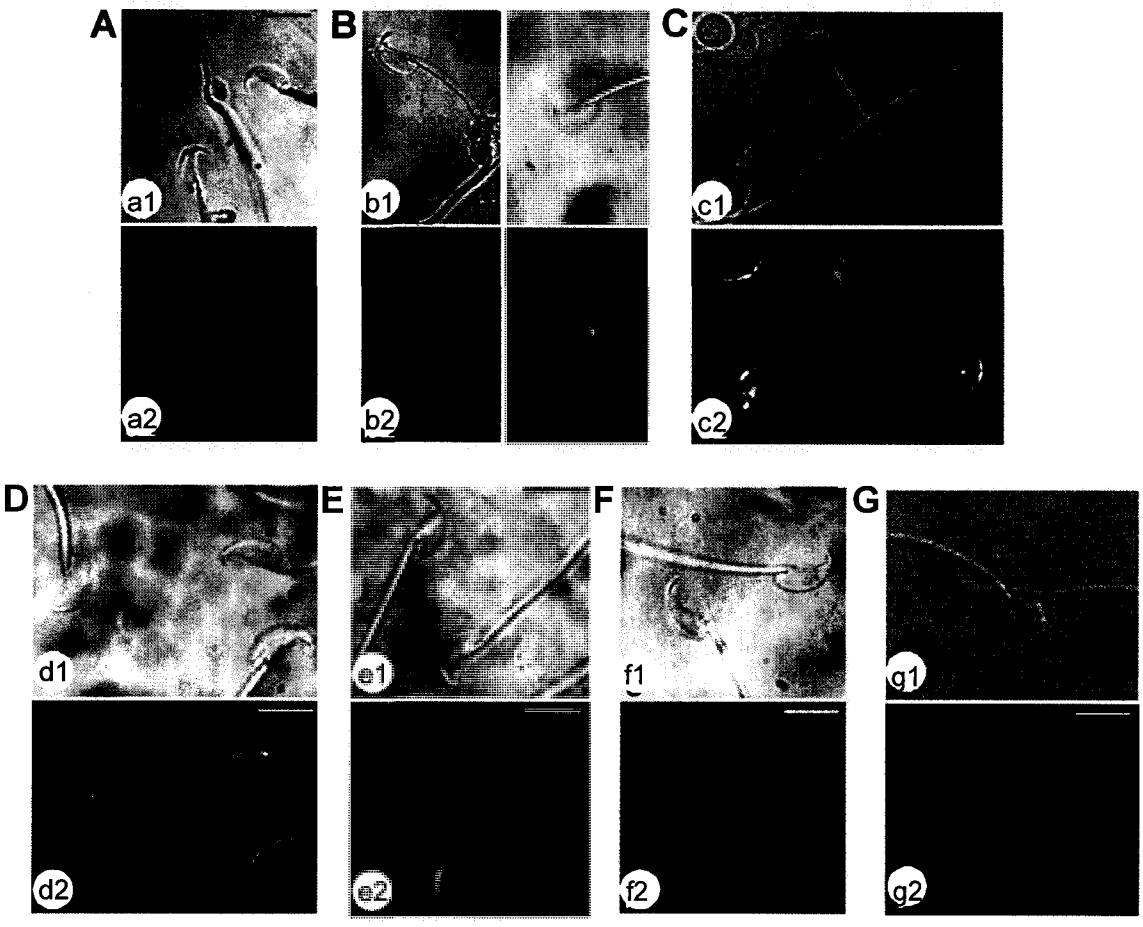
A
a1
a2
B
b1
b2
C
c1
c2
D
d1
d2
E
e1
e2
F
f1
f2
G
g1
g2

Figure 3.5. Indirect immunofluorescence for ASA on mouse sperm. Live testicular sperm (A), caput and corpus epididymal sperm (B), caudal epididymal and vas deferens sperm (C), oviductal/uterine sperm (D), aldehyde/methanol fixed caudal epididymal and vas deferens sperm (E) and aldehyde/methanol fixed caudal epididymal and vas deferens sperm treated with Triton X-100 (F) were exposed to anti-ASA IgG followed by fluorescent secondary antibodies. Preimmune IgG produced only background levels of fluorescence on the aldehyde-fixed and methanol-permeabilized sperm (G). Top panels (a1, b1, c1, d1, e1, f1, and g1) are phase contrast micrographs, and bottom panels (a2, b2, c2, d2, e2, f2, and g2) are immunofluorescent micrographs, respectively. Note the absence of ASA staining in testicular sperm (a2) and positive ASA staining in the head (convex ridge and postacrosome) of caudal epididymal and vas deferens sperm (c2). The majority of caput and corpus epididymal sperm did not show ASA staining, whereas the remainder revealed staining in the postacrosome of the sperm head (b2). Importantly, ASA was retained on the sperm head surface after in vivo capacitating in the oviduct (d2), implicating its role in ZP binding. The immunofluorescence of ASA on aldehyde/methanol fixed caudal epididymal and vas deferens sperm (e2) suggested its acrosomal localization. Bar = 10 μm

Consistent with the ASA localization on *in vitro* capacitated sperm, IIF of oviductal/uterine sperm revealed the presence of ASA staining on the sperm head at the convex ridge with similar levels of fluorescent staining (Figure 3.5D). This indicated that the enzyme was retained on the surface of these *in vivo* capacitated sperm. IIF of live noncapacitated caudal epididymal and vas deferens sperm showed staining of ASA with the same pattern as capacitated sperm collected from the same parts of the male reproductive tract, although the intensity of the fluorescent staining was lower in the former (data not shown). This suggested that ASA was on the surface on noncapacitated sperm but may be partially masked.

The existence of ASA in the sperm acrosome has been reported in several mammalian species (Dudkiewicz, 1984; Brandon et al., 1997), but not in mice. Attempts were therefore made to localize the enzyme intracellularly in mouse sperm. IIF of aldehyde-fixed and cold methanol-permeabilized sperm with anti-ASA IgG revealed the presence of ASA in the acrosomal region, suggesting the presence of the enzyme in the acrosome (Figure 3.5E). However, after treatment of sperm with 0.625% Triton X-100, the fluorescent staining of acrosomal ASA diminished (Figure 3.5F), corroborating the immunoblotting results showing a significant decrease of the ASA signal in the detergent-treated sperm (Figure 10A, lane 2). However, the decrease observed by IIF was more prominent than that revealed by immunoblotting. This may be due to several washing steps involved in IIF, which may have caused further release of ASA from sperm. In contrast, preimmune IgG produced only background levels of fluorescence on the aldehyde-fixed and methanol-permeabilized sperm (Figure 3.5G).

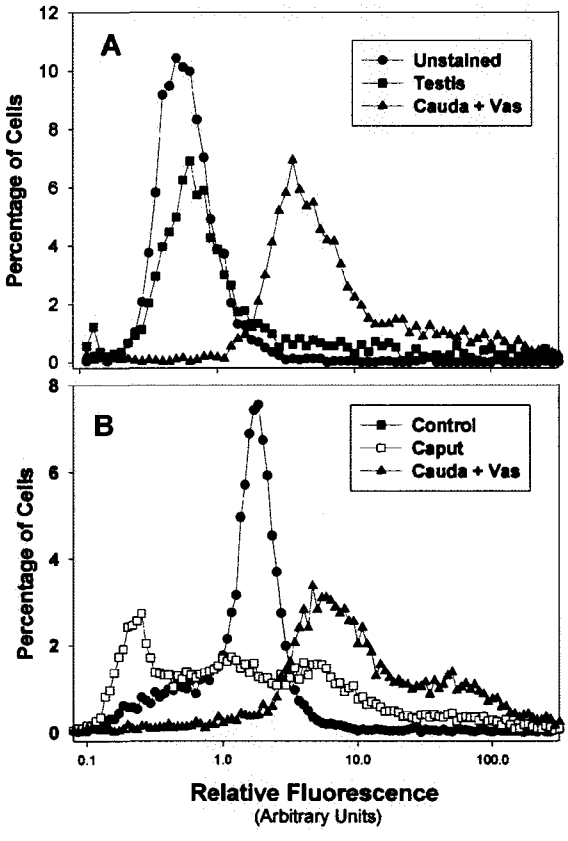
A
Unstained
Testis
Cauda + Vas
Percentage of Cells
12
10
8
6
4
2
0
B
Control
Caput
Cauda + Vas
Percentage of Cells
8
6
4
2
0
0.1
1.0
10.0
100.0
Relative Fluorescence
(Arbitrary Units)

Figure 3.6. Flow cytometry analysis of sperm surface ASA. Frequency histogram of ASA staining intensity of testicular (—■—), caput epididymal (—□—), and caudal epididymal and vas deferens (—▲—) mouse sperm analyzed by flow cytometry. Sperm exposed to PRS IgG served as a negative control (—●—). **A**) Comparison between testicular sperm and caudal epididymal and vas deferens sperm. **B**) Comparison between caput epididymal sperm and caudal epididymal and vas deferens sperm. Note the absence of ASA on testicular and caput sperm.

To determine whether acrosomal ASA is exposed on the sperm surface after acrosome reaction (AR), IIF of acrosome-reacted sperm using anti-ASA IgG was performed. Acrosome-reacted sperm were differentiated from acrosome-intact sperm by their dissimilar reactivity to an antibody against Izumo, a protein responsible for sperm/egg fusion (Okabe et al., 1987; Inoue et al., 2005). The reason for the use of this antibody was because Izumo is absent on the surface of acrosome-intact sperm, but is localized to the entire sperm head region only after the acrosome reaction (Inoue et al., 2005). I first validated the use of Izumo as an acrosome-reacted sperm marker by studying the correlation between OBF13 (a mouse monoclonal IgG against Izumo) (Inoue et al., 2005) immunoreactivity of live sperm and their acrosomal status (which was revealed by Coomassie blue G-250 staining (Moller et al., 1990) (Figure 3.8B)). Only live sperm were evaluated for anti-ASA immunostaining (Figure 3.8A). Live sperm were identified by positive staining with Mito tracker, a cell-permeant probe that is readily sequestered by the actively respiring mitochondria in living cells. Capacitated sperm were induced to undergo acrosome reaction by treatment with 10 μM calcium ionophore (A23187) for 30 min (37°C, 5% CO_2). Half of the treated sperm were subject to IIF with OBF13 and the other half was stained with Coomassie blue to verify the use of Izumo as the marker of acrosome-reacted sperm. Coomassie blue staining revealed that 75 ± 10% of the treated sperm became acrosome reacted, while 73 ± 10% of the sperm were stained positive by OBF13. The correlation coefficient for the two methods was 0.996. The spontaneous acrosome reaction rates (that is, ZP agonist-independent) were 12 ± 4% and 9 ± 4%, as revealed by Coomassie blue staining and OBF13 labelling,

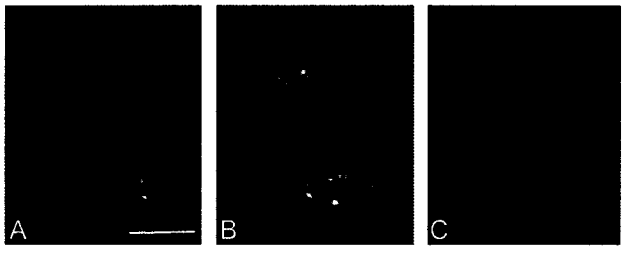
A
B
C

Figure 3.7. IIF for SGG on live mouse testicular (A) and caudal epididymal and vas deferens (B) sperm. **A** and **B)** Sperm were incubated with affinity-purified anti-SGG IgG. **C**) Caudal epididymal and vas deferens sperm were exposed to PRS IgG. Note the presence of SGG staining on the convex ridge and postacrosomal region in both testicular sperm and mature sperm. Bar = 10 μm

respectively (Figure 3.8D). The results suggested that Izumo can be used as an acrosome-reacted sperm marker.

To localize ASA in acrosome-reacted sperm, capacitated sperm were treated with A23187 (10 μM) for 10 min to induce the acrosome reaction. Under this condition, ~50% of sperm underwent acrosome reaction. With the acrosomal status being distinguished by the OBF13 labeling (Figure 3.8A and C, green fluorescence), IIF with anti-ASA IgG revealed positive staining at the dorsal ridge (presumably over the inner acrosomal membrane) of the acrosome-reacted sperm as well as on the plasma membrane of acrosome-intact sperm (Figure 3.8C, red fluorescence). The localization of ASA to this region on the capacitated acrosome-intact sperm head surface was consistent with our previously published results (see above and (Tantibhedhyangkul et al., 2002)). In contrast, background fluorescence was observed when these sperm were exposed to preimmune IgG or normal mouse IgM instead of anti-ASA IgG or OBF13 (data not shown). This result indicated that ASA was on the plasma membrane of the convex ridge of acrosome-intact sperm as well as on the surface of acrosome-reacted sperm (presumably the inner acrosomal membrane).

3.1.2.3.2. Immunogold Transmission Electron Microscopy

The localization of ASA in sperm as revealed by IIF was further confirmed by electron microscopic immunoprotein-A gold labeling (Figure 3.9). At the transmission electron microscopy level, live caudal epididymal and vas deferens sperm were treated with anti-ASA IgG, and the antibody-antigen complexes were detected by incubating treated sperm with protein A-gold. Gold particles were observed on the plasma membrane in the dorsal part and the postacrosomal region of capacitated sperm

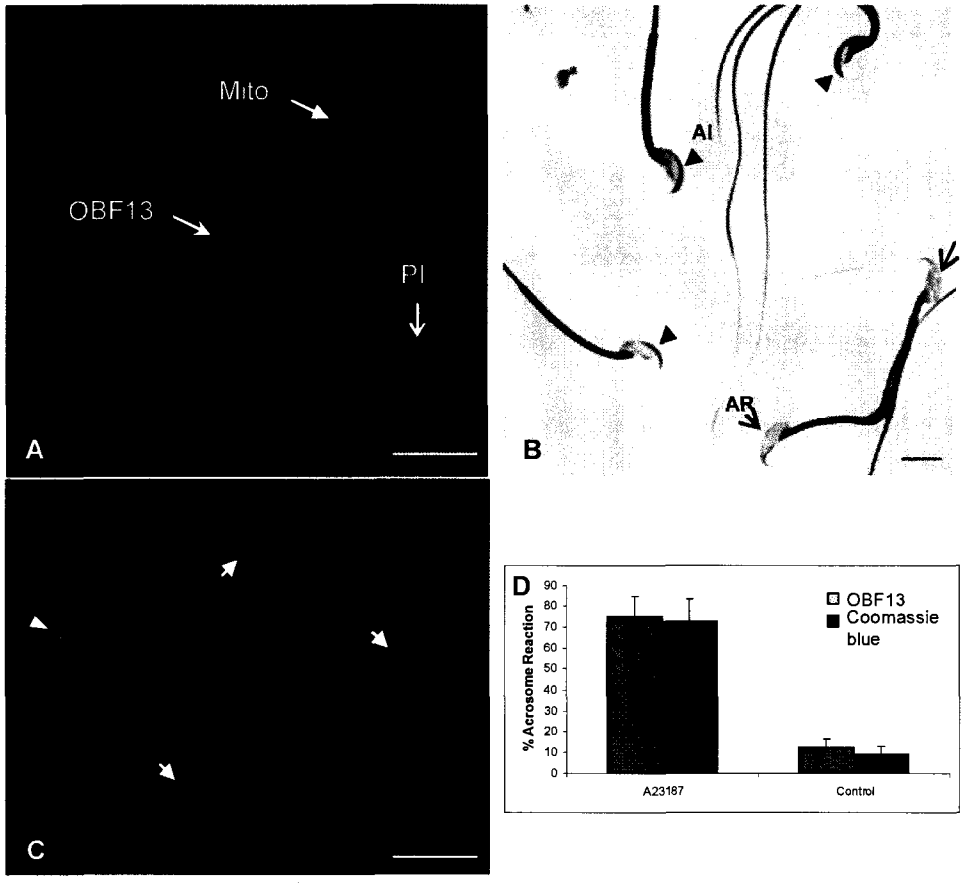
Mito
OBF13
PI
A
AI
AR
B
C
D
% Acrosome Reaction
90
80
70
60
50
40
30
20
10
0
OBF13
Coomassie blue
A23187
Control

Figure 3.8. IIF for ASA on acrosome reacted sperm. Caudal epididymal + vas deferens sperm were capacitated in vitro in KRB-BSA for 30 min and then induced to undergo acrosome reaction with calcium ionophore A23187 for 10 min. The acrosomal status of the sperm revealed by the labeling with OBF13, a monoclonal antibody against Izumo which is localized to the entire sperm head only after acrosome reaction (A) and by Coomassie blue staining (B) showed high correlation (D). The viability of the sperm was shown by the positive staining with MitoTracker (Mito) and the negative staining of propidium Iodide (PI) (A). (C) The sperm were simultaneously labeled with OBF13 (green) and anti-ASA IgG (red). The nuclei were shown by Hoechst (blue). Note that ASA was present on acrosome intact (arrow head) as well as on acrosome reacted (arrow) sperm. Bar = 10 μm.

(Figure 3.9a, see enlargements of these regions in a2 and a3). In contrast, preimmune IgG produced minimal numbers of gold particles (Figure 3.9b). This work was done by Dr. Weerachatyanukul.

3.1.2.3.3. Biochemical Characterization of Mouse Sperm ASA

Using purified pig sperm ASA (purified to a single band on SDS-PAGE (Carmona et al., 2002a)) as a standard, the mouse sperm ASA was quantified to be ~70 fg/sperm by immunoblotting and Typhoon imaging analysis. To quantify ASA on the sperm surface and in the acrosome separately, differential extraction methods for membrane proteins and/or acrosomal soluble proteins were used. The sperm plasma membrane and acrosomal soluble components were extracted by 0.625% Triton X-100 solution (Kim et al., 2001). Immunoblotting results indicated that ~70% of ASA was present in this detergent extract, whereas the remainder was in the Triton X-100 insoluble fraction (Figure 3.10A, lanes 1 and 2). This suggested that ASA existed mainly on the membrane and/or in the acrosomal soluble fraction. A sucrose solution (AES) containing a low amount of ATP (1 mM) and EDTA (1 mM) was previously used to extract peripheral plasma membranes from fibroblast cells (Carter and Hakomori, 1977) and from mouse and pig sperm (Tanphaichitr et al., 1993; Tanphaichitr et al., 1998a). Figure 3.10B showed that ASA was indeed present in the AES extract of mouse sperm. Within 20 min of the first ASA treatment, there was no leakage of acrosin, an acrosomal protein marker (Yanagimachi, 1994). This was deduced by the immunoblotting results showing no reactivity of the AES extract with anti-acrosin antibody (data not shown). Therefore, ASA present in this first AES extract would reflect its entity on the plasma membrane. Notably, plasma membrane ASA had the same molecular mass (68 kDa) as ASA

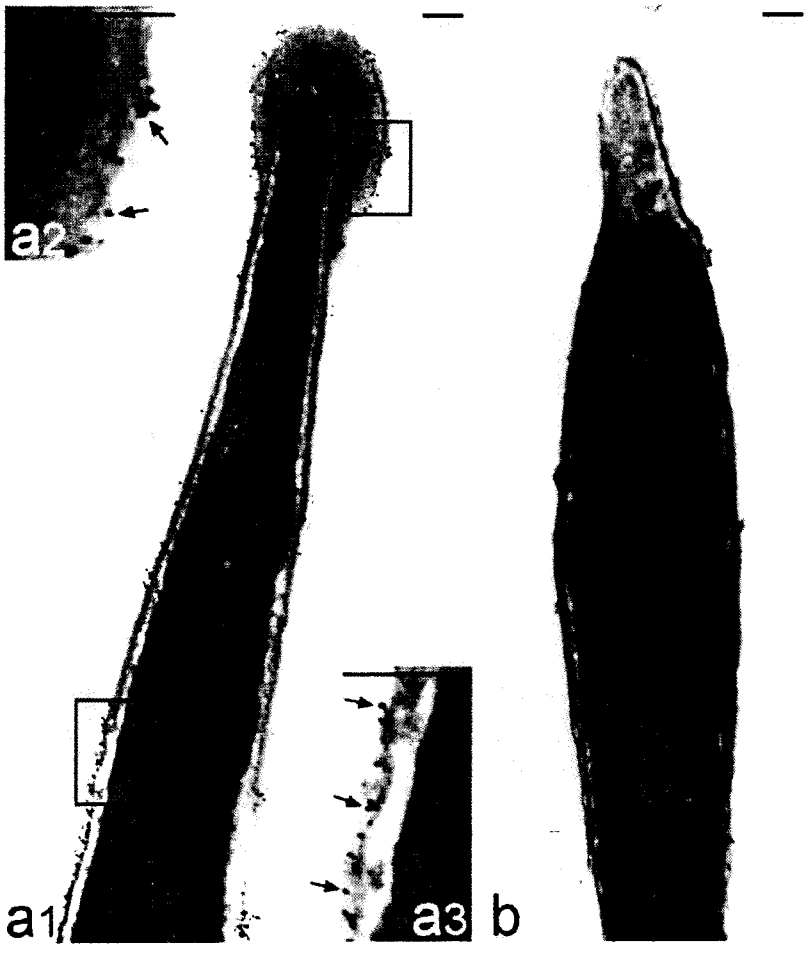
a2
a1
a3
b

Figure 3.9. Immunogold transmission electron microscopy of live sperm. Panel a1: caudal epididymal and vas deferens sperm were exposed to anti-ASA IgG followed by protein A-gold. Enlargements of the selected areas of the sperm head (boxed) were shown in panels a2 and a3. Panel b: negative control, sperm were exposed to PRS IgG instead of anti-ASA IgG. Note the presence of gold particles on the head plasma membrane. Bar = 0.2 μm.

extracted by Triton X-100 from the sperm plasma membrane and the soluble acrosomal components. The amount of plasma membrane ASA in the first AES extract was quantified to be ~0.5% of total ASA in mouse sperm. However, this might be an underestimate of the total amount of plasma membrane ASA. Repeating the AES extraction, which also involved sperm centrifugation, led to leakage of acrosin from sperm, and acrosomal ASA would be expected to be present in the second AES extract. Therefore, the exact amount of ASA on the sperm plasma membrane could not be quantified because plasma membrane ASA and acrosomal ASA appeared to have the same molecular mass. The presence of ASA in mouse sperm was further supported by NCS desulfation activity of plasma membrane-intact (i.e., 0.35 mU/10^6 sperm) and sonicated mouse sperm (i.e., 7.2 mU/10^6 sperm). Although the ASA activity assay of intact sperm was performed at pH 5.0, sperm resuspended in buffer at this pH were viable as evidenced by their exclusion of propidium iodide (>95%). The presence of ASA in the AES extract and the presence of NCS desulfation activity on membrane-intact sperm corroborated the immunolocalization results showing that ASA is present on the sperm plasma membrane.

3.1.2.3.4. Cauda Epididymal and Vas Deferens Sperm Acquire their Surface ASA through its Affinity to SGG

Since ASA has high affinity (K_d = 8.9 nM) for SGG coated as monolayers on microwell plates (Carmona et al., 2002b), it is possible that ASA in the caudal epididymal fluid is deposited onto the epididymal sperm surface, provided that SGG on intact sperm has similar affinity to ASA. To verify this hypothesis, affinity of ASA binding to caudal epididymal and vas deferens sperm was first determined. To confirm that ASA binds

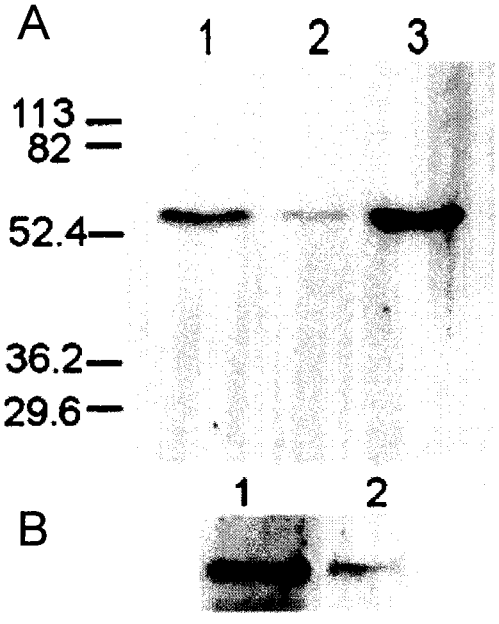
A
1
2
3
113
82
52.4
36.2
29.6
B
1
2

Figure 3.10. Western blot of mouse sperm with anti-ASA antiserum. (A) Mouse sperm (1.2×10^6) were treated with 0.625% Triton X-100 solution, and the Triton X-100 extract is shown in lane 1. Lane 2 displays proteins from the Triton X-100-treated sperm solubilized in SDS-PAGE sample buffer. Lane 3: proteins from 2×10^6 intact mouse sperm solubilized in SDS-PAGE sample buffer. (B) Mouse sperm (4×10^6) were treated with the AES solution, and the AES extract is shown in lane 2. Mouse sperm (2×10^6) solubilized in SDS-PAGE sample buffer is shown in lane 1. Positions of molecular mass markers (in kDa) on the polyacrylamide gel are marked by arrows on the left. Results shown here are representative of those obtained from two replicate experiments.

directly to SGG at the sperm level with similar affinity as that of SGG monolayers is important because the orientation of SGG molecules coated as monolayers may not be the same as that on sperm surface. Figure 3.11 shows that Alexa-430 ASA bound to caudal epididymal sperm in a concentration-dependent manner (Figure 3.11A, open circles). At 60 nM, the binding of Alexa-430 ASA to sperm was approaching saturation (Figure 3.11A). However, binding of Alexa-430 ovalbumin to caudal epididymal sperm was at a very low level (~2% of that observed for Alexa-430 ASA throughout all concentrations used; Figure 3.11A, closed triangles, inset right). The binding of sperm to Alexa-430 ovalbumin was then considered nonspecific, and the values obtained were used for subtraction from the fluorescence values of Alexa-430 ASA binding to sperm prior to kinetic analysis (Figure 3.11B). Fluorescence microscopy revealed that Alexa-430 ASA bound to the sperm head at the convex ridge and the postacrosomal region (Figure 3.11A, insert left). Both of these sites contain SGG (Figure 3.7) (White et al., 2000). When 600 nM unlabeled ASA was included with 60 nM Alexa-430 ASA for sperm incubation, binding of Alexa-430 ASA to sperm was abolished to the background level, implicating specificity of the binding. Analysis of the Alexa-430 ASA-sperm binding curve revealed a K_d of 46.0 ± 15.0 nM ASA (Figure 3.11B), a value within the same range as that of ASA binding to SGG monolayers (Carmona et al., 2002b). The high SD of this K_d value may reflect inherent heterogeneity of sperm quality. When testicular sperm were used in place of caudal epididymal sperm for incubation with Alexa-430 ASA, binding of the enzyme to the sperm surface was not observed (data not shown). Possibly, the sperm surface needed to be modified as part of the continuing

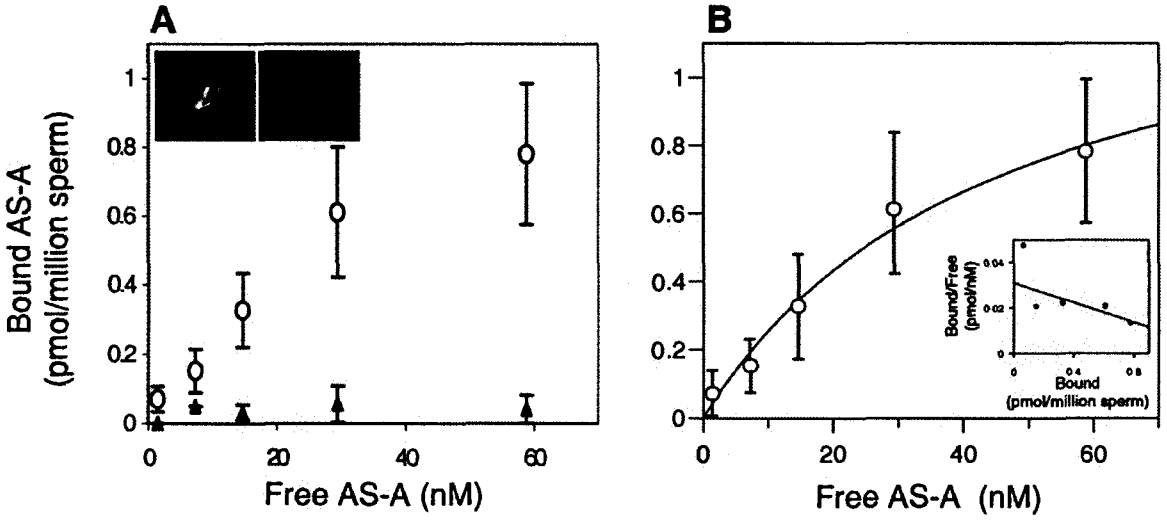
A
B
Bound AS-A
(pmol/million sperm)
Free AS-A (nM)
Free AS-A (nM)
Bound/Free
(pmol/nM)
Bound
(pmol/million sperm)

Figure 3.11. Binding of Alexa-430 ASA to caudal epididymal sperm. Alexa-430 ASA (0–60 nM) was incubated with caudal epididymal sperm (1.2×10^6). After washing the unbound protein from sperm, the level of Alexa-430 ASA binding to sperm (○) was measured spectrofluorometrically. Sperm incubated with 60 nM Alexa-430 ovalbumin (▲) show minimal fluorescence. The amount of Alexa-430 ASA and Alexa-430 ovalbumin bound to sperm was determined from the standard curve of Alexa-430 ASA and Alexa-430 ovalbumin, respectively. **A)** Raw data show the fluorescent pattern of Alexa-430 ASA binding to caudal epididymal sperm included in the left panel of the inset. In contrast, minimal fluorescence observed in sperm incubated with Alexa-430 ovalbumin is shown in the inset right panel. **B)** To eliminate the level of nonspecific binding of Alexa-430 ASA binding to sperm, the fluorescence background of Alexa-430 ovalbumin adhered to sperm was used to subtract the fluorescence reading of sperm-bound Alexa-430 ASA. Inset: Linear Scatchard plot revealed a K_d of 46 nM. Data at each Alexa-430 ASA concentration are expressed as mean ± SD from at least three experimental days. Six replicates of sperm samples were used for Alexa-430 ASA binding for each experimental day.

sperm maturation process during migration through the epididymis to gain the ASA binding ability.

Next, we investigated whether SGG was involved in the acquisition of sperm surface ASA by using anti-SGG IgG to block the sulfoglycolipid. Sperm treated with anti-SGG Fab showed a dramatic decrease in Alexa-430 ASA binding, compared with untreated sperm (Table 3.1). In contrast, sperm treated with PRS Fab did not show any decrease in Alexa-430 ASA binding (Table 3.1). The results strongly suggest that deposition of ASA onto the sperm surface was via its affinity to SGG on the sperm plasma membrane. Because α-mannosidase, an acidic glycohydrolase present in the epididymal fluid, deposits onto sperm via interaction with mannose-6-phosphate receptor on the sperm surface (Belmonte et al., 1998) and because phosphorylation has been identified on the mannose residues of testis ASA *N*-linked oligosaccharides (Sommerlade et al., 1994), ASA deposition onto the sperm surface may also be through its interaction with mannose-6-phosphate receptor. To test this hypothesis, mannose-6-phosphate (having affinity for mannose-6-phosphate receptor) was included in Alexa-430 ASA-sperm coincubates. Mannose-6-phosphate, even at 1 mM, did not inhibit Alexa-430 ASA binding to sperm, indicating that deposition of Alexa-430 ASA onto sperm was not through the mannose-6-phosphate receptor mechanism (Table 3.1).

Table 3.1. Binding of Alexa-430 ASA to mouse sperm is inhibited by anti-SGG Fab but not by mannose-6-phosphate.

Treatment	Concentration (nmol/treatment)	% Control	% Inhibition
None		100	0
Anti-SGG Fab[b]	0.15	44.7 ± 11.5[c]	55
	0.7	38.9 ± 15.1[c]	61
	1.5	32.7 ± 8.1[c]	67
PRS Fab	0.15	109.2 ± 6.3	0
	0.7	119.1 ± 2.2	0
	1.5	116.5 ± 9.8	0
Mannose-6-phosphate	7	98.6 ± 3.6	0
	70	97.5 ± 4.8	0
	350	95.9 ± 6.3	0

[a]200,000 mouse sperm, containing 0.12 nmol SGG, were used for each treatment (see Material and Methods).
[b]The concentration of antiSGG Fab used ranged from 1-10 times of total SGG in the treated sperm.
[c]$P < 0.005$, as compared to controls (no treatment).

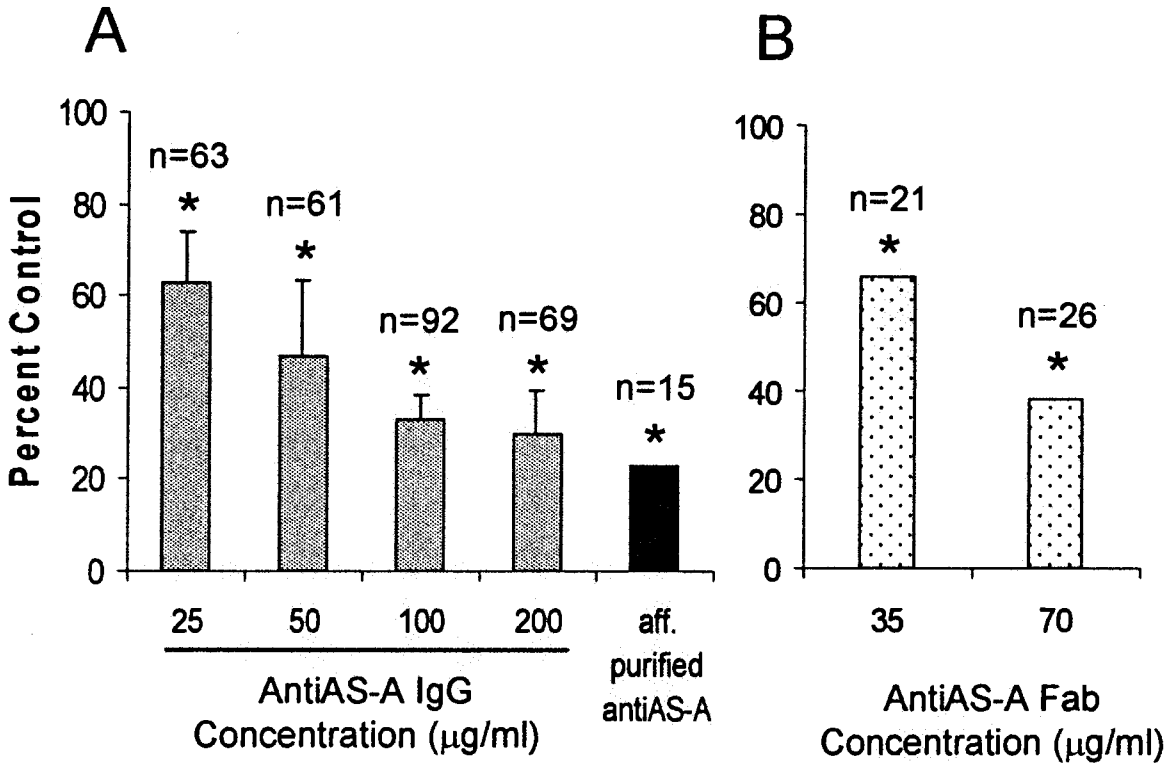
A
B
Percent Control
100
80
60
40
20
0
n=63
n=61
n=92
n=69
n=15
n=21
n=26
*
25
50
100
200
aff. purified antiAS-A
35
70
AntiAS-A IgG Concentration (μg/ml)
AntiAS-A Fab Concentration (μg/ml)

Figure 3.12. Inhibitory effects of sperm pretreatment with anti-ASA on sperm-ZP binding. **A**) Sperm were pretreated with anti-ASA IgG at various concentrations or with affinity-purified anti-ASA IgG before coincubation with eggs. Control sperm were pretreated with 100 μg/ml PRS IgG and coincubated with eggs likewise. **B**) Anti-ASA Fab (35 and 70 μg/ml) and PRS Fab (70 μg/ml) were used in place of anti-ASA IgG and PRS IgG, respectively. The number of sperm bound to egg ZP was counted and expressed as percent control, as compared with the corresponding number of PRS IgG/Fab-treated sperm. n = number of total eggs assessed in each sample. Data are expressed as mean ± SD of percent control of means from three experiments or more, except for the experiments using affinity-purified anti-ASA IgG or anti-ASA Fab, which were done once. * denotes significant difference ($P < 0.05$) from the control samples as determined by ANOVA of raw data (i.e., number of sperm bound/egg).

3.1.3. Roles of Sperm Surface ASA in Sperm-ZP Binding

3.1.3.1. Anti-ASA IgG Inhibited Sperm-Egg Binding

Since ASA was present at the convex ridge and the postacrosomal region of the sperm head, both of which are involved in ZP binding (Yanagimachi, 1994; Chen and Cardullo, 1994; Kerr et al., 2002), its role in sperm-ZP binding was assessed by competitive sperm-egg binding assays. Sperm pretreated with anti-ASA IgG had reduced ability to bind to the egg ZP in a dose-dependent manner, with maximal inhibition of ~70% at the antibody concentration of >100 μg/ml (Figure 3.12A). Affinity-purified anti-ASA IgG also showed inhibitory effects on gamete interaction to the same extent as its equivalent non-affinity-purified anti-ASA IgG (i.e., concentration of 200 μg/ml) (Figure 3.12A), and this suggested that the anti-ASA IgG-induced inhibition of gamete binding was specific to the masking of sperm surface AS-A. This inhibition was not due to steric hindrance attributed by the bivalent nature of IgG, since anti-ASA Fab fragments also exerted similar inhibitory effects (Figure 3.12B). However, the degree of inhibition, when compared with IgG concentrations of the same antigen binding valency, was less pronounced with the Fab fragments (i.e., 34% inhibition for 35 μg/ml anti-ASA Fab versus 54% for 50 μg/ml anti-ASA IgG and 62% inhibition for 70 μg/ml anti-ASA Fab versus 70% for 100 μg/ml anti-ASA IgG) (Figure 3.12B). The lower degree of inhibition of sperm-ZP binding caused by anti-ASA Fab may be due to its lower affinity for ASA compared with anti-ASA IgG.

The decrease of sperm-ZP binding following sperm pretreatment with anti-ASA antibody was not due to an increase in premature acrosome reaction. The majority of sperm (~90%) treated with either 100 μg/ml anti-ASA IgG or 100 μg/ml PRS IgG

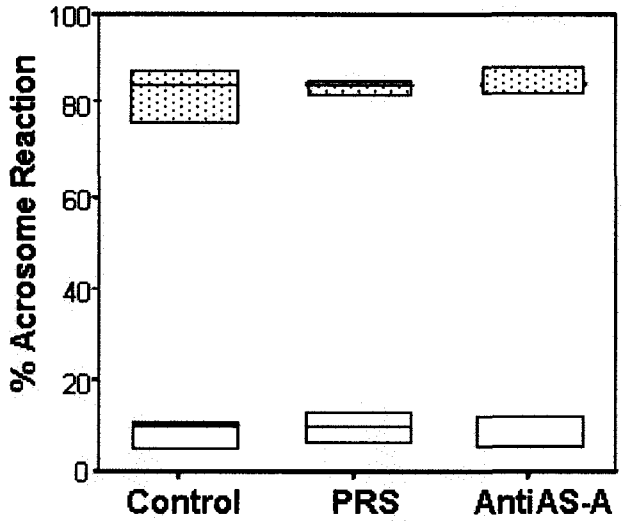
% Acrosome Reaction
100
80
60
40
20
0
Control
PRS
AntiAS-A

Figure 3.13. Effects of sperm treatment with anti-ASA IgG on the acrosome reaction. Empty boxes: spontaneous acrosome reaction (sperm were treated with 100 μg/ml PRS IgG or 100 μg/ml anti-ASA IgG or untreated [control]) (n = 6); dot-filled boxes: ZP-induced acrosome reaction (sperm were treated as those appearing as empty boxes, followed by solubilized ZP) (n = 6). Data were expressed as box plots of medians with the 25–75th percentile range.

remained acrosome intact,. similar to those untreated sperm (Figure 3.13, empty boxes). In addition, these antibody-treated sperm, like the untreated sperm, were able to undergo acrosome reaction upon ZP induction; ~90% of them underwent the acrosome reaction when exposed to 10 solubilized ZP/μl (Figure 3.13, dot-filled boxes).

3.1.3.2. In Vivo Contraceptive Effect of Sperm Treatment with ASA

Our in vitro results indicated the involvement of sperm surface ASA in ZP binding. These studies were conducted in well-defined conditions, where male and female factors were not taken into account. To confirm the physiological significance of ASA in fertilization, effects of anti-ASA IgG treatment on sperm were evaluated in artificial insemination experiments. This was done by comparing the number of eggs fertilized in vivo following insemination of the superovulated females with anti-ASA IgG or PRS IgG treated sperm. Eighty percent of eggs retrieved from females inseminated with PRS IgG treated sperm were fertilized. In contrast, the average percentage of fertilized eggs collected from females inseminated with anti-ASA IgG treated sperm was only 42%, a value significantly lower than that of the controls (PRS IgG treated sperm, $P < 0.001$; Figure 3.14A). When the numbers of fertilized eggs were compared between the paired females inseminated with sperm treated with anti-ASA IgG or PRS IgG (control; Figure 3.14B), the range of in vivo fertilization inhibition was from 20% to 70% of the control values, with an average of 46%. The lower inhibitory effects on in vivo fertilization by sperm treatment with anti-ASA, compared with the results obtained from the in vitro binding assay (Figure 3.12), may be due to the fact that the treated sperm

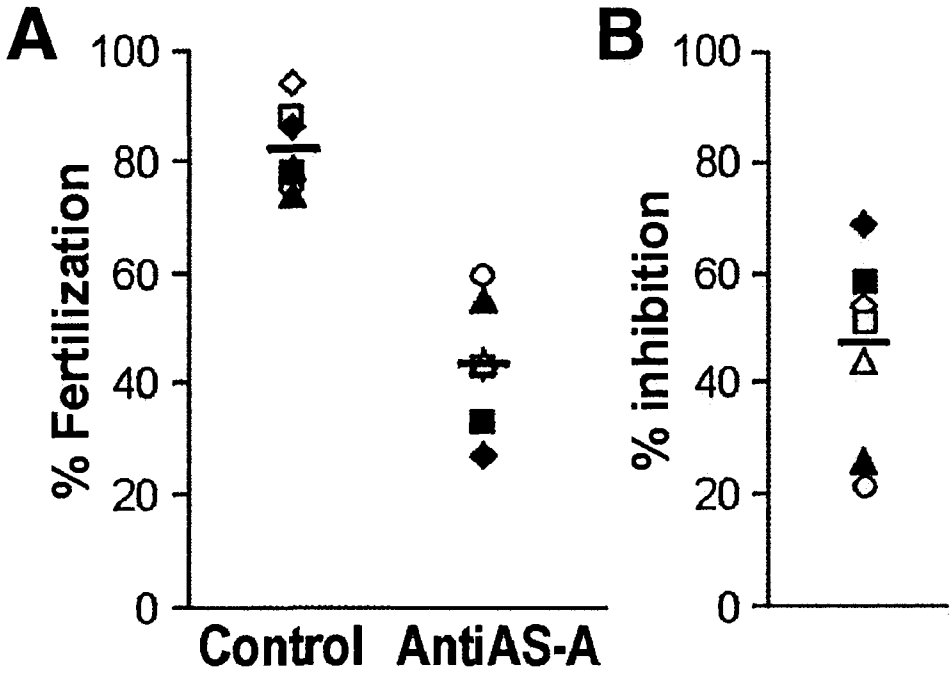
A
100
80
60
40
20
0
% Fertilization
Control
AntiAS-A
B
100
80
60
40
20
0
% inhibition

Figure 3.14. Effects of anti-ASA treatment of sperm on in vivo fertilization. (**A**) Percent fertilization of total eggs (fertilized + unfertilized) retrieved from each female inseminated with the sperm suspension containing either PRS IgG (control) or anti-ASA IgG (200 μg/ml). Each female pair (see *Materials and Methods*) was represented by different symbols. (**B**) Percent inhibition of in vivo fertilization in each female pair. The number of fertilized eggs retrieved from individual females inseminated with the PRS IgG containing sperm suspension was assigned as 100%. Horizontal bars in both **A** and **B** represent means of 7 data points.

suspension used for artificial insemination still contained epididymal fluid, which may have impeded the binding of the antibody to the sperm surface.

3.1.4. Binding of ASA to the ZP and ZP Glycoproteins

3.1.4.1. Binding of Alexa-430 ASA to the Mouse ZP

The results shown above (in Figures 3.5 and 3.12) implicated a direct involvement of sperm surface ASA in ZP binding. To confirm this, direct binding of purified sperm ASA to both intact and solubilized ZP was investigated. Figure 3.15 revealed that Alexa-430 ASA bound to the ZP of unfertilized eggs (A, panel a), while Alexa-430 ovalbumin (A, panel b) did not. All unfertilized eggs incubated with Alexa-430 ASA exhibited similar fluorescent staining. When non-fluorescently labeled ASA (100 x) was included in the coincubation of Alexa-430 ASA and unfertilized mouse eggs, the fluorescent signal on the egg ZP was minimal (data not shown). Furthermore, Alexa-430 ASA bound to solubilized ovarian ZP adhered to the wells of a microtiter plate, and the binding level increased and approached saturation with increasing amounts of Alexa-430 ASA (Figure 3.15B). Scatchard plotting (Figure 3.15B) revealed a K_d of this binding to be 0.21 μM. In contrast, ASA did not bind to the ZP of fertilized eggs (Figure 3.15A, panel c).

3.1.4.2. Characterization of Isolated Mouse Ovarian ZP and Purified ZP Glycoproteins

The localization of ASA to the sperm head surface (Figure 3.5) and the inhibitory effects of sperm treatment with anti-ASA antibodies on sperm-ZP binding (Figure 3.12) suggested that the sperm surface ASA is involved in the primary binding to the ZP. Since ASA is also present in the acrosome (Figure 3.5E) and is detectable on the surface

A

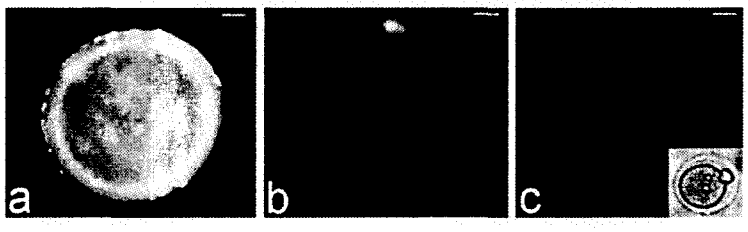
a
b
c

B

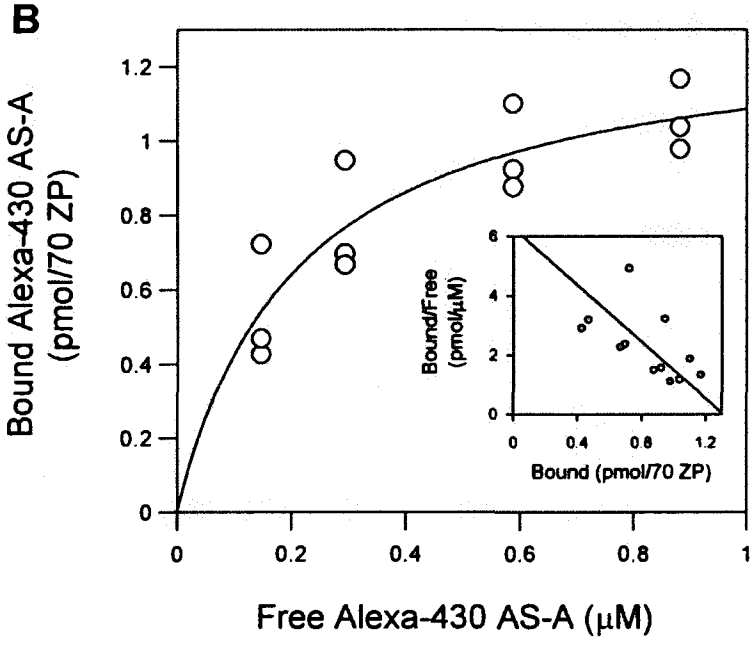
Bound Alexa-430 AS-A (pmol/70 ZP)
Free Alexa-430 AS-A (μM)
0
0.2
0.4
0.6
0.8
1
1.2
Bound/Free (pmol/μM)
Bound (pmol/70 ZP)
0
2
4
6
0.4
0.8
1.2

Figure 3.15. Binding of ASA to the mouse ZP. (**A**) ZP-intact eggs. Unfertilized eggs (20–30) were incubated with 0.15 μM Alexa-430 AS-A (**a**) or with 0.15 μM Alexa-430 ovalbumin (**b**) in a 60-μl droplet of medium. Fertilized eggs (20–30) were also incubated with 10 μg/ml Alexa-430 AS-A (**c**) under the same conditions as those used for unfertilized eggs. Bar = 0.2 μm. Note that only the unfertilized eggs showed the intense fluorescent staining, indicating ASA binding. Results shown here are representative of those obtained from two replicate experiments. (**B**) Solubilized ZP. Seventy solubilized ovarian mouse ZPs were attached to each microtiter plate well and incubated with 0–0.9 μM Alexa-430 ASA, and the fluorescence intensity of Alexa-430 ASA bound to the ZP was measured spectrofluorometrically. The background fluorescence of ZP incubated with 0.9 μM Alexa-430 ovalbumin was used as a blank. The amount of Alexa-430 ASA bound to ZP was determined from the standard curve of Alexa-430 ASA. Open circles represent individual sample points. Linear Scatchard plot analysis (inset) revealed a K_d of 0.21 μM.

of acrosome-reacted sperm (Figure 3.8C), this second entity of ASA may be involved in the secondary ZP binding. If sperm ASA is involved in the primary and secondary ZP binding, it should also possess affinity for the ZP3 and ZP2 sulfoglycoproteins, respectively.

To determine which of the zona glycoproteins could serve as the putative ligand for ASA, the affinity of ASA to ZP1, ZP2 and ZP3 was investigated. These experiments required isolation of ZP in large quantity in order to purify individual ZP glycoproteins. A large-scale ZP isolation protocol was used for this purpose (Litscher et al., 2008), which was based mainly on the physical properties of ZP, e.g., resistance to physical force and a specific sedimentation velocity value. Thus, ZP could be purified from a mouse ovarian homogenate by centrifugation on a Percoll gradient. At the conclusion of centrifugation, ZP banded at a position about one-fourth from the top of the tube (at a density of 1.02 g/ml) (Figure 3.16A). The yield of ZP by this method was about 300 ZP/ovary. The quality and purity of the isolated ZP were evaluated by SDS-PAGE under non-reducing condition. Three zona glycoproteins were resolved on the gel with apparent molecular mass of ~ 200 kDa (ZP1 dimer), ~ 120 kDa (ZP2) and ~ 83 kDa (ZP3), as previously described (Bleil and Wassarman, 1980b). No other protein bands were detected (Figure 3.16B, total ZP).

Individual zona glycoproteins were purified from heat-solubilized ZP by electroelution or size exclusion high performance liquid chromatography (HPLC). Complete solubilization of ZP takes about 15 min, and was monitored under a stereo microscope by the disappearance of intact ZP. Following electroelution, the yield of ZP1, ZP2 and ZP3 was about 35, 200 and 150 ng/ovary, respectively. Silver staining of

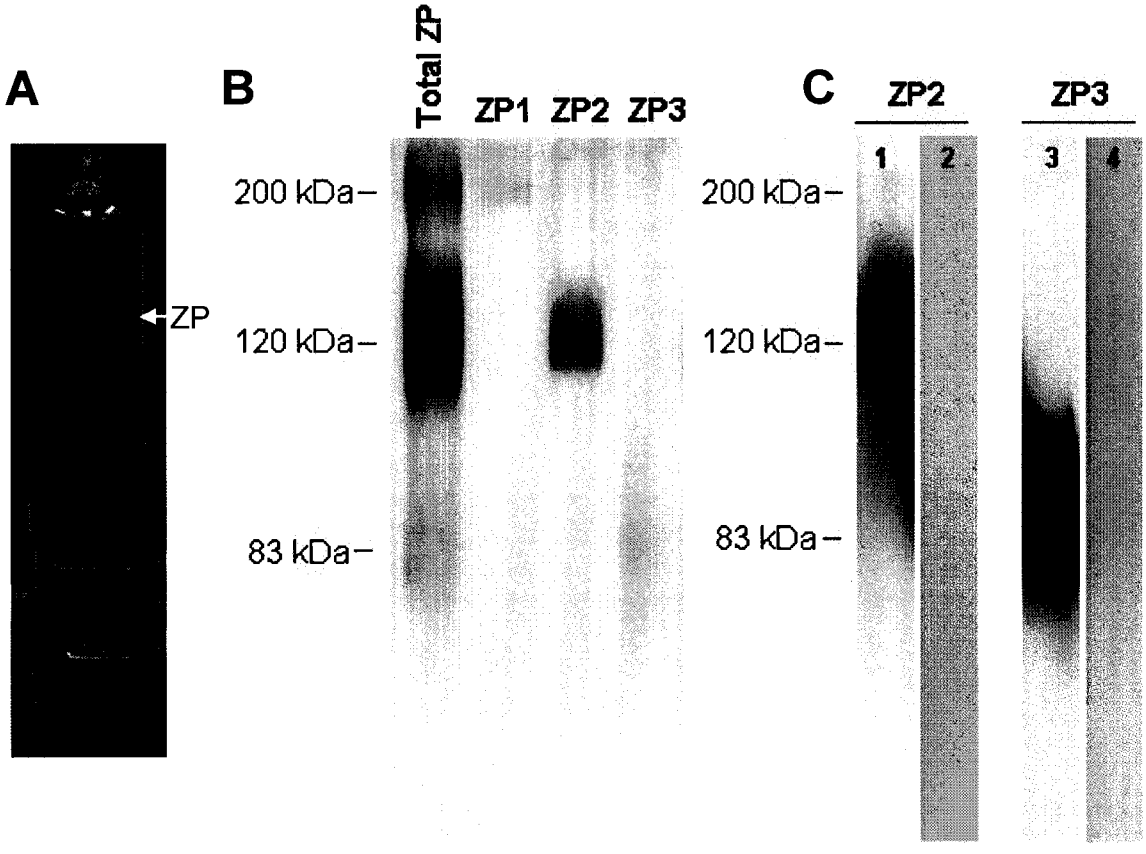
A
ZP
B
Total ZP
ZP1
ZP2
ZP3
200 kDa–
120 kDa–
83 kDa–
C
ZP2
ZP3
1
2
3
4
200 kDa–
120 kDa–
83 kDa–

Figure 3.16. Isolation and Characterization of purified ZP glycoproteins. Mouse ovarian ZP was isolated from ovary homogenate by centrifugation on Percoll gradient, and the ZP banded at a position about one-fourth from the top of the tube (at a density of 1.02 g/ml) (**A**). The isolated ZP was solubilized in 0.2 M sodium phosphate buffer, pH 6.8, containing 0.1% SDS by heating at 65°C for 10 min and then subject to SDS-PAGE followed by electroelution to purify ZP glycoproteins. Solubilized ZP and purified ZP glycoproteins were resolved by non-reducing SDS-PAGE. Purity of each protein was assessed by silver staining (**B**), and the identities of the proteins confirmed by Western blot analyses using monoclonal antibodies against ZP2 and ZP3 (**C**). Lanes 1 and 2 in panel C were purified ZP2 probed with anti-ZP2 and anti-ZP3, respectively. Lanes 3 and 4 in panel C were purified ZP3 probed with anti-ZP3 and anti-ZP2, respectively. The apparent molecular masses of ZP1, 2 and 3 are 200, 120 and 83 kDa, respectively, as indicated.

SDS-PAGE-resolved zona glycoproteins revealed that each of the electroeluted glycoprotein appeared as a single band, free from other ZP glycoproteins (Figure 3.16B). The identities of the mZP2 and mZP3 were confirmed by immunoblotting using monoclonal antibodies specific for ZP2 (East et al., 1984) and ZP3 (East et al., 1985), respectively (Figure 3.16C). Characterization of solubilized ZP by size exclusion HPLC also revealed three distinct peaks (retention time) that corresponded to mZP1 (57.3 min), mZP2 (62.2 min), and mZP3 (66.8 min) (Figure 3.17).

To ensure that isolated ZP glycoproteins were biologically active, I opted to test for the ability of isolated ZP3 on the induction of the acrosome reaction (see INTRODUCTION section 1.6) (Bleil and Wassarman, 1983). Solubilized mouse ZP at the concentration of 8 ZP/μl have been shown previously to induce the acrosome reaction of capacitated sperm effectively (Tantibhedhyangkul et al., 2002). Here, I showed that the isolated mouse ZP, when heat solubilized to the same concentration (8 ZP/μl), induced 64% of capacitated sperm to undergo the acrosome reaction (Figure 3.18). Since ZP3 exists at ~ 35% of total ZP weight, I further tested whether my isolated ZP3 at 9.8 ng/ μl (equivalent to total 8 ZP/μl) could induce the sperm acrosome reaction to the same extent. Figure 3.18 showed that 62% of capacitated sperm underwent acrosome reaction in response to treatment with ZP3, suggesting that the purified ZP3 retained its biological activity. In contrast, sperm incubated in KRB-BSA alone or in KRB-BSA containing ovalbumin or fetuin, two glycosylated proteins that are unable to induce acrosome reaction (Carmona et al., 2002b), showed a similar rate of acrosome reaction (8%, 11% and 14%, respectively), which was a spontaneous type (that is, ZP agonist-independent) (Figure 3.18). Since ovalbumin and fetuin used in these experiments were also subject to

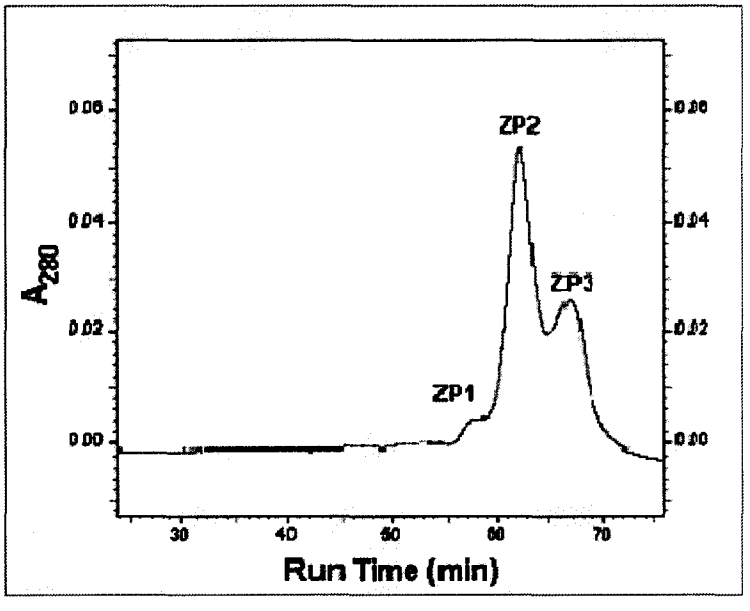
ZP1
ZP2
ZP3
A_{280}
0.00
0.02
0.04
0.06
30
40
50
60
70
Run Time (min)

Figure 3.17. High-performance liquid chromatography (HPLC) of mouse ZP glycoproteins. Shown is an absorption profile at 280 nm following HPLC fractionation of solubilized mouse ovarian ZP purified by centrifugation of an ovarian homogenate on a Percoll gradient (essentially as described in the M & M). Isolated ZP was heat-solubilized in HPLC buffer. After centrifugation to remove insoluble material, the solubilized content was fractionated on a Bio-Sil SEC 250 size-exclusion column. The material was separated into three distinct peaks (retention time) that correspond to mZP1 (57.3 min), mZP2 (62.2 min), and mZP3 (66.8 min).

the electroelution purification process, the induced acrosome reaction by ZP3 was not attributed to the presence of any residual components of the SDS-PAGE buffer (i.e., SDS) or other contaminants incurring during the electroelution process. As a positive control, 74% of capacitated sperm treated with 10 μM calcium ionophore A13287 underwent acrosome reaction, consistent with previously published results (Figure 3.18) (Ward and Storey, 1984). As anticipated, ZP1 and ZP2 lacked this capacity to induce AR (Bleil and Wassarman, 1983), only 8% and 13% of sperm treated with purified ZP2 and ZP1 underwent acrosome reaction, respectively (Figure 3.18).

3.1.4.3. Binding of ASA to ZP Glycoproteins

The direct binding of ASA to solubilized total mouse ovarian ZP and each ZP glycoproteins were tested by Dot-immunoblotting. The amounts of ZP1, ZP2 and ZP3 which reflected their physiological composition (weight ratio of ZP1/ZP2/ZP3 being 15%/50%/35%) were initially used for this binding assay. The results showed that purified sperm ASA bound to solubilized total ZP (1 μg), as well as to the ZP2 (1 μg) and ZP3 glycoproteins (0.7 μg) (Figure 3.19A). However, ASA showed minimal binding to the ZP1 glycoprotein (0.3 μg) (Figure 3.19A). The binding appeared to be specific to the ZP and ZP glycoproteins since ASA exhibited no affinity towards ovalbumin and fetuin immobilized on the same nitrocellulose membrane (Figure 3.19A). Furthermore, when ASA was incubated with 10 x solubilized ZP prior to the incubation with ZP-dotted membrane, the binding of ASA to the ZP on the membrane was minimal (Figure 3.19C, mZP). Similar experiments were performed to determine the specificity of the binding of ASA to ZP2 and ZP3. Due to limited quantities of purified ZP2 and ZP3, ten times the

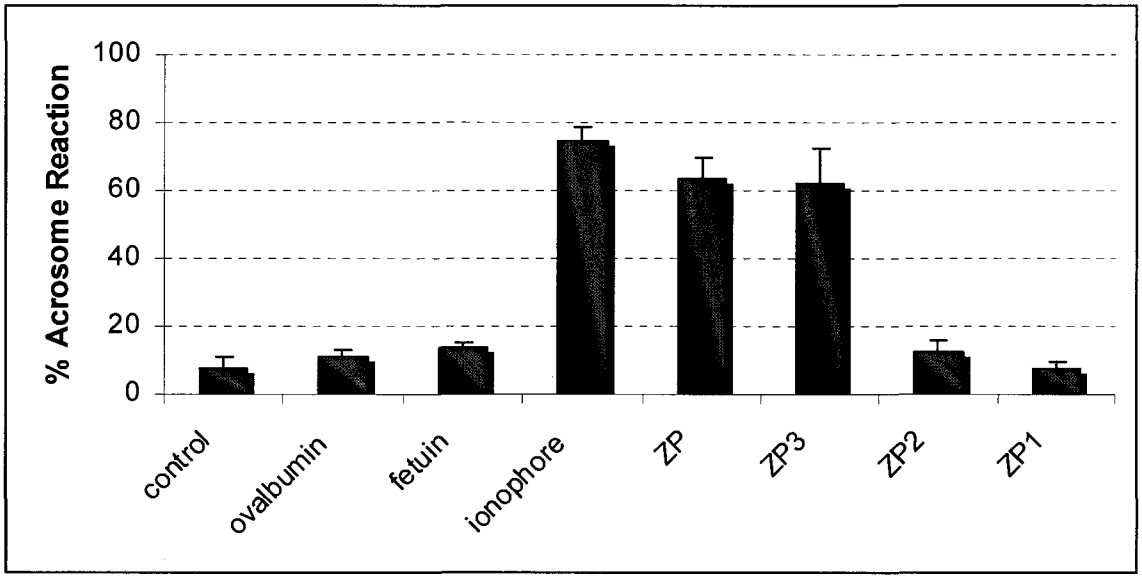
% Acrosome Reaction
100
80
60
40
20
0
control
ovalbumin
fetuin
ionophore
ZP
ZP3
ZP2
ZP1

Figure 3.18. Solubilized mouse ovarian ZP and purified ZP3 retained their biological activity. Capacitated sperm were incubated with solubilized mouse ZP, and purified mZP1, mZP2 and mZP3 at a final concentration of 8 ZP/μl or equivalent for 30 min (37°C, 5% CO_2). Capacitated sperm untreated or treated with ovalbumin (40 ng/μl) and fetuin (40 ng/μl) served as negative controls. Sperm treated with 10 μM A23187 served as a positive control. Ovalbumin and fetuin used had been subject to the same electroelution purification process as that for ZP glycoproteins.

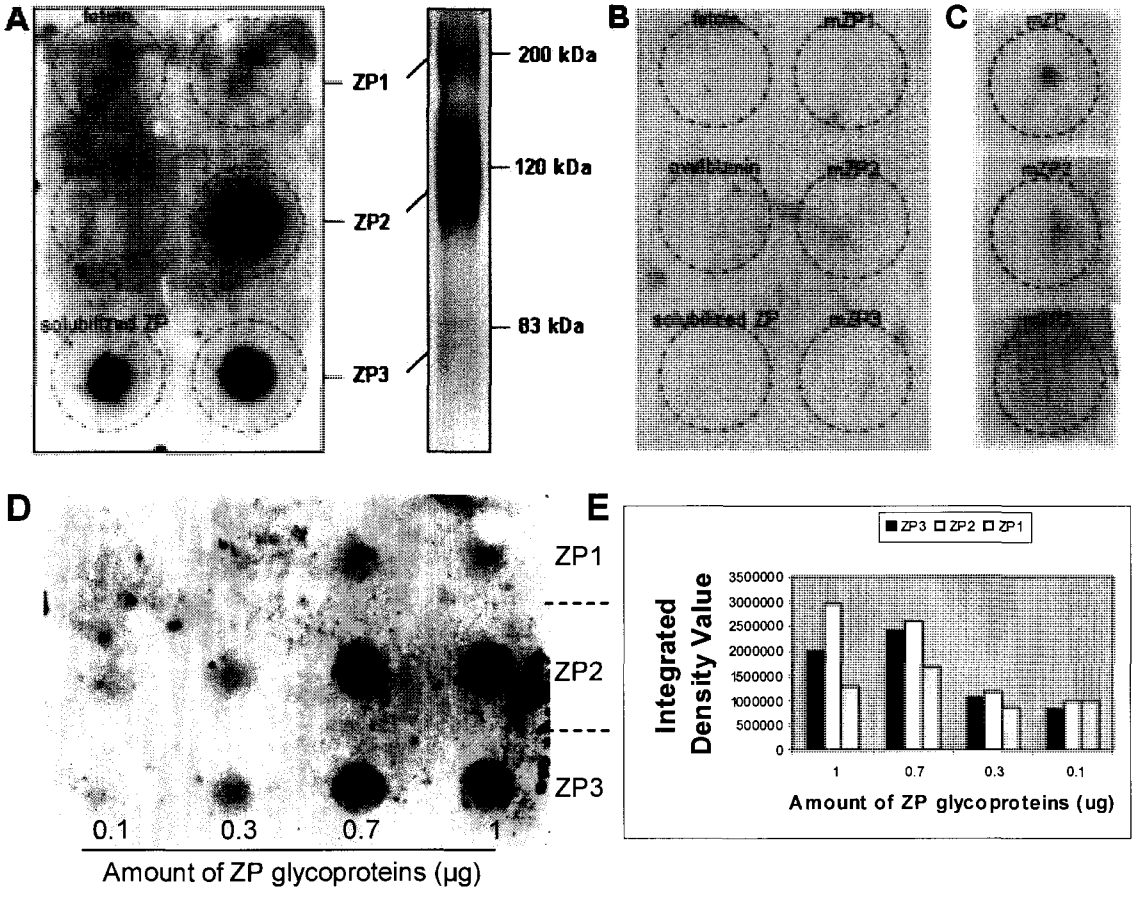
A
ZP1
ZP2
ZP3
200 kDa
120 kDa
83 kDa
B
C
D
ZP1
ZP2
ZP3
0.1
0.3
0.7
1
Amount of ZP glycoproteins (µg)
E
ZP3 ZP2 ZP1
Integrated Density Value
3500000
3000000
2500000
2000000
1500000
1000000
500000
0
1
0.7
0.3
0.1
Amount of ZP glycoproteins (ug)

Figure 3.19. Binding of purified sperm ASA to solubilized mouse ovarian ZP and individual ZP glycoproteins. (**A**) and (**B**) One microgram of fetuin, ovalbumin and slubilized ZP, 0.3 μg of ZP1, 1 μg of ZP2 and 0.7 μg of ZP3 were dotted onto nitrocellular membrane and air dried. After blocking for non-specific binding with 5% skim milk in TBS-0.05% Tween, the membrane was incubated with 3 μg of ASA in 1 ml of TBST in the absence (**A**) and presence (**B**) of 1 μM dextran sulfate and the bound ASA was immunodetected using anti-ASA IgG. The amount of ZP glycoproteins used was based on the weight ratio of ZP1:ZP2:ZP3 to be 15%:50%:35%. (**C**) One microgram each of ZP, ZP2 and ZP3 were immobilized on the membrane. ASA was preincubated with 10 x solubilized ZP prior to the incubation with the membrane (**D**) Different amounts of ZP glycoproteins were dotted onto nitrocellular membrane for the detection of ASA binding as described for **A** and **B**. The relative amount of ASA bound to each ZP glycoprotein was measured by densitometry and results were plotted in (**E**).

amount of solubilized ZP instead of ZP2 or ZP3 was used to incubate with ASA prior to the incubation of ASA and the membranes with dotted ZP2 and ZP3. The results showed that pre-treatment of ASA with excess amount of solubilized ZP reduced the binding of ASA to ZP2 and ZP3 to background level (Figure 3.19C).

When different amounts of zona glycoproteins (in the range of 0.1 to 1 μg) were dotted onto the membrane, ASA bound to the ZP2 and ZP3 glycoproteins in a dose dependent manner (Figure 3.19 D & E). The binding appeared to have reached saturation when 0.7 μg of ZP2 and ZP3 was dotted (Figure 3.19 D & E). When the binding of ASA to equal amounts of different ZP glycoproteins was compared, ASA appeared to have the highest affinity for ZP2 (Figure 3.19 D & E). The binding of ASA to the ZP glycoproteins was likely dependent on the sulfated sugar moieties in the ZP glycans since it was blocked by dextran sulfate (MW 500 kDa) (0.5 mg/ml) (Figure 3.19B).

3.1.4.4. Production, Purification and Characterization of Recombinant WT and Mutant ASA

The results presented above suggested that purified ASA might bind to the ZP and purified ZP glycoproteins via their sulfated sugar moieties. This raised a question whether the active site pocket of ASA, which is the most positively charged area (see INTRODUCTION, Figure 1.9), is required for this binding. In this active site pocket, FGly69 (formylglycine 69, posttranslationally modified from C69) is the active site amino acid, and K302 and K123 are the two amino acids that capture the sulfate group of the substrate for the initial interaction with FGly69 (Schenk et al., 2009; Von Bulow et al., 2001). Although the hydrolysis of arylsulfates occurs at the optimum pH of 5, the

capturing of an arylsulfate/sulfated sugar by K302 and K123 should also take place at neutral pH, since this active site pocket area still remains the most positively charged even at this pH (Figure 1.9) (Schenk et al., 2009). In addition, it is possible that when ASA interacts with the ZP, the negative charges of the ZP glycan moieties may bring their microenvironment into the acidic range and this would endow the highest capacity for K302 and K123 to capture the sulfate group of the substrate. Therefore, two ASA mutants C69A/K123A/K302A, possessing no substrate binding ability & desulfation activity, and C69A without desulfation activity but still with affinity for the substrate were produced. Should the ZP bind to the active site pocket of ASA, we expect that this binding would not be observed with the ASA mutant, C69A/K123A/K302A, but would be so with the C69A mutant.

Since ASA is a lysosomal enzyme, the over expressed recombinant WT and mutant ASA would presumably accumulate in the lysosomes of the transfected CHO cells; this would make purification of the recombinant ASA from other intracellular/intralysosomal proteins difficult. Primary amines were reportedly able to cause newly synthesized lysosomal enzymes to diverge from the lysosomal route to a secretory pathway (Chang et al., 1988). Therefore, transfected CHO cells were treated with 10 mM ammonium chloride in serum free culture medium to induce secretion of newly synthesized ASA into culture medium (see *Materials and Methods*). The spent culture media, containing mainly over-expressed recombinant ASA (called wild type, C69A, CKK and pcDNA from cells transfected with pcDNA3.1 containing unaltered ASA cDNA, C69A ASA construct, C69A/K123A/K302A ASA construct and blank

pcDNA3.1, respectively), were collected for the purification of recombinant ASAs. Notably, the amounts of total proteins in the media of transfected CHO cells were similar for all transfection plasmids (Table 3.2). As expected, recombinant WT ASA exhibited NCS desulfation activity, whereas C69A and CKK mutant ASA possessed only background activity towards NCS, similar to that of pcDNA (Table 3.2).

Recombinant ASAs were initially purified from the spent media by cation exchange using a slurry of Q-Sepharose Fast Flow resin. The total protein profiles of the recombinant ASAs after Q-Sepharose, as revealed by silver staining, showed that recombinant ASAs and transferrin were the major proteins in these samples (Figure 3.20A, left panel). Western blotting confirmed the presence of recombinant ASAs in all preparations except for pcDNA, as expected (Figure 3.20A, right panel). Recombinant ASAs were further enriched following the removal of transferrin by affinity chromatography using anti human transferrin IgG matrix. Purity of the expressed ASA, as assessed by SDS-PAGE and silver staining (Figure 3.20B, left panel), revealed a main protein band of 68 kDa, which was confirmed by Western blot as ASA (Figure 3.20B, right panel). The following five people have contributed to the making of these recombinant ASA. Dr. E. Carmona, former research associate, designed most of the experimental plans. Dr. K. Chakrabandhu (former postdoctoral fellow) was involved in the construct designing and recombinant ASA production. Ms. D. Costa Santos (former research assistant), Mr. M. Schenk (former exchanged graduate student), and Ms. F. Liu (former research assistant) were involved in the production.

Table 3.2. Production of recombinant WT and mutant ASA

	WT	C69	CKK	pcDNA	
protein (mg)	3.67	5.51	6.69	6.76	
total activity (U)	17.90	2.90	2.42	1.94	medium
specific activity (U/mg)	4.88	0.53	0.36	0.29	
protein (mg)	0.57	1.98	1.12	2.79	
total activity (U)	21.1	2.65	0.65	0.68	after OS
specific activity (U/mg)	37.02	1.34	0.58	0.24	

CHO cells transfected with full length ASA cDNA, C69A construct, C69A/K123A/K302A construct and empty vector pcDNA3.1 were treated with 10 mM ammonium chloride in serum free culture medium to induce secretion of newly synthesized ASA. The spent culture media were collected and an aliquot was used for protein quantification and NCS desulfation activity assay (medium). ASA in the remaining media was further purified through Q-sepharose chromatography and the total protein obtained and NCS desulfation activity was measured (after QS).

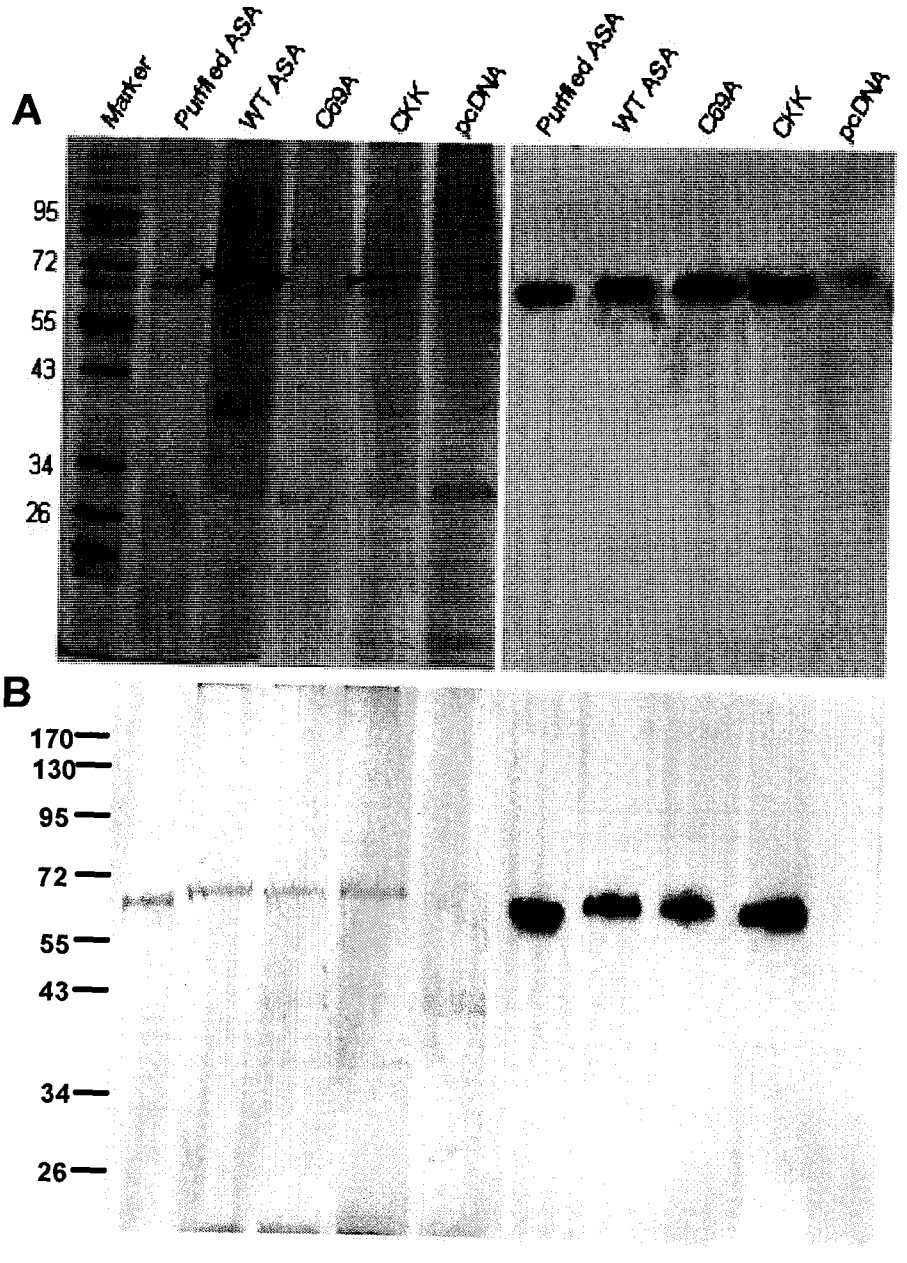
A
Marker
Purified ASA
WT ASA
C68A
CKK
pcDNA
Purified ASA
WT ASA
C68A
CKK
pcDNA
95
72
55
43
34
26
B
170
130
95
72
55
43
34
26

Figure 3.20. Protein profiles of purified recombinant ASAs. (**A**) Recombinant ASAs in the spent culture media (see M & M) were purified through Q-Sepharose ion exchange. Left panel: silver staining of these partially purified recombinant ASAs. Arrow heads indicate transferrin, the major contaminating protein. Right panel: Western blot for ASA of the same set of samples shown on the silver-stained gel. Positions of molecular mass markers (kDa) are marked on the left. (**B**) The partially purified recombinant ASAs were further enriched by removing major contaminating protein transferrin using anti human transferrin IgG covalently linked to AminoLink resin. An aliquot of each purified recombinant ASA was run on the same SDS-PAGE in duplicates in two sets. Purified pig sperm ASA was used as a positive control. One set of the samples was stained with silver to reveal protein profiles (left) and the other set was transferred to nitrocellulose membrane for Western blot (right). Silver staining showed that the purified recombinant ASA consists primarily of a single protein band of 68 kDa. The identities of these major protein bands were confirmed to be ASA by Western blot using anti-ASA antibodies (right).

3.1.4.5. Binding of Recombinant ASA to the ZP

The ability of the recombinant mutant ASAs to bind to the ZP was tested by Dot-immunoblotting with equal amount of ZP (1 μg) immobilized on the membrane. My result showed that the recombinant WT ASA bound to the ZP at a similar level as that of purified ASA (Figure 3.21). This result validated our experimental approach of using recombinant mutant ASAs to test for their ZP binding ability. Both recombinant mutant ASAs, C69A/K123A/K302A (possessing no substrate binding ability & desulfation activity) and C69A (without desulfation activity but still with affinity for the substrate) were still able to bind to the ZP (Figure 3.21), suggesting that the active site pocket of ASA is not involved in ZP binding. The signals detected were specific for ASA since pcDNA gave no signal at all (Figure 3.21). The bindings were also specific to the ZP, since purified sperm ASA showed no detectable binding towards ovalbumin (Figure 3.21).

3.1.5. Summary of Section 3.1

The first part of my thesis research was focused on the roles of sperm surface ASA in sperm-ZP interactions. The results presented support the involvement of ASA in mouse gamete recognition. I described that mouse sperm had two entities of ASA, one in the acrosome that was synthesized in spermatogenic cells, and the other was on the head surface that was captured by SGG from the epididymal fluid. On mature sperm, surface ASA was confined to the plasma membrane overlying the acrosome, the known location for sperm binding to the ZP. ASA on the sperm head surface had direct affinity for the ZP and was involved in the primary sperm-ZP binding. This was further confirmed by

the direct binding of purified sperm ASA to the ZP3 glycoprotein, the primary sperm receptor for acrosome-intact sperm. The presence of ASA on the head of acrosome-reacted sperm, together with its affinity for the ZP2 glycoprotein (the secondary sperm receptor for acrosome-reacted/reacting sperm), suggested that the acrosomal ASA might be involved in the secondary sperm-ZP binding. We speculated that ASA, as a desulfating enzyme, might use its active site pocket to recognize the sulfated sugar moieties of the zona glycoproteins. However, my results argued against this hypothesis, e.g., the active site pocket of ASA was not involved in binding to the ZP.

Unlike its role as an adhesion molecule, the physiological significance of ASA as an active enzyme in maintaining male fertility is largely unknown. SGC has been suggested as a natural substrate of ASA, since it is accumulated in the brains of individuals who suffer metachromatic leukodystrophy (MLD), a neurological disorder due to ASA deficiency. However, SGG, being structurally analogous to SGC, has not been proven as a natural substrate of ASA in vivo. Both SGC and SGG can be desulfated by ASA in vitro, provided that the sulfoglycolipids are presolubilized by saposin B (a "physiological detergent") or a chemical detergent. In the second part of my thesis, I described the use of a mouse model of MLD, the *ASA* null mice, to confirm the physiological significance of ASA in fertilization in vivo, and to study changes of sperm and testicular SGG levels as a result of ASA deficiency and male fertility defects associated with these changes.

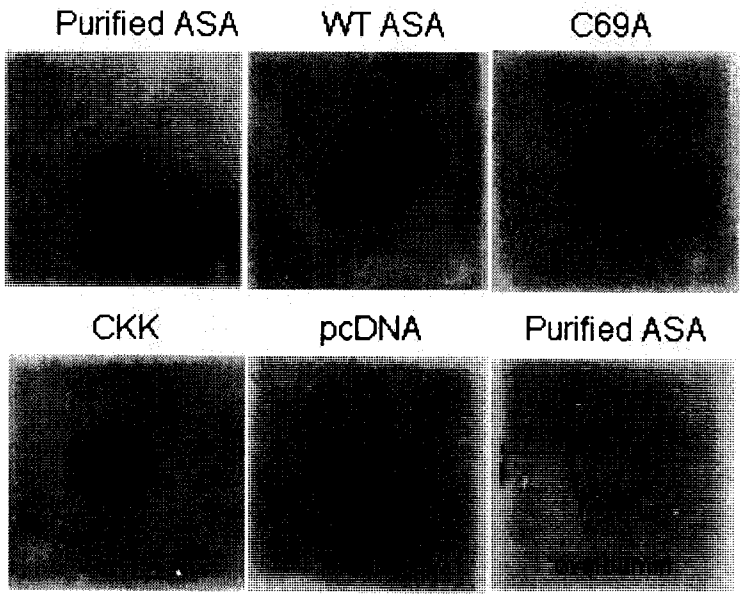
Purified ASA
WT ASA
C69A
CKK
pcDNA
Purified ASA

Figure 3.21. Binding of recombinant mutant ASAs to solubilized mouse ovarian ZP. One microgram of solubilized ZP or ovalbumin (labeled with ovalbumin) was dotted onto nitrocellular membranes and air dried. After blocking for non-specific binding with 5% skim milk in TBS-0.05% Tween, the membranes were incubated with 1 μg of purified sperm ASA or recombinant ASAs (as indicated) in 1 ml of TBST, and the bound ASA was immunodetected using anti-ASA IgG.

3.2. Fecundity of ASA Null Male Mice

Results presented thus far have clearly demonstrated that sperm ASA has direct affinity for the ZP and is involved in sperm-ZP binding. The overall significance of ASA in fertilization is evidenced by strong inhibitory effects of anti-ASA on mouse in vivo fertilization (Tantibhedhyangkul et al., 2002). However, roles of sperm ASA in male fecundity still needed to be validated. It would therefore be logical to examine the fecundity and sperm fertilizing ability of *ASA* null males in comparison with the parameters of wild type mice.

3.2.1. Compromised in Vitro Sperm Fertilizing Ability in Aging ASA Null Mice

To examine whether *Asa* null mutation affected sperm fertilizing ability, in vitro fertilization (IVF) assays were performed. Sperm isolated from the cauda epididymis and vas deferens of 5-month-old *ASA* null mice showed similar capacity to fertilize eggs in vitro compared to WT sperm (75.8 ± 17.7% of WT sperm value), when an equal number of motility-selected swim-up sperm were used for insemination (5 x 10^5 sperm in a 500 µl of KSOM) (Figure 3.22B). Under the same gamete coincubation conditions, however, the IVF rate of 8-month-old *ASA* null sperm was only 10.7 ± 4.6% of the WT value ($p < 0.001$) (Figure 3.22D). Since sperm must first bind to the ZP in order to fertilize an egg, defects in sperm ZP binding ability may be one of the causes that led to the markedly reduced capacity of sperm from older *ASA* null mice to fertilize eggs in vitro. Therefore, in vitro gamete binding assays were performed. Cauda epididymal and vas deferens sperm of 5-month-old *ASA* null mice bound to the ZP at similar levels as wild-type (WT) sperm, i.e., 22.0 ± 5.0 sperm/egg versus 25.9 ± 4.6 sperm/egg using WT sperm

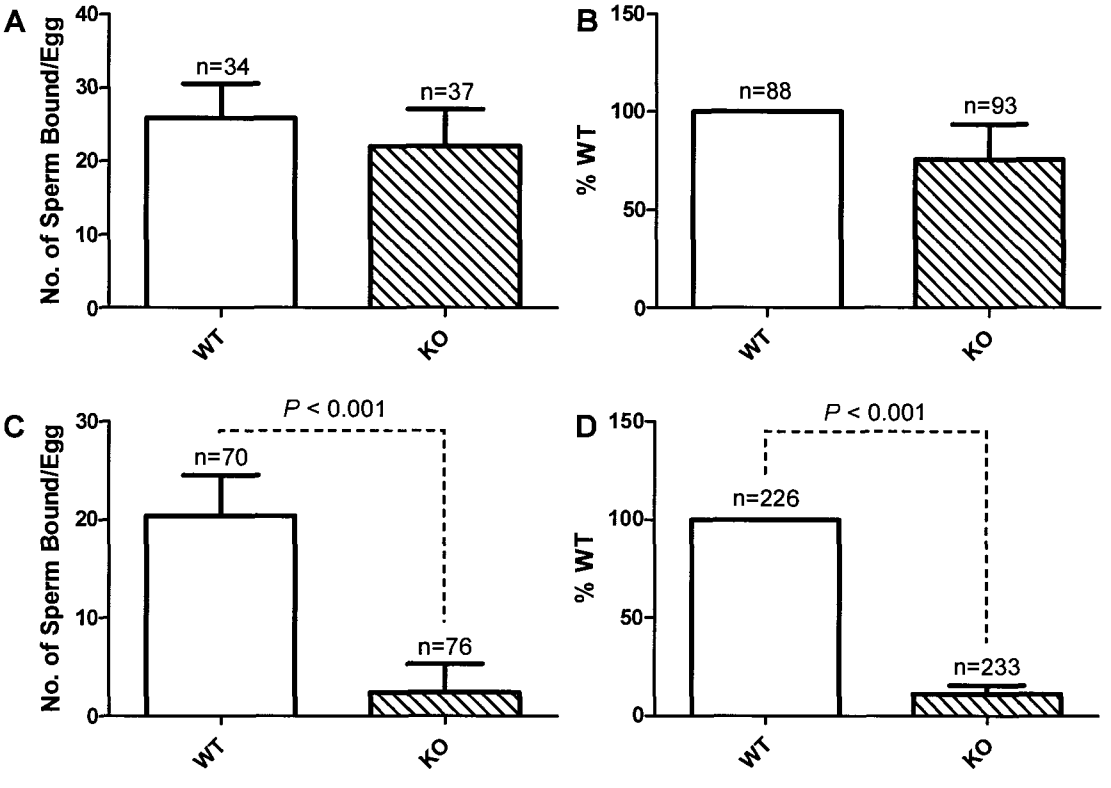
A
No. of Sperm Bound/Egg
40
30
20
10
0
n=34
n=37
WT
KO
B
% WT
150
100
50
0
n=88
n=93
WT
KO
C
No. of Sperm Bound/Egg
30
20
10
0
P < 0.001
n=70
n=76
WT
KO
D
% WT
150
100
50
0
P < 0.001
n=226
n=233
WT
KO

Figure 3.22. In vitro fertilizing ability of WT and ASA null mouse sperm. **A** and **C**. Sperm-ZP binding ability of 5-month old (A) and 8-month old (C) WT and ASA null mice. Data were expressed as the mean ± SD of the average number of bound sperm/egg from three or more experiments. **B** and **D**. In vitro fertilizing ability of sperm from 5-month old (B) and 8-month old (D) WT and ASA null mice. Data were expressed as mean ± SD of percent control of means from three experiments. n = total number of eggs assessed in each sample. Significant difference ($P < 0.001$) from the control samples as determined by ANOVA of raw data was indicated.

(Figure 3.22A), when an equal number of motility-selected swim-up sperm were used for insemination (6 x 10^4 sperm in a 60 µl droplet of egg coincubate). Under the same experimental conditions, the ZP binding ability of 8-month-old *ASA* null sperm were significantly decreased, the average number of *ASA* null sperm bound to the ZP per egg was 2.4 ± 2.8, only 12% of the WT value (20.4 ± 4.1, $p < 0.001$) (Figure 3.22C). Notably, sperm from 5- and 8-month-old WT mice exhibited similar ZP binding ability and *in vitro* fertilizing capacity (Figure 3.22).

The number of epididymal and vas deferens sperm retrieved from the 8-month-old *ASA* null mice (21.5 ± 3.5 million) was significantly lower compared to age-matched WT (45.3 ± 6.0 million) ($P < 0.001$) (Table 3.3). Similarly, the number of swim-up sperm obtained from the 8-month-old *ASA* null mice (4.3 ± 0.6 million) was also significantly reduced compared with that of WT (32.0 ± 3.0 million) ($P < 0.001$) (Table 3.3). In addition, 38 ± 13% of these mutant sperm showed morphological abnormality (mostly found in the non-swim-up population), including hairpin morphology with folding in the tail, multiple bends or kinks of the tail, headless sperm, and sperm with the tail folded and enclosed in the cytoplasmic residue (Figure 3.23). However, since equal number of motile WT and *ASA* null swim-up sperm were used for insemination, and since the percentage of spontaneous acrosome reaction in the swim-up population was similar between WT and *ASA* null samples (Table 3.3), the results from gamete functional assays indicated that the sperm fertilizing ability of 8-month-old *ASA* null mice was compromised. In contrast, the number of epididymal and vas deferens sperm, and the number of swim-up sperm were similar between 5-month-old WT and *ASA* null mice (Table 3.3), corroborating results from IVF and sperm-ZP binding experiments.

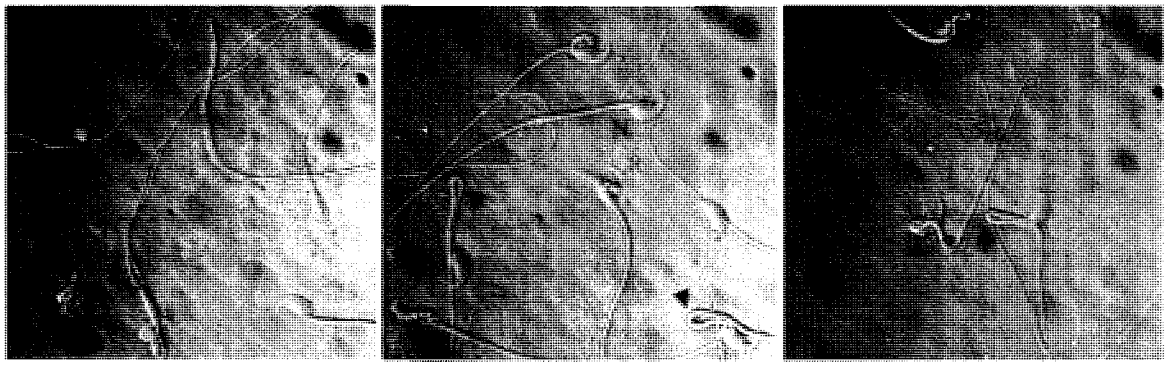

Figure 3.23. Abnormal sperm morphology in 8-month-old *ASA* null mice. Around 40% of the sperm retrieved from the cauda epididymis and vas deferens of 8-month-old *ASA* null mice exhibited various morphological abnormalities, including hairpin morphology with folding in the tail (arrow), bends or kinks of the tail (arrow heads), headless sperm (empty arrow head), and sperm with the tail folded and enclosed in the cytoplasmic residue (stars). A morphologically normal sperm is indicated with a letter "N".

Table 3.3. Basic sperm parameters of WT and ASA null mice.

Phenotype/genotype	+/+		-/-	
Age of mice (months)	5	8	5	8
# sperm (x 10^6)/male	48.9 ± 5.2 (4)	45.3 ± 6.0 (3)	48.5 ± 6.8 (5)	21.5 ± 3.5 (4)
# swim-up sperm (x 10^6)/male	33.8 ± 2.5 (4)	32.0 ± 3.0 (3)	28.5 ± 8.1 (5)	4.3 ± 0.6 (4)
% motile sperm*	79.3 ± 3.1 (4)	75.1 ± 2.7 (3)	80.3 ± 5.2 (5)	69.0 ± 3.0 (4)
% basal AR-sperm	3.3 ± 1.5 (3)	2.7 ± 1.5 (3)	3.7 ± 2.1 (3)	3.7 ± 2.5 (3)
Spontaneous AR-sperm/60 min	20.7 ± 2.1 (3)	19.0 ± 3.6 (3)	21.0 ± 2.0 (3)	19.0 ± 2.6 (3)
% ZP-induced AR-sperm	64.7 ± 1.5 (3)	62.0 ± 4.6 (3)	63.3 ± 4.0 (3)	61.3 ± 4.0 (3)

Considering that both WT and *ASA* null sperm underwent acrosome reaction at a similar rate upon ZP induction (Table 3.3), the drastic decrease in the ZP binding of sperm from 8-month-old *ASA* null mice would explain the also marked decrease in IVF.

3.2.2. Eight-month-old ASA Null Males are Subfertile

The reduced ZP binding ability and in vitro fertilization capacity of 8-month-old *ASA* null mice is consistent with the function of ASA in ZP binding. Based on the results obtained from in vitro sperm functional assays, mating studies were designed in such a way that fecundity of *ASA* null male mice could be evaluated as a function of their age. Basically, 8 *ASA* null and 4 WT males (7.5 and 8 weeks of age, respectively) were individually caged with WT females (~ 8 weeks of age) for 25 weeks to allow natural mating. During these 6 months, the eight *ASA* null males produced 37 litters (4.6 litters/male) with an average litter size of 6.2 ± 2.4 pups/litter, which was significantly smaller ($P < 0.05$) than the average litter size from 22 litters (5.5 litters/male) produced by the four WT males (7.9 ± 1.3 pups/litter) (Figure 3.24B). Litter sizes resulting from the 4 WT mating pairs were generally similar with each other (ranging from the average of 6.3 to 8.5 pups/litter). In marked contrast, the litter sizes from the 8 *ASA* null mating pairs varied considerably among the breeding pairs (from the average of 4.8 pups/litter (KO4) to 8 pups/litter (KO2)), as well as among litters at different times from the same mating pair. For example, *ASA* null male mouse # 7 (KO7) produced the lowest litter size of 1 pup and the highest litter size of 9 pups (Figure 3.24B). The average accumulated pup numbers produced per *ASA* null male grew in a linear mode and were indistinguishable from those of WT males within 5 months of the male age (within the

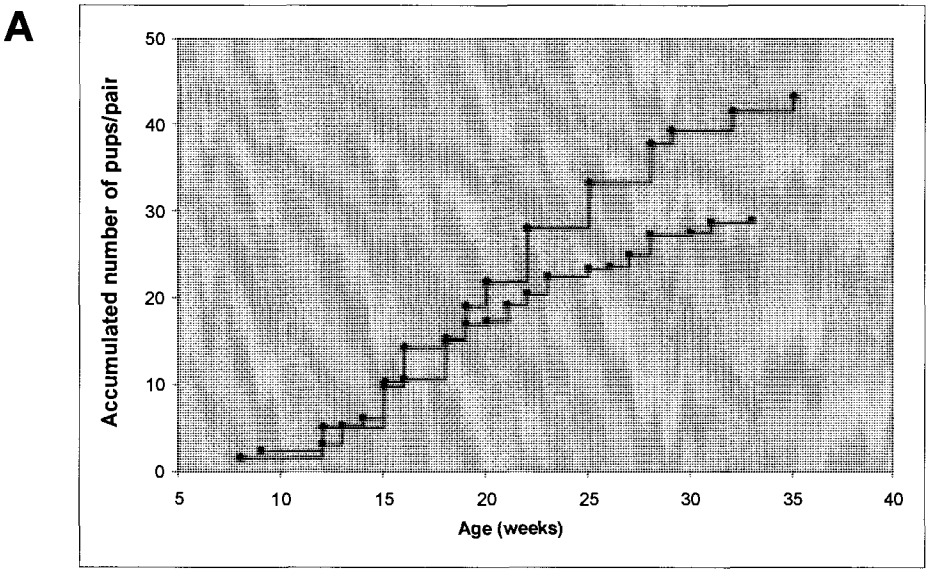
A
Accumulated number of pups/pair
0
10
20
30
40
50
5
10
15
20
25
30
35
40
Age (weeks)

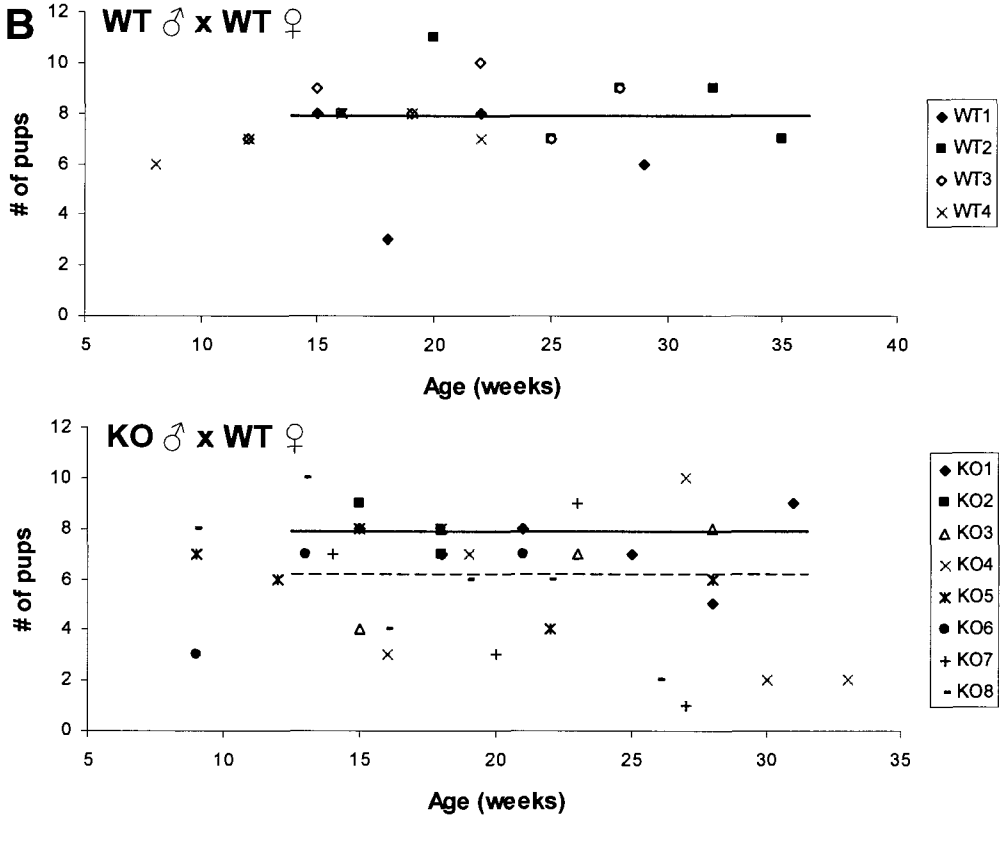
B
WT ♂ x WT ♀
# of pups
Age (weeks)
WT1
WT2
WT3
WT4
KO ♂ x WT ♀
# of pups
Age (weeks)
KO1
KO2
KO3
KO4
KO5
KO6
KO7
KO8

Figure 3.24. Reduced fecundity of older ASA null males. The fecundity of ASA null males were evaluated by natural mating studies with WT females starting when the males were ~ 2 months of age for a duration of ~6 months. (**A**) The average accumulated numbers of pups produced by 4 WT ♂x WT ♀ (blue line) and 8 KO ♂x WT ♀ (pink line) mating pairs were presented. The total number of litters produced by WT and ASA null males during the whole mating period was 5.5 and 4.6, respectively. (**B**) Scatter plot of litter sizes resulting from each breeding pair. Each dot represents the number of pups born. Solid horizontal line indicates the average litter size resulting from WT mating pairs (7.9 ± 1.3 pups/litter), whereas the dashed horizontal line represents the average litter size produced by ASA *null* males (6.2 ± 2.4 pups/litter, $P < 0.05$).

first 24 weeks of the mating study) (Figure 3.24A). However, when the males became more than 5 months of age, the increase in the accumulated pup numbers produced by *ASA* null males became much more gradual, as compared with WT males; the accumulated number of pups born from *ASA* null males was apparently at a much gradual slope, relative to the corresponding plot from WT males, which was still rising linearly with the same slope as when the animals were at a younger age (Figure 3.24A). During this six-month mating period, the mating behavior of the *ASA* null male mice was not different from that of the WT.

3.2.3. Localization and Quantification of SGG in ASA Null Sperm

ASA and SGG have a close association with each other. ASA docks onto the sperm surface via its non-enzymatic affinity for SGG, and this results in their co-localization on the sperm head plasma membrane, where they likely collaborate in ZP interaction (Weerachatyanukul et al., 2003; Schenk et al., 2009). The spatial association between ASA and SGG in testicular germ cells is still unknown. ASA newly glycosylated in Golgi bodies may cross-path with SGG newly synthesized in the same organelle. Thus, ASA in these entities of male germ cells may have desulfation activity on SGG. In the same vein, ASA in the late residual bodies of Sertoli cells may be involved in desulfation of SGG phagocytosed as membrane remnants of apoptotic cells or residual bodies of elongated spermatids (see INTRODUCTION section 1.2). Yet, in the normal situation, SGG accumulation in Sertoli cells has not been described. It is possible that the catabolism of the phagocytosed SGG occurs in a rapid manner. While this is still a matter of further investigation, the availability of *ASA* null mice offers a convenient

opportunity to evaluate this concept. Therefore, the localization and the amount of SGG were first determined in the *ASA* null sperm from 8-month-old mice. SGG localization was examined, since major changes of its quantity in *ASA* null sperm would expectedly result in the lipid relocalization. My immunofluorescence results using affinity purified anti-SGG IgG indicated the presence of SGG on the convex ridge of live *ASA* null sperm head surface, a pattern indistinguishable from that of WT sperm (Figure 3.25A). This result suggested that ASA deficiency did not lead to aberrant localization of SGG on the sperm surface. HPTLC results revealed the same trend of similarity in SGG amounts between WT and ASA null sperm from mice 8 months of age (Figure 3.25B & C). However, when the much more sensitive method of SGG quantitation by ESI-MS approach (using deuterated SGG (Franchini et al., 2008) as an internal standard) was used, the amount of SGG in 8-month-old *ASA* null sperm (0.116 ± 0.061 μg/million sperm) was found to be decreased almost by half, compared with that of the age matched WT sperm (0.213 ± 0.039 μg/million sperm) ($P < 0.05$) (Figure 3.26). In contrast, the amounts of SGG in WT (0.200 ± 0.015 μg/million sperm) and *ASA* null sperm (0.219 ± 0.015 μg/million sperm) from 5-month-old mice were similar (Figure 3.26). It is important to note that the amount of SGG in 5- and 8-month-old WT sperm was comparable (Figure 3.26). These results were in great contrast to what was expected, since ASA is a catabolic enzyme involved in the first step of SGG degradation. However, the results were consistent with the sperm fertilizing capacity of the *ASA* null males at both ages, i.e., the dissimilarity of sperm fertilizing ability and sperm SGG

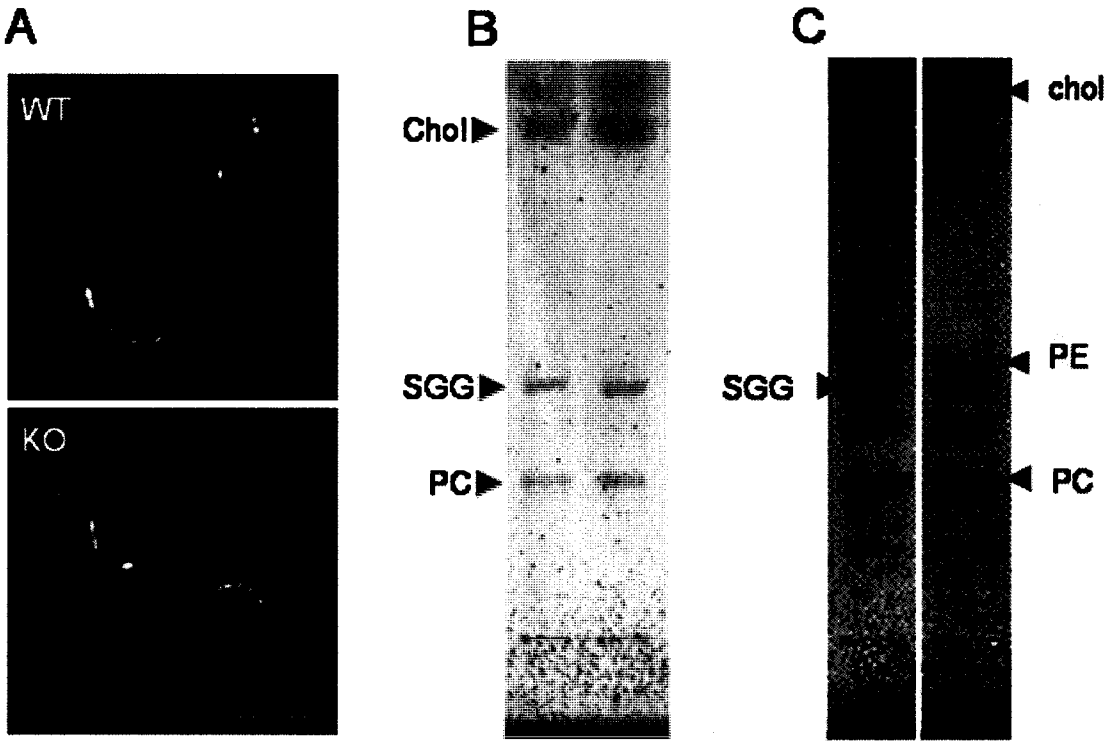
A
WT
KO
B
Chol
SGG
PC
C
chol
SGG
PE
PC

Figure 3.25. Normal SGG localization and lipid profiles of 8-month old *ASA* null sperm. (A) IIF for SGG on live caudal epididymal and vas deferens sperm of WT and ASA null sperm. Bar = 10 μm. Total sperm lipids were separated by HPTLC using the solvent system $CHCl_3/CH_3OH/0.2\%$ aqueous $CaCl_2$ = 60:35:8 (v/v/v). The glycolipid profile was revealed by orcinol charring (**B**), and the total sperm lipid profile was revealed by coomassie blue staining (**C**). Chol, Cholesterol; PE, phosphatidylethanolamine; PC, phosphatidylcholine.

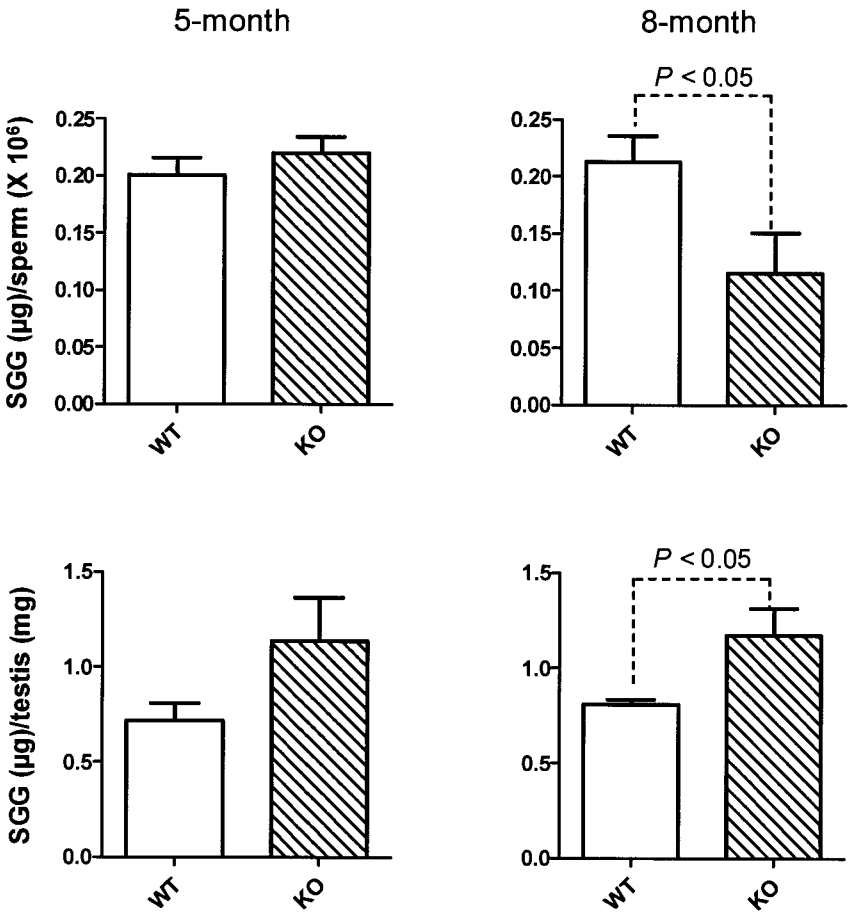
5-month
8-month
P < 0.05
SGG (µg)/sperm (X 10⁶)
0.25
0.20
0.15
0.10
0.05
0.00
WT
KO
P < 0.05
SGG (µg)/testis (mg)
1.5
1.0
0.5
0.0
WT
KO

Figure 3.26. Quantification of WT and ASA null testes and sperm SGG by ESI-MS/MS. Quantification of SGG was performed using the multiple-reaction monitoring (MRM) mode. $^{2}H_3$-SGG (100 pmol in 20 µl of chloroform/methanol, 1/1, v/v) was added to each testis (from 0.2 mg of testis wet weight) or sperm (from 0.7 million sperm) lipid extract dissolved in acetonitrile/methanol/water/acetic acid (41/23/36/1, v/v/v/v, 180 µl). Aliquots of this solution (100 µl) were subject to reverse phase HPLC and the effluent was passed to an Ionspray source connected to a triple-quadrupole mass spectrometer (Sciex API III^{+} Perkin Elmer-Sciex Instruments, Thornhill, Ontario, Canada). Data were collected in the MS/MS mode by MRM of transitions selected for SGG (m/z 795.6→ 97.0 and 795.6→ 539.5) and $^{2}H_3$-SGG (m/z 798.6→97.0 and 798.6→ 542.3) under conditions previously optimized for maximal signal production from SGG (orifice 120 volts, collision gas (argon) thickness at an instrumental (CGT) setting of 200). Quantification was achieved by relating the peak areas and heights of sample SGG to those of the $^{2}H_3$-SGG internal standard using software (MacSpec version 3.3) supplied by the instrument manufacturer. Significant differences between corresponding WT and KO values were indicated ($P < 0.05$).

levels in 5-month-old WT and *ASA* null males, and the decreases in these two parameters in 8-month-old *ASA* null males, as compared with those in WT males of the same age. The results suggested that the impaired sperm fertilizing ability of 8-month-old *ASA* null mice may be due to the reduced sperm SGG levels and further confirmed the significance of sperm SGG in sperm-ZP binding and fertilization. To determine whether other sperm lipids were affected by the null mutation of ASA, the glycolipid and total lipid profiles of sperm from 8-month-old *ASA* null and WT mice were examined by HPTLC, and the results showed no apparent differences between sperm of the two genotypes (Figure 3.25B & C). However, due to limited detection sensitivity of HPTLC, minor changes in lipid profiles might not have been detected.

3.2.4. *ASA Null Sperm Exhibited Normal Plasma Membrane Fluidity*

Since mouse sperm must capacitate to gain fertilization competence (Yanagimachi, 1994), the markedly reduced ability of sperm from 8-month-old *ASA* null males to bind to the ZP and to fertilize eggs in vitro may be due to their inability to fully capacitate in vitro. One of the hallmarks of sperm capacitation is an increase in plasma membrane fluidity (Gadella et al., 1999a; Gadella and Harrison, 2000; Gadella and Harrison, 2002; de Vries et al., 2003; Rathi et al., 2001), which can be monitored by flow cytometry using merocyanine 540 (MC 540) (Harrison et al., 1996). MC 540 is a fluorescent lipophilic dye, which has been shown to intercalate into plasma membrane lipid bilayers more efficiently if the membrane lipids are in a higher state of disorder (Williamson et al., 1983; Langner and Hui, 1993). Thus the ability of the *ASA* null sperm to capacitate in vitro was evaluated by monitoring changes in their plasma membrane

fluidity under capacitating conditions. Since BSA in capacitating medium may interfere with the fluorescence of merocyanine (Harrison et al., 1996), capacitated sperm samples were washed with PBS-PVA (0.1% w/v) by low speeed centrifugation followed by resuspension in PBS-PVA to ~2 x 10^6 sperm/ml for flow cytometry analysis. It has been shown previously that the merocyanine fluorescence in capacitated boar sperm is enhanced as a result of increased membrane fluidity (Harrison et al., 1996). Here, I showed the same result for the first time in mouse sperm (Figure 3.27A & B); Capacitation of caudal epididymal and vas deferens sperm resulted in a significant increase in the percentage of sperm exhibiting a high intensity of merocyanine fluorescence (71 ± 7%), compared with non-capacitated sperm that were incubated in PBS-PVA (28% ± 5%; $P < 0.001$) (Figure 3.27A & B). When swim-up sperm were evaluated for plasma membrane fluidity, the percentages of *ASA* null sperm (67% and 64% for 5- and 8-month-old mice, respectively) (Figure 3.27C & E) that exhibited high intensity of MC540 fluorescence were similar to those of WT sperm (67% and 66% for 5- and 8-month-old mice, respectively) (Figure 3.27D & F), suggesting that the overall sperm plasma membrane fluidity was comparable between WT and *ASA* null animals. These results suggested that the increase in sperm plasma membrane fluidity associated with capacitation may have occurred normally in *ASA* null sperm.

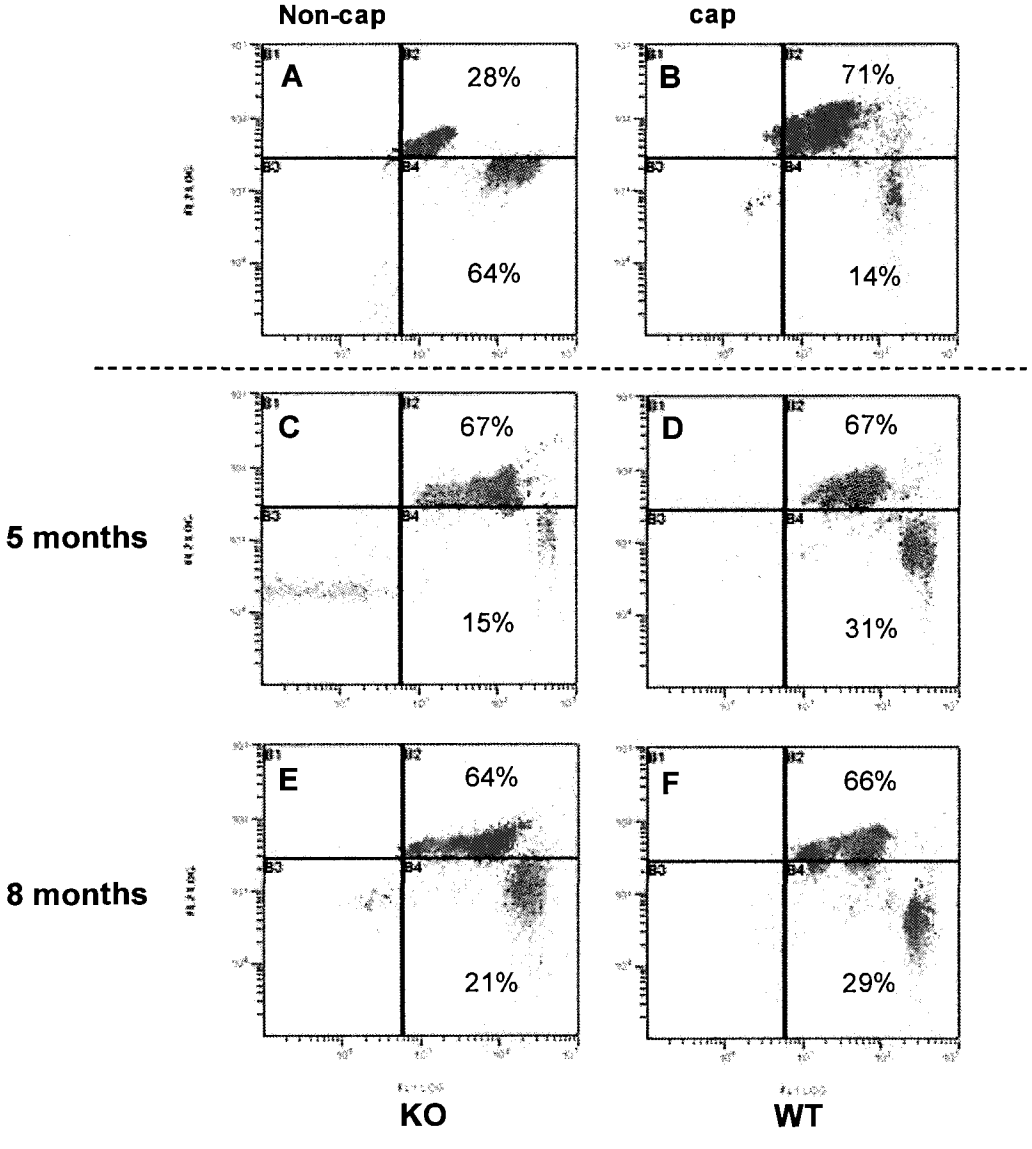
Non-cap
cap
A
28%
64%
B
71%
14%
5 months
C
67%
15%
D
67%
31%
8 months
E
64%
21%
F
66%
29%
KO
WT

Figure 3.27. Plasma membrane fluidity of WT and *ASA* null sperm under capacitating condition. Swim-up sperm were incubated with 2.7 μM MC540 and 1 μM calcein AM (Molecular Probes) in PBS-0.1% PVA in the dark for 15 min at 37 °C, and were then analyzed by flow cytometry. Typical flow cytograms of MC540 staining of non-capacitated (**A**) and capacitated (**B**) sperm, 5-month-old WT (**D**) and KO (**C**) and 8-month-old WT (**F**) and KO (**E**) sperm are shown. The X-axis represents calcein staining, with high fluorescence (quadrants to the right of the vertical line) for live cells, and low fluorescence (quadrants to the left of the vertical line) for dead cells. The Y-axis indicates merocyanine fluorescence, with high fluorescence (above the horizontal line) for high membrane fluidity and low fluorescence (below the horizontal line) for low membrane fluidity. The subpopulation of cells with high calcein and merocyanine fluorescence (top right quadrant) indicates live cell with higher membrane fluidity, representing capacitated sperm population, while the subpopulation of sperm cells with high calcein but low merocyanine fluorescence (bottom right quadrant) indicates live cells with lower membrane fluidity, representing non-capacitated sperm population.

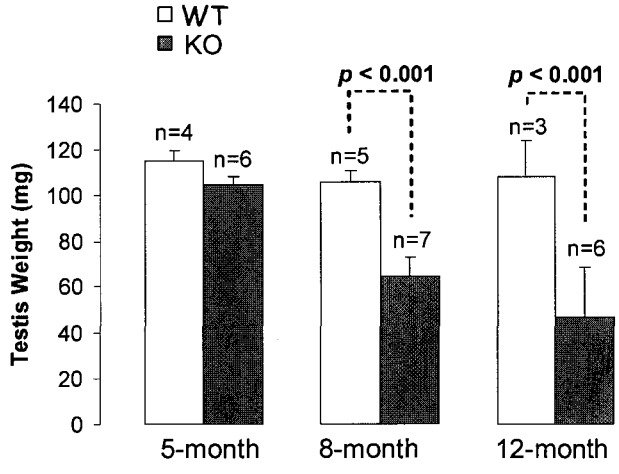
WT
KO
Testis Weight (mg)
140
120
100
80
60
40
20
0
n=4
n=6
n=5
n=7
n=3
n=6
p < 0.001
p < 0.001
5-month
8-month
12-month

Figure 3.28. Testis weight of WT and *ASA* null mice of different ages. Data were expressed as Mean ± SD of the average weight of both testes. n = number of animals examined. Significant difference ($P < 0.001$) from the control values as determined by ANOVA of raw data is indicated.

3.2.5. Reduced Testis Weight in 8-Month-Old ASA Null Mice

When becoming more than 5 months old, *ASA* null mice showed an age-dependent testis weight loss compared with their WT counterparts. The average testis weight of 5-month-old *ASA* null mice was 104.9 ± 3.4 mg (n=6), which did not differ from that of age-matched WT animals (115.2 ± 4.1 mg, n=6) (Figure 3.28). In contrast, the average testis weight of 8-month-old *ASA* null mice (64.5 ± 8.5 mg (n=7)) decreased significantly (a 39% reduction, $P<0.001$) in relation to that of WT males of the same age (105.7 ± 5.0 mg, n=5) (Figure 3.28). At 12 months old, the testis weight of *ASA* null mice was further reduced to 47.0 ± 21.7 mg (n=4), a 57% reduction from the value of WT counterparts (108.4 ± 15.5 mg, n=6) (Figure 3.28). The drastically decreased testis weights of *ASA* null mice suggested that their spermatogenesis might be disrupted or proceed at a reduced rate.

3.2.6. Impairment of Spermatogenesis in ASA Null Testes

Histological examination of the seminiferous tubules of 5-month-old *ASA* null mice revealed normal organization of the epithelium, with sperm seen in the lumen, the same as WT (Figure 3.29a & b). However, abnormalities and irregularities in the seminiferous tubules of 8-month-old *ASA* null mice were evident, with apparent reduction in the epithelium area and the number of germ cells, as compared with those in WT mice (Figures 3.29e & f; 3.30a & b). The number of sperm seen in the luman was also greatly reduced (Figures 3.29f & 3.30b). Quantification (means ± 95% confidence interval) of the tubule area (T_{area}) of the seminiferous tubules of WT (44969 ± 10848 μm^2, a total of 78 tubule sections from 4 WT mice) and *ASA* null mice (30767 ± 7404 μm^2, a total of 76

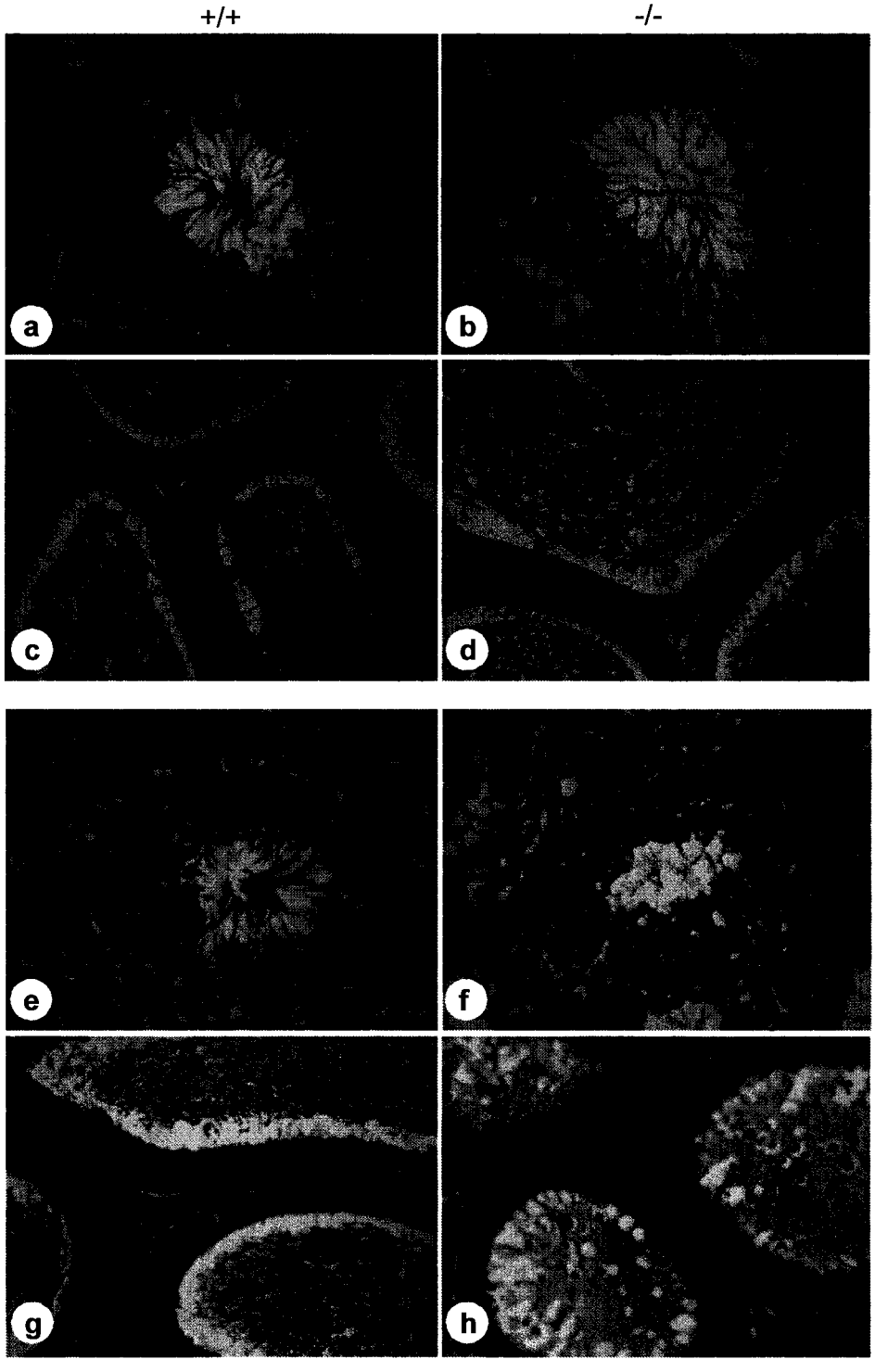
+/+
-/-
a
b
c
d
e
f
g
h

Figure 3.29. Light microscopic examination of the testes and epididymides of WT and *ASA* null mice. Testes and epididymides were fixed in Bouin's fixative. The tissues were sectioned at 5-μm thickness and stained with heamatoxylin and eosin (H&E). Genotypes of the tissues were labeled on the top. (a), (b), (e) and (f) were cross sections of the seminiferous tubules. (c), (d), (g) and (h) were cross sections of the caput epididymides. (x 200).

tubule sections from 4 *ASA* null mice) revealed that the seminiferous tubules of *ASA* null mice were significantly reduced in size when compared with those of WT mice ($P < 0.001$) (Figure 3.30c). This reduction was due to a decrease in epithelial areas (E_{area}) (37297 ± 8501 μm^2 and 24189 ± 6587 μm^2 for WT and *ASA* null mice, respectively) since there was no significant difference in the luminal areas (L_{area}) (7672 ± 5046 μm^2 and 6579 ± 2365 μm^2 for WT and *ASA* null mice, respectively) (Figure 3.30c). An increased number of vacuoles in the 8-month-old *ASA* null testes was also apparent (Figures 3.29f; 3.30b), which was not seen in age-matched WT testis (Figures 3.29e; 3.30a). This suggested there might be a germ cell loss or reduced generation of spermatogenic cells. The quantitative measurements of the seminiferous epithelia were performed by Dr. L. Hermo and Mr. P. Turmel.

One possible mechanism of germ cell loss in the seminiferous tubules is an elevated rate of germ cell apoptosis. Although during normal spermatogenesis, more than half of the diferentiating spermatogenic cells at various developmental stages die by apoptosis before they mature into spermatozoa (Huckins, 1978; Allan DJ, 1987; Billig et al., 1995), only a limited number of apoptotic spermatogenic cells are detectable when WT testis sections are examined histochemically, due to rapid removal of the apoptotic germ cells by Sertoli cells through phagocytosis. However, an increased rate of germ cell apoptosis has been observed in a number of mouse models genetically null of proteins (e.g., Msh5, a member of the family of mismatch repair proteins (de Vries et al., 1999) and Atm, a member of a family of kinases involved in DNA metabolism and cell cycle checkpoint control (Xu et al., 1996; Hamer et al., 2004) essential for spermatogenesis

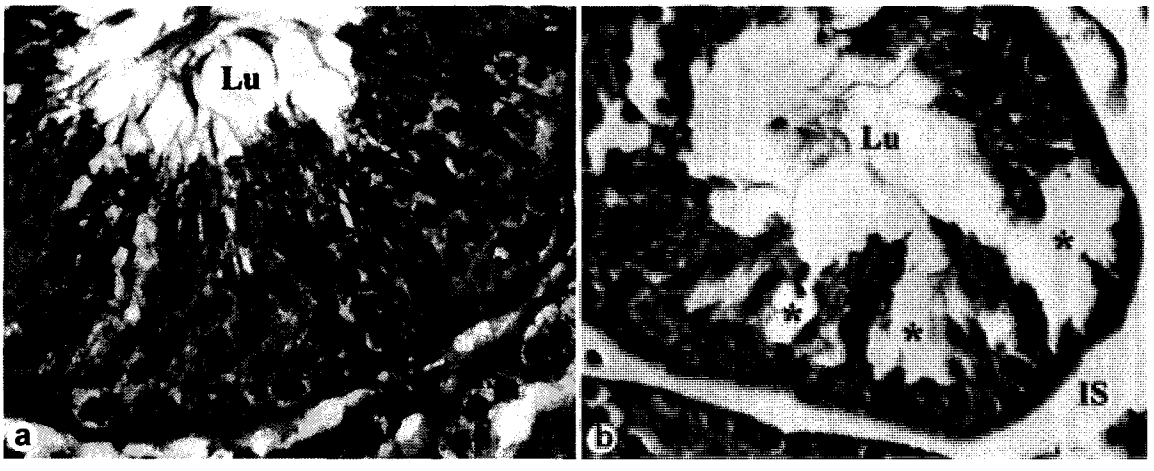
Lu
a
Lu
IS
b

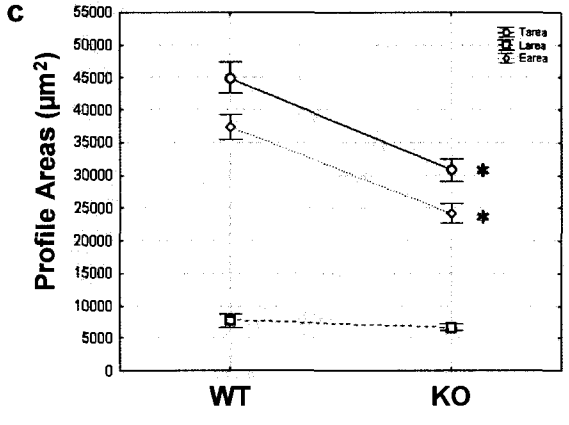
c
Profile Areas (µm²)
55000
50000
45000
40000
35000
30000
25000
20000
15000
10000
5000
0
Tarea
Larea
Earea
WT
KO

Figure 3.30. Qualitative and quantitative analyses of light micrographs of testes of 8-month old WT and ASA null mice. Light microscopic examination of testis sections of 8-month old ASA null mice (b) revealed abnormalities and irregularities in numerous seminiferous tubules, with apparent reduction in profile area of the epithelium and a loss of germ cells as compared to those of WT mice (a). Lu, Lumen; SE, Seminiferous Epithelium; IS, Interstitial Space; asterisks (*), spaces in seminiferous epithelium. (x 250). Quantification of profile areas (T_{area}) of seminiferous tubules of WT (n=78) and ASA KO mice (n=76) with 95% confidence interval showed that the seminiferous tubules of ASA null mice were significantly reduced in size when compared to WT mice (c). This was due to a reduction in Epithelial areas (E_{area}), but not Luminal areas (L_{area}). The asterisk (*, $P < 0.001$) indicates a significant difference between WT and ASA null mice.

(de Rooij and de Boer, 2003). Therefore, I examined the rate of apoptosis in male germ cells on the testis sections by DNA fragmentation staining using the TUNEL (terminal deoxynucleotidyltransferase-mediated dUTP-biotin nick end labeling) method. Five-month-old *ASA* null testes did not display any increase in the number of apoptotic cells compared to WT testes, i.e., 11.3 ± 4.0 versus 12.3 ± 4.2 apoptotic cells per 100 randomly selected seminiferous tubules in the testes of ASA null and WT mice, respectively (Figure 3.31a, b & e). However, this number was significantly higher in 8-month-old *ASA* null testes (196.3 ± 20.5) compared with that of age-matched WT mice (12.3 ± 2.5) ($P < 0.001$) (Figure 3.31c, d & e). In the *ASA* null testes, the majority of the labeled nuclei were found in primary spermatocytes (Figure 3.31f).

3.2.7. Normal Cellular Organization of the Epididymis of ASA Null Mice

Examination of hemotoxyline/eosin-stained epididymis sections of *ASA* null mice revealed no significant changes of cellular organization compared with those of WT animals (Figure 3.29c, d, g & h). Quantitatively, the Tubular areas (T_{area}), Epithelial areas (E_{area}), and Luminal areas (L_{area}) of the proximal initial segments (PIS) (31062 ± 8386 μm^2, 24851± 5857 μm^2, 6211 ± 3034 μm^2, respectively) (a total of 39 sections from 4 mice) and caput (a total of 40 sections from 4 mice) regions of the epididymis (15695 ± 3814 μm^2, 9912 ± 2019 μm^2, 5783 ± 2350 μm^2, respectively) of the WT were not significantly different from those of the *ASA* null mice (34836 ± 9870 μm^2, 27195 ± 6865 μm^2, 7641 ± 3502 μm^2, respectively, for the PIS (a total of 37 sections from 4 mice), and 15327 ± 3332 μm^2, 10201± 2013 μm^2, 5127 ± 1523 μm^2, respectively, for the

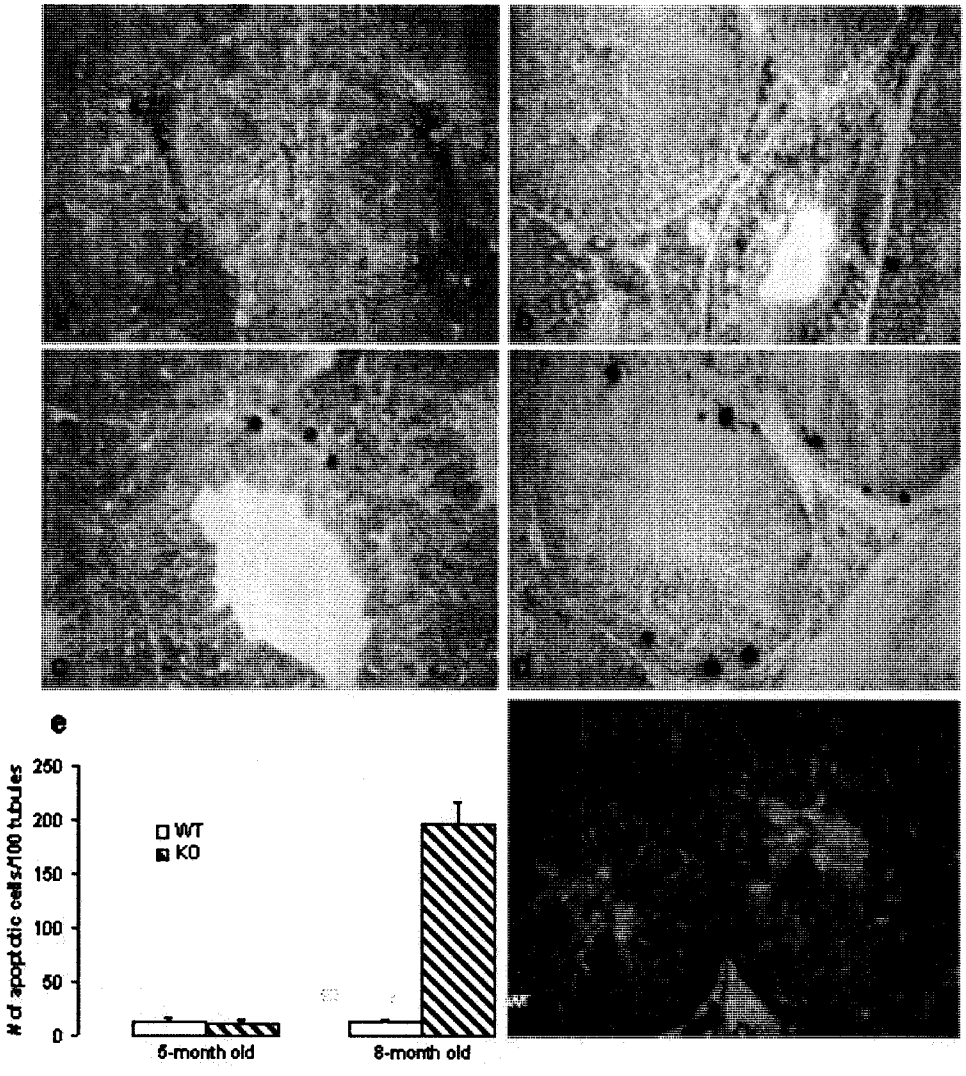
e
# of apoptotic cells/100 tubules
250
200
150
100
50
0
WT
KO
6-month old
8-month old

Figure 3.31. Higher number of apoptotic germ cells in 8-month-old *ASA* null testes. In situ terminal deoxynucleotidyltransferase-mediated dUTP–biotin nick end labeling (TUNEL) staining of seminiferous tubule of 5-month-old WT (a) and *ASA* null mice (b), as well as of 8-month-old WT (c) and *ASA* null mice (d). An increase in the apoptotic germ cells (brown) of the 8-month-old mutant mice is evident (d). The total number of apoptotic germ cells within each cross section of seminiferous tubules was counted on at least 200 randomly selected tubule sections, and the data were presented as Mean ± SD of the number of apoptotic germ cells/100 tubule sections from 3 mice for each genotype at each age (e). The cells that underwent apoptosis were identified to be mainly primary spermatocytes (f, arrow heads) on slides counterstained with hematoxylin and eosin (H & E).

caput regions (a total of 41 sections from 4 mice) (Figure 3.32). There was a significant reduction in the number of sperm in the epididymal lumen of the 8-month-old *ASA* null mice (Figure 3.29h), compared with those in WT and 5-month-old mutant mice (Figure 3.29c, g & d). The former was also accompanied by a marked increase in the number of round cells within the epididymal lumen (Figure 3.29h). These cells were presumably germ cells that were sloughed off the seminiferous tubule epithelium. The quantitative measurements of the epithelia area were performed by Dr. L. Hermo and Mr. P. Turmel.

3.2.8. Sperm Parameters

The epididymal sperm counts were reduced in 8-month-old *ASA* null mice and the decrease was to a greater extent with age. Five-month-old WT and *ASA* null mice had similar number of sperm retrieved from the cauda epididymis and vas deferens, i.e., 48.9 ± 5.2 million/male (n=4) versus 48.5 ± 6.8 million/male (n=5) (Table 3.3). However, at 8 months of age, the number of sperm retrieved from the cauda epididymis and vas deferens of *ASA* null mice (22.0 ± 3.9 million/male, n=4) was significantly decreased (by 51%), as compared with that of age-matched WT (45.3 ± 6.0 million/male, n=3) (Table 3.3). More strikingly, there was barely any sperm seen in the luminal content retrieved from the cauda epididymis and vas deferens of 1-year old *ASA* null mice. The reduced testis weight and decreased epididymal sperm number manifested that normal spermatogenesis in the testis was discontinued in the aging ASA-null mice.

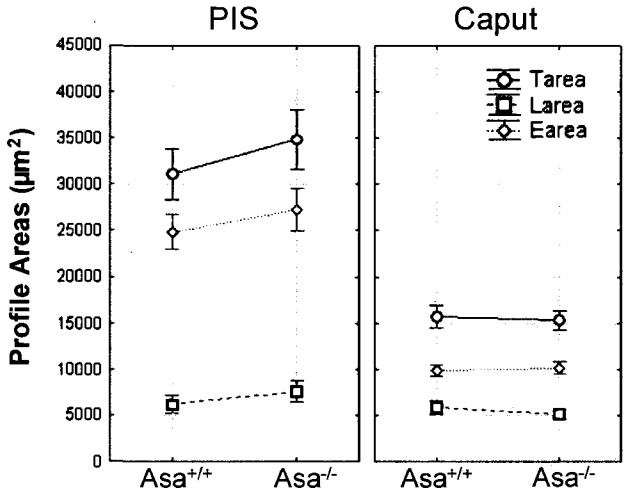
PIS
Caput
Profile Areas (µm²)
45000
40000
35000
30000
25000
20000
15000
10000
5000
0
Tarea
Larea
Earea
Asa+/+
Asa-/-
Asa+/+
Asa-/-

Figure 3.32. Quantitative analysis of light micrographs of proximal initial segment and caput of 8-month-old WT and *ASA* null mice. Graphs of means ± 95% confidence interval summarizing results of quantification of profile areas of epididymal tubules of WT and *ASA* null mice for proximal initial segment (PIS) (WT: n=39; *ASA* null: n=37) and caput (WT: n=40; *ASA* null: n=41) regions of the epididymis. There was no significant difference in the Tubular areas (Tarea), Epithelial areas (Earea), or Luminal areas (Larea) in both regions (PIS and caput) between WT and *ASA* null mice.

3.2.9. Androgen Production Appeared to be Normal in ASA Null Male Mice

It is well known that androgen plays a key role in the initiation and maintenance of spermatogenesis (Sharpe, 1994; Singh et al., 1995; McLachlan, 2000). Therefore, we determined whether the discontinued spermatogenesis observed in 8-month-old *ASA* null mice was a result of androgen withdrawal. Conventional radioimmunoassay revealed the serum testosterone concentration in the 8-month-old *ASA* null mice to be 632 ± 565 ng/dl, a value lower than that of age-matched WT mice (1321 ± 494 ng/dl) (Figure 3.33). However, due to the large variations among samples, no statistically significant difference between WT and *ASA* null mice was detected. The large variations in serum testosterone concentrations were expected and due to the pulsatile pattern of testosterone secretion in adulthood in response to the intermittent discharge of LH from the pituitary (Plant, 1981; Keeney and Ewing, 1990; Ramaswamy et al., 1998; Ramaswamy et al., 2000). The testosterone concentrations were measured by our collaborator Dr. P. Sretarugsa.

Since results from serum testosterone analyses were not sufficient to draw a conclusion as to whether or not androgen production was affected in the 8-month-old *ASA* null mice, the ultrastructure of androgen producing Leydig cells in these animals were examined as an alternate. Transmission electron microscopy revealed morphological similarity between Leydig cells of WT and *ASA* null mice (Figure 3.34a & b). Leydig cells from both WT and KO animals possessed numerous mitochondria (m) that were scattered over the cytoplasm. Lipid droplets (Lp) were also found with a high variation in frequency from cells to cells. Smooth endoplasmic reticuli (SER) were also observed to be interconnecting with each other throughout the cytoplasm in both animal

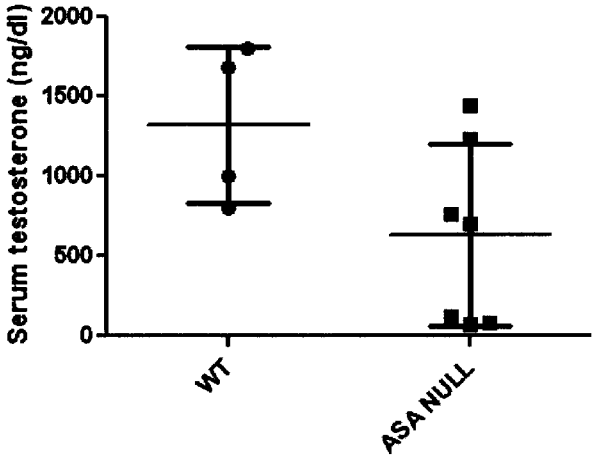
Serum testosterone (ng/dl)
2000
1500
1000
500
0
WT
ASA NULL

Figure 3.33. Serum testosterone levels of 8-month-old WT and *ASA* null mice. Serum testosterone concentrations were not affected by ASA deficiency. No significant difference was detected between WT and ASA null males by student *t*-test (P=0.0734). Data are presented as Mean ± SD.

groups. Furthermore, concentric membrane systems of rough endolasmic reticuli (RER), which arranged around lipid droplets or other inclusions were observed among the two groups (Figure 3.34a & b). All of these features are typical of functioning Leydig cells in normal mice. Therefore, according to these observations, the Leydig cells of 8-month-old *ASA* null mice appeared to be normal structurally and functionally. This experiment was performed by Dr. L. Hermo and Mr. P. Turmel.

Since the seminal vesicle is a target tissue of testosterone, its weight and morphology/anatomy can be used to reflect changes of testosterone levels. Our analyses revealed that the seminal vesicles from 8-month-old WT and *ASA* null mice showed no overt changes in morphology and weight (312.3 ± 22.0 mg, (n = 5) versus 325.7 ± 35.6 mg (n = 6), respectively) (Figure 3.34c). Furthermore, the weight of the caput epididymis, another major target tissue of testosterone, was similar in the 8-month-old WT (23.6 ± 0.6 mg, n = 4) and *ASA* null mice (17.7 ± 1.5 mg, n = 7) (Figure 3.34d). These results corroborated the observation that the epithelia of the caput epididymis of the 8-month-old *ASA* null mice were normal (Figure 3.32). All of these results implicated no changes of testosterone levels in *ASA* null mice, and argued against the possibility that the aberrant phenotypes of the testis and sperm of these 8-month-old knockout mice were testosterone dependent.

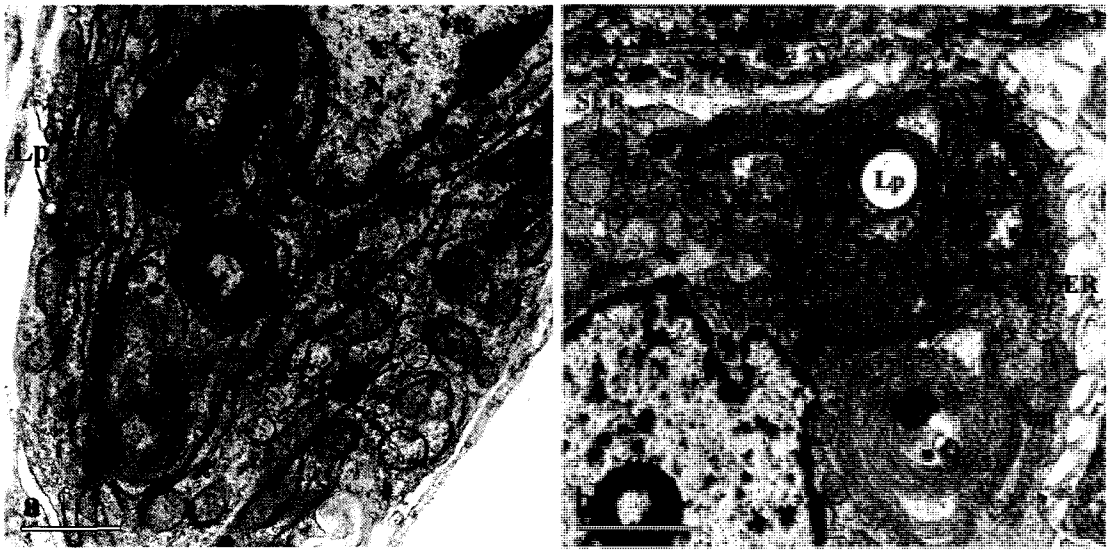
Lp
Lp
ER

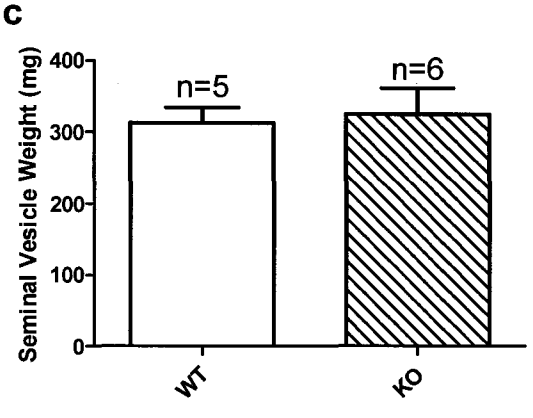
c
Seminal Vesicle Weight (mg)
400
300
200
100
0
n=5
n=6
WT
KO

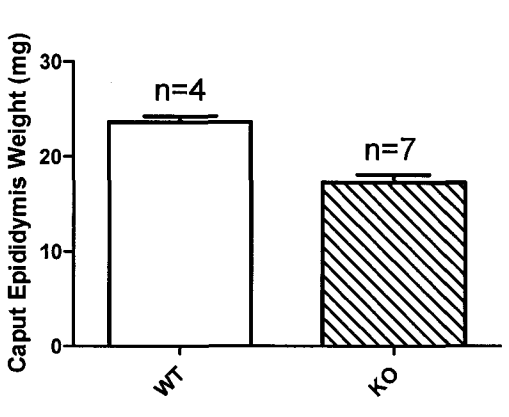
d
Caput Epididymis Weight (mg)
30
20
10
0
n=4
n=7
WT
KO

Figure 3.34. Ultrastructure of Leydig cells and weights of seminal vesicle and caput epididymis were normal in 8-month-old *ASA* null mice. (a & b) Thin sections of testes (40 to 70-nm thickness) were stained with uranyl acetate and lead citrate and examined at 120kV with a FEI Tecnai-12 electron microscope. The analyses revealed similarities in appearance between Leydig cells of WT (b) and *ASA* null mice (a). In both groups, the cells presented numerous mitochondria (m) scattered over the cytoplasm. Lipid droplets (Lp) were present in the cytoplasma, which varied greatly in frequency from cell to cell. The interconnecting tubules of smooth endoplasmic reticulum (SER) were also observed throughout the cytoplasm in both groups. Furthermore, concentric membrane systems of rough endolasmic reticulum (RER) which arrange around lipid droplets or other inclusions were observed among the two groups. All of these are features of Leydig cells that have been well described previously in normal mice. SE: Seminiferous Epithelium. ((a): x 16,500; (b): x 9,900). (c) Data of seminal vesicle weight were expressed as Mean ± SD. n = number of animals examined. (d) Data of caput epididymis weight were expressed as Mean ± SD. n = number of animals examined.

3.2.10. Summary of Reproductive Physiology and Morphology in ASA Null mice

Mating studies over a period of 5 months revealed that the fecundity of *ASA* null males declined with age, in particular when the knockout mice became older than 5 months. Corroborating these results, in vitro studies revealed marked decreases in ZP binding ability and IVF rate of sperm from older *ASA* null mice. The reduced sperm fertilizing ability of the older *ASA* null mice were not due to a lack of increase in membrane fluidity during capacitation or inability to undergo ZP-induced acrosome reaction, two prerequisites to successful ZP binding and fertilization. The apparent normal sperm fertilizing ability of 5-month-old *ASA* null mice suggested that the role of ASA in ZP binding was not essential. This may be due to a strong backup mechanism for ZP interaction in sperm. The reduced male fecundity and sperm fertilizing ability of 8-month-old mutant mice implied that secondary damages to the male reproductive system may have occurred as a result of ASA deficiency.

When becoming more than 5 months old, *ASA* null mice showed an age-dependent testis weight loss accompanied by a reduction in cauda epididymal and vas deferens sperm number. These results suggested a disruption of spermatogenesis. Histological examination indeed revealed a significantly higher number of apoptotic germ cells in the testis of 8-month-old *ASA* null mice compared with age-matched WT. A large number of round cells (presumably germ cell sloughed off seminiferous epithelium) were also seen in the lumen of epididymis of the older *ASA* null mice. Such changes were not observed in the testis or epididymis of 5-month-old mutant mice. Although ASA is also expressed in the epididymis, null mutation of *ASA* did not seem to

affect gross morphology of the tissue. Rather, it was ASA secreted into the epididymal fluid that was important for endowing sperm fertilizing ability (see Section 3.1).

3.2.11. Quantification of SGG in ASA Null Testes

As stated above, ASA deficiency is likely to cause its substrates to accumulate in tissues where ASA is present. This has been the case for sulfatides in the brains of MLD patients and ASA null mice (Hess et al., 1996). In the testes, since SGG is the major sulfoglycolipid that can be degraded by ASA, it is logical to speculate that ASA deficiency would lead to the accumulation of SGG. Thus, age-dependent changes in the levels of SGG in the testes of *ASA* null mice were determined by quantitative electrospray ionization mass spectrometry (ESI-MS). In the testes of 5-month-old animals, the amount of SGG in *ASA* null males (1.139 ± 0.392 μg/mg of testis weight, n = 3) was ~58% higher than that of age-matched WT counterparts (0.717 ± 0.160 μg/mg of testis weight, n = 3) (Figure 3.26). When the animals became 8 months old, similar results were still observed; the level of SGG in the testes of *ASA* null mice (1.173 ± 0.244 μg/mg of testis weight, n = 3) was ~45% more than that of WT mice (0.811 ± 0.040 μg/mg of testis weight, n = 3) (Figure 3.26). SGG has been shown to be a substrate of ASA in vitro (Schenk et al., 2009) and the data presented here support the in vitro results, suggesting that SGG is a natural substrate of ASA. Notably, the levels of SGG in the WT testes at both ages were comparable (Figure 3.26) and were similar to what was previously reported (Tadano-Aritomi et al., 2003). Interestingly, the testicular SGG levels were also similar between 5- and 8-month old *ASA* null mice (Figure 3.26). This result implicated that the biosynthesis of SGG might be inhibited once SGG is

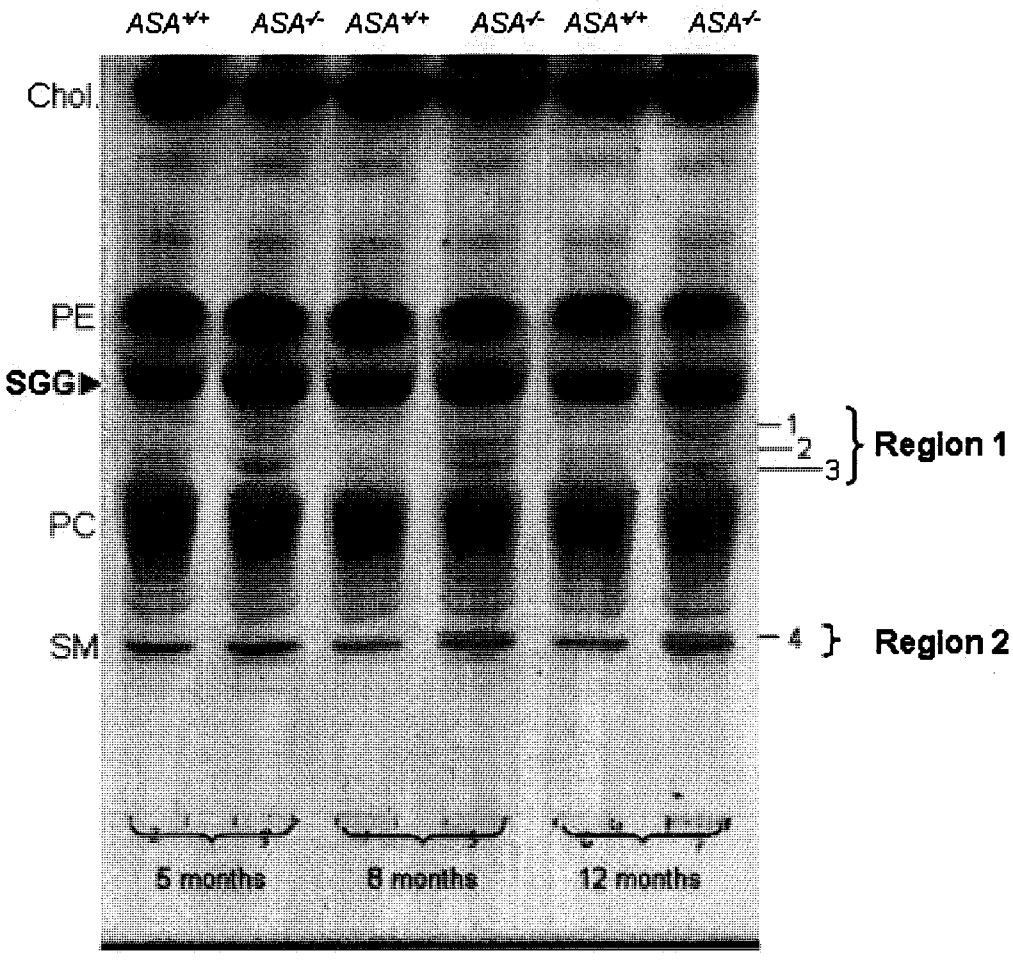
ASA+/+
ASA-/-
ASA+/+
ASA-/-
ASA+/+
ASA-/-
Chol.
PE
SGG
PC
SM
1
2
3
4
Region 1
Region 2
5 months
8 months
12 months

Figure 3.35. Glycolipid profiles of WT and *ASA* null testis. Lipid extracts from 10 mg of testis (wet tissue weight) of 5, 8, and 12 months old WT and *ASA* null mice were separated by HPTLC using the solvent system $CHCl_3$/MeOH/0.22%$CaCl_2$ = 60:35:8. The HPTLC plate was subject to orcinol charring to stain glycolipids purple. Phospholipids appeared yellow with orcinol charring (PE and PC). SGG appeared to be the most abundant glycolipid in the testis, and its level in the *ASA* null samples seemed to be higher than those of corresponding WT samples. Note the presence of extra glycolipid bands in the ASA-null testicular lipids (marked as 1, 2, and 3 in region1, and 4 in region 2). Chol, Cholesterol; PE, phosphatidylethanolamine; PC, phosphatidylcholine.

accumulated in the testis (e.g., through the inhibition of CGT and/or CST activities), and/or the SGG biosynthetic pathway is shuttled to alternative ones (e.g., the synthesis of sulfatide). The SGG quantification by ESI-MS was carried out in our collaborator Dr. K. Faull's laboratory. Ms. K. Kongmanas performed the actual sample analysis.

3.2.12. Other Changes in Lipid Profiles of ASA Null Testes

To determine whether ASA deficiency caused accumulation of other sulfoglycolipids in the testes, testicular total glycolipid profiles were examined by HPTLC (Figure 3.35), and sulfolipid profiles were examined by HPTLC (Figure 3.36) and ESI-MS (Figure 3.37). HPTLC of the total testis lipid extracts revealed several extra glycolipid bands present only in *ASA* null testes (regions 1 & 2 in Figure 3.35). Three of these lipid bands (region 1 of Figure 3.35) were present in all knockout lipid samples but were absent from the WT, and they migrated to the similar position as bovine brain sulfatide on HPTLC plate. Another glycolipid band, at a position just above sphingomyeline (band 4 in Figure 3.35), was present selectively in 8-month-old or older *ASA* null testes. The presence of this lipid closely correlated with the reduced sperm fertilizing ability of these mice. Azure A staining of HPTLC separated testicular lipids revealed only one sulfated lipid band, corresponding to SGG (Figure 3.36). The total testicular sulfolipid profiles were further characterized by a much more sensitive ESI-MS. Precursor ion scan for sulfate (m/z 97) confirmed that SGG was the major sulfolipid in the testis (Figure 3.37). Interestingly, there was a selective appearance of an ion at m/z 778.5 in the *ASA* null testis lipid samples (Figure 3.37). To determine which of the above mentioned two regions on HPTLC (Figure 3.35) that contained the extra lipid bands gave

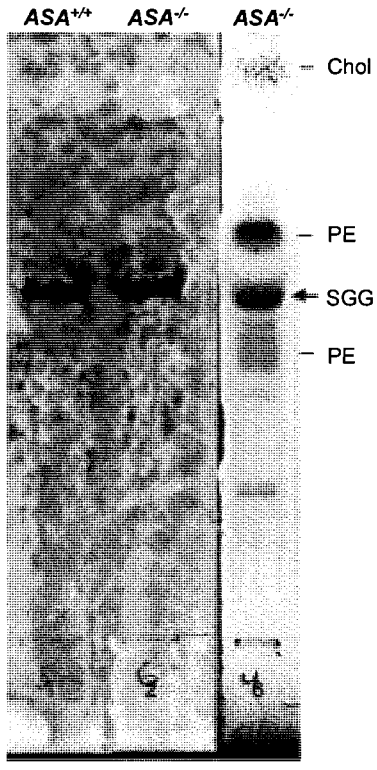
ASA+/+
ASA-/-
ASA-/-
Chol
PE
SGG
PE

Figure 3.36. HPTLC showing sulfolipid profiles of 8-month-old WT and *ASA* null testis. Lipid extracts from 15 mg of testis of 8-month-old WT (Lane 1) and *ASA* null (lanes 2 & 3) mice were separated by HPTLC using the solvent system $CHCl_3$/MeOH/0.22%$CaCl_2$ = 60:35:8. A duplicate of the *ASA* null lipid samples were applied in lanes 2 and 3. Lane 3 was cut off the HPTLC plate and subject to orcinol staining/charring, whereas the other lanes (lane 1 & 2) were stained with azure A. Glycolipids stained purple, and phospholipids appeared yellow with orcinol staining/charring (lane 3). Sulfolipids were stained blue with azure A. Note that SGG is the only detectable sulfolipid in both WT and *ASA* null samples. Data shown are representative of duplicate experiments. Chol, Cholesterol; PE, phosphatidylethanolamine; PC, phosphatidylcholine.

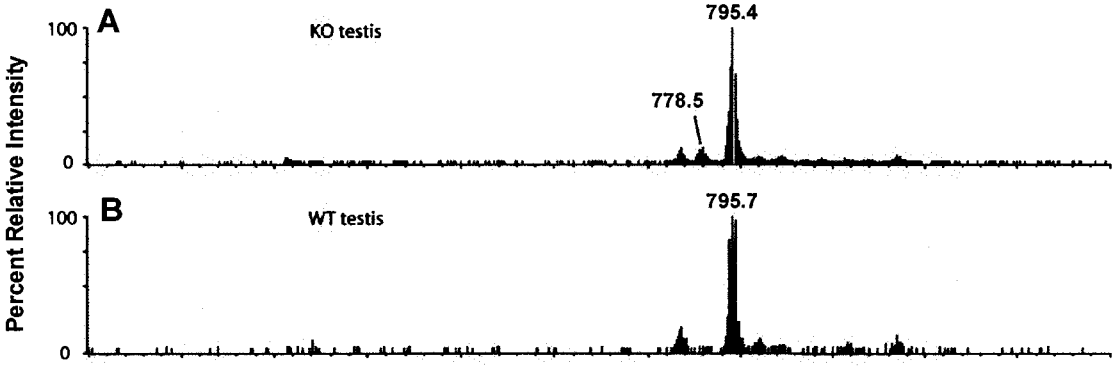
A
KO testis
795.4
778.5
100
0
B
WT testis
795.7
100
0
Percent Relative Intensity

Figure 3.37. ESI precursor ion mass spectra of lipid extracts from 8-month-old *ASA* null (A) and WT testes (B). Lipid extracts from testis (34 mg) were subject to reverse phase HPLC and 1 ml fractions were collected. All fractions collected for each sample were analyzed by a precursor ion scan for sulfate (m/z 97) in negative-ion mode to obtain the sulfated lipid profiles of the WT and *ASA* null testis. Note the selective presence of the ion m/z 778.5 in the KO sample. The ion m/z 795.4/795.7 represents $[M-H]^-$ of SGG.

rise to this ion peak, lipids in the two regions were re-extracted from scraped silica from preparative TLC plates and subject to ESI-MS. In negative ion MS mode, a signal at m/z 778.5 was apparent in lipid extracts from region 1 of 8-month-old *ASA* null testis but it was absent in age-matched WT testis (Figure 3.38). This result indicated that the extra lipid bands in region 1 on HPTLC plates gave rise to the ion at m/z 778.5. We speculated that this lipid was palmitoyl sulfatide based on the following observations: 1) the lipid was sulfated; 2) it migrated on HPTLC plates to the similar position as commercial bovine brain sulfatides; and 3) the m/z 778.5 matched $[M-H]^-$ of palmitoyl sulfatide. To confirm this, tandem mass spectrum after collisionally activated dissociation (CAD) of the parent ion at m/z 778.5 was obtained and compared with that of authentic palmitoyl sulfatide (Figure 3.39). The two spectra appeared very similar and both spectra contained common ions at m/z 97 (HSO_4^-) and m/z 241 (Figure 3.39). The latter was likely a dehydrated product of galactose-sulfate (Hsu et al., 1998). Since sulfated glucosylceramide would also give rise to an ion at m/z 778.5 $[M-H]^-$, tandem mass spectrum was obtained for HPLC-purified rat kidney sulfated glucosylceramide. Apparently, except for the presence of sulfate ion at m/z 97, the sulfated glucosylceramide spectra showed no similarities to those of m/z 778.5 ion of *ASA* null testes and palmitoyl sulfatide (Figure 3.39). This excluded the possibility that the m/z 778.5 peak was sulfated glucosylceramide. The identity of the ion at m/z 778.5 being palmitoyl sulfatide was further confirmed by Fourier Transform Mass Spectrometry (FTMS). By electrospray ionization from nanotip emitters (Proxeon) on a Thermo LTQ-FTMS, which was externally calibrated in the positive ion mode, authentic palmitoyl sulfatide (Matreya) gave a signal in the negative ion mode at m/z 778.5189 corresponding

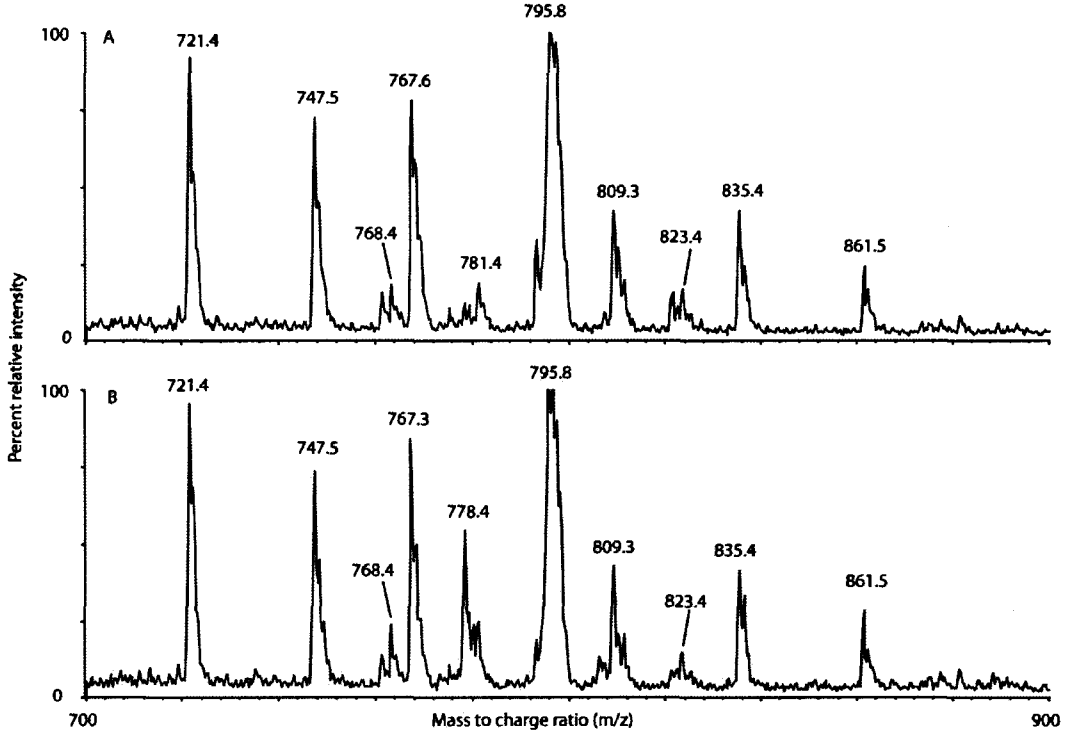
A
100
0
721.4
747.5
767.6
768.4
781.4
795.8
809.3
823.4
835.4
861.5
B
100
0
721.4
747.5
767.3
768.4
778.4
795.8
809.3
823.4
835.4
861.5
Percent relative intensity
700
Mass to charge ratio (m/z)
900

Figure 3.38. ESI-MS analysis of partially purified testis lipids. Preparative TLC was used to partially purify testis lipids corresponding to region I on HPTLC plate of total testis lipids (see Figure 3.35). The purified lipids were then subject to ESI-MS analysis in negative ion mode to scan for all negatively charged lipids. Total ion current profiles of 8-month-old WT (A) and *ASA* null (B) testis lipids (in region I) are shown. Note the selective presence of ion at m/z 778.4 in the *ASA* null sample. All the other ions are present in both lipid samples.

to the $(M-H)^-$ anion (calculated 778.5139 for $C_{40}H_{76}NO_{11}S$, difference = 5 mDa or 6.4 ppm). Under the same conditions an HPTLC partially purified sample from *ASA* null mouse testis gave a signal at m/z 778.5224 (different by 8.5 mDa or 10.9 ppm from authentic palmitoyl sulfatide). When the samples of authentic palmitoyl sulfatide and the testis lipid extract were mixed in proportions predicted to give equivalent signal strengths for their m/z 778 components, a single signal at m/z 778.5 emerged with no indication of splitting even at resolution up to 1×10^6. Furthermore, when the spectrum of the partially-purified lipid extract was re-calibrated using the signal at m/z 795 as an internal calibrant (assigned as coming from the testis lipid SGG, elemental composition $C_{41}H_{79}O_{12}S$, calculated as 796.5292), the m/z 778.5 signal was re-measured at 778.51447, different by 0.57 mDa or 0.7 ppm from authentic palmitoyl sulfatide. Based on our MS data, we concluded that the ion at m/z 778.5 in *ASA* null testis lipids was palmitoyl sulfatide. The MS analyses were performed in our collaborator Dr. K. Faull's laboratory. Ms. K. Kongmanas purified the rat kidney sulfated glucosylceramide by HPLC and helped Dr. Faull run the lipid samples on mass spectrometer.

3.2.13. Flow Cytometric Analysis of SGG in Isolated Testicular Germ Cells

SGG quantification results indicated that the sulfoglycolipid was not accumulated in *ASA* null sperm and in fact was decreased in amount in sperm of 8-month-old mice. In contrast, SGG was accumulated in the *ASA* null testes at both 5 and 8 months. Total testicular lipids were extracted from all testicular cell types, including germ cells, Sertoli cells, Leydig cells, connective tissue cells and blood cells. However, only the first two

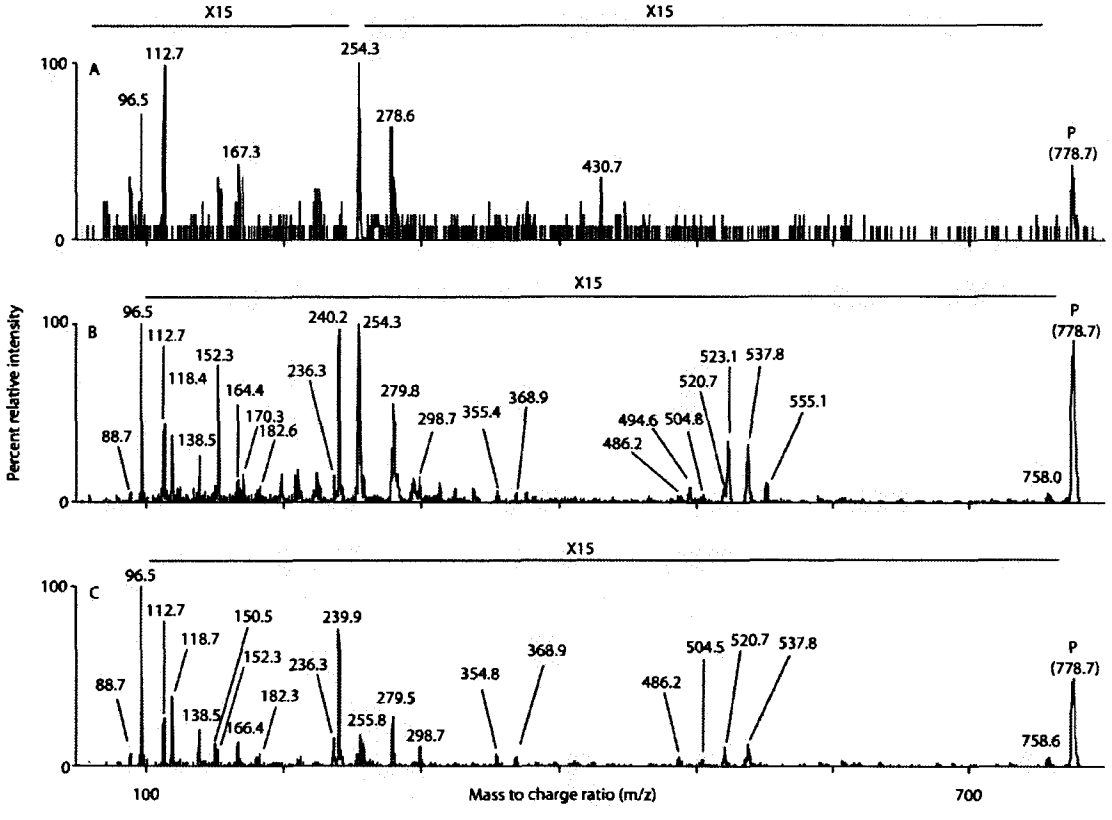
X15
X15
A
100
0
112.7
254.3
96.5
278.6
167.3
430.7
P
(778.7)
X15
B
100
0
96.5
112.7
240.2
254.3
152.3
118.4
236.3
164.4
279.8
170.3
182.6
298.7
355.4
368.9
88.7
138.5
523.1
537.8
520.7
555.1
494.6
504.8
486.2
758.0
P
(778.7)
X15
C
100
0
96.5
112.7
150.5
239.9
118.7
152.3
236.3
354.8
368.9
504.5
520.7
537.8
88.7
182.3
279.5
138.5
166.4
255.8
298.7
486.2
758.6
P
(778.7)
Percent relative intensity
100
Mass to charge ratio (m/z)
700

Figure 3.39. Tandem mass spectra of (A) sulfated glucosylceramide, (B) unknown ion at m/z 778.7 from the ASA *null* testis and (C) palmitoylsulfatide (C16). HPLC purified sulfated glucosylceramide from rat kidney (A) and commercial palmitoyl sulfatide (Matreya) (C) were analyzed by ESI-MS/MS. Lipid extracts from 8-month-old *ASA* null testes were subject to reverse phase HPLC and the effluent was continuously monitored by ESI-MS in the negative-ion mode for the fractions that gave rise to the ion at m/z 778.7. Tandem mass spectra from CAD of this parent ion at m/z 778.7 was recorded (B).

types of cells possess ASA (Figure 3.2). Therefore, it is very likely that SGG would only be accumulated in these two cell types when ASA is missing. Quantification of SGG in both testicular germ cells of various developmental stages and Sertoli cells in *ASA* null and WT mice would have given a better understanding of how SGG metabolism changes in the mutant mice. While the most desirable approach for this SGG quantification would be through ESI-MS of isolated lipids from each stage of testicular germ cells and Sertoli cells, this methodology requires a large number of animals for the preparation of each cell type for lipid extraction, and would not be suitable for the *ASA* null animals. I took an alternative approach by using flow cytometry with our affinity-purified anti-SGG IgG to analyze changes of SGG levels in testicular germ cells of *ASA* null mice in comparison with those of WT germ cells. Using DNA flow cytometry to distinguish germ cell DNA content, different stages of isolated testicular germ cells could be identified. Their positioning in the flow cytogram was based on the fluorochrome (DRAQ5) binding to their DNA; the fluorescence emission intensities of each germ cell stage were proportional to their DNA content (C values) (Figure 3.40A). The major cell populations were classified as 4C (diploid primary spermatocytes), 2C (spermatogonia), 1C (haploid round spermatids) and apparently hypohaploid (haploid elongating/elongated spermatids). The hypohaploid peak is due to the compaction of elongating/elongated spermatid DNA, thus causing incomplete accessibility to the DNA dye (Clausen et al., 1982; Evenson et al., 1986). In WT mice at both 5 months and 8 months of age, the SGG intensities were highest in primary spermatocytes, second in round spermatids and lowest in elongating/elongated spermatids, with an approximate ratio of 4:1:0.4. Since one primary spermatocyte gives rise to four spermatids, a ratio of ~ 4:1 for SGG intensities in

these cell types is expected. This result was also consistent with a previous report on the onset of SGG synthesis in primary spermatocytes (Kornblatt, 1979). Cells with 2C DNA (mainly spermatogonia and some somatic cells) had no SGG intensity, which was consistent with immunolocalization results showing SGG in pachytene spermatocytes, and spermatids, but not in spermatogonia and Sertoli cells (Lingwood, 1981). The SGG intensities on primary spermatocytes, round and elongated spermatids of 5-month-old *ASA* null mice were 84 ± 8%, 84 ± 12% and 91 ± 11% of the values of age-matched WT males, respectively, showing no significant difference (Figure 3.40). In contrast, the SGG intensities on primary spermatocytes, and elongated spermatids of 8-month-old *ASA* null mice were significantly reduced to 49 ± 16% ($P < 0.05$), and 52 ± 17% ($P < 0.05$) of the age-matched WT values, respectively (Figure 3.40). The SGG intensity on round spermatids of 8-month-old *ASA* null mice was also decreased (77 ± 21% of the WT value), although the difference was not statistically significant. This may be due to insufficient number of animals analyzed. These results were consistent with the decrease of SGG levels on epididymal sperm of 8-month-old *ASA* null mice, as determined by quantitative ESI-MS. However, the flow cytometry results did not agree with the biochemical data showing SGG accumulation in the *ASA* null testes. This discrepancy may be explained by the possibility that the extra SGG as determined by ESI-MS belonged to non-germ cells in the testis, i.e., the Sertoli cells and this argument will be elaborated in the DISCUSSION section.

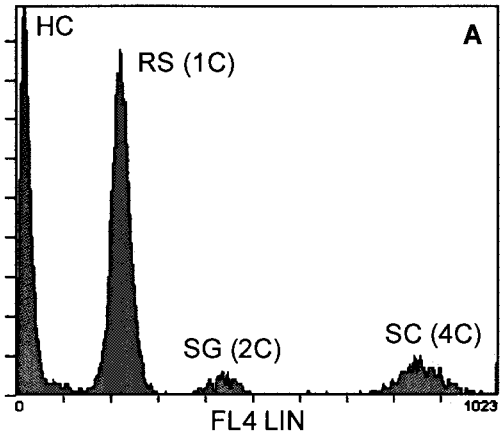
A
HC
RS (1C)
SG (2C)
SC (4C)
0
1023
FL4 LIN

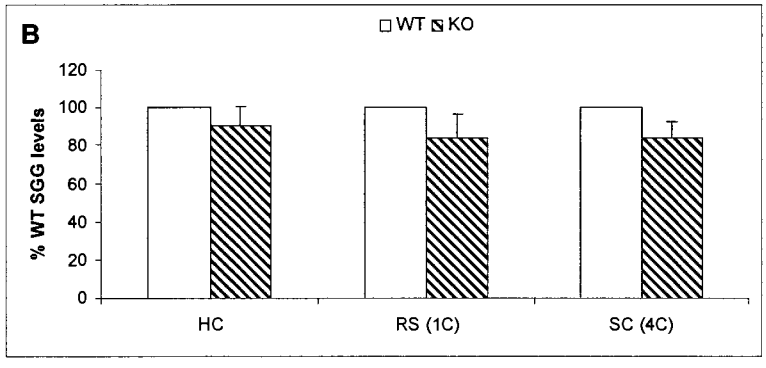
B
WT KO
% WT SGG levels
120
100
80
60
40
20
0
HC
RS (1C)
SC (4C)

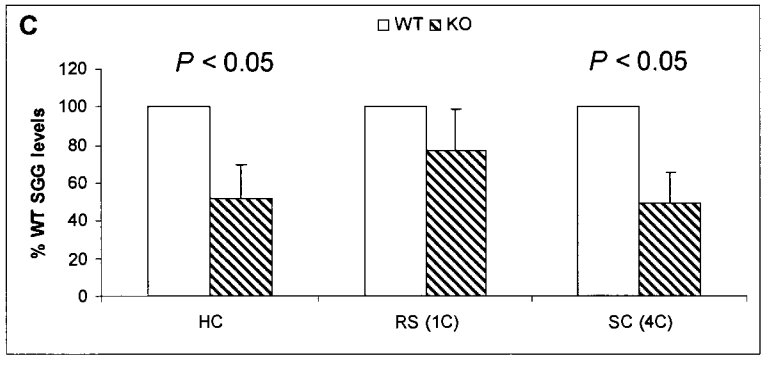
C
WT KO
P < 0.05
P < 0.05
% WT SGG levels
120
100
80
60
40
20
0
HC
RS (1C)
SC (4C)

Figure 3.40. Flow cytometric analysis of SGG levels on primary spermatocytes (SC), round spermatids (RS) and elongated spermatids (HC). (**A**) Representative flow cytograms showing the distribution of testicular germ cell populations based on their DNA content (C value, denoted in parenthesis). (**B**) Percent WT SGG levels in different germ cell populations of 5-month-old *ASA* null mice. (**C**) Percent WT SGG levels on different germ cell populations of 8-month-old *ASA* null mice. Data were expressed as mean ± SD of percent control of means from three experiments. Significant differences between corresponding WT and KO values were indicated ($P < 0.05$).

3.2.14. Testis and Sperm Cholesterol Levels were not Affected by the Null Mutation of ASA

Since SGG is an ordered lipid (Tanphaichitr et al., 2003) and it interacts with other ordered lipids, such as saturated phospholipids (Tanphaichitr et al., 2003; Attar et al., 1998; Attar et al., 2000) and cholesterol (Bou et al., 2006), to form lipid raft microdomains on the sperm plasma membrane (Bou et al., 2006), the aberrant SGG levels in sperm and testes of the ASA null mice may affect cellular/membrane cholesterol levels. Biochemical quantification of cholesterol revealed 0.590 ± 0.019 μg free cholesterol (n = 3) and 0.618 ± 0.022 μg free cholesterol + cholesteryl ester (total cholesterol) (n = 3) in one million of *ASA* null sperm from 5-month-old animals. These values were not dissimilar to those in WT sperm of the same number collected from age-matched animals, i.e., 0.577 ± 0.03 μg (n = 3) and 0.607 ± 0.036 μg (n = 3), respectively (Figure 3.41). When mice reached 8 months of age, *ASA* null sperm had 0.737 ± 0.048 $\mu g/10^6$ sperm (n = 3) and 0.757 ± 0.044 $\mu g/10^6$ sperm (n = 3) of free cholesterol and total cholesterol, respectively. These values were also similar to those in WT sperm from animals of the same age, i.e., 0.705 ± 0.037 $\mu g/10^6$ sperm (n = 3) and 0.728 ± 0.040 $\mu g/10^6$ sperm (n = 3), respectively (Figure 3.41). Of note was an increase in both free and total sperm cholesterol levels in the older animals (both WT and *ASA* null) (Figure 3.41). As well the difference between total and free sperm cholesterol became smaller at the age of 8 months (Figure 3.41). A similar trend of no alteration of cholesterol levels was observed in testes of *ASA* null mice, as compared with WT animals, in both ages (Figure 3.41). At 5 months old, *ASA* null males had free and total cholesterol of 1.538 ± 0.266 (n = 3) and 1.635 ± 0.308 (n = 3) μg/mg testis, respectively (Figure 3.41). The

corresponding values in WT males of the same age were 1.446 ± 0.162 (n = 3) and 1.565 ± 0.200 (n = 3) μg/mg testis respectively (Figure 3.41). When the animals were 8 months old, slight but significant ($P < 0.05$) decreases of free and total testis cholesterol levels were observed in both *ASA* null and WT males, i.e., 1.134 ± 0.052 (n = 3) and 1.290 ± 0.071 (n = 3) μg/mg testis, respectively, for *ASA* nulls, and 1.199 ± 0.061 (n = 3) and 1.324 ± 0.078 (n = 3) μg/mg testis, respectively, for the WT (Figure 3.41).

3.2.15. Summary of the Levels of SGG and other Lipids in ASA Null Mice

Since SGG is expressed in male germ cells, and it can be desulfated by ASA in vitro, accumulation of SGG in the testis and sperm of *ASA* null mice was expected. By using a very sensitive quantitative ESI-MS with a proper internal standard (deuterated SGG), we did not detect any significant changes in sperm SGG amount in 5-month-old *ASA* null mice, as compared with age-matched WT. In contrast, the amount of sperm SGG in 8-month-old mutant mice was significantly reduced. Although these results were contradictory to what was expected, they may explain, at least in part, the reduced sperm fertilizing ability of the older *ASA* mice (since SGG has been shown to play roles in sperm-egg interaction). In the testis of mutant mice at both ages, however, SGG was indeed accumulated, as expected. To understand the discrepancy between the levels of SGG in the *ASA* null testes and sperm, testicular germ cells were isolated and their SGG levels were determined by flow cytometry using anti-SGG antibodies. Consistent with the SGG quantification data on sperm, my results showed that the levels of SGG in testicular germ cells of the 5-month-old mutant mice were similar to those of the WT,

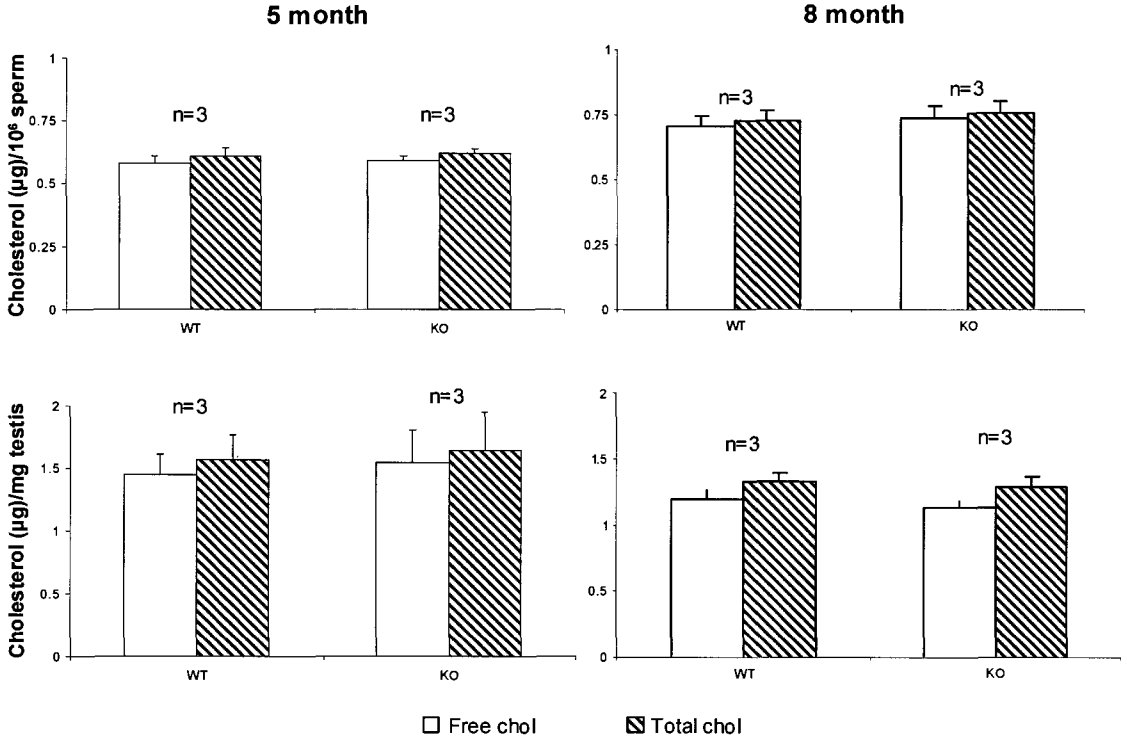
5 month
8 month
Cholesterol (µg)/10⁶ sperm
Cholesterol (µg)/mg testis
n=3
WT
KO
Free chol
Total chol

Figure 3.41. Similar levels of sperm and testis cholesterol in 5- and 8-month-old WT and *ASA* null mice. Total cholesterol (free cholesterol + cholesterol ester) and free cholesterol were quantified fluorometrically using the Amplex Red (Molecular Probes) assay with or without the inclusion of cholesterol esterase in the reaction, respectively, from total sperm (top two plots) and testis (bottom tow plots) lipid extracts. Ages of the mice used were indicated on the top. n = number of mice assayed. Empty bars represent free cholesterol, while the striped bars represent total cholesterol.

whereas a significantly reduced SGG levels were detected in germ cells of the older mutant mice. These results suggested that SGG was unlikely to be accumulated in testicular germ cells. Since ASA is expressed in Sertoli cells and Sertoli cells are known for their phagocytotic activity toward membrane remnants of apoptotic germ cells and residual bodies, SGG might have been accumulated in these cells. The accumulation of SGG may become toxic to Sertoli cells, which in turn impaired their cellular functions, leading to aberrant sperm SGG levels and disruption of spermatogenesis. This is discussed in more detail in DISCUSSION.

In addition to SGG, palmitoylsulfatide, a sulfoglycolipid not normally present in WT testis at an appreciable amount, was also found to be accumulated in the mutant testis. The appearance of this lipid may reflect a shunting of the SGG/SGC biosynthetic pathway as a result of SGG accumulation. We also found another glycolipid whose presence in the mutant testis correlated with the onset of reduced sperm fertilizing ability (present only in 8-month-old *ASA* null testis). Efforts were made to determine the identity of this lipid, but we have not been successful due to insufficient amount of lipid samples. Apart from changes in these lipids, the presence of other major lipids (e.g., phospholipids, sphingomyeline, and cholesterol) did not seem to be affected by ASA deficiency.

CHAPTER FOUR

DISCUSSION

This thesis consists of two parts. The first part describes the localization of ASA in the male reproductive system and its role on the sperm surface in fertilization. ASA was localized to the acrosomal system of spermatogenic cells, and the acrosome of mature sperm. ASA also existed on the mature sperm surface. This ASA entity originated from the epididymal fluid; it was a secreted product of the epithelial cells of the epididymis. This extracellular ASA deposited onto the sperm surface via its high affinity for SGG on the plasma membrane of transiting sperm. Sperm surface ASA was involved in sperm-ZP binding. Moreover, purified sperm ASA had affinity for the ZP by binding to both ZP3 and ZP2, suggesting a role in the primary and secondary sperm-ZP interaction. ASA is also present in Sertoli cells-in lysosomes, and late residual bodies. However, its role in Sertoli cells is unknown. In the second part of my thesis, the physiological significance of Sertoli cell ASA was investigated using *ASA* null mice as a model. Results presented in this thesis indicated that ASA was important in keeping SGG balance in the testis and sperm, suggesting that SGG was a natural substrate of ASA in vivo. SGG was accumulated in the mutant testes, most likely in Sertoli cells, which in turn might lead to Sertoli cell dysfunction and subsequently to spermatogenesis disruption in the mutant mice older than 5 months of age. The decrease of sperm SGG levels in older *ASA* null mice may account for their reduced fecundity and their sperm in vitro fertilizing competence. However, it remains to be verified that SGG is indeed accumulated in Sertoli cells and this accumulation has adverse effects on Sertoli cell

functions. Results on ASA localization, acquisition of sperm surface ASA and its role in sperm-egg interaction have been published in two manuscripts. The involvement of sperm surface and acrosomal ASA in primary and secondary ZP binding, respectively, as well as the work on *ASA* null mice have not been published yet.

4.1. Sperm ASA as a ZP Binding Molecule

4.1.1. Acquisition of Sperm Surface ASA from the Epididymal Fluid

The results presented here demonstrated that sperm ASA is involved in mouse gamete recognition. Immunocytochemistry showed that ASA was expressed in the acrosome and acrosomal processes of round and elongating spermatids, respectively. However, IIF and flow cytometry analysis revealed the absence of ASA on the live testicular sperm surface. Its absence was unlikely due to masking of testicular sperm surface, since SGG rising only a short distance from the sperm plasma membrane was readily detectable by IIF. Therefore, the negative IIF staining of ASA on live testicular sperm strongly suggested its absence on the surface of these sperm and argued against the possibility that acrosomal ASA might be secreted onto the maturing sperm surface.

ASA immunoreactivity was also present in Sertoli cells. In the majority of these cells, the globular body-like staining patterns of ASA, regionalized mainly in the supranuclear region, might reflect lysosomal localization of the enzyme. This postulation was supported by previous reports of the presence of ASA in lysosomes of Sertoli cells (Moviglia et al., 1982) and other somatic cells (Stein et al., 1989a; Fujii et al., 1992; Leznicki and Rozanska, 1991; Kelly et al., 1989; Leznicki and Bleszynski, 1970; Clendenon and Allen, 1970). Late residual bodies present in Sertoli cells at certain stages

of the spermatogenic cycle were also stained intensely with anti-ASA, although early residual bodies showed negative staining. Because the late residual bodies eventually fuse with the Sertoli cell lysosomes (Morales et al., 1986), the results suggested that ASA present in the late residual bodies was derived from Sertoli cell lysosomes following their fusion. The exact roles of ASA in the Sertoli cells are currently unclear. We postulate that it might be involved in the degradation of SGG phagocytosed from residual bodies during spermiogenesis or from apoptotic spermatogenic cells, thus contributing to the homeostasis of SGG. Nonetheless, SGG is hardly detectable in Sertoli cells in normal testis, possibly due to its fast degradation by ASA. However, SGG may become accumulated in Sertoli cells when ASA is absent, such as the case in ASA deficient animals.

Immunocytochemistry results revealed ASA staining in strips of principal cells in the cauda epididymis (Figure 3.2) and most of the principal cells in the vas deferens (Figure 3.2). Principal cells are recognized for their secretory activities (Hermo and Robaire, 2002; Hermo et al., 2002). The network patterns of ASA staining in principal cells (Figure 3.2, inset), resembling the endoplasmic reticulum and Golgi apparatus (Robaire and Hermo, 1988), suggested that ASA was synthesized in these cells. Similar staining patterns have been noted in principal cells for SGP-2, immobilin, and other known secreted proteins of the epididymis (Hermo et al., 1994). Corroborating the immunolocalization results, ASA was shown to be expressed in the epididymis by RT-PCR (Figure 3.3), and its protein was present in the epididymal fluid as revealed by Western blot (Figure 3.4). These results strongly suggested that ASA was secreted by epididymal epithelial cells into the lumen.

Although immunocytochemistry also revealed the presence of ASA in the initial segment, caput, and corpus epididymis, the enzyme was restricted to apical cells, narrow cells, and adsorptive clear cells (Figure 3.2). As demonstrated for other lysosomal enzymes, immunocytochemical reaction and electron microscopic immunogold labeling in these cell types appear to represent the targeting of these enzymes from the Golgi apparatus via small vesicles directly to their lysosomes, which were abundant in these cells (Hermo and Robaire, 2002; Morales et al., 1986; Hermo et al., 1992b; Igdoura et al., 1994). This may also be the case for ASA. Alternatively, because narrow cells, apical cells, and clear cells are known for their endocytotic activities (Hermo and Robaire, 2002; Hermo and Robaire, 2002), ASA in these cells may have originated from transit sperm with damaged acrosomes through the endocytosis mechanism. ASA in these cells may function in desulfation of SGG, endocytosed from remnant membrane vesicles in the epididymal fluid. These vesicles could originate from the shedding of excess plasma membranes of round spermatids during their differentiation to testicular spermatozoa and/or from plasma membranes of damaged sperm in transit through the initial segment and the proximal region of the caput epididymis.

On mature live sperm, ASA expression was confined to the plasma membrane overlying the acrosome, the known site for sperm binding to the ZP (Figure 3.5). However, results from IIF and flow cytometry analyses indicated the absence of ASA on live testicular sperm, caput and corpus epididymal sperm (Figures 3.5 and 3.6). This implied that ASA was acquired by sperm during their transit through the epididymis. As discussed above, the principal cells of the cauda epididymis and vas deferens were likely the source of this sperm surface ASA. In fact, ASA in the epididymal fluid and that on

sperm surface had the same molecular mass (Figure 3.4). Since ASA has very high affinity for SGG or SGC (K_d = 8.9 nM for both SGG and SGC) immobilized as monolayers in microwells (Carmona et al., 2002b), deposition of ASA onto the mature sperm surface most likely occurred through the tight interaction between ASA and sperm SGG (K_d = 46 nM). Indeed, the binding of Alexa-430 ASA to sperm was inhibited by anti-SGG Fab (Figure 3.11 and Table 3.1). Available information implies that ASA can bind to SGG non-enzymatically via electrostatic interaction: 1) SGG, coexisting with ASA on the surface of mature caudal epididymal and ejaculated sperm, is not desulfated , and binding of ASA to sperm does not lead to SGG desulfation in vitro (Carmona et al., 2002b); 2) sperm surface ASA is enzymatically active (using NCS as a substrate) (Tantibhedhyangkul et al., 2002); therefore the active site pocket of ASA is not involved in binding to sperm surface SGG; 3) ASA contains numerous positively charged amino acids on the surface of its 3-D structure (Schenk et al., 2009) (Figure 1.9) (Lukatela et al., 1998). Besides the active site pocket of ASA with the highest positive charge, the electrostatic potential of ASA revealed a surface cleft formed by amino acid residues Arg496 and Ile487, with the second highest positive charge density (Figure 1.9). Structural docking of SGG to ASA 3-D structure, performed by our collaborator, Dr. P-G Nyholm, Goteborg University, using AUTODOCK program (developed at Scripps Research Institute to dock flexible substrates into protein active sites) suggests that Arg496 and Ile487 (7-9 Å apart, a distance comparable to the size of SGG) are crucial residues for SGG binding (Figure 1.9). Arg496 would interact with the SO_4^{-2} group of SGG electrostatically, while Ile487 would interact with the hydrophobic sugar ring of SGG. This structural docking approach has been used previously to identify SGC

(SGG's analog) binding amino acids (Arg342 and Phe198, 11 Å apart) of Heat Shock Protein 70 (Mamelak and Lingwood, 2001). Since ASA is known to be targeted to the lysosome via the mannose-6-phosphate receptor (Rahi and Srivastava, 1983), and since this receptor is present on the sperm surface (Barbieri et al., 1995), the involvement of mannose-6-phosphate receptor in targeting ASA onto the sperm surface was studied. At millimolar concentrations, mannose-6-phosphate did not inhibit Alexa-430 ASA binding to intact cauda sperm (Table 3.1), suggesting that deposition of ASA onto sperm surface was not dependent on mannose-6-phosphate receptor. The interaction between ASA and mannose-6-phosphate receptor on the sperm surface may be of a low affinity, making it impossible for mannose-6-phosphate to compete with ASA binding to sperm surface SGG, which occurred with high affinity. Collectively, these results indicate that sperm surface ASA is acquired from the epididymal fluid via tight interaction with SGG during sperm transit through the epididymis.

ASA was a minor protein in the caudal epididymal and vas deferens fluid- it was only 0.13% by weight of total proteins in the fluid. This result and the strong implication that sperm surface ASA originated from the epididymal fluid explain why ASA existed in very small amount on the surface of mature mouse sperm (1 pmole/million sperm) (data from my work published in manuscript Tantibhedhyangkul et al., 2002). As part of my thesis research, the physiological significance of sperm surface ASA has been demonstrated. ASA remained on the anterior head surface of uterine mouse sperm (Figure 3.5 D) and was involved in sperm-egg interaction both in vitro (Figure 3.12) and in vivo (Figure 3.14) (Tantibhedhyangkul et al., 2002). Therefore, the molar ratio of ASA to SGG in mature sperm was very low (600 pmoles of SGG/million sperm

(Furimsky et al., 2005) vs. 1 pmole/million sperm). This low ratio may be essential for maintaining the integrity of the sperm plasma membrane since exogenously added purified sperm ASA at a nonphysiological high concentration induced sperm to prematurely acrosome react (Carmona et al., 2002b). Since SGG is also a ZP binding molecule (White et al., 2000), the distribution of free SGG molecules (unbound by ASA) may be beneficial for interaction between sperm and the ZP glycans. ASA, being a peripheral plasma membrane protein (Tantibhedhyangkul et al., 2002), may first bind to the ZP glycans and bring them next to the sperm surface for interaction with the sulfated galactose head groups of SGG molecules, which extend only a short distance from the sperm plasma membrane lipid bilayers (Figure 1.8). Restricted secretion of ASA by the epididymis may thus regulate the low ratio of ASA to SGG with a beneficial consequence of better binding of mature sperm to the ZP. As with other molecules involved in egg interaction (e.g., P26H (Legare et al., 1999), α-mannosidase (Tulsiani et al., 1995a), SED1 (Ensslin and Shur, 2003) and protein DE (Ellerman et al., 1998; Moore et al., 1994), acquisition of ASA by the sperm surface would constitute part of the sperm maturation process, which prepares sperm with optimal ZP-binding capacity.

4.1.2. Involvement of ASA in Both Primary and Secondary Sperm-ZP Binding

The current investigation showed that ASA on mouse sperm was present in two different cellular locations, the plasma membrane overlying the acrosome and within the acrosome itself. The sperm head plasma membrane ASA was involved in the primary binding of acrosome-intact sperm to the ZP, as shown by the inhibition of affinity-purified anti-ASA IgG and Fab fragments on sperm-ZP binding (Figure 3.12). The

decrease of sperm-ZP binding following sperm pretreatment with anti-ASA antibody was not from an increase in premature acrosome reaction (Figure 3.13). The majority of sperm (~90%) treated with either 100 μg/ml anti-ASA IgG or 100 μg/ml PRS IgG remained acrosome intact, similar to those untreated sperm (Figure 3.13, empty boxes). In addition, these antibody-treated sperm, like the untreated sperm, contained the functional machinery necessary for the ZP-induced acrosome reaction; ~90% of them underwent the acrosome reaction when exposed to 10 solubilized ZP/ml (Figure 3.13, dot-filled boxes). This result also indicated that ASA was not involved in ZP induced acrosome reaction. The role of ASA in mediating primary sperm-ZP interaction was further confirmed in this report by the direct demonstration that purified sperm ASA bound to mouse ZP3 glycoprotein (Figure 3.19), previously documented for its role in primary binding to acrosome-intact sperm (Bleil and Wassarman, 1980a; Litscher et al., 2009; Wassarman and Litscher, 2008).

In addition to its localization on the head surface of plasma membrane intact sperm, ASA was also detectable on the head of acrosome-reacted sperm (Figure 3.8c). Indirect immunofluorescence localization of ASA on fixed and permeabilized mouse sperm revealed the existence of ASA in the acrosome (Figures 3.5E), consistent with previous report on the de novo synthesis of acrosomal ASA in the primary spermatocytes (Dudkiewicz et al., 1979; Dudkiewicz, 1984; Nikolajczyk and O'Rand, 1992; Kreysing et al., 1994b). These results implied that ASA might be involved in secondary sperm-ZP binding. In the mouse, binding of membrane-intact sperm to ZP3 induces acrosome reaction thereby making components within the acrosomal matrix and its surrounding membranes available for binding to the ZP glycoproteins. Mouse ZP2 is considered as

the secondary sperm receptor for the binding of acrosome-reacted sperm based on the observations that purified mouse ZP2 binds to acrosome-reacted sperm (Bleil and Wassarman, 1986) but does not inhibit binding of acrosome-intact sperm to the ZP (Bleil and Wassarman, 1980a). Therefore, the complementary binding molecule(s) for the ZP2 on sperm must be within the acrosome (i.e., in the acrosomal matrix and/or on the inner acrosomal membrane). While these perspectives still hold true, the scenario of sperm-ZP interactions may be much more complex. This is mostly because of the realization that acrosome reaction is not an all or none event where the acrosome is either "intact" or "reacted" (Kim and Gerton, 2003; Buffone et al., 2008). It is thus conceivable that, after the initial binding of acrosome-intact sperm to the ZP and the induction of acrosome reaction, acrosome reacting sperm are also involved in ZP binding. Since acrosome-reacting sperm have not lost their entire plasma membrane and outer acrosomal membrane yet, molecules present on these membranes as well as in the acrosome should be involved in this transitional binding event. It is also reasonable to speculate that both ZP2 and ZP3 are involved in this binding. In this thesis, I demonstrated that ASA was part of the acrosomal component; as well it existed on the convex ridge surface of acrosome reacted sperm (presumably inner acrosomal membrane). Most importantly, my results revealed the affinity of ASA for ZP2 in addition to ZP3. All these findings therefore suggested that ASA in the acrosome was involved in secondary ZP binding. Considering that ASA also has affinity for ZP3, it is possible that ASA in the acrosome still retained the ability to bind to ZP3, thus contributing to the binding of acrosome-reacting sperm to the ZP. Taken together, my results strongly suggested that sperm ASA was involved in the continuation of ZP binding. First, sperm surface ASA was involved

in the primary binding of acrosome-intact sperm to ZP3. After initiation of acrosome reaction, ASA in the acrosomal matrix contributeed to the transitional binding of acrosome-reacting sperm to both ZP2 and ZP3. Finally, ASA on the inner acrosomal membrane of acrosome-reacted sperm was involved in the secondary binding to ZP2.

The binding of ASA to purified ZP3 and ZP2 glycoproteins described above was shown by immuno-dot blot analyses (Figure 3.19). However, ZP2 appeared to have a higher degree of ASA binding (Figure 3.19), which may suggest that ASA played a more important role in securing acrosome-reacting/reacted sperm on the ZP. This binding may be mediated by ionic interactions between polysulfated groups on the ZP glycoproteins and the basic amino acid residues on ASA, since it was abolished by 1 μM of dextran sulfate (500 kDa) (Figure 3.19B). Interestingly, a similar mechanism has been described for the binding of proacrosin (Howes et al., 2001) and sp38 (Mori et al., 1993) to mouse and porcine ZP2, respectively, as well as for the interaction between sea urchin bindin and sulfated fucans of the vitelline envelope (DeAngelis and Glabe, 1987). Thus, such a mechanism appears to be evolutionary conserved. All three ZP glycoproteins contain sulfated glycans (Dunbar et al., 2001; Harris et al., 1994; Wassarman et al., 2004; Takasaki et al., 1999; Noguchi and Nakano, 1992; Hokke et al., 1994; Topfer-Petersen et al., 2008; Nixon et al., 2007). Sulfation predominantly occurs at the C-6 position of GlcNAc residue within the ZP glycans, and to a small but significant extent at the C-3 position of the reducing terminal GlcNAc (Hokke et al., 1994; Takasaki et al., 1999). As an arylsulfatase, ASA may bind to the ZP via its active site pocket, since the active site pocket of sperm surface ASA is still available (Tantibhedhyangkul et al., 2002). On the ZP, the sulfated sugar residues may be exposed enough to access the active site pocket of

ASA. However, the demonstration that both recombinant ASA mutants, C69A and CKK (Cys69, Lys302 and Lys123-all mutated to Ala) with no SGG/SGC desulfation activity (Schenk et al., 2009), bound to the ZP immobilized on nitrocellulose membrane (Figure 3.21) suggested that ASA's active site pocket was not involved in binding to the ZP.

X-ray crystallography and computational studies have revealed positively charged patches and clefts on the ASA molecular surface (Lukatela et al., 1998; Schenk et al., 2009). These surface areas may be the binding sites of ZP sulfated sugar residues. As discussed above, computational and structural docking studies of ASA-SGG interactions revealed that the sulfated galactose group of SGG docks with the second lowest energy into the ASA surface cleft (containing R496 and I487) (Figure 1.9). The same mechanism may apply to the interaction between ASA and the ZP. Unfortunately, structural docking of ZP glycans cannot be accomplished with accuracy because of the unpredictable flexibility of the glycans. Since ASA exists as a dimer at physiological pH, one monomer may bind to the sperm surface SGG while the other one may interact with the sulfated sugar moieties of the ZP glycan. Work is currently ongoing to determine whether the positively charged ASA surface cleft is involved in ZP binding. Should this surface cleft be involved in ZP binding, recombinant mutant ASA (R496A/I487A) wound have minimal affinity for the ZP.

4.2. Fecundity of ASA Null Male Mice

ASA is a ubiquitously expressed lysosomal enzyme. In the male reproductive system, ASA was expressed in spermatogenic cells, Sertoli cells, and principal cells of the caudal epididymis and vas deferens (Figure 3.2). On mature sperm, ASA was

present in the acrosome and on the head surface (Figure 3.5) (Tantibhedhyangkul et al., 2002). The acrosomal ASA is from de novo synthesis in primary spermatocytes (Kreysing et al., 1994b), whereas the surface ASA is acquired during sperm epididymal transit (see part 1). We have demonstrated that sperm surface ASA is involved in sperm-ZP interaction (Figure 3.12) (Tantibhedhyangkul et al., 2002; Carmona et al., 2002a) and dispersion of the viscoelastic cumulus matrix of expanded COCs (Wu et al., 2007a). In the first part of my thesis, I further demonstrated that purified sperm ASA bound directly to the ZP3 sulfoglycoprotein (Figure 3.19), confirming the role of sperm surface ASA in primary ZP binding. I also demonstrated the direct affinity of ASA to purified mouse ZP2 sulfoglycoprotein (Figure 3.19), suggesting a role of acrosomal ASA in the secondary binding of acrosome-reacting/reacted sperm to the egg ZP. The overall significance of sperm ASA was evidenced by strong inhibitory effects of anti-ASA in mouse in vivo fertilization (Figure 3.14) (Tantibhedhyangkul et al., 2002; Tanphaichitr et al., 1992). As a catabolic enzyme, the roles of ASA activity in the acrosome and in Sertoli cells are less clear. In order to confirm the physiological significance of sperm ASA in fertilization, detailed fecundity of *ASA* null male mice was studied. This study also provided an opportunity to investigate whether ASA's enzymatic activity was required to regulate SGG (a known substrate of ASA in vitro) balance in the testis, which in turn is pertinent for spermatogenesis.

4.2.1. Effects of ASA Null Mutation on Sperm Fertilizing Ability

Natural mating studies over a period of ~6 months (starting when the males were ~ 3 months old till they were ~ 8 months of age) revealed that *ASA* null males produced

smaller litters than WT controls (Figure 3.24). Upon closer examination, the average accumulated litters produced by each mating pair were similar between WT and *ASA* null males up to 5 months of age, but this number of *ASA* null males started to decline when the mice became older, suggesting subfertility in these mice (Figure 3.24A). Consistent with the mating results, sperm from 5-month-old *ASA* null males showed almost normal levels of ZP binding ability, and were fully capable of fertilizing eggs in vitro, while near background levels of sperm-ZP binding and in vitro fertilization were observed for sperm from 8-month-old *ASA* null males (Figure 3.22). The latter was not due to an inability of the *ASA* null sperm to capacitate in vitro (Figure 3.27). Nor was it due to a higher rate of spontaneous acrosome reaction (which would render sperm incapable of binding to the ZP). In addition, the *ASA* null sperm showed similar rate of ZP-induced acrosome reaction as the WT sperm (Table 3.3). Thus, ASA may not be involved directly in regulating these events. In addition, the severe defects of *ASA* null sperm from 8-month-old mice in ZP binding and IVF were not the secondary result of abnormal sperm morphology, number, or percent motility, because sperm were motility-selected by the swim-up technique and equal number of sperm with similar percent motility was used for insemination in these experiments. Notably, the percent motility of the swim-up sperm population was similar between WT and *ASA* null males (in the range of ~70 to 80%) (Table 3.3). Nonetheless, the number of sperm retrievable from the cauda epididymis and vas deferens of 8-month-old *ASA* null mice was significantly lower compared with that from the age-matched WT animals (Table 3.3). Further histological studies indicated that this reduction in epididymal and vas deferens sperm in *ASA* null mice was likely a

consequence of partial arrest of spermatogenesis in the mutant testes (Figures 3.28, 3.29 & 3.30).

The apparent normal fecundity of 5-month-old *ASA* null mice as revealed by natural mating and the normal ability of their sperm to bind to the ZP and to fertilize eggs in vitro suggested that ASA was not essential for these events at this animal age. These findings do not corroborate our previous results describing the significance of sperm ASA in egg interaction and fertilization (Figure 3.12 and 3.14) (Tantibhedhyangkul et al., 2002). In our previous in vitro experimentation, anti-ASA antibody was used as a tool to mask ASA on the surface of sperm retrieved from the cauda epididymal and vas deferens of WT animals (Tantibhedhyangkul et al., 2002). Direct binding of purified ASA to the ZP was also illustrated (Tantibhedhyangkul et al., 2002). These approaches have been used by a number of investigators to first demonstrate the significance of a specific sperm surface molecule in egg interaction and fertilization. Invariably, like what we have observed herein with ASA, results from these types of in vitro experimentation are different from those of the gene targeting knockout mouse approach. For example, acrosin, PH-20, GalT, and CD52, present on the sperm surface, have all been established by in vitro experimentation to be important for fertilization, but male mice with the respective gene disrupted can still sire offspring (Okabe and Cummins, 2007; Yamaguchi et al., 2008). In fact, none of the ZP binding molecules identified so far through in vitro assays are indispensable for fertilization in vivo; the mutant mice are either fertile or subfertile (Table 4.1). These discrepancies have been explained by the likelihood that the interaction between sperm and eggs is not solely dependent on a single molecule on the sperm surface. A lack of one ZP binding molecule can be compensated by other sperm

surface molecules having similar ZP affinity. A number of sperm surface molecules that have ZP affinity have been discovered (see INTRODUCTION), and these molecules may act cooperatively or in sequence to achieve optimal sperm binding to the ZP. Deletion of one of these molecules will initiate the compensation of other molecules in the ZP binding process. These ZP binding molecules may exist in the same membrane domains (such as lipid rafts) on the sperm surface. Emerging evidence has implicated a role of sperm lipid rafts as a platform for these sperm proteins. In fact, a number of ZP binding molecules have been found in isolated sperm lipid rafts, including ASA and SGG (Bou Khalil et al., 2006; Nixon et al., 2009), PH-20 (Nixon et al., 2009), basigin, IZUMO, CRISP1 (Sleight et al., 2005; Nixon et al., 2009), TESP1 (Sleight et al., 2005), GalT, Adam1b, Sp56, SED1, mannosidase 2, and Ace (Angiotensin converting enzyme) (Nixon et al., 2009). Most importantly, ASA and its substrate SGG have been identified in isolated pig sperm lipid rafts (Bou Khalil et al., 2006; Nixon et al., 2009). SGG not only contributes to the adhesion property of the sperm lipid rafts to homologous ZP, but also serves as a structural molecule important for raft formation (Bou Khalil et al., 2006). It is conceivable that the presence and proper presentation of all required molecules within the membrane microdomains would favor optimal binding between sperm and eggs, whereas disruption of a single molecule in this class would probably lead to suboptimal binding rather than a complete loss of interaction between sperm and eggs (Table 4.1).

Alternate routes of gamete interaction may also be used in sperm from mutant mice. This was first evidenced in *Galt* null mice, whose sperm could not interact with ZP3 and could not undergo the acrosome reaction upon induction with solubilized ZP (Lu and Shur, 1997). Yet, the mutant sperm were still able to bind to the ZP, and some small

percentage of these sperm could still fertilize eggs. This was explained by the subsequent discovery that there exists also a ZP3-independent sperm ligand on the ZP glycomatrix, which is a 250 kDa, WGA-reactive glycoprotein with a basic isoelectric point. This large sized ligand is a secreted product of the oviductal epithelium and it deposits onto the ZP glycomatrix during egg transport through the oviduct (Rodeheffer and Shur, 2004). When the GalT-ZP3 interaction does not exist in *Galt* knockout mice, this 250 kDa WGA reactive glycoprotein would compensate for the ZP3 interaction by binding to an unknown receptor on the sperm surface (Rodeheffer and Shur, 2004; Ensslin et al., 2007). Since *Galt* null sperm were still able to undergo spontaneous acrosome reaction when incubated in capacitating medium, these acrosome reacted sperm (which presumably form immediately after the initial sperm binding to the 250 kDa WGA reactive protein) would then still be able to penetrate through the ZP layer to reach and interact with the egg plasma membrane (Lu and Shur, 1997).

A defect in sperm-egg interaction occurring at one site in the reproductive tract as a result of targeted genetic disruption may also be compensated at the other site in the reproductive system. This is evidenced in *Tesp5* (testicular serine protease 5) null epididymal sperm, which had severe disability to bind to and undergo the ZP induced acrosome reaction in vitro. However, the reduced in vitro fertilizing ability of these *Tesp5* null epididymal sperm could be restored by exposing the sperm to uterine fluid, a result underscoring a positive/compensatory contribution of uterine secretion to normal fertility (Yamashita et al., 2008).

Nevertheless, the discrepancy in the fertilizing ability of sperm from 5- and 8-month-old *ASA* null mice suggested that sperm defects secondary to the lack of ASA

might account for the impaired functions of sperm from 8-month-old mice, and it would take some time (3 months or so) to have these secondary defects manifesting in the form of reduced fecundity. With regard to male fertility, 8-month old mice are equivalent to ~ 40-year old human males. Notably, physiologic aging has been linked to human male subfertility (Kuhnert and Nieschlag, 2004). For instance, elderly human males produce less testosterone (Pirke et al., 1980), and have fewer motile sperm in the ejaculate (Auger et al., 1995; Andolz et al., 1999; Eskenazi et al., 2003; Elzanaty, 2007; Ng et al., 2004). In rodents, decreased fertility has also been observed in aged males, and is caused by a variety of endocrine, spermatogenic, and environmental factors (Parkening et al., 1988; Parkening, 1989; Wang et al., 1993). The fact that ASA deficiency resulted in reduced male fecundity only in mice ≥8 months of age but not in younger ones suggested that the aging *ASA* null mice might be used as an animal model for the study of reproductive aging in males.

4.2.2. Reduced Level of SGG in Sperm of 8-Month Old ASA Null Mice May Account for Decreased Sperm Fertilizing Ability

A number of studies have revealed that ASA can hydrolyze detergent/saposin B presolubilized SGG in vitro (Yamato et al., 1974; Fluharty et al., 1974; Yamaguchi et al., 1975; Schenk et al., 2009). Although ASA on acrosome intact sperm does not desulfate sperm SGG (Carmona et al., 2002b), ASA in Sertoli cells and acrosome may still be able to exert its enzymatic activity on saposin B presolubilized SGG. In other words, the likelihood that SGG is a substrate of ASA in the male reproductive system must not be excluded. SGG is the main sulfoglycolipid of mammalian sperm (Tanphaichitr et al.,

2003; Ishizuka et al., 1973; Kornblatt et al., 1974; Suzuki et al., 1973) and it has been localized to the sperm head plasma membrane and shown to be involved in sperm-ZP binding (White et al., 2000; Weerachatyanukul et al., 2001; Bou Khalil et al., 2006; Tanphaichitr et al., 2003, Tanphaichitr et al., 2007c). SGG is also enriched in isolated lipid rafts from capacitated pig sperm, which had ZP affinity (Bou Khalil et al., 2006; Tanphaichitr et al., 2007b; Tanphaichitr et al., 2007c). Therefore, ASA depletion in *ASA* null mice may affect SGG levels, which in turn may modify SGG localization on sperm; both of these putative consequences would have adversely affected sperm-egg interaction. Results from both HPTLC and IIF, however, showed that the overall levels and localization of SGG, respectively, in *ASA* null sperm were indistinguishable from those of WT sperm (Figure 3.25). However, HPTLC is not a sensitive method to detect refined changes of lipid quantities. Therefore, a much more sensitive method, ESI-MS, was used to quantify SGG. By using combined liquid chromatography electrospray ionization mass spectrometry (LC-ESI-MS), it was shown that sperm SGG levels were indeed lower in 8-month-old *ASA* null mice (0.116 ± 0.061 μg SGG/million sperm) compared with age-matched WT counterparts (0.213 ± 0.039 μg SGG/million sperm, $P < 0.05$, and Figure 3.26), albeit no differences were seen between WT and *ASA* null sperm from 5-month-old males (0.200 ± 0.026 and 0.219 ± 0.026 μg SGG/million sperm, respectively). Our SGG quantification by ESI-MS was carried out with a proper internal standard (i.e., deuterium-labelled SGG isotopomer with the same chemical structure as the analyte and the same fragmentation patterns), and this was the first time that SGG was quantified in biological samples by this method.

Since ASA is a catabolic enzyme, the results obtained were opposite to what was expected. Nonetheless, the findings suggested that the reduced levels of SGG on sperm from 8-month-old *ASA* null mice might account for the impaired sperm fertilizing ability. It is interesting to note that the sperm plasma membrane fluidity, as revealed by MC540 staining, did not change even though the sperm SGG level was reduced by about half in 8-month-old *ASA* null mice (Figures 3.25 & 3.26). MC540 is used to detect membrane fluidity based on its property to intercalate into disordered membrane lipids, this result thus suggested that the fluid domains might not change in the *ASA* null sperm. The decrease in SGG levels in the *ASA* null sperm might still lead to a decrease in membrane domains with rigidity, since SGG is an ordered lipid; but this decrease might be of such a small degree that it did not increase the fluid domains that would have been detected by MC540 staining.

4.2.3. SGG, the Substrate of ASA, was Accumulated in ASA Null Testes

The unexpected decrease of SGG levels in *ASA* null sperm raised further questions. First, since ASA is present in testicular male germ cells and Sertoli cells, would testicular SGG exist at reduced levels as well? Second, what was the molecular mechanism for the decrease in sperm SGG levels in *ASA* null sperm? Quantification of SGG in total testicular lipid extracts by LC-ESI-MS revealed increased levels of SGG in *ASA* null testes of both age groups (1.139 ± 0.227 and 1.173 ± 0.141 μg/mg of testis for 5-month and 8-month old *ASA* null mice, respectively), compared with those of age-matched WT (0.717 ± 0.092 and 0.811 ± 0.023 μg/mg of testis for 5-month and 8-month old *ASA* null mice, respectively) (Figure 3.26), representing approximately 159% and

145% of the normal SGG levels in the testes at 5 and 8 months of age, respectively. These results were as expected and corroborated the previous findings on SGG accumulation in the brain of *ASA* null mice and MLD patients (Molander-Melin et al., 2004; von Figura et al., 2001). Also, a similar SGG accumulation in the testis has been documented in *prosaposin*$^{-/-}$ mice that lack saposin B, a co-enzyme of ASA that solubilizes SGG into the micelle form (Tadano-Aritomi et al., 2003). Although other saposins (saposins A, C and D) were also missing in the prosaposin$^{-/-}$ mice, owing to the specificity of saposin B as a co-enzyme for ASA (Matzner et al., 2009), the SGG accumulation in the knockout mouse testis was likely due to inability of ASA to desulfate the sulfoglycolipid. Unfortunately, it was impossible to ascertain experimentally whether the *prosaposin*$^{-/-}$ males were fertile because they died before reaching sexual maturity (Tadano-Aritomi et al., 2003).

The mechanisms why SGG levels in *ASA* null sperm of 8-month-old mice were decreased (instead of an increase according to the enzymatic function of ASA) was thus addressed. These extracted lipids were from total testicular homogenates, contributed from male germ cells, Sertoli cells, Leydig cells, connective tissue cells and blood cells. However, only the first two types of cells in the testis possess ASA (Figure 3.2), and in the case of testicular germ cells, it is well documented that they also contain SGG, all or part of which would remain in testicular and epididymal sperm. Considering that saposin B, the activator of ASA, is not expressed in germ cells (Morales et al., 1998; Sprecher-Levy et al., 1993), germ cell ASA is unlikely involved in SGG degradation. In addition, SGG is present mainly on the surface of male germ cells, which except for a very minor population of spermatids (step 7) do not contain lysosomes. Therefore, the degradation

rate of spermatogenic cells is not expected to be high. On the other hand, ASA in Sertoli cells exists in late residual bodies (Figure 3.2), which are partly derived from lysosomes. Sertoli cells are known for their phagocytic activities toward cellular remnants of apoptotic germ cells and residual bodies (the cytoplasmic portions of elongated spermatids, which are gathered on one side of the posterior end of the elongated spermatid head for the engulfment by Sertoli cells; this event occurring as part of spermiogenesis results in the formation of testicular sperm with little cytoplasmic content) (Maeda et al., 2002; Nakagawa et al., 2005; Kerr and de Kretser, 1974). It is therefore possible that Sertoli cell ASA may function in the degradation of SGG-containing membranes, which are originated from apoptotic germ cells or residue bodies. SGG may therefore transiently reside in Sertoli cells. Thus, quantification of SGG in both testicular germ cells of various developmental stages and Sertoli cells in *ASA* null and WT mice would have given a better understanding of how SGG metabolism changes in the mutant mice. While the most desirable approach for this SGG quantification would be through ESI-MS of isolated lipids from each stage of testicular germ cells, this methodology requires a large number of germ cells and Sertoli cells for the initial lipid extraction. After the preparation of a loose cell suspension from seminiferous tubules prepared by collagenase and then trypsin digestion of the testis tissue, Sertoli cells have to be separated from germ cells. Testicular germ cells of various developmental stages (mainly pachytene spermatocytes and round/elongated spermatids, comprising ~ 15% and 75% of the total germ cell population, respectively (Bellve et al., 1977)) would subsequently be separated by sedimentation velocity at unit gravity on an albumin gradient in a Staput chamber (Romrell et al., 1976; Grabske et al., 1975). Lipids would

finally be isolated from Sertoli cells cultured on the substratum and from the purified pachytene spermatocytes and round spermatids for ESI-MS quantification of SGG. Our initial attempt in quantifying SGG in pachytene spermatocytes and round spematids of WT mice following these tedious steps indicated that 50 mice were needed to prepare enough lipids for two repeats. It would probably require more mice to prepare lipids of comparable amounts from Sertoli cells, which constitute about 5% of total cells in the seminiferous tubule (Bellve et al., 1977). Therefore, this approach would not be suitable to be applied to the *ASA* knockout animals, which are available in limited numbers. Therefore, I chose to use flow cytometry employing our affinity-purified anti-SGG IgG to analyze changes of SGG levels in testicular germ cells of *ASA* null mice in comparison with those of WT germ cells. I was fully aware, however, that the data obtained did not give absolute amounts of SGG in these cells.

In the 5-month-old *ASA* null testes, SGG levels on primary spermatocytes, round spermatids and elongated spermatids were not different from those in age-matched WT testes, showing 84 ± 8.4%, 84 ± 12.2%, 91 ± 11%, respectively, of the WT values on corresponding cell types (Figure 3.40). In contrast, SGG levels on primary spermatocytes and elongated spermatids of 8-month-old ASA null mice were significantly lower than those of age-matched WT (49 ± 16% and 52 ± 17% of the WT values, respectively, $P < 0.05$, and Figure 3.40). A decrease in SGG level on round spermatids of the mutant mice was also observed (77 ± 21% of the WT value, and Figure 3.40), although the difference was not statistically significant. This lack of significant difference may be due to insufficient number of samples analyzed. These flow cytometry results in testicular germ cells were consistent with the SGG levels in WT and *ASA* null

sperm, as analyzed by ESI-MS (Figure 3.26) (i.e., no changes relative to the WT samples in germ cells and sperm from 5-month-old *ASA* knockout animals, but decreased levels of the corresponding cells from 8-month-old *ASA* null mice). All of these results suggested that SGG accumulation did not occur in male germ cells (either testicular germ cells or sperm) in *ASA* null males, 8 months of age.

One of the most likely sites where SGG may be accumulated in the *ASA* null testis is in the Sertoli cells. It was reasoned based on the observation that ASA was present in the late residual bodies of Sertoli cells (Figure 3.2) and the presence of prosaposin in their lysosomes (Morales et al., 1998). In addition, Sertoli cells are known for their phagocytotic functions (Nakanishi and Shiratsuchi, 2004). Therefore, Sertoli cells may be involved in degradation of phagocytosed resdidual bodies and membrane remnants of apoptotic germ cell (both of which should contain SGG). Although the presence of SGG in Sertoli cells in wild type mice may not be that apparent due to rapid degradation of the sulfoglycolipid, accumulation of SGG in *ASA* null Sertoli cells is expected due to the failure of SGG to become degraded. Due to the absence of ASA, phagocytosed SGG cannot be desulfated and its level is built up in Sertoli cells. Further experiments are needed to verify whether SGG is indeed accumulated in Sertoli cells. This can be achieved by conventional immunohistochemistry technique using affinity-purified anti-SGG IgG on frozen testis sections. A more precise and sensitive method would be imaging mass spectrometry, which has been used successfully to detect cellular and subcellular distribution of sulfatide molecular species in the rat cerebellum (Pernber et al., 2007).

To date, limited information is available on testicular SGG metabolism. As evidenced by my results that ASA is important for spermatogenesis and sperm fertilizing ability in aging animals, the understanding of how ASA is involved in these processes, in particular, with the relationship to SGG, the sulfoglycolipid that exists specifically in male germ cells will shed more light to a better understanding of SGG metabolism in the testis and the importance of keeping SGG balance on male fertility.

4.2.4. Higher Incidence of Germ Cell Apoptosis in 8-Month Old ASA Null Testes

Compared with WT animals, epididymal sperm number and testis weight of 8-month-old *ASA* null mice were significantly reduced (Figure 3.28 & Table 3.3), suggesting that spermatogenesis of the mutant mice might be partially impaired. Histological examination of the testes of 8-month-old *ASA* null mice revealed a higher number of vacuolation within the seminiferous tubules and apparent reduction in the epithelial area (Figures 3.28 & 3.29). These data suggested that there was a loss of developing germ cells in the testes. This was also accompanied by a marked increase in the number of round cells (presumably germ cells that were sloughed off the seminiferous epithelium) in the epididymal lumen of the mutant mice (Figure 3.29 h). All of these observations suggested that the spermatogenesis process in the 8-month-old *ASA* knockout mice was aberrant and this presumably was the cause of the reduced number of sperm in the epididymis. It is interesting, however, that deficiency in ASA did not seem to have any apparent effects on the gross morphology of the epididymis (Figure 3.29 c, d, g & h), although ASA is expressed in the epididymis (Figures 3.2 f & g; 3.3) (Weerachatyanukul et al., 2003). This observation may suggest that ASA is not essential

in maintaining the cellular organization and communication of epididymal epithelial cells and it would rather be ASA secreted by the epididymal epithelial cells in the epididymal lumen that is important for the physiology of transiting sperm, in particular for partially endowing ZP binding ability to mature sperm (Weerachatyanukul et al., 2003).

TUNEL staining indicated a higher incidence of germ cell apoptosis at the primary spermatocyte stage in the 8-month-old *ASA* null testes (Figure 3.31). This may account, at least in part, for the reduced sperm production (Table 3.3). Apoptosis has been recognized as an important mechanism during spermatogenesis (Rodriguez et al., 1997). It has been estimated that about 50-70% of germ cells at different stages of spermatogenesis are eliminated through apoptosis. However, few apoptotic germ cells can be readily detected in the normal testis upon histological examination, due to rapid and efficient clearance of apoptotic germ cells by Sertoli cells (Sinha Hikim and Swerdloff, 1999; Nakanishi and Shiratsuchi, 2004). While Sertoli cells are known for their supportive and nourishing roles in the development of spermatogenic cells (Dym, 1977; Griswold, 1998), they also have phagocytotic activity. They engulf residual bodies, the extracytoplasmic remnants shed from elongated spermatids during spermiogenesis. Sertoli cells are also known for the ability to phagocytose subcellular remnants of degrading germ cells (Nakanishi and Shiratsuchi, 2004; Nakagawa et al., 2005). This latter function of Sertoli cells would allow the remaining testicular germ cells to proceed in their development (Nakagawa et al., 2005). Without this "clean-up" function of Sertoli cells, certain molecular components of the cellular remnants (i.e., glycolipids) may be accumulated and become toxic to the remaining germ cells and Sertoli cells. In this regard, it is known that accumulation of glycosphingolipids is

deleterious to cells, as evidenced in several human diseases including Niemann-Pick type C (NPC) disease and MLD (te et al., 2004; Ellinwood et al., 2004). Similarly, too much SGG may also adversely affect cellular functions.

Androgen is known to play a key role in the control of spermatogenesis (Sharpe, 1994; Singh et al., 1995; McLachlan, 2000); androgen withdrawal in hypophysectomized rats results in germ cell death (Russell and Clermont, 1977). Thus, reduced androgen level could be a cause of the reduced rate of spermatogenesis observed in 8-month-old *ASA* null mice. However, our data did not reveal marked changes in androgen levels in *ASA* null mice (Figure 3.33). Although serum testosterone levels seemed to be somewhat reduced in 8-month-old *ASA* null mice, when compared with those in age-matched WT mice, the differences were not statistically significant due to large variations. The pulsatile pattern of testosterone secretion in adulthood in response to the intermittent discharge of LH from the pituitary is known to account for this variation (Plant, 1981, Keeney and Ewing, 1990, Ramaswamy et al., 1998, Ramaswamy et al., 2000). As an alternative to testosterone measurement, the androgen producing cells, the Leydig cells, and target tissues of testosterone were examined to determine whether circulating androgen levels were affected in these mice. At the electron microscopic level, the ultrastructure of the Leydig cell was indistinguishable between WT and *ASA* null mice. The presence of lipid droplets in the cytoplasm, a characteristic of normal Leydig cells, was also observed in 8-month-old *ASA* null males (Figure 3.34 a & b), suggesting that their Leydig cells functioned normally. The comparable weight of seminal vesicles and caput epididymis (Figure 3.3 c & d), and the normal morphology and size of the caput

epididymal epithelia of the *ASA* null mice further suggested that the circulating androgen levels were unaffected (Figures 3.28 c, d, g ,h & 3.31).

Although the level of testosterone may not have changed in 8-month-old *ASA* knockout mice, the exertion of its action could still be problematic, a cause of the reduced spermatogenesis rate. Testosterone functions through Sertoli cells by binding to androgen receptor in the cytoplasm and influences tubular microenvironment. Sertoli cells secrete a number of molecules that are pertinent to germ cell development, including androgen binding protein (ABP), growth factors (e.g., transforming growth factor-β (TGF-β), stem cell factor (SCF), and insulin-like growth factor I (IGF-I) (Jegou, 1993)), and lactate. This secretory function of Sertoli cells may be impaired in 8-month-old *ASA* null mice. It is possible that the synthesis of androgen receptors in Sertoli cells may also be reduced, and this could lead to a topical decrease in androgen levels in the male reproductive system. The observed apoptosis in spermatogenic cells may therefore reflect the compromised functions of Sertoli cells due to the toxicity exerted by accumulated intracellular SGG.

4.2.5. Presence of C16:0 sulfatide in ASA null testes

HPTLC revealed several new glycolipid bands in *ASA* null testes (Figure 3.35). We reasoned that these lipids might be sulfated, since ASA is a catabolic enzyme that can desulfate sulfoglycolipids. ESI precursor ion scan for sulfate MS analysis of total testicular lipids indeed revealed a sulfolipid with an m/z 778.5 that was selectively present in the *ASA* null testes, regardless of their age (Figure 3.37). ESI-tandem mass spectrometry revealed that the fragmentation patterns of this ion at m/z 778.5 were very

similar to those of palmitoylsulfatide (C16:0 fatty acid containing sulfatide) (Figure 3.39). The identification of this lipid being palmitoylsulfatide was further confirmed by precise mass measurement using LTQ-FTMS. Since C16:0 fatty acid containing sulfated glucosylceramide may also give rise to the same m/z value of 778.5, the MS/MS spectrum of HPLC-purified rat kidney sulfated glucosylceramide was obtained and compared with that of palmitoylsulfatide (Figure 3.39). This possibility was excluded because the fragmentation pattern of sulfated glucosylceramide was completely different from that of the *ASA* null testis lipid at m/z of 778.5 (Figure 3.39).

Since CGT, the enzyme required to synthesize SGC/SGG, is only expressed in germ cells in the testis (Fujimoto et al., 2000), the C16:0 sulfatide was most likely synthesized in these cells in the *ASA* null testes. Under normal conditions, this lipid is undetectable in the testes. Palmitoylsulfatide may be synthesized at a very low level, and it is rapidly turned over by ASA after being phagocytosed as part of residue bodies. Alternatively, the putative SGG accumulation in ASA mutant Sertoli cells might create a signal for a reduced synthesis of SGG precursor, PPG. Yet, the CGT and CST may still be active. With a small amount of ceramide available in testicular germ cells, sulfoglycolipid biosynthesis is shunted towards the production of SGC. Since palmitic acid is the main fatty acid in testicular germ cells (Davis et al., 1966; Coniglio, 1994), C16:0 fatty acid containing SGC is produced. Eventually, SGG accumulation would lead to inhibition of SGG synthesis (presumably through inhibition of CST activity) in older mutant mice (i.e., 8 months of age).

We also tried to get the identity of another glycolipid that migrated with lower mobility and was present only in testes of ASA null mice of 8 months old or older

(Figure 3.35, band 4 in region 2). We have not yet been successful on this attempt. This was likely due to the insufficient amounts of the extracted lipid to be detected by our MS setups.

4.2.6. Age-Dependent Decline of Male Fertility of ASA Null Mice

Results presented in this study demonstrated that ASA was critical for the maintenance of adult male fertility. Young ASA null mice up to 5 months of age were able to carry out normal spermatogenesis and produce motile sperm with normal fertilizing ability. However, by 8 months of age, *ASA* null mice were subfertile, with significantly reduced testis weight and epididymal sperm counts as a result of increased rates of germ cell apoptosis and sloughing of germ cells from the seminiferous epithelium. Many of the sperm that reached the epididymis were immotile with abnormal morphology. By 12 months of age, virtually no sperm were found in the epididymis of ASA null mice. These reproductive defects of the older *ASA* null males may result from the toxicity of accumulated SGG. Since SGG was accumulated in the *ASA* null testis, while SGG levels in testicular germ cells and sperm were in fact reduced (in 8-month-old mutant mice), the accumulation mostly likely occurred in the Sertoli cells.

The expression of ASA in Sertoli cells and its localization in the late residue bodies (formed as a result of fusion between residue bodies and lysosomes) of these cells strongly suggests that the ASA activity may be involved in degrading SGG from remnant membranes of apoptotic cells or residual bodies. Supporting this hypothesis, prosaposin, the precursor of saposins including ASA's activator protein saposin B, has been shown to be exclusively expressed in Serotli cells in the seminiferous tubules (Morales et al.,

1998). More specifically, prosaposin is localized to the lysosomes and phagolysosomes containing residual bodies but not on endosomes or luminal (early) residual bodies (Morales et al., 1998). Based on these observations, a role of lysosomal prosaposin in the degradation of membrane glycolipids from residue bodies phagocytosed by Sertoli cells has been proposed (Morales et al., 1998). Similar to the cytotoxicity described for other accumulated glycolipids (te et al., 2004; Ellinwood et al., 2004), it is likely that accumulation of SGG would result in adverse effects to the cells, and various integrative corrective mechanisms may be needed to adjust the SGG levels close to normal in situations where its metabolisms are challenged. The first example is the observation in *Saposin A* null mice. Saposin A is the activator for galactosylceramidase that degrades GG. In these mutant mice, the levels of GG are increased. Yet, SGG amounts in the testis are normal; this indicates that the synthesis of SGG is tightly regulated and is not driven by the excess amount of its precursor. In a similar vein, overexpression of CGT in oligodendrocytes did only slightly increase GC levels; there was no increase in the steady-state level of SGC in the brain of transgenic mice (Fewou et al., 2005; Zoller et al., 2005). On the other hand, mice genetically ablated of *Cgt* of *Cst* could not have SGG/SGC synthesized, indicating that there is no alternative route for the sulfoglycolipid biosynthesis. Spermatogenesis is thus disrupted in these mice; their neurological system also shows abnormalities in myelin and paranodal junction structures, and the mice suffer tremor, ataxia and hindlimb paralysis (Fujimoto et al., 2000; Coetzee et al., 1996; Honke et al., 2002). Nonetheless, recent work in our laboratory indicates that $Cgt^{+/-}$ male mice have normal fecundity and neurological behavior. In these heterozygous mice, the expression of CGT polypeptide is similar to the wild type value (assessed

semiquantitatively by immunoblotting) despite the 50% expression of the *Cgt* mRNA, indicating that the translation of the enzyme is compensated towards the normal level. As a result, the levels of SGG in the testis and sperm of $Cgt^{+/-}$ mice are 75% and 80%, as quantitated by ESI-MS of the normal values (Kongmanas, 2007). This would explain why these mice are fully fertile, although the exact mechanism on how SGG is essential for spermatogenesis still needs to be discerned. Perhaps, SGG molecules on the testicular germ cell surface interact with themselves or their binding proteins (which are yet to be identified) on adjacent spermatogenic cells or Sertoli cells, thus contributing to the cell adhesion process required during spermatogenesis. Nonetheless, all of these previously described observations indicate that the turnover and biosynthesis of SGG and SGC are tightly regulated, so that the concentrations of these major sulfoglycolipids can be maintained within a narrow range of the normal values that are essential for the ongoing spermatogenesis event and the functioning of the stable myelin sheath.

One of the expected consequences of ASA deficiency in the testis would be accumulation of its substrate SGG, which was indeed detected in the *ASA* null testis. As discussed above, the most possible site where SGG might have been accumulated in the *ASA* null testes is Sertoli cells. As a result of the sulfoglycolipid accumulation, I speculate that the following might have happened in the mutant testes: (1) Sertoli cells may send an inhibitory signal to primary spermatocytes to reduce SGG synthesis; (2) Sertoli cell functions may become compromised; (3) the Sertoli-germ cell interaction may be disrupted (Figure 4.1).

SGG accumulation in Sertoli cells may serve as a feed-back signal for germ cells to decrease or cease further SGG synthesis, possibly through the down regulation of

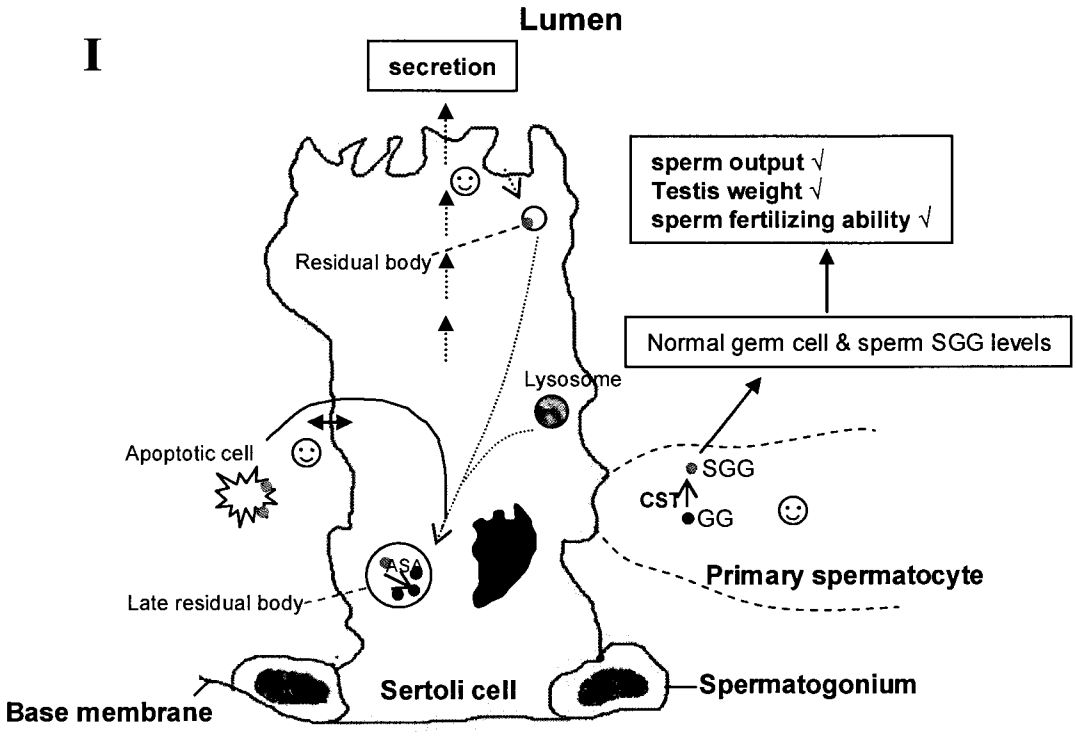
I
Lumen
secretion
sperm output √
Testis weight √
sperm fertilizing ability √
Residual body
Normal germ cell & sperm SGG levels
Lysosome
Apoptotic cell
SGG
CST
GG
Primary spermatocyte
Late residual body
Sertoli cell
Spermatogonium
Base membrane

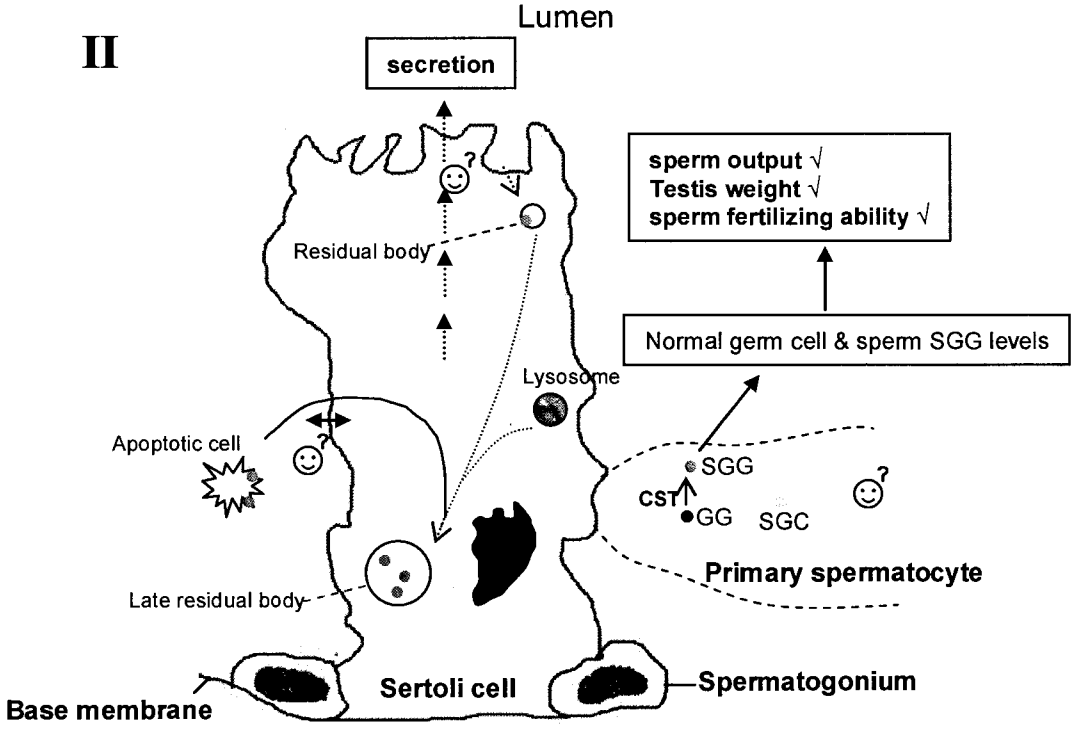
II
Lumen
secretion
sperm output √
Testis weight √
sperm fertilizing ability √
Residual body
Normal germ cell & sperm SGG levels
Lysosome
Apoptotic cell
SGG
CST
GG
SGC
Primary spermatocyte
Late residual body
Sertoli cell
Spermatogonium
Base membrane

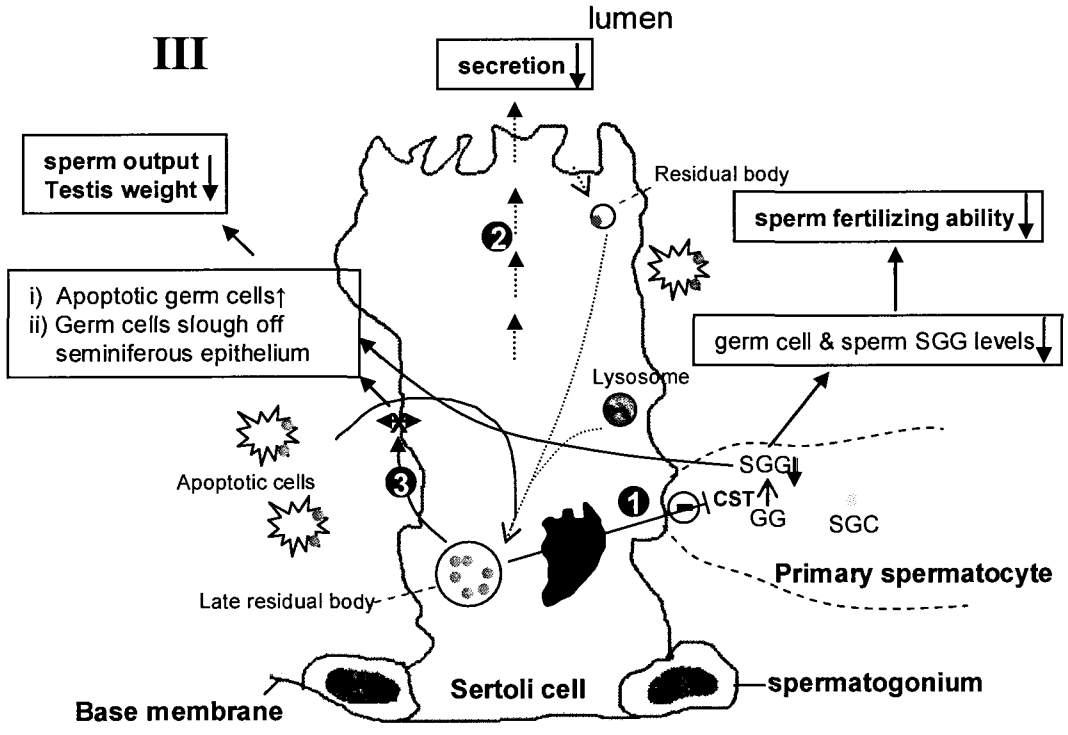
III
lumen
secretion
sperm output
Testis weight
Residual body
sperm fertilizing ability
i) Apoptotic germ cells↑
ii) Germ cells slough off
seminiferous epithelium
germ cell & sperm SGG levels
Lysosome
Apoptotic cells
SGGI
CST
GG
SGC
Primary spermatocyte
Late residual body
Sertoli cell
spermatogonium
Base membrane

Figure 4.1. Illustrations of SGG turnover in the testes of WT (I) and ASA null (II & III) mice. In the WT testis (I), SGG phagocytosed from apoptotic cells and residual bodies is targeted to the late residual bodies in Sertoli cells for degradation via starting with desulfation by ASA. Efficient degradation of the phagocytosed SGG may be important for maintaining germ cell SGG balance and continuation of spermatogenesis. In *ASA* null testis from animals 5 months (II) and 8 months (III) of age, SGG is accumulated in Sertoli cells due to ASA deficiency. Excess amounts of glycolipids likely induce toxicity to the cells (te et al., 2004; Ellinwood et al., 2004) and Sertoli cells may become dysfunctional by SGG accumulation. However, this accumulation may not have reached a threshold in Sertoli cells of 5-month-old knockout animals. Therefore, Sertoli cells in these animals may still be able to perform most of their functions and spermatogenesis still appeared normal, and sperm produced showed similar fertilizing ability as WT sperm (II). In contrast, the amount of SGG accumulated in the Sertoli cells of 8-month-old *ASA* null mice may have become intolerable by these cells. This may lead to: (1) inhibition of SGG synthesis in primary spermatocytes possibly via decreased activity of the enzymes in the biosynthesis pathway (e.g., CST); the reduction of sperm SGG levels likely accounts for decreased sperm fertilizing ability; (2) Sertoli cell dysfunction with reduced secretion capacity; and (3) disruption of Sertoli-germ cell interactions. All of these changes would lead to a slower rate of spermatogenesis (lower sperm production and reduced testis weight) and subsequently germ cell death.

testicular galactolipid sulfotransferase by an endogenous inhibitor (Lingwood et al., 1994). Although the amount of SGG accumulated per testis weight was similar between 5- and 8-month-old *ASA* null mice (Figure 3.26), the amount of SGG accumulated per Sertoli cell in the 8-month-old *ASA* null mice was likely much higher than that in the 5-month-old mutant mice. This statement was deduced from the fact that there was a significant loss of germ cells in the older mutant testes, resulting in the higher proportion of Sertoli cells. In addition, flow cytometry results indicated a decrease in SGG levels in testicular germ cells, relative to wild type values, in 8-month-old knockout mice, whereas the correspondence decrease was not observed in the younger mice (Figure 3.40). This implicated an even higher level of SGG accumulated in Sertoli cells of the older *ASA* null animals. Therefore, it is possible that in the testes of young *ASA* null mice, the extent of SGG accumulation may still be under the threshold level. This may explain the apparently normal phenotype of the 5-month-old *ASA* null mice. In contrast, the accumulation of the sulfoglycolipid may become intolerable by the Sertoli cells in older mutant mice. As a result, SGG synthesis by the primary spermatocytes would have been inhibited. The decreased levels of SGG on the primary spermatocytes of the 8-month-old *ASA* null mice may reflect this inhibition of SGG synthesis (Figure 4.1).

The reduced levels of SGG on testicular germ cells may directly lead to the decrease of SGG on mature sperm. Since SGG is a ZP binding molecule (White et al., 2000; Bou Khalil et al., 2006 Weerachatyanukul et al., 2001), the reduced sperm SGG levels likely resulted in compromised sperm fertilizing ability. However, although the SGG level of sperm from 8-month-old *ASA* null mice was reduced to ~50% of that of the WT, the levels of sperm-ZP binding and IVF rates were nearly zero (Figures 3.25 &

3.22). This may be due to altered membrane organization on these sperm. Besides being a ZP adhesion molecule, SGG also contributes to the formation of sperm lipid rafts which serve as a platform for sperm-ZP binding (Bou Khalil et al., 2006). Perhaps, the ~50% reduction of SGG had led to formation of abnormal sperm lipid rafts, with aberrant presentation of the ZP-binding molecules that no longer supports sperm-egg interaction needed for successful fertilization.

The presence of palmitoylsulfatide (C16) in the *ASA* null testis may be another consequence of SGG accumulation (see Section 4.2.5). Interestingly, saturated short chain (i.e., C18:0) fatty acid-containing SGC has also been found to be the predominant sulfatide molecular species accumulated in the neurons and astrocytes of *ASA* null mouse brain (Isaac et al., 2006). It has been speculated that the fatty acid chain length of a sulfatide dictates its cellular localization (i.e., with short chain sulfatide localized intracellularlly and long chain localized on the plasma membrane) and thus its function. In this regard, the C18:0 sulfatide was found to be accumulated in large cytoplasmic vesicles, presumably lysosomes of astrocytes, in *ASA* null mice, rather than targeted to the cell plasma membrane (Isaac et al., 2006). The elevated levels of intracellular sulfatide (C18 and C16) may be toxic to the cells, and this may be one of the underlying mechanisms for the pathology in the brain and testis of the *ASA* null mice.

The presence of palmitoylsulfatide in the testis may be one of the signals that induced germ cell apoptosis in the 8-month-old *ASA* null mice. It has recently been reported that abnormal sulfatide metabolism/trafficking in cultured neuroblastoma cells and primary neurons upon exogenous sulfatide administration induces neuronal cell apoptosis (Zeng et al., 2008). Apart from the expected sulfatide accumulation in the

lysosomes of these cells, an increase in endosomal ceramide content was detected. This ceramide was shown to be generated by a β-galactosidase activity that directly hydrolyzes sulfatide to ceramide without the initial desulfation step (Zeng et al., 2008). Interestingly, β-galactosidase was reported to be expressed in spermatocytes and spermatids (round, elongated/condensed) in the rat testis (Skudlarek et al., 2000; Abou-Haila and Tulsiani, 2001). The endosome-generated ceramide accumulation (Spinedi et al., 1999; Ravid et al., 2003; Wu et al., 2005) and sulfatide toxicity (te et al., 2004; Ellinwood et al., 2004) were thought to be responsible for the induction of apoptosis. Interestingly, in testes of mice treated with doxorubicin (an anti-neoplasic drug with adverse side effects in causing male infertility by inducing apoptosis of spermatogonia and primary spermatocytes), the loss of spermatogonia and primary spermatocytes through apoptosis was accompanied by a transient increase in ceramide with C16:0 as the predominant fatty acyl chain (Zanetti et al., 2007). One puzzling issue is that the incidence of germ cell apoptosis was only elevated in the testes of 8-month-old but not 5-month-old *ASA* null mice, even though palmitoylsulfatide was present in the mutant testes of both ages. These results suggested that palmitoylsulfatide may not be directly involved in causing germ cell death. Nonetheless, it could be a matter of having a high enough concentration of palmitoylsulfatide and the putative degraded product, ceramide, in older *ASA* null animals for the observed adverse effects in the testes of these mice. It would be interesting to assess whether 8-month-old *ASA* null mouse testes have high ceramide content.

Accumulation of SGG in Sertoli cells may also have compromised their functions (Figure 4.1). Not much is known about the pathology of cells/integrative body system

that is induced by SGG accumulation. However, there is wealth of information regarding alterations of SGC metabolism, trafficking and homeostasis in several human diseases. Sulfatides are essential for a variety of biological processes, including cell growth, intracellular protein trafficking, signal transduction, cell-cell/extracellular matrix recognition and cell morphogenesis (Vos et al., 1994; Ishizuka, 1997; Merrill, Jr. et al., 1997; Blomqvist et al., 2002; Marcus et al., 2006; Marinier et al., 1997). The accumulation of SGC caused by ASA deficiency is responsible for MLD (von Figura et al., 2001). In addition, SGC accumulation has been revealed in post-mortem brain tissues from subjects with Parkinson's disease, although the underlying mechanism is currently unknown (Cheng et al., 2003).

Compromised Sertoli cell functions may lead to reduced production and secretion of important molecules. One of such molecules is androgen binding protein (ABP) that carries testosterone and dihydrotestosterone to the target cells including germ cells (Hagenas and Ritzen, 1975; Cheng et al., 1985; Gerard et al., 1988; Gerard, 1995; Gueant et al., 1991; Turner and Roddy, 1990). Although our data suggested that circulating androgen levels were unchanged in the mutant mice, it is still possible that local androgen levels within the seminiferous tubules might have been affected. It has been reported that concentrations of intratesticular testosterone in adult rats are approximately 50 to 100-fold higher than that found in serum. The higher testicular levels of testosterone are important because full spermatogenic capacity requires 70 ng/ml and spermatogenesis is dramatically compromised at testosterone concentrations below 20 ng/ml (Zirkin et al., 1989). In this regard, ABP has been postulated to be required for maintaining high levels of testosterone inside the seminiferous tubules (Dohle et al., 2003). Thus, reduced ABP

secretion may cause spermatogenesis disruption and germ cell death. The synthesis and transport of other important nutrients and regulatory molecules into germ cells, including lactate, tranferrin, metalloproteases, clusterin, and cathepsin L, may also have been affected (Jegou, 1993; Griswold, 1998).

Sertoli cell dysfunction and aberrant germ cell SGG levels may both contribute to perturbation of Sertoli-germ cell interaction (Figure 4.1). Since cellular communication between Sertoli cell and germ cells plays an essential role in spermatogenesis (Jegou, 1993; Griswold, 1998), disruption of this communication may likely also account for germ cell apoptosis. In the testes of 8-month-old ASA null mice, on the one hand, Sertoli cells may have lost part of their normal functionality. On the other hand, the reduced SGG levels on germ cells may have rendered them less capable of adhering to the Sertoli cells. Although proper balance of germ cell SGG level is known to be essential for normal spermatogenesis (Fujimoto et al., 2000; Honke et al., 2002; Kongmanas, 2007), the functions of SGG during this process remain to be elucidated. One possible role of germ cell SGG is to interact with L-selectin that is present on the Sertoli cell surface (Freeman et al., 2002; Suzuki et al., 1993; Brockhausen and Kuhns, 1997), thus contributing to the adhesion of germ cells to Sertoli cells. In addition, SGG may contribute to the organization of lipid raft microdomains in developing germ cells, which may also be involved in interaction with Sertoli cells. It is thus conceivable that the reduced level of SGG in the germ cells of 8-month-old *ASA* null mice would compromise germ cell-Sertoli cells interaction. On the other hand, the expression of L-selectin in Sertoli cells may also be altered as a result of compromised cell functionality. Consequently, some germ cells may lose support from the Sertoli cells, and become

sloughed off from the seminiferous epithelium or die through apoptosis. The end results of all these are reduced sperm production and testicular atrophy (Figure 4.1).

4.3. Conclusions

Mouse epididymal sperm have two entities of ASA; one in the acrosome that is synthesized in spermatogenic cells and the other one on the cell surface that is acquired from the epididymal fluid during sperm transit in the epididymis. Sperm surface and acrosomal ASA may be involved in the primary and secondary binding to the ZP3 anad ZP2 sulfoglycoproteins, respectively, independent of the active site pocket of ASA. The overall significance of sperm ASA is evidenced by the strong inhibitory effect of sperm treatment with anti-ASA antibodies on fertilization in vivo.

The roles of ASA in male fertility were further investigated using *ASA* null mice. Sperm from 5-month-old *ASA* null mice exhibited normal fertilizing ability, whereas sperm from 8-month-old null mice had minimal fertilizing competence in vitro. Consistent with the in vitro results, fecundity of *ASA* null males also decreased when the mice became older ($\geq$ 8 months). The reduction of sperm SGG levels may be a cause of the decrease in sperm fertilizing ability in the older mutant mice. Testis weight and epididymal sperm number were reduced in the *ASA* null mice at 8 months of age. An increase in the number of apoptotic testicular germ cells may account partly for these changes. *ASA* null mice accumulated SGG in their testes, suggesting for the first time that SGG is a natural substrate for ASA in vivo. This accumulation is likely to occur in Sertoli cells due to their phagocytotic activity towards apoptotic germ cells and residual bodies, both of which should contain SGG. The accumulation of phagocytosed SGG

might lead to Sertoli cell dysfunction and subsequently spermatogenesis disruption. Testes of the mutant mice also uniquely contained palmitoylsulfatide. These two attributes may be the causes of germ cell lose in the *ASA* null mice.

4.4. Scientific Significance and Future Directions

Acquisition of ZP binding molecules by sperm during their epididymal transit is one of the major events associated with sperm epididymal maturation. Here, I have provided evidence that cauda epididymal sperm acquire ASA from the epididymal fluid via tight interaction with sperm surface SGG, thus contributing to this maturation process. Furthermore, the demonstration that ASA binds to both ZP3 and ZP2 sulfoglycoproteins has led to the better understanding of the molecular mechanism for ASA-ZP binding; its possible role in both primary and secondary ZP binding. However, it is still unknown which ASA surface domain is involved in ZP binding, although the active site pocket of ASA is unlikely involved. It remains to be determined whether the positively charged "cleft" on the ASA molecular surface, identified by computational studies (Schenk et al., 2009), is involved in binding to the ZP sulfated glycans.

The study on the fecundity of *ASA* null male mice has provided implication that SGG is a natural substrate of ASA in vivo. Importantly, as evidenced by the results that ASA is important for spermatogenesis and sperm fertilizing ability in aging animals, the current study has shed some light to the understanding of the mechanisms of ASA involvement in these processes, in particular, with the relationship to SGG, the sulfoglycolipid that exists specifically in male germ cells. This work has also led to a better understanding of how SGG degradation occurs in the testis under normal and

pathological conditions, and how changes in SGG balance in the testis would affect male fertility. Although my data suggested that SGG is most likely accumulated in Sertoli cells of the *ASA* null testis, this postulation still needs to be confirmed experimentally to ultimately understand the mechanism of SGG degradation. Most significantly, the information obtained will warrant ASA and SGG as biomarkers for male fertility/subfertility, especially in older males. To date, these markers are not available and thus invasive reproductive technology with likelihood of long-term adverse effects is often applied in infertility clinics without precise information on the male infertility status.

Collectively, the understanding of the molecular mechanisms of mammalian sperm-ZP interaction will provide information necessary for the development of male fertility markers and non-hormonal vaginal contraceptives, with fewer systemic side effects compared to oral estrogen birth control pills. Using antibodies/inhibitors generated against a group of ZP binding molecules should effectively interfere with sperm-egg binding. In addition, compounds that can also prevent sexually transmitted diseases (STD) are the most desirable as vaginal contraceptives. Since pathogenic STD-associated microbials also bind to SGG (Harouse et al., 1991; Gadella et al., 1998; Piomboni and Baccetti, 2000), the use of antibodies/inhibitors generated against SGG may also prevent STD by masking/interfering with the functions SGG.

Reference List

Abou-Haila,A. and Tulsiani,D.R. (2001). Acid Glycohydrolases in Rat Spermatocytes, Spermatids and Spermatozoa: Enzyme Activities, Biosynthesis and Immunolocalization. Biol. Proced. Online. *3*, 35-42.

Acevedo,J.J., Mendoza-Lujambio,I., de la Vega-Beltran JL, Trevino,C.L., Felix,R., and Darszon,A. (2006). KATP channels in mouse spermatogenic cells and sperm, and their role in capacitation. Dev. Biol. *289*, 395-405.

Acott,T.S. and Hoskins,D.D. (1978). Bovine sperm forward motility protein. Partial purification and characterization. J. Biol. Chem. *253*, 6744-6750.

Ahn,V.E., Faull,K.F., Whitelegge,J.P., Fluharty,A.L., and Prive,G.G. (2003). Crystal structure of saposin B reveals a dimeric shell for lipid binding. Proc. Natl. Acad. Sci. U. S. A *100*, 38-43.

Ahnonkitpanit,V., White,D., Suwajanakorn,S., Kan,F., Namking,M., Wells,G., and Tanphaichitr,N. (1999). Role of egg sulfolipidimmobilizing protein 1 (SLIP1) on sperm-egg plasma membrane binding. Biology of Reproduction *61*, 749-756.

Aitken,R.J. (1997). Molecular mechanisms regulating human sperm function. Molecular Human Reproduction *3*, 169-173.

Aitken,R.J. and McLaughlin,E.A. (2007). Molecular mechanisms of sperm capacitation: progesterone-induced secondary calcium oscillations reflect the attainment of a capacitated state. Soc. Reprod. Fertil. Suppl *63*, 273-293.

Akama,T.O., Nakagawa,H., Sugihara,K., Narisawa,S., Ohyama,C., Nishimura,S., O'Brien,D.A., Moremen,K.W., Millan,J.L., and Fukuda,M.N. (2002). Germ cell survival through carbohydrate-mediated interaction with Sertoli cells. Science *295*, 124-127.

Allan DJ, Harmon BV Kerr JFR. Cell death in spermatogenesis. In: Potten CS, editor. Perspectives on mammalian cell death. 229-258. 1987. London, Oxford University Press.

Alvarez,J.G., Storey,B.T., Hemling,M.L., and Grob,R.L. (1990). High-resolution proton nuclear magnetic resonance characterization of seminolipid from bovine spermatozoa. Journal of Lipid Research *31*, 1073-1081.

Andolz,P., Bielsa,M.A., and Vila,J. (1999). Evolution of semen quality in North-eastern Spain: a study in 22,759 infertile men over a 36 year period. Hum. Reprod. *14*, 731-735.

Aravinda,S., Gopalakrishnan,B., Dey,C.S., Totey,S.M., Pawshe,C.H., Salunke,D., Kaur,K., and Shaha,C. (1995). A testicular protein important for fertility has glutathione S-transferase activity and is localized extracellularly in the seminiferous tubules. J. Biol. Chem. *270*, 15675-15685.

Asquith,K.L., Baleato,R.M., McLaughlin,E.A., Nixon,B., and Aitken,R.J. (2004). Tyrosine phosphorylation activates surface chaperones facilitating sperm-zona recognition. J. Cell Sci. *117*, 3645-3657.

Asquith,K.L., Harman,A.J., McLaughlin,E.A., Nixon,B., and Aitken,R.J. (2005). Localization and significance of molecular chaperones, heat shock protein 1, and tumor rejection antigen gp96 in the male reproductive tract and during capacitation and acrosome reaction. Biol. Reprod. *72*, 328-337.

Attar,M., Kates,M., Bou Khalil,M., Carrier,D., Wong,P.T.T., and Tanphaichitr,N. (2000). A Fourier-transform infrared study of the interaction between germ-cell specific sulfogalactosylglycerolipid and dimyristoylglycerophosphocholine. Chemistry and Physics of Lipids *106*, 101-114.

Attar,M., Wong,P.T.T., Kates,M., Carrier,D., Jaklis,P., and Tanphaichitr,N. (1998). Interaction between sulfogalactosylceramide and dimyristoylphosphatidylcholine increases the orientational fluctuations of the lipid hydrocarbon chains. Chemistry and Physics of Lipids *94*, 228-238.

Auger,J., Kunstmann,J.M., Czyglik,F., and Jouannet,P. (1995). Decline in semen quality among fertile men in Paris during the past 20 years. N. Engl. J. Med. *332*, 281-285.

Aumuller,G., Schulze,C., and Viebahn,C. (1992). Intermediate filaments in Sertoli cells. Microsc. Res. Tech. *20*, 50-72.

Baba,T., Azuma,S., Kashiwabara,S., and Toyoda,Y. (1994a). Sperm from mice carrying a targeted mutation of the acrosin gene can penetrate the oocyte zona pellucida and effect fertilization. J. Biol. Chem. *269*, 31845-31849.

Baba,T., Kashiwabara,S., Watanabe,K., Itoh,H., Michikawa,Y., Kimura,K., Takada,M., Fukamizu,A., and Arai,Y. (1989). Activation and maturation mechanisms of boar acrosin zymogen based on the deduced primary structure. J. Biol. Chem. *264*, 11920-11927.

Baba,T., Niida,Y., Michikawa,Y., Kashiwabara,S., Kodaira,K., Takenaka,M., Kohno,N., Gerton,G.L., and Arai,Y. (1994b). An acrosomal protein, sp32, in mammalian sperm is a binding protein specific for two proacrosins and an acrosin intermediate. Journal of Biological Chemistry *269*, 10133-10140.

Baibakov,B., Gauthier,L., Talbot,P., Rankin,T.L., and Dean,J. (2007). Sperm binding to the zona pellucida is not sufficient to induce acrosome exocytosis. Development *134*, 933-943.

Baldi,E., Luconi,M., Bonaccorsi,L., and Forti,G. (2002). Signal transduction pathways in human spermatozoa. Journal of Reproductive Immunology *53*, 121-131.

Baldi,E., Luconi,M., Bonaccorsi,L., Muratori,M., and Forti,G. (2000). Intracellular events and signaling pathways involved in sperm acquisition of fertilizing capacity and acrosome reaction. Front Biosci. *5*, E110-E123.

Barbieri,A.M., Sosa,M.A., Grimalt,P., Mayorga,L.S., and Bertini,F. (1995). Phosphomannosyl receptors on the surface of spermatozoa from the cauda epididymis of the rat. International Journal of Andrology *18*, 113-119.

Baum,H., Dodgson,K.S., and Spencer,B. (1959). The assay of arylsulphatases A and B in human urine. Clinical Chimica Acta *4*, 453-455.

Bedford,J.M. (1977). Sperm/egg interaction: the specificity of human spermatozoa. Anat. Rec. *188*, 477-487.

Bellve,A.R., Cavicchia,J.C., Millette,C.F., O'Brien,D.A., Bhatnagar,Y.M., and Dym,M. (1977). Spermatogenic cells of the prepuberal mouse. Isolation and morphological characterization. J. Cell Biol. *74*, 68-85.

Belmonte,S.A., Challa,A., Gutierrez,L.S., Bertini,F., and Sosa,M.A. (1998). à-Mannosidase from rat epididymal fluid is a ligand for phosphomannosyl receptors on the sperm surface. International Journal of Andrology *21*, 277-288.

Benau,D.A. and Storey,B.T. (1988). Relationship between two types of mouse sperm surface sites that mediate binding of sperm to the zona pellucidae. Biology of Reproduction *39*, 235-244.

Benoff,S. (1997). Carbohydrates and fertilization an overview. Molecular Human Reproduction *3*, 599-637.

Bigler,D., Chen,M., Waters,S., and White,J.M. (1997). A model for sperm-egg binding and fusion based on ADAMs and integrins. Trends Cell Biol. *7*, 220-225.

Billig,H., Furuta,I., Rivier,C., Tapanainen,J., Parvinen,M., and Hsueh,A.J. (1995). Apoptosis in testis germ cells: developmental changes in gonadotropin dependence and localization to selective tubule stages. Endocrinology *136*, 5-12.

Blackmore,P.F. (1999). Extragenomic actions of progesterone in human sperm and progesterone metabolites in human platelets. Steroids *64*, 149-156.

Bleil,J.D., Greve,J.M., and Wassarman,P.M. (1988). Identification of a secondary sperm receptor in the mouse egg zona pellucida: role in maintenance of binding of acrosome-reacted sperm to eggs. Developmental Biology *128*, 376-385.

Bleil,J.D. and Wassarman,P.M. (1980a). Mammalian sperm-egg interaction: identification of a glycoprotein in mouse egg zonae pellucidae possessing receptor activity for sperm. Cell *20*, 873-882.

Bleil,J.D. and Wassarman,P.M. (1980b). Structure and function of the zona pellucida: identification and characterization of the proteins of the mouse oocyte's zona pellucida. Developmental Biology *76*, 185-202.

Bleil,J.D. and Wassarman,P.M. (1983). Sperm-egg interactions in the mouse: sequence of events and induction of the acrosome reaction by a zona pellucida glycoprotein. Developmental Biology *95*, 317-324.

Bleil,J.D. and Wassarman,P.M. (1986). Autoradiographic visualization of the mouse egg's sperm receptor bound to sperm. J. Cell Biology. *102*, 1363-1371.

Bleil,J.D. and Wassarman,P.M. (1988). Galactose at the nonreducing terminus of O-linked oligosaccharides of mouse egg zona pellucida glycoprotein ZP3 is essential for the glycoprotein's sperm receptor activity. Proceedings of the National Academy of Science USA *854*, 6778-6782.

Bleil,J.D. and Wassarman,P.M. (1990). Identification of a ZP3-binding protein on acrosome intact mouse sperm by photoaffinity crosslinking. Proceedings of the National Academy of Science USA *87*, 5563-5567.

Bligh,E.G. and Dyer,W.J. (1959). A rapid method of total lipid estraction and purification. Canadian Journal of Biochemistry and Physiology *31*, 911-917.

Blomqvist,M., Osterbye,T., Mansson,J.E., Horn,T., Buschard,K., and Fredman,P. (2002). Sulfatide is associated with insulin granules and located to microdomains of a cultured beta cell line. Glycoconj. J. *19*, 403-413.

Boerke,A., Tsai,P.S., Garcia-Gil,N., Brewis,I.A., and Gadella,B.M. (2008). Capacitation-dependent reorganization of microdomains in the apical sperm head plasma membrane: functional relationship with zona binding and the zona-induced acrosome reaction. Theriogenology *70*, 1188-1196.

Boettger-Tong,H., Biegler,B., Lee,T., and Poirier,G.R. (1992). Competition between zonae pellucidae and a proteinase inhibitor for sperm binding. Biology of Reproduction *47*, 716-722.

Boggs,J.M., Koshy,K.M., and Rangaraj,G. (1988). Interdigitated lipid bilayers oflong acyl chain species of cerebroside sulfate. A fatty acid spin label study. Biochimica et Biophysica Acta *938*, 373-385.

Boggs,J.M., Menikh,A., and Rangaraj,G. (2000). Trans interactions between galactosylceramide and cerebroside sulfate across apposed bilayers. Biophysical Journal *78*, 874-885.

Bojesen,A. and Gravholt,C.H. (2007). Klinefelter syndrome in clinical practice. Nat. Clin. Pract. Urol. *4*, 192-204.

Bonduelle,M., Wennerholm,U.B., Loft,A., Tarlatzis,B.C., Peters,C., Henriet,S., Mau,C., Victorin-Cederquist,A., Van Steirteghem,A., Balaska,A., Emberson,J.R., and Sutcliffe,A.G. (2005). A multi-centre cohort study of the physical health of 5-year-old children conceived after intracytoplasmic sperm injection, in vitro fertilization and natural conception. Hum. Reprod. *20*, 413-419.

Bou Khalil,M., Carmona,E., Carrier,D., Kates,M., and Tanphaichitr,N. (2001). The mammalian male germ cell specific sulfogalactosylglycerolipid imparts rigidity to ram testis phospholipid bilayers. Biology of Reproduction *64 Suppl.1*, 218.

Bou Khalil, M., Chakrabandhu,K., Xu,H., Weerachatyanukul,W., Buhr,M., Berger,T., Carmona,E., Vuong,N., Kumarathasan,P., Wong,P.T., Carrier,D., and Tanphaichitr,N. (2006). Sperm capacitation induces an increase in lipid rafts having zona pellucida binding ability and containing sulfogalactosylglycerolipid. Dev. Biol. *290*, 220-235.

Boulanger,J., Faulds,D., Eddy,E.M., and Lingwood,C.A. (1995). Members of the 70 kDa heat shock protein family specifically recognize sulfoglycolipids: role in gamete recognition and mycoplasma-related infertility. Journal of Cellular Physiology *165*, 7-17.

Boulanger,J., Huesca,M., Arab,S., and Lingwood,C.A. (1994). Universal method for the facile production of glycolipid/lipid matrices for the affinity purification of binding ligands. Analytical Biochemistry *217*, 1-6.

Bowen,J.R., Gibson,F.L., Leslie,G.I., and Saunders,D.M. (1998). Medical and developmental outcome at 1 year for children conceived by intracytoplasmic sperm injection. Lancet *351*, 1529-1534.

Brandon,C.I., Srivastava,P.N., Heusner,G.L., and Fayrer-Hosken,R.A. (1997). Estraction and quantification of acrosin, á-N-acetylglucosaminidase, and arylsulfatase-A from equine ejaculated spermatozoa. Journal of Experimental Zoology *279*, 301-308.

Breitbart,H. (2002a). Intracellular calcium regulation in sperm capacitation and acrosomal reaction. Mol. Cell Endocrinol. *187*, 139-144.

Breitbart,H. (2002b). Role and regulation of intracellular calcium in acrosomal exocytosis. J. Reprod. Immunol. *53*, 151-159.

Breitbart,H. and Spungin,B. (1997). The biochemistry of the acrosome reaction. Mol. Hum. Reprod. *3*, 195-202.

Breuss,J.M., Gillett,N., Lu,L., Sheppard,D., and Pytela,R. (1993). Restricted distribution of integrin beta 6 mRNA in primate epithelial tissues. J. Histochem. Cytochem. *41*, 1521-1527.

Brock,W.A., Trostle,P.K., and Meistrich,M.L. (1980). Meiotic synthesis of testis histones in the rat. Proc. Natl. Acad. Sci. U. S. A *77*, 371-375.

Brockhausen,I. and Kuhns,W. (1997). Role and metabolism of glycoconjugate sulfation. Trends in Glycoscience and Glycotechnology *9*, 379-398.

Brown,C.R. and Jones,R. (1987). Binding of zona pellucida proteins to a boar sperm polypeptide of M{-r}53 000 and identification of zona moieties involved. Development *99*, 333-339.

Buhi,W.C. (2002). Characterization and biological roles of oviduct-specific, oestrogen-dependent glycoprotein. Reproduction. *123*, 355-362.

Cardullo,R.A., Armant,D.R., and Millette,C.F. (1989). Characterization of fucosyltransferase activity during mouse spermatogenesis: Evidence for a cell surface fucosyltransferase. Biochemistry *28*, 1611-1617.

Carmona,E., Weerachatyanukul,W., Soboloff,T., Fluhary,A.L., White,D., Promdee,L., Ekker,M., Berger,T., Buhr,M., and Tanphaichitr,N. (2002a). Arylsulfatase A is present on the pig sperm surface and is involved in sperm-zona pellucida binding. Developmental Biology *247*, 182-196.

Carmona,E., Weerachatyanukul,W., Xu,H., Fluharty,A.L., Anupriwan,A., Shoushtarian,A., Chakrabandhu,K., and Tanphaichitr,N. (2002b). Binding of arylsulfatase A to mouse sperm inhibits gamete interaction and induces the acrosome reaction. Biology of Reproduction *66*, 1820-1827.

Carter,W.G. and Hakomori,S. (1977). Isolation and partial characterization of "galactoprotein a" (LETS) and "galactoprotein b" from hamster embryo fibroblasts. Biochemical and Biophysical Research Communications *76*, 299-308.

Chalabi,S., Panico,M., Sutton-Smith,M., Haslam,S.M., Patankar,M.S., Lattanzio,F.A., Morris,H.R., Clark,G.F., and Dell,A. (2006). Differential O-glycosylation of a conserved domain expressed in murine and human ZP3. Biochemistry *45*, 637-647.

Chang,P.L., Ameen,M., Yu,C.Z., and Kelly,B.M. (1988). Effect of ammonium chloride on subcellular distribution of lysosomal enzymes in human fibroblasts. Experimental Cell Research *176*, 258-267.

Chang,P.L. and Moudgil,G. (1984). A specific ultrastructural stain for arylsulfatase A activity in human cultured fibroblasts. Journal of Histochemistry and Cytochemistry *32*, 617-624.

Chapman,N., Kessopoulou,E., Andrews,P., Hornby,D., and Barratt,C.R. (1998). The polypeptide backbone of recombinant human zona pellucida glycoprotein-3 initiates acrosomal exocytosis in human spermatozoa in vitro. Biochemical Journal *330*, 839-845.

Chen,S. and Cardullo,R. (1994). Characterization and localization of fluorescent zonae pellucidae on mouse sperm. Molecular Biology of the Cell *5*, 224a.

Chen,Y., Cann,M.J., Litvin,T.N., Iourgenko,V., Sinclair,M.L., Levin,L.R., and Buck,J. (2000). Soluble adenylyl cyclase as an evolutionarily conserved bicarbonate sensor. Science *289*, 625-628.

Cheng,C.Y. and Mruk,D.D. (2002). Cell junction dynamics in the testis: Sertoli-germ cell interactions and male contraceptive development. Physiol Rev. *82*, 825-874.

Cheng,C.Y., Musto,N.A., Gunsalus,G.L., Frick,J., and Bardin,C.W. (1985). There are two forms of androgen binding protein in human testes. Comparison of their protomeric variants with serum testosterone-estradiol binding globulin
3. J. Biol. Chem. *260*, 5631-5640.

Cheng,H., Xu,J., McKeel,D.W., Jr., and Han,X. (2003). Specificity and potential mechanism of sulfatide deficiency in Alzheimer's disease: an electrospray ionization mass spectrometric study. Cell Mol. Biol. (Noisy. -le-grand) *49*, 809-818.

Cherr,G.N., Yudin,A.I., and Overstreet,J.W. (2001). The dual functions of GPI-anchored PH-20: hyaluronidase and intracellular signaling. Matrix Biol. *20*, 515-525.

Chiu,P.C., Chung,M.K., Koistinen,R., Koistinen,H., Seppala,M., Ho,P.C., Ng,E.H., Lee,K.F., and Yeung,W.S. (2007). Glycodelin-A interacts with fucosyltransferase on human sperm plasma membrane to inhibit spermatozoa-zona pellucida binding. J. Cell Sci. *120*, 33-44.

Clark,G.F. and Dell,A. (2006). Molecular models for murine sperm-egg binding
1. J. Biol. Chem.

Clausen,O.P., Parvinen,M., and Kirkhus,B. (1982). Stage-related variations in DNA fluorescence distribution during rat spermatogenic cycle measured by flow cytometry
2. Cytometry *2*, 421-425.

Clendenon,N.R. and Allen,N. (1970). Assay and subcellular localizaiton of the arylsulphatases in rat brain. Journal of Neurochemistry *17*, 865-879.

Clermont,Y. (1972). Kinetics of spermatogenesis in mammals: seminiferous epithelium cycle and spermatogonial renewal. Physiol Rev. *52*, 198-236.

Coetzee,T., Fujita,N., Dupree,J., Shi,R., Blight,A., Suzuki,K., Suzuki,K., and Popko,B. (1996). Myelination in the absence of galactorcerebroside and sulfatide: Normal structure with abnormal function and regional instability. Cell *86*, 209-219.

Contreras,H.R. and Llanos,M.N. (2001). Detection of progesterone receptors in human spermatozoa and their correlation with morphological and functional properties. Int. J. Androl *24*, 246-252.

Cooper,T.G. (1995). Role of the epididymis in mediating changes in the male gamete during maturation. Adv. Exp. Med. Biol. *377*, 87-101.

Cooper,T.G. (1998). Interactions between epididymal secretions and spermatozoa. Journal of Reproduction and Fertility Supplement *53*, 119-136.

Cooper,T.G. and Yeung,C.H. (1997). Physiology of sperm maturation and fertilization. In Andrology: Male Reproductive Health and Dysfunction, E.Nieschlag, ed. (Berlin Heidelberg: Springer-Verlag), pp. 61-78.

Cornwall,G.A., Cameron,A., Lindberg,I., Hardy,D.M., Cormier,N., and Hsia,N. (2003). The cystatin-related epididymal spermatogenic protein inhibits the serine protease prohormone convertase 2. Endocrinology *144*, 901-908.

Cornwall,G.A., Tulsiani,D.R.P., and Orgebin-Crist,M.C. (1991). Inhibition of the mouse sperm surface à-D-mannosidase inhibits sperm-egg binding in vitro. Biology of Reproduction *44*, 913-921.

Crook,S.J., Stewart,R., Boggs,J.M., Vistnes,A.I., and Zalc,B. (1987). Characterization of anti-cerebroside sulfate antisera using a theoretical model to analyze liposome immune lysis data. Molecular Immunology *24*, 1135-1143.

Cross,N.L. (1998). Role of cholesterol in sperm capacitation. Biology of Reproduction *59*, 7-11.

Dacheux,J.L., Gatti,J.L., and Dacheux,F. (2003). Contribution of epididymal secretory proteins for spermatozoa maturation. Microsc. Res. Tech. *61*, 7-17.

Darszon,A., Acevedo,J.J., Galindo,B.E., Hernandez-Gonzalez,E.O., Nishigaki,T., Trevino,C.L., Wood,C., and Beltran,C. (2006). Sperm channel diversity and functional multiplicity. Reproduction. *131*, 977-988.

DasGupta,S., Mills,C.L., and Fraser,L.R. (1993). Ca(2+)-related changes in the capacitation state of human spermatozoa assessed by a chlortetracycline fluorescence assay. J. Reprod. Fertil. *99*, 135-143.

Davis,B.K. (1982). Uterine fluid proteins bind sperm cholesterol during capacitation in the rabbit. Experentia *38*, 1063-1064.

Davis,B.K. and Davis,N.V. (1983). Binding by glycoproteins of seminal plasma membrane vesicles accelerates decapacitation in rabbit spermatozoa. Biochimica et Biophysica Acta *727*, 70-76.

Davis,J.T., Bridges.RB, and Coniglio,J.G. (1966). Changes in lipid compositon of the maturing rat testis. Biochemical Journal *98*, 342-346.

De Blas,G., Michaut,M., Trevino,C.L., Tomes,C.N., Yunes,R., Darszon,A., and Mayorga,L.S. (2002). The intraacrosomal calcium pool plays a direct role in acrosomal exocytosis. J. Biol. Chem. *277*, 49326-49331.

de Kretser,D.M. and Kerr,J.B. (1994). The Cytology of the Testis. In The Physiology of Reproduction, E.Knobil and J.D.Neill, eds. (New York: Raven press), pp. 1177-1290.

De Lamirande,E., Leclerc,P., and Gagnon,C. (1997). Capacitation as a regulatory event that primes spermatozoa for the acrosome reaction and fertilization. Molecular Human Reproduction *3*, 175-194.

de Rooij,D.G. and de Boer,P. (2003). Specific arrests of spermatogenesis in genetically modified and mutant mice. Cytogenet. Genome Res. *103*, 267-276.

de Vries,K.J., Wiedmer,T., Sims,P.J., and Gadella,B.M. (2003). Caspase-independent exposure of aminophospholipids and tyrosine phosphorylation in bicarbonate responsive human sperm cells. Biol. Reprod. *68*, 2122-2134.

de Vries,S.S., Baart,E.B., Dekker,M., Siezen,A., de Rooij,D.G., de Boer,P., and te,R.H. (1999). Mouse MutS-like protein Msh5 is required for proper chromosome synapsis in male and female meiosis. Genes Dev. *13*, 523-531.

DeAngelis,P. and Glabe,C. (1987). Polysaccharide structural features that are critical for the binding of sulfated fucans to bindin, the adhesive protein from sea urchin sperm. Biological Chemistry Hoppe Seyler *262*, 13946-13952.

Delacour,D., Gouyer,V., Zanetta,J.P., Drobecq,H., Leteurtre,E., Grard,G., Moreau-Hannedouche,O., Maes,E., Pons,A., Andre,S., Le Bivic,A., Gabius,H.J., Manninen,A., Simons,K., and Huet,G. (2005). Galectin-4 and sulfatides in apical membrane trafficking in enterocyte-like cells. J. Cell Biol. *169*, 491-501.

Dell,A., Morris,H.R., Easton,R.L., Patankar,M., and Clark,G.F. (1999). The glycobiology of gametes and fertilisation. Biochimica et Biophysica Acta *1473*, 196-205.

Demarco,I.A., Espinosa,F., Edwards,J., Sosnik,J., De La Vega-Beltran JL, Hockensmith,J.W., Kopf,G.S., Darszon,A., and Visconti,P.E. (2003). Involvement of a Na+/HCO-3 cotransporter in mouse sperm capacitation. J. Biol. Chem. *278*, 7001-7009.

Deng,X., He,Y., and Martin-Deleon,P.A. (2000). Mouse Spam1 (PH-20): evidence for its expression in the epididymis and for a new category of spermatogenic-expressed genes. J. Androl *21*, 822-832.

Dias,G.M., Retamal,C.A., Tobella,L., Arnholdt,A.C., and Lopez,M.L. (2006). Nuclear status of immature and mature stallion spermatozoa. Theriogenology *66*, 354-365.

Ding,Z., Qu,F., Guo,W., Ying,X., Wu,M., and Zhang,Y. (2007). Identification of sperm forward motility-related proteins in human seminal plasma. Mol. Reprod. Dev. *74*, 1124-1131.

Dohle,G.R., Halley,D.J.J., Van Hemel,J.O., van den Ouweland,A.M.W., Pieters,M.H.E.C., Weber,R.F.A., and Govaerts,L.C.P. (2002). Genetic risk factors in

infertile men with severe oligozoospermia and azoospermia. Human Reproduction *17*, 13-16.

Dohle,G.R., Smit,M., and Weber,R.F. (2003). Androgens and male fertility. World J. Urol. *21*, 341-345.

Dohle,G.R., Veeze,H.J., Overbeek,S.E., van den Ouweland,A.M., Halley,D.J., Weber,R.F., and Niermeijer,M.F. (1999). The complex relationships between cystic fibrosis and congenital bilateral absence of the vas deferens: clinical, electrophysiological and genetic data. Hum. Reprod. *14*, 371-374.

Dudkiewicz,A.B. (1984). Purification of boar acrosomal arylsulfatase A and possible role in the penetration of cumulus cells. Biol. Reprod. *30*, 1005-1014.

Dunbar,B.S., Timmons,T.M., Skinner,S.M., and Prasad,S.V. (2001). Molecular analysis of a carbohydrate antigen involved in the structure and function of zona pellucida glycoproteins. Biology of Reproduction *65*, 951-960.

Dym,M. (1977). The male reproductive system. In Histology, L.Weiss, ed. (New York: McGraw-Hill Book Company), pp. 979-1038.

Dym,M. (1994). Spermatogonial stem cells of the testis. Proc. Natl. Acad. Sci. U. S. A *91*, 11287-11289.

Dym,M. and Cavicchia,J.C. (1977). Further observations on the blood-testis barrier in monkeys. Biol. Reprod. *17*, 390-403.

East,I.J., Gulyas,B.J., and Dean,J. (1985). Monoclonal antibodies to the murine zona pellucida protein with sperm receptor activity: effects on fertilization and early development. Dev. Biol. *109*, 268-273.

East,I.J., Keenan,A.M., Larson,S.M., and Dean,J. (1984). Scitigraphy of normal mouse ovaries with monoclonal antibodies to ZP-2, the major zona pellucida protein. Science *225*, 938-941.

Eckhardt,M., Hedayati,K.K., Pitsch,J., Lullmann-Rauch,R., Beck,H., Fewou,S.N., and Gieselmann,V. (2007). Sulfatide storage in neurons causes hyperexcitability and axonal degeneration in a mouse model of metachromatic leukodystrophy. J. Neurosci. *27*, 9009-9021.

Ecroyd,H., Jones,R.C., and Aitken,R.J. (2003). Tyrosine phosphorylation of HSP-90 during mammalian sperm capacitation. Biol. Reprod. *69*, 1801-1807.

Eddy,E.M., Muller,C.H., and Lingwood,C.A. (1985). Preparation of monoclonal antibody to sulfatoxygalactosylglycerolipd by in vitro immunizationwith a glycolipid-glass conjugate. Journal of Immunological Methods *81*, 137-146.

Eddy,E.M. and O'Brien,D.A. (1994). The spermatozoon. In The Physiology of Reproduction, E.Knobil, ed. (New York: Raven Press), pp. 29-77.

Eddy,E.M., Toshimori,K., and O'Brien,D.A. (2003). Fibrous sheath of mammalian spermatozoa. Microsc. Res. Tech. *61*, 103-115.

Ehrenwald,E., Foote,R.H., and Parks,J.E. (1990). Bovine oviductal fluid components and their potential role in sperm cholesterol efflux. Mol. Reprod. Dev. *25*, 195-204.

Ekhlasi-Hundrieser,M., Sinowatz,F., Greiser,D.W., I, Waberski,D., and Topfer-Petersen,E. (2002). Expression of spermadhesin genes in porcine male and female reproductive tracts. Mol. Reprod. Dev. *61*, 32-41.

Ellerman,D.A., Brantua,V.S., Martinez,S.P., Cohen,D.J., Conesa,D., and Cuasnicu,P.S. (1998). Potential contraceptive use of epididymal proteins: immunization of male rats with epididymal protein DE inhibits sperm fusion ability. Biology of Reproduction *59*, 1029-1036.

Ellinwood,N.M., Vite,C.H., and Haskins,M.E. (2004). Gene therapy for lysosomal storage diseases: the lessons and promise of animal models. J. Gene Med. *6*, 481-506.

Elzanaty,S. (2007). Association between age and epididymal and accessory sex gland function and their relation to sperm motility. Arch. Androl *53*, 149-156.

Ensslin,M., Vogel,T., Calvete,J.J., Thole,H.H., Schmidtke,J., Matsuda,T., and Topfer-Petersen,E. (1998). Molecular cloning and characterization of P47, a novel boar sperm-associated zona pellucida-binding protein homologous to a family of mammalian secretory proteins. Biol. Reprod. *58*, 1057-1064.

Ensslin,M.A., Lyng,R., Raymond,A., Copland,S., and Shur,B.D. (2007). Novel gamete receptors that facilitate sperm adhesion to the egg coat. Soc. Reprod. Fertil. Suppl *63*, 367-383.

Ensslin,M.A. and Shur,B.D. (2003). Identification of mouse sperm SED1, a bimotif EGF repeat and discoidin-domain protein involved in sperm-egg binding. Cell *114*, 405-417.

Eskenazi,B., Wyrobek,A.J., Sloter,E., Kidd,S.A., Moore,L., Young,S., and Moore,D. (2003). The association of age and semen quality in healthy men. Hum. Reprod. *18*, 447-454.

Esposito,G., Jaiswal,B.S., Xie,F., Krajnc-Franken,M.A., Robben,T.J., Strik,A.M., Kuil,C., Philipsen,R.L., Van Duin,M., Conti,M., and Gossen,J.A. (2004). Mice deficient for soluble adenylyl cyclase are infertile because of a severe sperm-motility defect. Proc. Natl. Acad. Sci. U. S. A *101*, 2993-2998.

Evenson,D., Darzynkiewicz,Z., Jost,L., Janca,F., and Ballachey,B. (1986). Changes in accessibility of DNA to various fluorochromes during spermatogenesis. Cytometry *7*, 45-53.

Fewou,S.N., Bussow,H., Schaeren-Wiemers,N., Vanier,M.T., Macklin,W.B., Gieselmann,V., and Eckhardt,M. (2005). Reversal of non-hydroxy:alpha-hydroxy galactosylceramide ratio and unstable myelin in transgenic mice overexpressing UDP-galactose:ceramide galactosyltransferase. J. Neurochem. *94*, 469-481.

Ficarro,S., Chertihin,O., Westbrook,V.A., White,F., Jayes,F., Kalab,P., Marto,J.A., Shabanowitz,J., Herr,J.C., Hunt,D.F., and Visconti,P.E. (2003). Phosphoproteome analysis of capacitated human sperm. Evidence of tyrosine phosphorylation of a kinase-anchoring protein 3 and valosin-containing protein/p97 during capacitation. J. Biol. Chem. *278*, 11579-11589.

Flesch,F.M., Brouwers,J.F., Nievelstein,P.F., Verkleij,A.J., Van Golde,L.M., Colenbrander,B., and Gadella,B.M. (2001). Bicarbonate stimulated phospholipid scrambling induces cholesterol redistribution and enables cholesterol depletion in the sperm plasma membrane. J. Cell Sci. *114*, 3543-3555.

Flesch,F.M. and Gadella,B.M. (2000). Dynamics of the mammalian sperm plasma membrane in the process of fertilization. Biochimica et Biophysica Acta *1469*, 197-235.

Florman,H.M. (1994). Sequential focal and global elevations of sperm intracellular Ca{+2+} are initiated by the zona pellucida during acrosomal exocytosis. Developmental Biology *165*, 152-164.

Florman,H.M., Bechtol,K.B., and Wassarman,P.M. (1984). Enzymatic Dissection of the Functions of the Mouse Egg's Receptor for Sperm. Developmental Biology *106*, 243-255.

Florman,H.M. and Ducibella,T. (2006). Fertilization in mammals. In Knobil and Neil's Physiology of Reproduction, J.D.Neill, ed. (New York: Elsevier), pp. 55-112.

Florman,H.M. and Wassarman,P.M. (1985). O-linked oligosaccharides of mouse egg ZP3 account for its sperm receptor activity. Cell *41*, 313-324.

Fluharty,A.L. and Edmond,J. (1978). Arylsulfatase A and B from human liver. Methods in Enzymology *50*, 537-547.

Fluharty,A.L., Stevens,R.L., Goldstein,E.B., and Kihara,H. (1979). The activity of arylsulfatase A and B on tyrosine O-sulfates. Biochim. Biophys. Acta *566*, 321-326.

Fluharty,A.L., Stevens,R.L., Miller,R.T., and Kihara,H. (1974). Sulfoglycerogalactolipid from rat testis: A substrate for pure; human arylsulfatase A. Biochemical and Biophysical Research Communications *61*, 348-354.

Forti,G., Baldi,E., Krausz,C., Luconi,M., Bonaccorsi,L., Maggi,M., Bassi,F., and Scarselli,G. (1999). Effects of progesterone on human spermatozoa: clinical implications. Ann. Endocrinol. (Paris) *60*, 107-110.

Foster,L.J., De Hoog,C.L., and Mann,M. (2003). Unbiased quantitative proteomics of lipid rafts reveals high specificity for signaling factors. Proc. Natl. Acad. Sci. U. S. A *100*, 5813-5818.

Fouchecourt,S., Metayer,S., Locatelli,A., Dacheux,F., and Dacheux,J.L. (2000). Stallion epididymal fluid proteome: Qualitative and quantitative characterization; Secretion and dynamic changes of major proteins. Biology of Reproduction *62*, 1790-1803.

Franca,L.R., Ogawa,T., Avarbock,M.R., Brinster,R.L., and Russell,L.D. (1998). Germ cell genotype controls cell cycle during spermatogenesis in the rat. Biol. Reprod. *59*, 1371-1377.

Francavilla,S., Gabriele,A., Romano,R., Gianaroli,L., Ferraretti,A.P., and Francavilla,F. (1994). Sperm-zona pellucida binding of human sperm is correlated with the immunocytochemical presence of proacrosin and acrosin in the sperm heads but not with the proteolytic activity of acrosin. Fertility and Sterility *62*, 1226-1233.

Franchini,L., Panza,L., Kongmanas,K., Tanphaichitr,N., Faull,K.F., and Ronchetti,F. (2008). An efficient and convenient synthesis of deuterium-labelled seminolipid isotopomers and their ESI-MS characterization. Chem. Phys. Lipids *152*, 78-85.

Frayne,J., McMillen,A., Love,S., and Hall,L. (1998). Expression of phosphatidylethanolamine-binding protein in the male reproductive tract: immunolocalisation and expression in prepubertal and adult rat testes and epididymides. Mol. Reprod. Dev. *49*, 454-460.

Fredman,P., Mattsson,L., Andersson,K., Davidsson,P., Ishizuka,I., Jeansson,S., Mansson,J.E., and Svennerholm,L. (1988). Characterization of the binding epitope of a monoclonal antibody to sulphatide. Biochemical Journal *251*, 17-22.

Freeman,E.A., Jani,P., and Millette,C.E. (2002). Expression and potential function of Rho family small G proteins in cells of the mammalian seminiferous epithelium. Cell Commun. Adhes. *9*, 189-204.

Fuentes-Prior,P., Fujikawa,K., and Pratt,K.P. (2002). New insights into binding interfaces of coagulation factors V and VIII and their homologues lessons from high resolution crystal structures. Curr. Protein Pept. Sci. *3*, 313-339.

Fujii,T., Kobayashi,T., Honke,K., Gasa,S., Ishikawa,M., Shimizu,T., and Makita,A. (1992). Proteolytic processing of human lysosomal arylsulfatase A. Biochimica et Biophysica Acta *1122*, 93-98.

Fujimoto,H., Tadano-Aritomi,K., Tokumasu,A., Ito,K., Hikita,T., Suzuki,K., and Ishizuka,I. (2000). Requirement of seminolipid in spermatogenesis revealed by UDP-galactose: Ceramide galactosyltransferase-deficient mice. J. Biol. Chem. *275*, 22623-22626.

Fukami,K., Nakao,K., Inoue,T., Kataoka,Y., Kurokawa,M., Fissore,R.A., Nakamura,K., Katsuki,M., Mikoshiba,K., Yoshida,N., and Takenawa,T. (2001). Requirement of phospholipase Cë4 for the zona pellucida-induced acrosome reaction. Science *292*, 920-923.

Furimsky,A., Vuong,N., Xu,H., Kumarathasan,P., Xu,M., Weerachatyanukul,W., Bou,K.M., Kates,M., and Tanphaichitr,N. (2005). Percoll gradient-centrifuged capacitated mouse sperm have increased fertilizing ability and higher contents of sulfogalactosylglycerolipid and docosahexaenoic acid-containing phosphatidylcholine compared to washed capacitated mouse sperm. Biol. Reprod. *72*, 574-583.

Furst,W. and Sandhoff,K. (1992). Activator proteins and topology of lysosomal sphingolipid catabolism. Biochimica et Biophysica Acta *1126*, 1-16.

Gadella,B.M., Colenbrander,B., Van Golde,L.M.G., and Lopes-Cardozo,M. (1993). Boar seminal vesicles secrete arylsulfatases into seminal plasma: Evidence that desulfation of seminolipid occurs only after ejaculation. Biology of Reproduction *48*, 483-489.

Gadella,B.M., Flesch,F.M., Van Golde,L.M.G., and Colenbrander,B. (1999a). Dynamics in the membrane organization of the mammalian sperm cell and functionality in fertilization. The Veterinary Quarterly *21*, 142-146.

Gadella,B.M., Gadella,T.W.J., Colenbrander,B., Van Golde,L.M., and Lopes-Cardozo,M. (1994). Visualization and quantification of glycolipid polarity dynamics in the plasma membrane of the mammalian spermatozoon. Journal of Cell Science *107*, 2151-2163.

Gadella,B.M. and Harrison,R.A. (2000). The capacitating agent bicarbonate induces protein kinase A-dependent changes in phospholipid transbilayer behavior in the sperm plasma membrane. Development *127*, 2407-2420.

Gadella,B.M. and Harrison,R.A. (2002). Capacitation induces cyclic adenosine 3',5'-monophosphate-dependent, but apoptosis-unrelated, exposure of aminophospholipids at the apical head plasma membrane of boar sperm cells. Biol. Reprod. *67*, 340-350.

Gadella,B.M., Miller,N.G.A., Colenbrander,B., Van Golde,L.M.G., and Harrison,R.A.P. (1999b). Flow cytometric detection of transbilayer movement of fluorescent phospholipid analogues across the boar sperm plasma membrane: Elimination of labeling artifacts. Molecular Reproduction and Development *53*, 108-125.

Gadella,B.M. and Van Gestel,R.A. (2004). Bicarbonate and its role in mammalian sperm function. Anim Reprod. Sci. *82-83*, 307-319.

Galbiati,F., Razani,B., and Lisanti,M.P. (2001). Emerging themes in lipid rafts and caveolae. Cell *108*, 403-411.

Gatti,J.L., Castella,S., Dacheux,F., Ecroyd,H., Metayer,S., Thimon,V., and Dacheux,J.L. (2004). Post-testicular sperm environment and fertility. Anim Reprod. Sci. *82-83*, 321-339.

Gaudreault,C., El Alfy,M., Legare,C., and Sullivan,R. (2001). Expression of the hamster sperm protein P26h during spermatogenesis. Biol. Reprod. *65*, 79-86.

Georgiou,I., Syrrou,M., Pardalidis,N., Karakitsios,K., Mantzavinos,T., Giotitsas,N., Loutradis,D., Dimitriadis,F., Saito,M., Miyagawa,I., Tzoumis,P., Sylakos,A., Kanakas,N., Moustakareas,T., Baltogiannis,D., Touloupides,S., Giannakis,D., Fatouros,M., and Sofikitis,N. (2006). Genetic and epigenetic risks of intracytoplasmic sperm injection method. Asian J Androl *8*, 643-673.

Gerard,A. (1995). Endocytosis of androgen-binding protein (ABP) by spermatogenic cells. J. Steroid Biochem. Mol. Biol. *53*, 533-542.

Gerard,A., Khanfri,J., Gueant,J.L., Fremont,S., Nicolas,J.P., Grignon,G., and Gerard,H. (1988). Electron microscope radioautographic evidence of in vivo androgen-binding protein internalization in the rat epididymis principal cells. Endocrinology *122*, 1297-1307.

Gibbons,R., Adeoya-Osiguwa,S.A., and Fraser,L.R. (2005). A mouse sperm decapacitation factor receptor is phosphatidylethanolamine-binding protein 1. Reproduction. *130*, 497-508.

Gieselmann,V. (2003). Metachromatic leukodystrophy: recent research developments. J. Child Neurol. *18*, 591-594.

Gong,X., Dubois,D.H., Miller,D.J., and Shur,B.D. (1995). Activation of a G protein complex by aggregation of á-1, 4-galactosyltransferase on the surface of the sperm. Science *269*, 1718-1721.

Gopalakrishnan,B., Aravinda,S., Pawshe,C.H., Totey,S.M., Nagpal,S., Salunke,D.M., and Shaha,C. (1998). Studies on glutathione S-transferases important for sperm function: evidence of catalytic activity-independent functions. Biochem. J. *329 (Pt 2)*, 231-241.

Grabske,R.J., Lake,S., Gledhill,B.L., and Meistrich,M.L. (1975). Centrifugal elutriation: separation of spermatogenic cells on the basis of sedimentation velocity. J. Cell Physiol *86*, 177-189.

Griswold,M.D. (1995). Interactions between germ cells and Sertoli cells in the testis. Biol. Reprod. *52*, 211-216.

Griswold,M.D. (1998). The central role of Sertoli cells in spermatogenesis. Semin. Cell Dev. Biol. *9*, 411-416.

Griswold,M.D., Heckert,L., and Linder,C. (1995). The molecular biology of the FSH receptor. J. Steroid Biochem. Mol. Biol. *53*, 215-218.

Gueant,J.L., Fremont,S., Felden,F., Nicolas,J.P., Gerard,A., Leheup,B., Gerard,H., and Grignon,G. (1991). Evidence that androgen-binding protein endocytosis in vitro is receptor mediated in principal cells of the rat epididymis. J. Mol. Endocrinol. *7*, 113-122.

Gyamera-Acheampong,C., Tantibhedhyangkul,J., Weerachatyanukul,W., Tadros,H., Xu,H., van de Loo,J.W., Pelletier,R.M., Tanphaichitr,N., and Mbikay,M. (2006). Sperm from mice genetically deficient for the PCSK4 proteinase exhibit accelerated capacitation, precocious acrosome reaction, reduced binding to egg zona pellucida, and impaired fertilizing ability Biol. Reprod. *74*, 666-673.

Hagenas,L. and Ritzen,E.M. (1975). Impaired Sertoli cell function in experimental cryptorchidism in the rat. Mol. Cell Endocrinol. *4*, 25-34.

Hakomori,S. (2000). Cell adhesion/recognition and signal transduction through glycosphingolipid microdomain. Glycoconjugate Journal *17*, 143-151.

Hakomori,S. and Handa,K. (2003). Interaction of glycosphingolipids with signal transducers and membrane proteins in glycosphingolipid-enriched microdomains. Methods Enzymol. *363*, 191-207.

Hamer,G., Kal,H.B., Westphal,C.H., Ashley,T., and de Rooij,D.G. (2004). Ataxia telangiectasia mutated expression and activation in the testis. Biol. Reprod. *70*, 1206-1212.

Hamil,K.G., Sivashanmugam,P., Richardson,R.T., Grossman,G., Ruben,S.M., Mohler,J.L., Petrusz,P., O'Rand,M.G., French,F.S., and Hall,S.H. (2000). HE2beta and HE2gamma, new members of an epididymis-specific family of androgen-regulated proteins in the human. Endocrinology *141*, 1245-1253.

Han,X., Cheng,H., Fryer,J.D., Fagan,A.M., and Holtzman,D.M. (2003). Novel role for apolipoprotein E in the central nervous system. Modulation of sulfatide content. J. Biol. Chem. *278*, 8043-8051.

Hanson,S.R., Best,M.D., and Wong,C.H. (2004). Sulfatases: structure, mechanism, biological activity, inhibition, and synthetic utility. Angew. Chem. Int. Ed Engl. *43*, 5736-5763.

Harder,T. and Simons,K. (1999). Clusters of glycolipid and glycosylphosphatidylinositol-anchored proteins in lymphoid cells: accumulation of actin regulated by local tyrosine phosphorylation. Eur. J. Immunol. *29*, 556-562.

Harlow,E. and Lane,D. (1988). Antibodies: A Laboratory Manual. (Cold Spring Harbor: Cold Spring Harbor Symposium).

Harris,J.D., Hibler,D.W., Fontenot,G.K., Hsu,K.T., Yurewicz,E.C., and Sacco,A.G. (1994). Cloning and characterization of zona pellucida genes and cDNAs from a variety

of mammalian species: The ZPA, ZPB and ZPC gene families. DNA Sequence *4*, 361-393.

Harrison,D.A., Carr,D.W., and Meizel,S. (2000). Involvement of protein kinase A and A kinase anchoring protein in the progesterone-initiated human sperm acrosome reaction. Biol. Reprod. *62*, 811-820.

Harrison,R.A. (1996). Capacitation mechanisms, and the role of capacitation as seen in eutherian mammals. Reprod. Fertil. Dev. *8*, 581-594.

Harrison,R.A. (1997). Sperm plasma membrane characteristics and boar semen fertility. J. Reprod. Fertil. Suppl *52*, 195-211.

Harrison,R.A. and Miller,N.G. (2000). cAMP-dependent protein kinase control of plasma membrane lipid architecture in boar sperm. Molecular Reproduction and Development *55*, 220-228.

Harrison,R.A.P., Ashworth,P.J.C., and Miller,N.G.A. (1996). Bicarbonate/CO2, an effector of capacitation, induces a rapid and reversible change in the lipid architecture of boar sperm plasma membranes. Molecular Reproduction and Development *45*, 378-391.

Hartmann,J.F., Gwatkin,R.B., and Hutchison,C.F. (1972). Early contact interactions between mammalian gametes in vitro: evidence that the vitellus influences adherence between sperm and zona pellucida. Proc. Natl. Acad. Sci. U. S. A *69*, 2767-2769.

Hemachand,T., Gopalakrishnan,B., Salunke,D.M., Totey,S.M., and Shaha,C. (2002). Sperm plasma-membrane-associated glutathione S-transferases as gamete recognition molecules. J. Cell Sci. *115*, 2053-2065.

Henderson,N.A., Cooke,G.M., and Robaire,B. (2006). Region-specific expression of androgen and growth factor pathway genes in the rat epididymis and the effects of dual 5alpha-reductase inhibition. J. Endocrinol. *190*, 779-791.

Henseler,M., Klein,A., Reber,M., Vanier,M.T., Landrieu,P., and Sandhoff,K. (1996). Analysis of a splice-site mutation in the sap-precursor gene of a patient with metachromatic leukodystrophy. Am. J. Hum. Genet. *58*, 65-74.

Hermo,L. and Andonian,S. (2003). Regulation of sulfated glycoprotein-1 and cathepsin D expression in adult rat epididymis. J. Androl *24*, 408-422.

Hermo,L., Badran,H., and Andonian,S. (2002). The structural organization and functins of the epithelium of the vas deferens. In The Epididymis: From Molecules to Clinical Practice, B.Robaire, ed. (New York: Kluwer Academic/Plenum Publishers), pp. 233-250.

Hermo,L., Barin,K., and Oko,R. (1994). Developmental expression of sulfated glycoprotein-2 in the epididymis of the rat. Anatomical Record *240*, 327-344.

Hermo,L., Morales,C., and Oko,R. (1992a). Immunocytochemical localization of sulfated glycoprotein-1 (SGP-1) and identification of its transcripts in epithelial cells of the extratesticular duct system of the rat. Anatomical Record *232*, 401-422.

Hermo,L., Oko,R., and Robaire,B. (1992b). Epithelial cells of the epididymis show regional variations with respect to the secretion of endocytosis of immobilin as revealed by light and electron microscope immunocytochemistry. Anatomical Record *232*, 202-220.

Hermo,L. and Robaire,B. (2002). Epididymal cell types and functions. In The Epididymis: From Molecules to Clinical Practice, B.Robaire, ed. (New York: Kluwer Academic/Plenum Publishers), pp. 81-102.

Hernandez-Gonzalez,E.O., Sosnik,J., Edwards,J., Acevedo,J.J., Mendoza-Lujambio,I., Lopez-Gonzalez,I., Demarco,I., Wertheimer,E., Darszon,A., and Visconti,P.E. (2006). Sodium and epithelial sodium channels participate in the regulation of the capacitation-associated hyperpolarization in mouse sperm. J. Biol. Chem. *281*, 5623-5633.

Hernandez-Gonzalez,E.O., Trevino,C.L., Castellano,L.E., de la Vega-Beltran JL, Ocampo,A.Y., Wertheimer,E., Visconti,P.E., and Darszon,A. (2007). Involvement of cystic fibrosis transmembrane conductance regulator in mouse sperm capacitation. J. Biol. Chem. *282*, 24397-24406.

Herrick,S.B., Schweissinger,D.L., Kim,S.W., Bayan,K.R., Mann,S., and Cardullo,R.A. (2005). The acrosomal vesicle of mouse sperm is a calcium store. J. Cell Physiol *202*, 663-671.

Hess,B., Saftig,P., Hartmann,D., Coenen,R., Lullmann-Rauch,R., Goebel,H.H., Evers,M., von Figura,K., D'Hooge,R., Nagels,G., De Deyn,P., Peters,C., and Gieselmann,V. (1996). Phenotype of arylsulfatase A-deficient mice: relationship to human metachromatic leukodystrophy. Proc. Natl. Acad. Sci. U. S. A *93*, 14821-14826.

Hess,K.C., Jones,B.H., Marquez,B., Chen,Y., Ord,T.S., Kamenetsky,M., Miyamoto,C., Zippin,J.H., Kopf,G.S., Suarez,S.S., Levin,L.R., Williams,C.J., Buck,J., and Moss,S.B. (2005). The "soluble" adenylyl cyclase in sperm mediates multiple signaling events required for fertilization. Dev. Cell *9*, 249-259.

Hinsch,E., Aires,V.A., Hedrich,F., Oehninger,S., and Hinsch,K.D. (2005). A synthetic decapeptide from a conserved ZP3 protein domain induces the G protein-regulated acrosome reaction in bovine spermatozoa. Theriogenology *63*, 1682-1694.

Hiraiwa,M., Martin,B.M., Kishimoto,Y., Conner,G.E., Tsuji,S., and O'Brien,J.S. (1997). Lysosomal proteolysis of prosaposin, the precursor of saposins (sphingolipid activator proteins): its mechanism and inhibition by ganglioside. Archives of Biochemistry and Biophysics *341*, 17-24.

Hiraiwa,M., O'Brien,J.S., Kishimoto,Y., Galdzicka,M., Fluharty,A.L., Binns,E.I., and Martin,B.M. (1993). Isolation, characterization, and proteolysis of human prosaposin, the

precursor of saposins (sphingolipid activator proteins). Archives of Biochemistry and Biophysics *304*, 110-116.

Hogan,B., Costantini,F., and Lacy,E. (1994). Manipulating the mouse embryo: a laboratory manual. (Cold Spring Harbor: Cold Spring Harbor Laboratory), pp. 1-497.

Hokke,C.H., Damm,J.B.L., Penninkhof,B., Aitken,R.J., Kamerling,J.P., and Vliegenthart,J.F.G. (1994). Structure of the O-linked carbohydrate chains of porcine zona pellucida glycoproteins. European Journal of Biochemistry *221*, 491-512.

Holland,M.K. and Nixon,B. (1998). The specificity of epididymal secretory proteins. J. Reprod. Fertil. Suppl *53*, 197-210.

Honda,A., Yamagata,K., Sugiura,S., Watanabe,K., and Baba,T. (2002). A mouse serine protease TESP5 is selectively included into lipid rafts of sperm membrane presumably as a glycosylphosphatidylinositol-anchored protein. Journal of Biological Chemistry *277*, 16976-16984.

Honke,K., Hirahara,Y., Dupree,J., Suzuki,K., Popko,B., Fukushima,K., Fukushima,J., Nagasawa,T., Yoshida,N., Wada,Y., and Taniguchi,N. (2002). Paranodal junction formation and spermatogenesis require sulfoglycolipids. Proc. Natl. Acad. Sci. U. S. A *99*, 4227-4232.

Hoodbhoy,T. and Dean,J. (2004). Insights into the molecular basis of sperm-egg recognition in mammals. Reproduction. *127*, 417-422.

Howes,E., Pascall,J.C., Engel,W., and Jones,R. (2001). Interactions between mouse ZP2 glycoprotein and proacrosin; a mechanism for secondary binding of sperm to the zona pellucida during fertilization. J. Cell Sci. *114*, 4127-4136.

Howes,L. and Jones,R. (2002). Interactions between zona pellucida glycoproteins and sperm proacrosin/acrosin during fertilization. J. Reprod. Immunol. *53*, 181-192.

Hsu,F.F., Bohrer,A., and Turk,J. (1998). Electrospay ionization tandem mass spectrometric analysis of sulfatide. Determination of fragmentation patterns and characterization of molecular species expressed in brain and in pancreatic islets. Biochimica et Biophysica Acta *1392*, 202-216.

Hsu,L.H., Narasimhan,R., and Levine,M. (1983). Studies of the biosynthesis and metabolism of rat testicular galactoglycerolipids. Can. J. Biochem. Cell Biol. *61*, 1272-1281.

Huckins,C. (1978). The morphology and kinetics of spermatogonial degeneration in normal adult rats: an analysis using a simplified classification of the germinal epithelium. Anat. Rec. *190*, 905-926.

Hunnicutt,G.R., Primakoff,P., and Myles,D.G. (1996). Sperm surface protein pH-20 is bifunctional: one activity is a hyaluronidase and second, distinct activity is required in secondary sperm-zona binding. Biology of Reproduction *55*, 80-86.

Hutt,D.M., Baltz,J.M., and Ngsee,J.K. (2005). Synaptotagmin VI and VIII and syntaxin 2 are essential for the mouse sperm acrosome reaction. J. Biol. Chem. *280*, 20197-20203.

Igdoura,S.A., Hermo,L., and Morales,C.R. (1994). Sulfated glycoprotein02 synthesized by nonciliated cells of the efferent ducts is targeted to the lysosomal compartment. Microscopy Research and Technique *29*, 468-480.

Iida,N., Toida,T., Kushi,Y., Handa,S., Fredman,P., Svenerholm,L., and Ishizuka,I. (1989). A sulfated glucosylceramide from rat kidney. Journal of Biological Chemistry *264*, 5974-5980.

Inoue,N., Ikawa,M., Isotani,A., and Okabe,M. (2005). The immunoglobulin superfamily protein Izumo is required for sperm to fuse with eggs. Nature *434*, 234-238.

Isaac,G., Pernber,Z., Gieselmann,V., Hansson,E., Bergquist,J., and Mansson,J.E. (2006). Sulfatide with short fatty acid dominates in astrocytes and neurons. FEBS J. *273*, 1782-1790.

Ishizuka,I. (1997). Chemistry and functional distribution of sulfoglycolipids. Progress in Lipid Research *36*, 245-319.

Ishizuka,I., Suzuki,M., and Yamakawa,T. (1973). Isolation and characterization of a novel sulfoglycolipid, seminolipid, from boar testis and spermatozoa. Journal of Biochemistry *73*, 77-87.

Iwabuchi,K., Yamamura,S., Prinetti,A., Handa,K., and Hakomori,S. (1998). GM3-enriched microdomain involved in cell adhesion and signal transduction through carbohydrate-carbohydrate interaction in mouse melanoma B16 cells. Journal of Biological Chemistry *273*, 9130-9138.

Jaffe,A. and Bush,A. (2001). Cystic fibrosis: review of the decade. Monaldi Arch. Chest Dis. *56*, 240-247.

Jaffe,T. and Oates,R.D. (1994). Genetic abnormalities and reproductive failure. Urol. Clin. North Am. *21*, 389-408.

Jegou,B. (1993). The Sertoli-germ cell communication network in mammals. Int. Rev. Cytol. *147*, 25-96.

Jegou,B. and Pineau,C. (1995). Current aspects of autocrine and paracrine regulation of spermatogenesis. Adv. Exp. Med. Biol. *377*, 67-86.

Jha,K.N., Shumilin,I.A., Digilio,L.C., Chertihin,O., Zheng,H., Schmitz,G., Visconti,P.E., Flickinger,C.J., Minor,W., and Herr,J.C. (2008). Biochemical and structural

characterization of apolipoprotein A-I binding protein, a novel phosphoprotein with a potential role in sperm capacitation. Endocrinology *149*, 2108-2120.

Jimenez-Gonzalez,C., Michelangeli,F., Harper,C.V., Barratt,C.L., and Publicover,S.J. (2006). Calcium signalling in human spermatozoa: a specialized 'toolkit' of channels, transporters and stores. Hum. Reprod. Update. *12*, 253-267.

Johnson,K.J., Patel,S.R., and Boekelheide,K. (2000). Multiple cadherin superfamily members with unique expression profiles are produced in rat testis. Endocrinology *141*, 675-683.

Johnson,L., Amann,R.P., and Pickett,B.W. (1978). Scanning electrons and light microscopy of the equine seminiferous tubule. Fertil. Steril. *29*, 208-215.

Johnston,D.S., Wright,W.W., Shaper,J.H., Hokke,C.H., Van den Eijnden,D.H., and Joziasse,D.H. (1998). Murine sperm-zona binding, a fucosyl residue is required for a high affinity sperm-binding ligand. Journal of Biological Chemistry *273*, 1888-1895.

Jones,R. (1998). Plasma membrane structure and remodelling during sperm maturation in the epididymis. J. Reprod. Fertil. Suppl *53*, 73-84.

Jovine,L., Janssen,W.G., Litscher,E.S., and Wassarman,P.M. (2006). The PLAC1-homology region of the ZP domain is sufficient for protein polymerisation. BMC. Biochem. *7*, 11.

Jovine,L., Qi,H., Williams,Z., Litscher,E., and Wassarman,P.M. (2002). The ZP domain is a conserved module for polymerization of extracellular proteins. Nat. Cell Biol. *4*, 457-461.

Jungnickel,M.K., Marrero,H., Birnbaumer,L., Lemos,J.R., and Florman,H.M. (2001). Trp2 regulates entry of Ca2+ into mouse sperm triggered by egg ZP3. Nature Cell Biology *3(5)*, 499-502.

Jungnickel,M.K., Sutton,K.A., Wang,Y., and Florman,H.M. (2007). Phosphoinositide-dependent pathways in mouse sperm are regulated by egg ZP3 and drive the acrosome reaction. Dev. Biol. *304*, 116-126.

Kan,F.W. and Esperanzate,P.W. (2006). Surface mapping of binding of oviductin to the plasma membrane of golden hamster spermatozoa during in vitro capacitation and acrosome reaction. Mol. Reprod. Dev. *73*, 756-766.

Kan,F.W.K., Roux,E., St.Jacques,S., and Bleau,G. (1990). Demonstration by lectin-gold cytochemistry of transfer of glyoconjugates of oviductal origin to the zona pellucida of oocytes after ovulation in hamsters. Anatomical Record *226*, 37-47.

Kan,F.W.K., Zalzal,S., Roux,E., and Nanci,A. (1994). Homogeneity in the distribution of matrix components in the hamster zona pellucida as revealed by backscattered electron imaging fracture-label. Anatomical Record *239*, 35-46.

Kongmanas K. (2007). Significance of sulfogalactosylglycerolipid in male fertility: studies using *Cgt* heterozygous mice. Department of Biochemistry, University of Ottawa.

Kates,M. (1986). Technique of lipidology: isolation, analysis and identification of lipids. In Laboratory Techniques in Biochemistry and Molecular Biology, R.H.Burdon, ed. (New York: Elsevier), pp. 100-278.

Kawano,N., Yoshida,K., Iwamoto,T., and Yoshida,M. (2008). Ganglioside GM1 mediates decapacitation effects of SVS2 on murine spermatozoa. Biol. Reprod. *79*, 1153-1159.

Kawano,N. and Yoshida,M. (2007). Semen-coagulating protein, SVS2, in mouse seminal plasma controls sperm fertility. Biol. Reprod. *76*, 353-361.

Kawasaki,Y., Nakagawa,A., Nagaosa,K., Shiratsuchi,A., and Nakanishi,Y. (2002). Phosphatidylserine binding of class B scavenger receptor type I, a phagocytosis receptor of testicular sertoli cells. J. Biol. Chem. *277*, 27559-27566.

Keeney,D.S. and Ewing,L.L. (1990). Effects of hypophysectomy and alterations in spermatogenic function on Leydig cell volume, number, and proliferation in adult rats 3. J. Androl *11*, 367-378.

Kelly,B.M., Yu,C.Z., and Chang,P.L. (1989). Presence of a lysosomal enzyme, aryluslfatase-A, in the prelysosome-endosome compartments of human cultured fibroblasts. European Journal of Cell Biology *48*, 71-78.

Kerr,C.L., Hanna,W.F., Shaper,J.H., and Wright,W.W. (2002). Characterization of zona pellucida glycoprotein 3 (ZP3) and ZP2 binding sites on acrosome-intact mouse sperm. Biology of Reproduction *66(6)*, 1585-1595.

Kerr,C.L., Hanna,W.F., Shaper,J.H., and Wright,W.W. (2004). Lewis X-containing glycans are specific and potent competitive inhibitors of the binding of ZP3 to complementary sites on capacitated, acrosome-intact mouse sperm. Biol. Reprod. *71*, 770-777.

Kerr,J.B. and de Kretser,D.M. (1974). Proceedings: The role of the Sertoli cell in phagocytosis of the residual bodies of spermatids. J. Reprod. Fertil. *36*, 439-440.

Kierszenbaum,A.L. (1994). Mammalian spermatogenesis in vivo and in vitro: a partnership of spermatogenic and somatic cell lineages. Endocr. Rev. *15*, 116-134.

Kierszenbaum,A.L. (2002). Histology and cell biology: an introduction to pathology. (St. Louis: Mosby, Inc.).

Kim,K.S., Cha,M.C., and Gerton,G.L. (2001). Mouse sperm protein sp56 is a component of the acrosomal matrix. Biology of Reproduction *64*, 36-43.

Kim,K.S. and Gerton,G.L. (2003). Differential release of soluble and matrix components: evidence for intermediate states of secretion during spontaneous acrosomal exocytosis in mouse sperm. Dev. Biol. *264*, 141-152.

Kim,T., Oh,J., Woo,J.M., Choi,E., Im,S.H., Yoo,Y.J., Kim,D.H., Nishimura,H., and Cho,C. (2006). Expression and relationship of male reproductive ADAMs in mouse. Biol. Reprod. *74*, 744-750.

Kirkman-Brown,J.C., Punt,E.L., Barratt,C.L., and Publicover,S.J. (2002). Zona pellucida and progesterone-induced Ca2+ signaling and acrosome reaction in human spermatozoa. J. Androl *23*, 306-315.

Kishimoto,Y., Hiraiwa,M., and O'Brien,J.S. (1992). Saposins: structure, function, distribution, and molecular genetics. Journal of Lipid Research *33*, 1255-1267.

Klymkowsky,M.W., Bachant,J.B., and Domingo,A. (1989). Functions of intermediate filaments. Cell Motil. Cytoskeleton *14*, 309-331.

Knapp,A., Kornblatt,M.J., Schachter,H., and Murray,R.K. (1973). Studies on the biosynthesis of testicular sulfoglycerogalactolipid: Demonstration of a golgi-associated sulfotransferase activity. Biochemical and Biophysical Research Communications *55*, 179-186.

Kolodny,E.H. and Fluharty,A.L. (1995). Lysosomal disorders. In The Metabolic and Molecular Bases of Inherited Disease, C.R.Scriver, ed. (New York: McGraw-Hill), pp. 2693-2741.

Kolter,T. and Sandhoff,K. (2005). Principles of lysosomal membrane digestion: stimulation of sphingolipid degradation by sphingolipid activator proteins and anionic lysosomal lipids. Annu. Rev. Cell Dev. Biol. *21*, 81-103.

Kornblatt,M.J. (1979). Synthesis and turnover of sulfogalactoglycerolipid, a membrane lipid, during spermatogenesis. Can. J. Biochem. *57*, 255-258.

Kornblatt,M.J., Knapp,A., Levine,M., Schachter,H., and Murray,R.K. (1974). Studies on the structure and formation during spermatogenesis of the sulfoglycerogalactolipid of rat testis. Can. J. Biochem. *52*, 689-697.

Kornblatt,M.J., Schachter,H., and Murray,R.K. (1972). Partial characterization of a novel glycerogalactolipid from rat testis. Biochemical and Biophysical Research Communications *48*, 1489-1494.

Koshy,K.M., Wang,J., and Boggs,J.M. (1999). Divalent cation-mediated interaction between cerebroside sulfate and cerebrosides: an investigation of the effect of structural variations of lipids by electrospray ionization mass spectrometry. Biophysical Journal *77*, 306.

Kreysing,J., Polten,A., Hess,B., von Figura,K., Menz,K., Steiner,F., and Gieselmann,V. (1994a). Structure of the mouse arylsulfatase A gene and cDNA. Genomics *19*, 249-256.

Kreysing,J., Polten,A., Lukatela,G., Matzner,U., van Figura,K., and Gieselmann,V. (1994b). Translational control of arylsulfatase A expression in mouse testis. Journal of Biological Chemistry *269*, 23255-23261.

Kuhnert,B. and Nieschlag,E. (2004). Reproductive functions of the ageing male 1. Hum. Reprod. Update. *10*, 327-339.

Kulkarni,V.S. and Brown,R.E. (1998). Thermotropic behavior of galactosylceramides with {Icis}-monoenoic fatty acyl chains. Biochimica et Biophysica Acta *1372*, 347-358.

Kuroda,Y., Kaneko,S., Yoshimura,Y., Nozawa,S., and Mikoshiba,K. (1999). Are there inositol 1,4,5-triphosphate (IP3) receptors in human sperm? Life Sci. *65*, 135-143.

Laemmli,U.K. (1970). Cleavage of structural proteins during the assembly of the head of bacteriophage T4. Nature *227*, 680-685.

Lamontagne,N., Legare,C., Gaudreault,C., and Sullivan,R. (2001). Identification and characterization of P31m, a novel sperm protein in Cynomolgus monkey (Macaca fascicularis). Mol. Reprod. Dev. *59*, 431-441.

Langlais,J., Kan,F.W.K., Granger,L., Raymond,L., Bleau,G., and Roberts,K.D. (1988). Identification of sterol acceptors that stimulate cholesterol efflux from human spermatozoa during in vitro capacitation. Gamete Research *20*, 185-201.

Langner,M. and Hui,S.W. (1993). Merocyanine interaction with phosphatidylcholine bilayers. Biochim. Biophys. Acta *1149*, 175-179.

Law,H., Itkonnen,O., and Lingwood,C.A. (1988). Sulfogalactolipid binding protein SLIP 1: A conserved function for a conserved protein. Journal of Cellular Physiology *137*, 462-468.

Leclerc,P., De Lamirande,E., and Gagnon,C. (1996). Cyclic adenosine 3',5' monophosphate-dependent regulation of protein tyrosine phosphorylation in relation to human sperm capacitation and motility. Biology of Reproduction *55*, 684-692.

Lee,D.C., Miller,I.R., and Chapman,D. (1986). An infrared spectroscopic study of metastable and stable forms of hydrated cerebroside bilayers. Biochimica et Biophysica Acta *859*, 266-270.

Legare,C., Berube,B., Boue,F., Lefievre,L., Morales,C.R., El Alfy,M., and Sullivan,R. (1999). Hamster sperm antigen P26h is a phosphatidylinositol-anchored protein. Molecular Reproduction and Development *52*, 225-233.

Letts,P.J., Hunt,R.C., Shirley,M.A., Pinteric,L., and Schachter,H. (1978). Late spermatocytes from immature rat testis: Isolation, electron microscopy, letin

agglutinability and capacity for glycoprotein and sulfogalactoglycerolipid biosynthesis. Biochimica et Biophysica Acta *541*, 59-75.

Leyton,L. and Saling,P. (1989). Evidence that aggregation of mouse sperm receptors by ZP3 triggers the acrosome reaction. The Journal of Cell Biology *108*, 2163-2168.

Leznicki,A. and Bleszynski,W. (1970). Histochemical localization of the soluble arylsulphatase activities in rat brain. Histochemie *24*, 251-265.

Leznicki,A.J. and Rozanska,M. (1991). Localizaiton of arylsulphatase A and B activities in rat kidney. Acta Biochim Pol *38*, 151-156.

Li,P., Chan,H.C., He,B., So,S.C., Chung,Y.W., Shang,Q., Zhang,Y.D., and Zhang,Y.L. (2001). An antimicrobial peptide gene found in the male reproductive system of rats. Science *291*, 1783-1785.

Lin,M.H., Lee,R.K., Hwu,Y.M., Lu,C.H., Chu,S.L., Chen,Y.J., Chang,W.C., and Li,S.H. (2008). SPINKL, a Kazal-type serine protease inhibitor-like protein purified from mouse seminal vesicle fluid, is able to inhibit sperm capacitation. Reproduction. *136*, 559-571.

Lingwood,C., Sakac,K., and Saltiel,A. (1994). Developmentally regulated testicular galactolipid sulfotransferase inhibitor is a phosphoinositol glycerolipid and insulin-mimetic. Molecular Reproduction and Development *37*, 462-466.

Lingwood,C. and Taylor,T. (1985). Synthesis and use of galactolipid sulfotransferase substrate-analogue affinity probes:possible localization of the testicular enzyme. Biochemistry and Cell Biology *64*, 631-637.

Lingwood,C.A. (1981). Localization of sulfatoxygalactosylacylalkylglycerol at the surface of rat testicular germinal cells by immunocytochemical techniques: pH dependence of a nonimmunological reaction between immunoglobulin and germinal cells. The Journal of Cell Biology *89*, 621-630.

Lingwood,C.A. (1985a). Developmental regulation of galactoglycerolipid and galactosphingolipid sulphation during mammalian spermatogenesis: Evidence for a substrate-selective inhibitor of testicular sulphotransferase activity in the rat. Biochemical Journal *231*, 393-400.

Lingwood,C.A. (1985b). Protein-glycolipid interactions during spermatogenesis. Binding of specific germ cell proteins to sulfatoxygalactosylacylalkylglycerol, the major glycolipid of mammalian male germ cells. Can. J. Biochem. Cell Biol. *63*, 1077-1085.

Lingwood,C.A. (1986). Colocalization of sulfogalactosylacylalkylglycerol (SGG) and its binding protein during spermatogenesis and sperm maturation. Topology of SGG defines a new testicular germ cell membrane domain. Biochemistry and Cell Biology *64*, 984-992.

Lingwood,C.A., Murray,R.K., and Schachter,H. (1980). The preparation of rabbit antiserum specific for mammalian testicular sulfogalactoglycerolipid. Journal of Immunology *124*, 769-774.

Lingwood,C.A. and Nutikka,A. (1991). Studies on the spermatogenic sulfogalactolipid binding protein SLIP1. Journal of Cellular Physiology *146*, 258-263.

Litscher,E.S., Janssen,W.G., Darie,C.C., and Wassarman,P.M. (2008). Purified mouse egg zona pellucida glycoproteins polymerize into homomeric fibrils under non-denaturing conditions. J. Cell Physiol *214*, 153-157.

Litscher,E.S., Juntunen,K., Seppo,A., Penttila,L., Niemela,R., Renkonen,O., and Wassarman,P.M. (1995). Oligosaccharide constructs with defined structures that inhibit binding of mouse sperm to unfertilized eggs in vitro. Biochemistry *34*, 4662-4669.

London,E. and Brown,D.A. (2000). Insolubility of lipids in Triton X-100: physical origin and relationship to sphingolipid/cholesterol membrane domains (rafts). Biochimica et Biophysica Acta *1508*, 182-195.

Lopez,L.C., Bayna,E.M., Litoff,D., Shaper,N.L., Shaper,J.H., and Shur,B.D. (1985). Receptor function of mouse sperm surface galactosyltransferase during fertilization. The Journal of Cell Biology *101*, 1501-1510.

Louis,A.I. and Fluharty,A.L. (1991). Activator-dependant hydrolysis of myelin cerebroside sulfate by arylsulfatase A. Developmental Neurosciences *13*, 41-46.

Lu,Q. and Shur,B.D. (1997). Sperm from á1,4-galactosyltransferase-null mice are refractory to ZP3-induced acrosome reactions and penetrate the zona pellucida poorly. Development *124*, 4121-4131.

Lukatela,G., Krauss,N., Theis,K., Selmer,T., Gieselmann,V., von Figura,K., and Saenger,W. (1998). Crystal structure of human arylsulfatase A: The aldehyde function and the metal ion at the active site suggest a novel mechanism for sulfate ester hydrolysis. Biochemistry *37*, 3654-3664.

Macek,M.B., Lopez,L.C., and Shur,B.D. (1991). Aggregation of á-1,4-galactosyltranferase on mouse sperm induces the acrosome reaction. Developmental Biology *147*, 440-444.

Macek,M.B. and Shur,B. (1988). Protein-carbohydrate complementarity in mammalian gamete recognition. Gamete Research *20*, 93-109.

Madara,J.L. (2000). Modulation of tight junctional permeability. Adv. Drug Deliv. Rev. *41*, 251-253.

Maeda,Y., Shiratsuchi,A., Namiki,M., and Nakanishi,Y. (2002). Inhibition of sperm production in mice by annexin V microinjected into seminiferous tubules: possible

etiology of phagocytic clearance of apoptotic spermatogenic cells and male infertility. Cell Death. Differ. *9*, 742-749.

Maehashi,E., Sato,C., Ohta,K., Harada,Y., Matsuda,T., Hirohashi,N., Lennarz,W.J., and Kitajima,K. (2003). Identification of the Sea Urchin 350-kDa Sperm-binding Protein as a New Sialic Acid-binding Lectin That Belongs to the Heat Shock Protein 110 Family: IMPLICATION OF ITS BINDING TO GANGLIOSIDES IN SPERM LIPID RAFTS IN FERTILIZATION. J. Biol. Chem. *278*, 42050-42057.

Mamelak,D. and Lingwood,C. (2001). The ATPase domain of hsp70 possesses a unique binding specificity for 3'-sulfogalactolipids. Journal of Biological Chemistry *276*, 449-456.

Marcus,J., Honigbaum,S., Shroff,S., Honke,K., Rosenbluth,J., and Dupree,J.L. (2006). Sulfatide is essential for the maintenance of CNS myelin and axon structure. Glia *53*, 372-381.

Marinier,A., Martel,A., Banville,J., Bachand,C., Remillard,R., Lapointe,P., Turmel,B., Menard,M., Harte,W.E.J., Wright,J.J., Todderud,G., Tramposch,K.M., Bajorath,J., Hollenbaugh,D., and Aruffo,A. (1997). Sulfated galactocerebrosides as potential antiinflammatory agents. Journal of Medical Chemistry *1997*, 3234-3247.

Matzner,U., Breiden,B., Schwarzmann,G., Yaghootfam,A., Fluharty,A.L., Hasilik,A., Sandhoff,K., and Gieselmann,V. (2009). Saposin B-dependent reconstitution of arylsulfatase A activity in vitro and in cell culture models of metachromatic leukodystrophy. J. Biol. Chem. *284*, 9372-9381.

Mayer,L.D., Hope,M.J., Cullis,P.R., and Janoff,A.S. (1985). Solute distributions and trapping efficienceies observed in freeze-thawed multilamellar vesicles. Biochimica et Biophysica Acta *817*, 193-196.

McLachlan,R.I. (2000). The endocrine control of spermatogenesis. Baillieres Best. Pract. Res. Clin. Endocrinol. Metab *14*, 345-362.

McLeskey,S.B., Dowds,C., Carballada,R., White,R.R., and Saling,P.M. (1998). Molecules involved in mammalian sperm-egg interaction. Int Rev Cytol *177*, 57-113.

Mehl,E. and Jatzkewitz,H. (1968). Cerebroside {-3-}sulfate as a physiological substrate of arylsulfatase A. Biochimica et Biophysica Acta *151*, 619-627.

Meistrich,M.L., Mohapatra,B., Shirley,C.R., and Zhao,M. (2003). Roles of transition nuclear proteins in spermiogenesis. Chromosoma *111*, 483-488.

Meizel,S. (1997). Amino acid neurotransmitter receptor/chloride channels of mammalian sperm and the acrosome reaction. Biology of Reproduction *56*, 569-574.

Merrill,A.H., Jr., Schmelz,E.M., Dillehay,D.L., Spiegel,S., Shayman,J.A., Schroeder,J.J., Riley,R.T., Voss,K.A., and Wang,E. (1997). Sphingolipids--the enigmatic lipid class: biochemistry, physiology, and pathophysiology. Toxicol. Appl. Pharmacol. *142*, 208-225.

Metayer,S., Dacheux,F., Dacheux,J.L., and Gatti,J.L. (2002a). Comparison, characterization, and identification of proteases and protease inhibitors in epididymal fluids of domestic mammals. Matrix metalloproteinases are major fluid gelatinases. Biol. Reprod. *66*, 1219-1229.

Metayer,S., Dacheux,F., Dacheux,J.L., and Gatti,J.L. (2002b). Comparison, characterization, and identification of proteases and protease inhibitors in epididymal fluids of domestic mammals. Matrix metalloproteinases are major fluid gelatinases. Biol. Reprod. *66*, 1219-1229.

Miller,D.J., Macek,M.B., and Shur,B.D. (1992). Complementarity between sperm surface á-1,4-galactosyltransferase and egg-coat ZP3 mediates sperm-egg binding. Nature *357*, 589-593.

Molander-Melin,M., Pernber,Z., Franken,S., Gieselmann,V., Mansson,J.E., and Fredman,P. (2004). Accumulation of sulfatide in neuronal and glial cells of arylsulfatase A deficient mice. J. Neurocytol. *33*, 417-427.

Moller,C.C., Bleil,J.D., Kinloch,R., and Wassarman,P.M. (1990). Structural and functional relationships between mouse and hamster zona pellucida glycoproteins. Developmental Biology *137*, 276-286.

Monne,M., Han,L., Schwend,T., Burendahl,S., and Jovine,L. (2008). Crystal structure of the ZP-N domain of ZP3 reveals the core fold of animal egg coats. Nature *456*, 653-657.

Montfort,L., Frenette,G., and Sullivan,R. (2002). Sperm-zona pellucida interaction involves a carbonyl reductase activity in the hamster. Mol. Reprod. Dev. *61*, 113-119.

Moore,A., Ensrud,K.M., White,T.W., Frethem,C.D., and Hamilton,D.W. (1994). Rat epididymis-specific sperm maturation antigens. I. Evidence that the 26 kD 4E9 antigen found on rat caudal epididymal sperm tail is derived from a protein secreted by the epididymis. Molecular Reproduction and Development *37*, 181-194.

Morales,C., Clermont,Y., and Nadler,N.J. (1986). Cyclic endocytic activity and kinetics of lysosomes in Sertoli cells of the rat: a morphometric analysis. Biology of Reproduction *34*, 207-218.

Morales,C.R., Hay,N., El Alfy,M., and Zhao,Q. (1998). Distribution of mouse sulfated glycoprotein-1 (prosaposin) in the testis and other tissues. J. Androl *19*, 156-164.

Mori,E., Baba,T., Iwanatsu,A., and Mori,T. (1993). Purification and characterization of a 38-kDa protein, sp38, with zona pellucida-binding property from porcine epididymal sperm. Biochemical and Biophysical Research Communications *196*, 196-202.

Mori,E., Hedrick,J.L., Wardrip,N.J., Mori,T., and Takasaki,S. (1998). Occurrence of reducing terminal {IN}-acetylglucosamine 3-sulfate and fucosylated outer chains in acidic N-glycans of porcine zona pellucida glycoproteins. Glycoconjugate Journal *15*, 447-456.

Moss,S.B., Challoner,P.B., and Groudine,M. (1989). Expression of a novel histone 2B during mouse spermiogenesis. Dev. Biol. *133*, 83-92.

Moss,S.B. and George,G.L. (2001). A-kinase anchor proteins in endocrine systems and reproduction. Trends in Endocrinology Metabolism *12*, 434-440.

Moviglia,G.A., Cavicchia,J.C., and Bertini,F. (1982). Lysosomal enzymes in cells separated from rat testis. Journal of Reproduction and Fertility *66*, 123-127.

Mruk,D.D. and Cheng,C.Y. (2004). Sertoli-Sertoli and Sertoli-germ cell interactions and their significance in germ cell movement in the seminiferous epithelium during spermatogenesis. Endocr. Rev. *25*, 747-806.

Munoz-Garay,C., De la Vega-Beltran JL, Delgado,R., Labarca,P., Felix,R., and Darszon,A. (2001a). Inwardly rectifying K(+) channels in spermatogenic cells: functional expression and implication in sperm capacitation. Dev. Biol. *234*, 261-274.

Munoz-Garay,C., De la Vega-Beltran JL, Delgado,R., Labarca,P., Felix,R., and Darszon,A. (2001b). Inwardly rectifying K(+) channels in spermatogenic cells: functional expression and implication in sperm capacitation. Dev. Biol. *234*, 261-274.

Murase,T. and Roldan,E.R. (1996). Progesterone and the zona pellucida activate different transducing pathways in the sequence of events leading to diacylglycerol generation during mouse sperm acrosomal exocytosis. Biochem. J. *320 (Pt 3)*, 1017-1023.

Murray,R.K. and Narasimhan,R. (1990). Glycoglycerolipids of animal tissues. In Glycolipids, Phosphoglycolipids, and Sulfoglycolipids, M.Kates, ed. (New York: Plenum Press), pp. 321-361.

Naaby-Hansen,S., Wolkowicz,M.J., Klotz,K., Bush,L.A., Westbrook,V.A., Shibahara,H., Shetty,J., Coonrod,S.A., Reddi,P.P., Shannon,J., Kinter,M., Sherman,N.E., Fox,J., Flickinger,C.J., and Herr,J.C. (2001). Co-localization of the inositol 1,4,5-trisphosphate receptor and calreticulin in the equatorial segment and in membrane bounded vesicles in the cytoplasmic droplet of human spermatozoa. Mol. Hum. Reprod. *7*, 923-933.

Nakagawa,A., Nagaosa,K., Hirose,T., Tsuda,K., Hasegawa,K., Shiratsuchi,A., and Nakanishi,Y. (2004). Expression and function of class B scavenger receptor type I on both apical and basolateral sides of the plasma membrane of polarized testicular Sertoli cells of the rat. Dev. Growth Differ. *46*, 283-298.

Nakagawa,A., Shiratsuchi,A., Tsuda,K., and Nakanishi,Y. (2005). In vivo analysis of phagocytosis of apoptotic cells by testicular Sertoli cells. Mol. Reprod. Dev. *71*, 166-177.

Nakanishi,Y. and Shiratsuchi,A. (2004). Phagocytic removal of apoptotic spermatogenic cells by Sertoli cells: mechanisms and consequences. Biol. Pharm. Bull. *27*, 13-16.

Neild,D.N., Gadella,B.M., Aguero,A., Stout,T.A., and Colenbrander,B. (2005). Capacitation, acrosome function and chromatin structure in stallion sperm. Anim Reprod. Sci. *89*, 47-56.

Newton,S.C., Blaschuk,O.W., and Millette,C.F. (1993). N-cadherin mediates Sertoli cell-spermatogenic cell adhesion. Dev. Dyn. *197*, 1-13.

Ng,K.K., Donat,R., Chan,L., Lalak,A., Di,P., I, and Handelsman,D.J. (2004). Sperm output of older men. Hum. Reprod. *19*, 1811-1815.

Nguyen,H.T., Amine,A.B., Lafitte,D., Waheed,A.A., Nicoletti,C., Villard,C., Letisse,M., Deyris,V., Roziere,M., Tchiakpe,L., Danielle,C.D., Comeau,L., and Hiol,A. (2006). Proteomic characterization of lipid rafts markers from the rat intestinal brush border 1. Biochem. Biophys. Res. Commun. *342*, 236-244.

Nikolopoulou,M., Soucek,D., and Vary,J. (1985). Changes in the lipid content of boar sperm plasma membranes during epididymal maturation. Biochimica et Biophysica Acta *815*, 486-498.

Nixon,B., Aitken,R.J., and McLaughlin,E.A. (2007). New insights into the molecular mechanisms of sperm-egg interaction. Cell Mol. Life Sci. *64*, 1805-1823.

Nixon,B., Bielanowicz,A., McLaughlin,E.A., Tanphaichitr,N., Ensslin,M.A., and Aitken,R.J. (2009). Composition and significance of detergent resistant membranes in mouse spermatozoa. J. Cell Physiol *218*, 122-134.

Nixon,B., MacIntyre,D.A., Mitchell,L.A., Gibbs,G.M., O'Bryan,M., and Aitken,R.J. (2006). The identification of mouse sperm-surface-associated proteins and characterization of their ability to act as decapacitation factors. Biol. Reprod. *74*, 275-287.

Noguchi,S., Hatanaka,Y., Tobita,T., and Nakano,M. (1992). Structural analysis of the N-linked carbohydrate chains of the 55-kDa glycoprotein family (PZP3) from porcine zona pellucida. European Journal of Biochemistry *204*, 1089-1100.

Noguchi,S. and Nakano,M. (1992). Structure of the acidic N-linked carbohydrate chains of the 55-kDa glycoprotein family (PZP3) from porcine zona pellucida. Journal of Biochemistry *209*, 883-894.

Norris,A.J., Whitelegge,J.P., Yaghoubian,A., Alattia,J.R., Prive,G.G., Toyokuni,T., Sun,H., Brooks,M.N., Panza,L., Matto,P., Compostella,F., Remmel,N., Klingenstein,R., Sandhoff,K., Fluharty,C., Fluharty,A., and Faull,K.F. (2005). A novel mass spectrometric assay for the cerebroside sulfate activator protein (saposin B) and arylsulfatase A. J. Lipid Res.

Norton,W.T. and Cammer,W. (1984). Isolation and characterization of myelin. In Myelin, P.Morell, ed. (New York: Plenum Press), pp. 147-195.

O'Brien,J.S. and Kishimoto,Y. (1991). Saposin proteins: structure, function, and role in human lysosomal storage disorders. FASEB Journal *5*, 301-308.

O'Toole,C.M., Arnoult,C., Darszon,A., Steinhardt,R.A., and Florman,H.M. (2000). Ca(2+) entry through store-operated channels in mouse sperm is initiated by egg ZP3 and drives the acrosome reaction. Mol. Biol. Cell *11*, 1571-1584.

O'Toole,C.M., Roldan,E.R., and Fraser,L.R. (1996). Protein kinase C activation during progesterone-stimulated acrosomal exocytosis in human spermatozoa. Mol. Hum. Reprod. *2*, 921-927.

Oehninger,S. (2001). Molecular basis of human sperm-zona pellucida interaction. Cells Tissues Organs *168*, 58-64.

Ohashi,T., Watabe,K., Sato,Y., Saito,I., Barranger,J.A., and Eto,Y. (1995). Successful transduction of oligodendrocytes and restoration of arylsulfatase A deficiency in metachromatic leukodystrophy fibroblasts using an adenovirus vector. Gene Ther. *2*, 443-449.

Ohta,K., Sato,C., Matsuda,T., Toriyama,M., Vacquier,V.D., Hirohashi,N., Lennarz,W.J., and Kitajima,K. (2000a). Lipid raft on gametic cells as a functional domain for sperm-egg interaction coupled with signal transduction. Zygote. *8 Suppl 1*, S63.

Ohta,K., Sato,C., Matsuda,T., Toriyama,M., Vacquier,V.D., Lennarz,W.J., and Kitajima,K. (2000b). Co-localization of receptor and transducer proteins in the glycosphingolipid-enriched, low density, detergent-insoluble membrane fraction of sea urchin sperm. Glycoconjugate Journal *17*, 205-214.

Okabe,M., Adachi,T., Takada,K., Oda,H., Yagasaki,M., Kohama,Y., and Mimura,T. (1987). Capacitation-ralated changes in antigen distribution on mouse sperm heads and its relation to fertilization rate in vitro. Journal of Reproductive Immunology *11*, 91-100.

Okabe,M. and Cummins,J.M. (2007). Mechanisms of sperm-egg interactions emerging from gene-manipulated animals. Cell Mol. Life Sci. *64*, 1945-1958.

Okamura,N., Tajima,Y., Soejima,A., Masuda,H., and Sugita,Y. (1985). Sodium bicarbonate in seminal plasma stimulated the motility of mammalian spermatozoa through direct activation of adenylate cyclase. Biological Chemistry Hoppe Seyler *260*, 9699-9705.

Orgebin-Crist,M.C., Hoffman,L.H., Olson,G.E., and Skudlarek,M.D. (1987). Secretion of proteins and glycoproteins by perifused rabbit corpus epididymal tubules: effect of castration. Am. J. Anat. *180*, 49-68.

Osheroff,J.E., Visconti,P.E., Valenzuela,J.P., Travis,A.J., Alvarez,J., and Kopf,G.S. (1999). Regulation of human sperm capacitation by a cholesterol efflux-stimulated signal transduction pathway leading to protein kinase A-mediated up-regulation of protein tyrosine phosphorylation. Mol. Hum. Reprod. *5*, 1017-1026.

Parkening,T.A. (1989). Fertilizing ability of spermatozoa from aged C57BL/6NNia mice 1. J. Reprod. Fertil. *87*, 727-733.

Parkening,T.A., Collins,T.J., and Au,W.W. (1988). Paternal age and its effects on reproduction in C57BL/6NNia mice. J. Gerontol. *43*, B79-B84.

Parks,J.E. and Lynch,D.V. (1992). Lipid composition and thermotropic phase behavior of boar, bull, stallion, and rooster sperm membranes. Cryobiology *29*, 255-266.

Parrish,J.J., Susko-Parrish,J.L., Ugus,C., and First,N.L. (1994). Differences in the role of cyclic adenosine 3',5'-monophosphate during capacitation of bovine sperm by heparin or oviduct fluid. Biology of Reproduction *51*, 1099-1108.

Pascher,I. and Sundell,S. (1977). Molecular arrangements in sphingolipids. The crystal structure of cerebroside. Chemistry and Physics of Lipids *20*, 175-191.

Patrat,C., Serres,C., and Jouannet,P. (2000). The acrosome reaction in human spermatozoa. Biol. Cell *92*, 255-266.

Pereira,B.M., Abou-Haila,A., and Tulsiani,D.R. (1998). Rat sperm surface mannosidase is first expresed on the plasma membrane of testicular germ cells. Biology of Reproduction *59*, 1288-1295.

Pernber,Z., Molander-Melin,M., Berthold,C.H., Hansson,E., and Fredman,P. (2002). Expression of the myelin and oligodendrocyte progenitor marker sulfatide in neurons and astrocytes of adult rat brain. J. Neurosci. Res. *69*, 86-93.

Pernber,Z., Richter,K., Mansson,J.E., and Nygren,H. (2007). Sulfatide with different fatty acids has unique distributions in cerebellum as imaged by time-of-flight secondary ion mass spectrometry (TOF-SIMS). Biochim. Biophys. Acta *1771*, 202-209.

Peterson,R., Russell,L., Bundman,D., Conway,M., and Freund,M. (1981). The interaction of living boar sperm and sperm plasma membrane vesicles with the porcine zona pellucida. Developmental Biology *84*, 144-156.

Pirke,K.M., Sintermann,R., and Vogt,H.J. (1980). Testosterone and testosterone precursors in the spermatic vein and in the testicular tissue of old men. Reduced oxygen supply may explain the relative increase of testicular progesterone and 17 alpha-hydroxyprogesterone content and production in old age. Gerontology *26*, 221-230.

Plant,T.M. (1981). Time courses of concentrations of circulating gonadotropin, prolactin, testosterone, and cortisol in adult male rhesus monkeys (Macaca mulatta) throughout the 24 h light-dark cycle. Biol. Reprod. *25*, 244-252.

Platt,M.D., Salicioni,A.M., Hunt,D.F., and Visconti,P.E. (2009). Use of Differential Isotopic Labeling and Mass Spectrometry To Analyze Capacitation-Associated Changes in the Phosphorylation Status of Mouse Sperm Proteins. J. Proteome. Res.

Ponce,R.H., Urch,U.A., and Yanagimachi,R. (1994). Inhibition of sperm-egg fusion in the hamster and mouse by carbohydrates. Zygote *2*, 253-262.

Popovic,Z.V., Sandhoff,R., Sijmonsma,T.P., Kaden,S., Jennemann,R., Kiss,E., Tone,E., Autschbach,F., Platt,N., Malle,E., and Grone,H.J. (2007). Sulfated glycosphingolipid as mediator of phagocytosis: SM4s enhances apoptotic cell clearance and modulates macrophage activity. J. Immunol. *179*, 6770-6782.

Prasad,S.V., Skinner,S.M., Carino,C., Wang,N., Cartwright,J., and Dunbar,B.S. (2000). Structure and function of the proteins of the mammalian zona pellucida. Cells Tissues Organs *166*, 148-164.

Primakoff,P. and Myles,D.G. (2002). Penetration, adhesion, and fusion in mammalian sperm-egg interaction. Science *296*, 2183-2185.

Quaas,A. and Dokras,A. (2008). Diagnosis and treatment of unexplained infertility. Rev. Obstet. Gynecol. *1*, 69-76.

Rahi,H. and Srivastava,P.N. (1983). Isolation and characterization of the pig endometrial arylsulphatase A. Biochemical Journal *211*, 649-659.

Rajendran,L. and Simons,K. (2005). Lipid rafts and membrane dynamics. J. Cell Sci. *118*, 1099-1102.

Ramakrishnan,H., Hedayati,K.K., Lullmann-Rauch,R., Wessig,C., Fewou,S.N., Maier,H., Goebel,H.H., Gieselmann,V., and Eckhardt,M. (2007). Increasing sulfatide synthesis in myelin-forming cells of arylsulfatase A-deficient mice causes demyelination and neurological symptoms reminiscent of human metachromatic leukodystrophy. J. Neurosci. *27*, 9482-9490.

Ramaswamy,S., Marshall,G.R., McNeilly,A.S., and Plant,T.M. (2000). Dynamics of the follicle-stimulating hormone (FSH)-inhibin B feedback loop and its role in regulating spermatogenesis in the adult male rhesus monkey (Macaca mulatta) as revealed by unilateral orchidectomy. Endocrinology *141*, 18-27.

Ramaswamy,S., Pohl,C.R., McNeilly,A.S., Winters,S.J., and Plant,T.M. (1998). The time course of follicle-stimulating hormone suppression by recombinant human inhibin A in the adult male rhesus monkey (Macaca mulatta). Endocrinology *139*, 3409-3415.

Rankin,T.L., Coleman,J.S., Epifano,O., Hoodbhoy,T., Turner,S.G., Castle,P.E., Lee,E., Gore-Langton,R., and Dean,J. (2003). Fertility and taxon-specific sperm binding persist after replacement of mouse sperm receptors with human homologs. Dev. Cell *5*, 33-43.

Rathi,R., Colenbrander,B., Bevers,M.M., and Gadella,B.M. (2001). Evaluation of in vitro capacitation of stallion spermatozoa. Biol. Reprod. *65*, 462-470.

Rathi,R., Colenbrander,B., Stout,T.A., Bevers,M.M., and Gadella,B.M. (2003). Progesterone induces acrosome reaction in stallion spermatozoa via a protein tyrosine kinase dependent pathway. Mol. Reprod. Dev. *64*, 120-128.

Ravid,T., Tsaba,A., Gee,P., Rasooly,R., Medina,E.A., and Goldkorn,T. (2003). Ceramide accumulation precedes caspase-3 activation during apoptosis of A549 human lung adenocarcinoma cells. Am. J. Physiol Lung Cell Mol. Physiol *284*, L1082-L1092.

Reijo,R., Lee,T.Y., Salo,P., Alagappan,R., Brown,L.G., Rosenberg,M., Rozen,S., Jaffe,T., Straus,D., Hovatta,O., de la Chapelle,A., Silber,S., and Page,D.C. (1995). Diverse spermatogenic defects in humans caused by Y chromosome deletions encompassing a novel RNA-binding protein gene. Nature Genetics *10*, 383-393.

Reiter,S., Fischer,G., and Jatzkewitz,H. (1976). Degradation of seminolipid by a lipase in secondary lysosomes. FEBS Letters *68*, 250-255.

Reyes-Moreno,C., Laflamme,J., Frenette,G., Sirard,M.A., and Sullivan,R. (2008). Spermatozoa modulate epididymal cell proliferation and protein secretion in vitro. Mol. Reprod. Dev. *75*, 512-520.

Ritter,M., Buechler,C., Boettcher,A., Barlage,S., Schmitz-Madry,A., Orso,E., Bared,S.M., Schmiedeknecht,G., Baehr,C.H., Fricker,G., and Schmitz,G. (2002). Cloning and characterization of a novel apolipoprotein A-I binding protein, AI-BP, secreted by cells of the kidney proximal tubules in response to HDL or ApoA-I. Genomics *79*, 693-702.

Robaire,B. and Viger,R.S. (1995). Regulation of epididymal epithelial cell functions. Biol. Reprod. *52*, 226-236.

Robaire,R. and Hermo,L. (1988). Efferent ducts, epididymis, and vas deferens: structure, functions and their regulation. In The Physiology of Reproduction, E.Knobil, ed. (New York: Raven Press, Ltd.).

Roberts,K.P., Ensrud-Bowlin,K.M., Piehl,L.B., Parent,K.R., Bernhardt,M.L., and Hamilton,D.W. (2008). Association of the protein D and protein E forms of rat CRISP1 with epididymal sperm. Biol. Reprod. *79*, 1046-1053.

Roberts,K.P., Johnston,D.S., Nolan,M.A., Wooters,J.L., Waxmonsky,N.C., Piehl,L.B., Ensrud-Bowlin,K.M., and Hamilton,D.W. (2007). Structure and function of epididymal protein cysteine-rich secretory protein-1. Asian J. Androl *9*, 508-514.

Rodeheffer,C. and Shur,B.D. (2004). Characterization of a novel ZP3-independent sperm-binding ligand that facilitates sperm adhesion to the egg coat. Development *131*, 503-512.

Rodemer,C., Thai,T.P., Brugger,B., Kaercher,T., Werner,H., Nave,K.A., Wieland,F., Gorgas,K., and Just,W.W. (2003). Inactivation of ether lipid biosynthesis causes male infertility, defects in eye development and optic nerve hypoplasia in mice. Hum. Mol. Genet. *12*, 1881-1895.

Rodriguez,I., Ody,C., Araki,K., Garcia,I., and Vassalli,P. (1997). An early and massive wave of germinal cell apoptosis is required for the development of functional spermatogenesis. EMBO J. *16*, 2262-2270.

Roldan,E.R.S., Murase,T., and Shi,Q. (1994). Exocytosis in spermatozoa in response to progesterone and zona pellucida. Science *266*, 1578-1581.

Romrell,L.J., Bellve,A.R., and Fawcett,D.W. (1976). Separation of mouse spermatogenic cells by sedimentation velocity. Developmental Biology *49*, 49-119.

Rossato,M., Di Virgilio,F., Rizzuto,R., Galeazzi,C., and Foresta,C. (2001). Intracellular calcium store depletion and acrosome reaction in human spermatozoa: role of calcium and plasma membrane potential. Mol. Hum. Reprod. *7*, 119-128.

Rudolph,C., Sigruener,A., Hartmann,A., Orso,E., Bals-Pratsch,M., Gronwald,W., Seifert,B., Kalbitzer,H.R., Verdorfer,I., Luetjens,C.M., Ortmann,O., Bornstein,S.R., and Schmitz,G. (2007). ApoA-I-binding protein (AI-BP) and its homologues hYjeF_N2 and hYjeF_N3 comprise the YjeF_N domain protein family in humans with a role in spermiogenesis and oogenesis. Horm. Metab Res. *39*, 322-335.

Russell,L.D. and Clermont,Y. (1977). Degeneration of germ cells in normal, hypophysectomized and hormone treated hypophysectomized rats. Anat. Rec. *187*, 347-366.

Russell,L.D. and Peterson,R.N. (1985). Sertoli cell junctions: morphological and functional correlates. Int. Rev. Cytol. *94*, 177-211.

Saether,T., Tran,T.N., Rootwelt,H., Christophersen,B.O., and Haugen,T.B. (2003). Expression and regulation of delta5-desaturase, delta6-desaturase, stearoyl-coenzyme A (CoA) desaturase 1, and stearoyl-CoA desaturase 2 in rat testis. Biol. Reprod. *69*, 117-124.

Sakac,D., Zachos,M., and Lingwood,C.A. (1992). Purification of the testicular galactolipid: 3'-phosphoadenoisine 5'-phosphosulfate sulfotransferase. Journal of Biological Chemistry *267*, 1655-1659.

Salicioni,A.M., Platt,M.D., Wertheimer,E.V., Arcelay,E., Allaire,A., Sosnik,J., and Visconti,P.E. (2007). Signalling pathways involved in sperm capacitation. Soc. Reprod. Fertil. Suppl *65*, 245-259.

Sanz,L., Calvete,J., Schafer,W., Mann,K., and Topfer-Petersen,E. (1992). Isolation and biochemical characterization of two isoforms of a boar sperm zona pellucida-binding protein. Biochimica et Biophysica Acta *1119*, 127-132.

Sarafian,T.A., Fluharty,A.L., Kihara,H., Helfand,G., and Edmond,J. (1982). Large-scale purification of pyrogen-free human arylsulfatase A. Journal of Applied Biochemistry *4*, 126-132.

Sato,K., Tokmakov,A.A., He,C.L., Kurokawa,M., Iwasaki,T., Shirouzu,M., Fissore,R.A., Yokoyama,S., and Fukami,Y. (2003). Reconstitution of Src-dependent phospholipase Cgamma phosphorylation and transient calcium release by using membrane rafts and cell-free extracts from Xenopus eggs. J. Biol. Chem. *278*, 38413-38420.

Sawada,H., Sakai,N., Abe,Y., Tanaka,E., Takahashi,Y., Fujino,J., Kodama,E., Takizawa,S., and Yokosawa,H. (2002). Extracellular ubiquitination and proteasome-mediated degradation of the ascidian sperm receptor. Proc. Natl. Acad. Sci. U. S. A *99*, 1223-1228.

Schenk,M., Koppisetty,C.A., Santos,D.C., Carmona,E., Bhatia,S., Nyholm,P.G., and Tanphaichitr,N. (2009). Interaction of arylsulfatase-A (ASA) with its natural sulfoglycolipid substrates: a computational and site-directed mutagenesis study. Glycoconj. J.

Schmidt,B., Selmer,T., Ingendoh,A., and von Figura,K. (1995). A novel amino acid modification in sulfatases that is defective in multiple sulfatase deficiency. Cell *82*, 271-278.

Schott,I., Hartmann,D., Gieselmann,V., and Lullmann-Rauch,R. (2001). Sulfatide storage in visceral organs of arylsulfatase A-deficient mice. Virchows Archive *439*, 90-96.

Schuck,S., Honsho,M., Ekroos,K., Shevchenko,A., and Simons,K. (2003). Resistance of cell membranes to different detergents. Proc. Natl. Acad. Sci. U. S. A *100*, 5795-5800.

Scully,N.F., Shaper,J.H., and Shur,B.D. (1987). Spatial and temporal expression of cell surface galactosyltransferase during mouse spermatogenesis and epididymal maturation. Developmental Biology *124*, 111-124.

Sharpe,R.M. (1994). Regulation of spermatogenesis. In The Physiology of Reproduction, E.Knobil, ed. (New York: Raven Press Ltd.), pp. 1363-1434.

Sharpe,R.M., Kerr,J.B., McKinnell,C., and Millar,M. (1994). Temporal relationship between androgen-dependent changes in the volume of seminiferous tubule fluid, lumen size and seminiferous tubule protein secretion in rats. J. Reprod. Fertil. *101*, 193-198.

Shi,Q.X. and Roldan,E.R. (1995). Evidence that a GABAA-like receptor is involved in progesterone-induced acrosomal exocytosis in mouse spermatozoa. Biol. Reprod. *52*, 373-381.

Shiratsuchi,A., Umeda,M., Ohba,Y., and Nakanishi,Y. (1997). Recognition of phosphatidylserine on the surface of apoptotic spermatogenic cells and subsequent phagocytosis by Sertoli cells of the rat. J. Biol. Chem. *272*, 2354-2358.

Shires,A., Carpenter,M.P., and Chalkley,R. (1975). New histones found in mature mammalian testes. Proc. Natl. Acad. Sci. U. S. A *72*, 2714-2718.

Shogomori,H. and Brown,D.A. (2003). Use of detergents to study membrane rafts: the good, the bad, and the ugly. Biol. Chem. *384*, 1259-1263.

Shur,B.D., Evans,S., and Lu,Q. (1998). Cell surface galactosyltransferase: current issues. Glycoconjugate Journal *15*, 537-548.

Shur,B.D. and Hall,N.G. (1982). A role for mouse sperm surface galactosyltransferase in sperm binding to the egg zona pellucida. The Journal of Cell Biology *95*, 574-579.

Shur,B.D., Rodeheffer,C., Ensslin,M.A., Lyng,R., and Raymond,A. (2006). Identification of novel gamete receptors that mediate sperm adhesion to the egg coat. Mol. Cell Endocrinol.

Simons,K. and Ehehalt,R. (2002). Cholesterol, lipid rafts, and disease. J. Clin. Invest *110*, 597-603.

Simons,K. and Ikonen,E. (1997). Functional rafts in cell membranes. Nature *387*, 569-572.

Simons,K. and Vaz,W.L. (2004). Model systems, lipid rafts, and cell membranes. Annu. Rev. Biophys. Biomol. Struct. *33*, 269-295.

Singh,J., O'Neill,C., and Handelsman,D.J. (1995). Induction of spermatogenesis by androgens in gonadotropin-deficient (hpg) mice. Endocrinology *136*, 5311-5321.

Sinha Hikim,A.P. and Swerdloff,R.S. (1999). Hormonal and genetic control of germ cell apoptosis in the testis. Rev. Reprod. *4*, 38-47.

Skudlarek,M.D., Abou-Haila,A., and Tulsiani,D.R. (2000). Rat spermatogenic cell beta-d-galactosidase: characterization, biosynthesis, and immunolocalization. Experimental Cell Research *261*, 139-149.

Sleight,S.B., Miranda,P.V., Plaskett,N.W., Maier,B., Lysiak,J., Scrable,H., Herr,J.C., and Visconti,P.E. (2005). Isolation and proteomic analysis of mouse sperm detergent-resistant membrane fractions: evidence for dissociation of lipid rafts during capacitation 1. Biol. Reprod. *73*, 721-729.

Slot,J.W. and Geuze,H.J. (1985). A new method of preparing gold probes for multiple-labeling cytochemistry. European Journal of Cell Biology *38*, 87-93.

Smith,T.T., McKinnon-Thompson,C.A., and Wolf,D.E. (1998). Changes in lipid diffusibility in the hamster sperm head plasma membrane during capacitation in vivo and in vitro. Molecular Reproduction and Development *50*, 86-92.

Sommerlade,H.J., Selmer,T., Ingendoh,A., Gieselmann,V., von Figura,K., Neifer,K., and Schmidt,B. (1994). Glycosylation and phosphorylation of arylsulfatase A. Journal of Biological Chemistry *269*, 20977-20981.

Song,Y., Withers,D.A., and Hakomori,S. (1998). Globoside-dependent adhesion of human embryonal carcinoma cells, based on carbohydrate-carbohydrate interaction, initiates signal transduction and induces enhanced activity of transcription factors AP1 and CREB. Journal of Biological Chemistry *273*, 2517-2525.

Spinedi,A., Di Bartolomeo,S., Di Sano,F., Rodolfo,C., Ambrosino,A., and Piacentini,M. (1999). Ceramide accumulation precedes caspase-dependent apoptosis in CHP-100 neuroepithelioma cells exposed to the protein phosphatase inhibitor okadaic acid 3. Cell Death. Differ. *6*, 618-623.

Sprong,H., Kruithof,B., Leijendekker,R., Slot,J.W., Van Meer,G., and van der,S.P. (1998). UDP-galactose:ceramide galactosyltransferase is a class I integral membrane protein of the endoplasmic reticulum. J. Biol. Chem. *273*, 25880-25888.

Spungin,B. and Breitbart,H. (1996). Calcium mobilization and influx during sperm exocytosis. J. Cell Sci. *109 (Pt 7)*, 1947-1955.

Spungin,B., Margalit,I., and Breitbart,H. (1995). Sperm exocytosis reconstructed in a cell-free system: evidence for the involvement of phospholipase C and actin filaments in membrane fusion. Journal of Cell Science *108*, 2525-2535.

Srivastav,A. (2000). Maturation-dependent glycoproteins containing both N- and O-linked oligosaccharides in epididymal sperm plasma membrane of rhesus monkeys (Macaca mulatta). J. Reprod. Fertil. *119*, 241-252.

Stein,C., Gieselmann,V., Kreysing,J., Schmidt,B., Pohlmann,R., Waheed,A., Meyer,H.E., O'Brien,J.S., and von Figura,K. (1989a). Cloning and expression of human arylsulfatase A. Journal of Biological Chemistry *264*, 1252-1259.

Stein,C., Hille,A., Seidel,J., Rijnbout,S., Waheed,A., Schmidt,B., Geuze,H., and von Figura,K. (1989b). Cloning and expression of human steroid-sulfatase. Membrane topology, glycosylation, and subcellular distribution in BHK-21 cells. J Biol. Chem. *264*, 13865-13872.

Stein,K.K., Go,J.C., Primakoff,P., and Myles,D.G. (2005). Defects in secretory pathway trafficking during sperm development in Adam2 knockout mice. Biol. Reprod. *73*, 1032-1038.

Stevens,R.L., Fluharty,A.L., Killgrove,A.R., and Kihara,H. (1976). Microheterogeneity of arylsulfatase A from human tissues. Biochimica et Biophysica Acta *445*, 661-671.

Suarez,S., Varosi,S.M., and Dai,X. (1993). Intracellular calcium increases with hyperactivation intact, moving hamster sperm and oscillates with the flagellar beat cycle. Cell Biology *90*, 4660-4664.

Sutovsky,P., Manandhar,G., McCauley,T.C., Caamano,J.N., Sutovsky,M., Thompson,W.E., and Day,B.N. (2004). Proteasomal interference prevents zona pellucida penetration and fertilization in mammals. Biol. Reprod. *71*, 1625-1637.

Suzuki,A., Ishizuka,I., Ueta,N., and Yamakawa,T. (1973). Isolation and characterization of seminolipd (1-O-Alkyl-2-O-Acyl-3-[3'-sulfogalactosyl] glycerol) from guinea pig testis and incorporation of {+35}S-sulfate into seminolipid in sliced testis. Japan J. Exp. Japan Journal of Experimental Medicine *43*, 435-442.

Suzuki,Y., Toda,Y., Tamatani,T., Watanabe,T., Suzuki,T., Nakao,T., Murase,K., Kiso,M., Hasegawa,A., Tadano-Aritomi,K., Ishizuka,I., and Miyasaka,M. (1993). Sulfated glycolipids are ligands for a lymphocyte homing receptor, L-selectin (LECAM-1), binding epitope in sulfated sugar chain. Biochemical and Biophysical Research Communications *190*, 426-434.

Tadano-Aritomi,K., Matsuda,J., Fujimoto,H., Suzuki,K., and Ishizuka,I. (2003). Seminolipid and its precursor/degradative product, galactosylalkylacylglycerol, in the testis of saposin A- and prosaposin-deficient mice. J. Lipid Res. *44*, 1737-1743.

Takahashi,Y., Bigler,D., Ito,Y., and White,J.M. (2001). Sequence-specific interaction between the disintegrin domain of mouse ADAM 3 and murine eggs: role of beta1 integrin-associated proteins CD9, CD81, and CD98. Mol. Biol. Cell *12*, 809-820.

Takasaki,S., Mori,E., and Mori,T. (1999). Structures of sugar chains included in mammalian zona pellucida glycoproteins and their potential roles in sperm-egg interaction. Biochimica et Biophysica Acta *1473*, 206-215.

Tanphaichitr,N., Bou Khalil,M., Weerachatyanukul,W., Kates,M., Xu,H., Carmona,E., Attar,M., and Carrier,D. (2003). Physiological and biophysical properties of male germ cell sulfogalactosylglycerolipid. In Lipid Metabolism and Male Fertility, S.De Vriese, ed. (Champaign, IL: AOCS Press).

Tanphaichitr,N., Carmona,E., Bou Khalil,M., Xu,H., Berger,T., and Gerton,G.L. (2007a). New insights into sperm-zona pellucida interaction: involvement of sperm lipid rafts. Frontiers in Bioscience *12*, 1748-1766.

Tanphaichitr,N., Carmona,E., Bou,K.M., Xu,H., Berger,T., and Gerton,G.L. (2007b). New insights into sperm-zona pellucida interaction: involvement of sperm lipid rafts. Front Biosci. *12*, 1748-1766.

Tanphaichitr,N., Faull,K.F., Yaghoubian,A., and Xu,H. (2007c). Roles of sperm lipid rafts and sulfogalactosyglycerolipid (SGG) in sperm functions: Consensus and controversy1. . Trends in Glycoscience and Glycotechnology *submitted.*

Tanphaichitr,N., Moase,C., Taylor,T., Surewicz,K., Hansen,C., Namking,M., B,rub,,B., Kamolvarin,N., Lingwood,C.A., Sullivan,R., Rattanachaiyanont,M., and White,D. (1998a). Isolation of antiSLIP1-reactive boar sperm P68/62 and its binding to mammalian zona pellucida. Molecular Reproduction and Development *49*, 203-216.

Tanphaichitr,N., Smith,J., and Kates,M. (1990). Levels of sulfogalactosylglycerolipid in capacitated motile and immotile mouse sperm. Biochemistry and Cell Biology *68*, 528-535.

Tanphaichitr,N., Smith,J., Mongkolsirikieart,S., Gradil,C., and Lingwood,C. (1993). Role of a gamete specific sulfoglycolipid-immobilizing protein on mouse sperm-egg binding. Developmental Biology *156*, 164-175.

Tanphaichitr,N., Tayabali,A., Gradil,C., Juneja,S., Leveille,M.C., and Lingwood,C. (1992). Role of germ cell-specific sulfolipidimmobilizing protein (SLIP1) in mouse in vivo fertilization. Molecular Reproduction and Development *32*, 17-22.

Tanphaichitr,N., Taylor,T., White,D., Rattanachaiyanont,M., and Moase,C. (1998b). Arylsulfatase-A is a component of boar sperm SLIP1 (P68) and may be involved in sperm-zona pellucida binding. Biology of Reproduction *58 Suppl.*, 158a.

Tanphaichitr,N., White,D., Taylor,T., Attar,M., Rattanachaiyanont,M., and Kates,M. (1999). Role of male germ-cell specific sulfogalactosylglycerolipid (SGG) and its binding protein, SLIP1, in mammalian sperm-egg interaction. In The Male Gamete: From Basic Knowledge to Clinical Applications, C.Gagnon, ed. (Vienna,IL: Cache Press), pp. 227-235.

Tantibhedhyangkul,J., Weerachatyanukul,W., Carmona,E., Xu,H., Anupriwan,A., Michaud,D., and Tanphaichitr,N. (2002). Role of sperm sufrace arylsulfatase A in mouse sperm-zona pellucida binding. Biology of Reproduction *67*, 212-219.

te,V.D., Lloyd-Evans,E., Veldman,R.J., Neville,D.C., Dwek,R.A., Platt,F.M., van Blitterswijk,W.J., and Sillence,D.J. (2004). Accumulation of glycosphingolipids in Niemann-Pick C disease disrupts endosomal transport. J. Biol. Chem. *279*, 26167-26175.

Thaler,C.D., Thomas,M., and Ramalie,J.R. (2006). Reorganization of mouse sperm lipid rafts by capacitation. Mol. Reprod. Dev. *73*, 1541-1549.

Thimon,V., Belghazi,M., Dacheux,J.L., and Gatti,J.L. (2006). Analysis of furin ectodomain shedding in epididymal fluid of mammals: demonstration that shedding of furin occurs in vivo. Reproduction. *132*, 899-908.

Thimon,V., Frenette,G., Saez,F., Thabet,M., and Sullivan,R. (2008). Protein composition of human epididymosomes collected during surgical vasectomy reversal: a proteomic and genomic approach. Hum. Reprod. *23*, 1698-1707.

Thimon,V., Metayer,S., Belghazi,M., Dacheux,F., Dacheux,J.L., and Gatti,J.L. (2005). Shedding of the germinal angiotensin I-converting enzyme (gACE) involves a serine protease and is activated by epididymal fluid. Biol. Reprod. *73*, 881-890.

Topfer-Petersen,E., Ekhlasi-Hundrieser,M., and Tsolova,M. (2008). Glycobiology of fertilization in the pig. Int. J. Dev. Biol. *52*, 717-736.

Topfer-Petersen,E., Romero,A., Varela,P.F., Ekhlasi-Hundrieser,M., Dostalova,Z., Sanz,L., and Calvete,J.J. (1998). Spermadhesins: a new protein family. Facts, hypotheses and perspectives. Andrologia *30*, 217-224.

Toshimori,K. (1998). Maturation of mammalian spermatozoa: modifications of the acrosome and plasma membrane leading to fertilization. Cell Tissue Research *293*, 177-187.

Towbin,H. and Gordon,J. (1984). Immunoblotting and dot immunobinding-current status and outlook. Journal of Immunological Methods *72*, 313-340.

Tres,L.L. and Kierszenbaum,A.L. (1983). Viability of rat spermatogenic cells in vitro is facilitated by their coculture with Sertoli cells in serum-free hormone-supplemented medium. Proc. Natl. Acad. Sci. U. S. A *80*, 3377-3381.

Trevino,C.L., Serrano,C., Beltran,C., Felix,R., and Darszon,A. (2001). Identification of mouse trp homlogs and lipid rafts from spermatogenic cells and sperm. FEBS Letters *509*, 119-125.

Trostle-Weige,P.K., Meistrich,M.L., Brock,W.A., and Nishioka,K. (1984). Isolation and characterization of TH3, a germ cell-specific variant of histone 3 in rat testis. J. Biol. Chem. *259*, 8769-8776.

Tsai,M.Y., Yeh,S.D., Wang,R.S., Yeh,S., Zhang,C., Lin,H.Y., Tzeng,C.R., and Chang,C. (2006). Differential effects of spermatogenesis and fertility in mice lacking androgen receptor in individual testis cells. Proc. Natl. Acad. Sci. U. S. A *103*, 18975-18980.

Tsai,P.S., de Vries,K.J., Boer-Brouwer,M., Garcia-Gil,N., Van Gestel,R.A., Colenbrander,B., Gadella,B.M., and Van Haeften,T. (2007). Syntaxin and VAMP association with lipid rafts depends on cholesterol depletion in capacitating sperm cells. Mol. Membr. Biol. *24*, 313-324.

Tsuji,Y., Fukuda,H., Iuchi,A., Ishizuka,I., and Isojima,S. (1992). Sperm immobilizing antibodies react to the 3-O-sulfated galactose residue of seminolipid on human sperm. Journal of Reproductive Immunology *22*, 225-236.

Tulsiani,D.R. (2003). Glycan modifying enzymes in luminal fluid of rat epididymis: are they involved in altering sperm surface glycoproteins during maturation? Microsc. Res. Tech. *61*, 18-27.

Tulsiani,D.R., Nagdas,S.K., Cornwall,G.A., and Orgebin-Crist,M.C. (1992). Evidence for the presence of high-mannose/hybrid oligosaccharide chain(s) on the mouse ZP2 and ZP3. Biology of Reproduction *46*, 93-100.

Tulsiani,D.R., Orgebin-Crist,M.C., and Skudlarek,M.D. (1998a). Role of luminal fluid glycosyltransferases and glycosidases in the modification of rat sperm plasma membrane glycoproteins during epididymal maturation. J. Reprod. Fertil. Suppl *53*, 85-97.

Tulsiani,D.R., Skudlarek,M.D., Araki,Y., and Orgebin-Crist,M.C. (1995a). Purification and characterization of two forms of beta-D-galactosidase from rat epididymal luminal fluid: evidence for their role in the modification of sperm plasma membrane glycoprotein(s). Biochem. J. *305 (Pt 1)*, 41-50.

Tulsiani,D.R.P. and Abou-Haila,A. (2001). Mammalian sperm molecules that are potentially important in interaction with female genital tract and egg vestments. Zygote *9*, 51-69.

Tulsiani,D.R.P., Abou-Hailaa,A., Loeser,C.R., and Pereira,B.M.J. (1998b). The biological and functional significance of the sperm acrosome and acrosomal enzymes in mammalian fertilization. Experimental Cell Research *240*, 151-164.

Tulsiani,D.R.P., Nagdas,S.K., Skudlarek,M.D., and Orgebin-Crist,M.C. (1995b). Rat sperm plasma membrane mannosidase: localization and evidence for proteolytic processing during epididymal maturation. Developmental Biology *167*, 584-595.

Tulsiani,R.P., Skudlarek,M.D., and Orgebin-Crist,M.C. (1989). Novel à-D-mannosidase of rat sperm plasma membranes:characterization and potential role in sperm-egg interaction. The Journal of Cell Biology *109*, 1257-1267.

Tupper,S., Wong,P.T.T., Kates,M., and Tanphaichitr,N. (1994). Interaction of divalent cations with germ cell specific sulfogalactosylglycerolipid and the effects on lipid chain dynamics. Biochemistry *33*, 13250-13258.

Tupper,S., Wong,P.T.T., and Tanphaichitr,N. (1992). Binding of Ca{+2+} to sulfogalactosylceramide and the sequential effects on the lipid dynamics. Biochemistry *31*, 11902-11907.

Turner,T.T. (1979). On the epididymis and its function. Invest Urol. *16*, 311-321.

Turner,T.T. and Roddy,M.S. (1990). Intraluminal androgen binding protein alters 3H-androgen uptake by rat epididymal tubules in vitro. Biol. Reprod. *43*, 414-419.

Van Meer,G. (2002). Cell biology. The different hues of lipid rafts. Science *296*, 855-857.

Vazquez,M.H., Phillips,D.M., and Wassarman,P.M. (1989). Interaction of mouse sperm with purified sperm receptors covalently linked to silica beads. J. Cell Sci. *92 (Pt 4)*, 713-722.

Visconti,P.E., Bailey,J.L., Moore,G.D., Pan,D., and Olds-Clarke,P. (1995a). Capacitation of mouse spermatazoa. Correlation between the capacitation state and protein tyrosine phosphorylation. Development *121*, 1129-1137.

Visconti,P.E. and Kopf,G.S. (1998). Regulation of protein phosphorylation during sperm capacitation. Biol. Reprod. *59*, 1-6.

Visconti,P.E., Moore,G.D., Bailey,J.L., Leclerc,P., Connors,S.A., Pan,D., Olds-Clarke,P., and Kopf,G.S. (1995b). Capacitation of mouse spermatozoa. II. Protein tyrosine phosphorylation and capacitation are regulated by a cAMP-dependent pathway. Development *121*, 1139-1150.

Visconti,P.E., Moore,G.D., Bailey,J.L., Leclerc,P., Connors,S.A., Pan,D., Olds-Clarke,P., and Kopf,G.S. (1995c). Capacitation of mouse spermatozoa. II. Protein tyrosine phosphorylation and capacitation are regulated by a cAMP-dependent pathway. Development *121*, 1139-1150.

Visconti,P.E., Westbrook,V.A., Chertihin,O., Demarco,I., Sleight,S., and Diekman,A.B. (2002). Novel signaling pathways involved in sperm acquisition of fertilizing capacity. J. Reprod. Immunol. *53*, 133-150.

Vogt,P.H. (2005). Azoospermia factor (AZF) in Yq11: towards a molecular understanding of its function for human male fertility and spermatogenesis. Reprod. Biomed. Online. *10*, 81-93.

Voigt,S., Gossrau,R., Baum,O., Loster,K., Hofmann,W., and Reutter,W. (1995). Distribution and quantification of alpha 1-integrin subunit in rat organs. Histochem. J. *27*, 123-132.

Von Bulow,R., Schmidt,B., Dierks,T., von Figura,K., and Uson,I. (2001). Crystal structure of an enzyme-substrate complex provides insight into the interaction betweeen human arylsulfatase A and its substrates during catalysis. Journal of Molecular Biology *305*, 269-277.

von Figura,K., Gieselmann,V., and Jaeken,J. (2001). Metachromatic Leukodystrophy. In The Online Metabolic & Molecular Bases of Inherited Disease, The McGraw-Hill Companies), pp. 3695-3724.

von Horsten,H.H., Derr,P., and Kirchhoff,C. (2002). Novel antimicrobial peptide of human epididymal duct origin. Biol. Reprod. *67*, 804-813.

Vos,J.P., Lopes-Cardozo,M.G., and Gadella,B.M. (1994). Metabolic and functional aspects of sulfogalactolipids. Biochimica et Biophysica Acta *1211*, 125-149.

Waheed,A. and Van Etten,R.L. (1980). Chemical characterization and substrate specificity of rabbit liver aryl sulfatase A. Biochimica et Biophysica Acta *614*, 92-101.

Wakayama,T., Nagata,K., Ohashi,K., Mizuno,K., Tanii,I., Yoshinaga,K., Oh-Oka,T., and Toshimori,K. (2000). The expression and cellular localization of the sperm flagellar protein MC31/CE9 in the rat testis: possible posttranscriptional regulation during rat spermiogenesis. Arch. Histol. Cytol. *63*, 33-41.

Walensky,L.D. and Snyder,S.H. (1995). Inositol 1,4,5-triphosphate receptors selectively localized to the acrosomes of mammalian sperm. The Journal of Cell Biology *130*, 857-869.

Walsh,A., Whelan,D., Bielanowicz,A., Skinner,B., Aitken,R.J., O'Bryan,M.K., and Nixon,B. (2008). Identification of the molecular chaperone, heat shock protein 1 (chaperonin 10), in the reproductive tract and in capacitating spermatozoa in the male mouse. Biol. Reprod. *78*, 983-993.

Wang,C., Leung,A., and Sinha-Hikim,A.P. (1993). Reproductive aging in the male brown-Norway rat: a model for the human. Endocrinology *133*, 2773-2781.

Wang,X., Sin,P., Al Qamari,A., Tai,T., Kawashima,I., and Paller,A.S. (2001). Carbohydrate-carbohydrate binding of ganglioside to integrin à{-5} modulates à{-5}á{-1} function. Journal of Biological Chemistry *276*, 8436-8444.

Ward,C.R. and Storey,B.T. (1984). Determination of the time course of capacitation in mouse spermatozoa using a chlortetracycline fluorescence assay. Dev. Biol. *104*, 287-296.

Wassarman,P. (1988). Zona pellucida glycoproteins. Annual Review of Biochemistry *57*, 415-442.

Wassarman,P.M. (1990). Profile of a mammalian sperm receptor. Development *108*, 1-17.

Wassarman,P.M. (1999). The Parkes Lecture. Zona pellucida glycoprotein mZP3: a versatile player during mammalian fertilization. J. Reprod. Fertil. *116*, 211-216.

Wassarman,P.M. (2008). Zona pellucida glycoproteins. J. Biol. Chem. *283*, 24285-24289.

Wassarman,P.M., Jovine,L., and Litscher,E.S. (2004). Mouse zona pellucida genes and glycoproteins. Cytogenet. Genome Res. *105*, 228-234.

Wassarman,P.M. and Litscher,E.S. (2001). Towards the molecular basis of sperm and egg interaction during mammalian fertilization. Cells Tissues Organs *168*, 36-45.

Wassarman,P.M. and Litscher,E.S. (2008). Mammalian fertilization: the egg's multifunctional zona pellucida. Int. J. Dev. Biol. *52*, 665-676.

Waters,S.I. and White,J.M. (1997). Biochemical and molecular characterization of bovine fertilin alpha and beta (ADAM 1 and ADAM 2): a candidate sperm-egg binding/fusion complex. Biology of Reproduction *56*, 1245-1254.

Weerachatyanukul,W., Rattanachaiyanont,M., Carmona,E., Furimsky,A., Mai,A., Shoushtarian,A., Sirichotiyakul,S., Ballakier,H., Leader,A., and Tanphaichitr,N. (2001). Sulfogalactosylglycerolipid is involved in human gamete interaction. Molecular Reproduction and Development *60(4)*, 569-578.

Weerachatyanukul,W., Xu,H., Anupriwan,A., Carmona,E., Wade,M., Hermo,L., da Silva,S.M., Rippstein,P., Sobhon,P., Sretarugsa,P., and Tanphaichitr,N. (2003).

Acquisition of arylsulfatase A onto the mouse sperm surface during epididymal transit. Biol. Reprod. *69*, 1183-1192.

Wertheimer,E.V., Salicioni,A.M., Liu,W., Trevino,C.L., Chavez,J., Hernandez-Gonzalez,E.O., Darszon,A., and Visconti,P.E. (2008). Chloride Is essential for capacitation and for the capacitation-associated increase in tyrosine phosphorylation. J. Biol. Chem. *283*, 35539-35550.

White,D., Weerachatyanukul,W., Gadella,B., Kamolvarin,N., Attar,M., and Tanphaichitr,N. (2000). Role of sperm sulfogalactosylglycerolipid in mouse sperm-zona pellucida binding. Biology of Reproduction *63*, 147-155.

Wikstrom,A.M. and Dunkel,L. (2008). Testicular function in Klinefelter syndrome. Horm. Res. *69*, 317-326.

Williamson,P., Mattocks,K., and Schlegel,R.A. (1983). Merocyanine 540, a fluorescent probe sensitive to lipid packing. Biochim. Biophys. Acta *732*, 387-393.

Wolf,D., Hagopian,S., and Ishijima,S. (1986). Changes in sperm plasma membrane lipid diffusibility after hyperactivation during in vitro capacitation in the mouse. The Journal of Cell Biology *102*, 1372-1377.

Wu,A., Anupriwan,A., Iamsaard,S., Chakrabandhu,K., Santos,D.C., Rupar,T., Tsang,B.K., Carmona,E., and Tanphaichitr,N. (2007b). Sperm surface arylsulfatase A can disperse the cumulus matrix of cumulus oocyte complexes. J Cell Physiol *213*, 201-211.

Wu,A., Anupriwan,A., Iamsaard,S., Chakrabandhu,K., Santos,D.C., Rupar,T., Tsang,B.K., Carmona,E., and Tanphaichitr,N. (2007a). Sperm surface arylsulfatase A can disperse the cumulus matrix of cumulus oocyte complexes. J. Cell Physiol *213*, 201-211.

Wu,J.T., Chiang,K.C., and Cheng,F.P. (2006). Expression of progesterone receptor(s) during capacitation and incidence of acrosome reaction induced by progesterone and zona proteins in boar spermatozoa. Anim Reprod. Sci. *93*, 34-45.

Wu,Z., Tandon,R., Ziembicki,J., Nagano,J., Hujer,K.M., Miller,R.T., and Huang,C. (2005). Role of ceramide in Ca2+-sensing receptor-induced apoptosis. J. Lipid Res. *46*, 1396-1404.

Xie,F., Garcia,M.A., Carlson,A.E., Schuh,S.M., Babcock,D.F., Jaiswal,B.S., Gossen,J.A., Esposito,G., Van Duin,M., and Conti,M. (2006). Soluble adenylyl cyclase (sAC) is indispensable for sperm function and fertilization. Dev. Biol. *296*, 353-362.

Xu,Y., Ashley,T., Brainerd,E.E., Bronson,R.T., Meyn,M.S., and Baltimore,D. (1996). Targeted disruption of ATM leads to growth retardation, chromosomal fragmentation during meiosis, immune defects, and thymic lymphoma. Genes Dev. *10*, 2411-2422.

Yamagata,K., Murayama,K., Okabe,M., Toshimori,K., Nakanishi,T., Kashiwabara,S., and Baba,T. (1998). Acrosin accelerates the dispersal of sperm acrosomal proteins during acrosome reaction. Journal of Biological Chemistry *273*, 10470-10474.

Yamagata,T. (1985). The role of saccharides in fertilization of the mouse. Development Growth & Differentiation *27*, 176-177.

Yamaguchi,R., Yamagata,K., Hasuwa,H., Inano,E., Ikawa,M., and Okabe,M. (2008). Cd52, known as a major maturation-associated sperm membrane antigen secreted from the epididymis, is not required for fertilization in the mouse. Genes Cells *13*, 851-861.

Yamaguchi,R., Yamagata,K., Ikawa,M., Moss,S.B., and Okabe,M. (2006). Aberrant distribution of ADAM3 in sperm from both angiotensin-converting enzyme (Ace)- and calmegin (Clgn)-deficient mice. Biol. Reprod. *75*, 760-766.

Yamaguchi,S., Aoki,K., Handa,S., and Yamakawa,T. (1975). Deficiency of seminolipid sulphatase activity in brain tissue of metachromatic leucodystrophy. J. Neurochem. *24*, 1087-1089.

Yamashita,M., Honda,A., Ogura,A., Kashiwabara,S., Fukami,K., and Baba,T. (2008). Reduced fertility of mouse epididymal sperm lacking Prss21/Tesp5 is rescued by sperm exposure to uterine microenvironment. Genes Cells *13*, 1001-1013.

Yamato,K., Handa,S., and Yamakawa,T. (1974). Purification of arylsulfatase a from boar testis and its activities toward seminolipid and sulfatide. Journal of Biochemistry *75*, 1241-1247.

Yanagimachi,R. (1994). Mammalian fertilization. In The Physiology of Reproduction, E.Knobil, ed. (New York: Raven Press Ltd.), pp. 189-317.

Yeh,S., Tsai,M.Y., Xu,Q., Mu,X.M., Lardy,H., Huang,K.E., Lin,H., Yeh,S.D., Altuwaijri,S., Zhou,X., Xing,L., Boyce,B.F., Hung,M.C., Zhang,S., Gan,L., and Chang,C. (2002). Generation and characterization of androgen receptor knockout (ARKO) mice: an in vivo model for the study of androgen functions in selective tissues. Proc. Natl. Acad. Sci. U. S. A *99*, 13498-13503.

Yenugu,S., Hamil,K.G., French,F.S., and Hall,S.H. (2004). Antimicrobial actions of the human epididymis 2 (HE2) protein isoforms, HE2alpha, HE2beta1 and HE2beta2. Reprod. Biol. Endocrinol. *2*, 61.

Yonezawa,N., Aoki,H., Hatanaka,Y., and Nakano,M. (1995). Involvement of N-linked carbohydrate chaines of pig zona pellucida in sperm-egg binding. European Journal of Biochemistry *233*, 35-41.

Yoshiizumi,K., Nakajima,F., Dobashi,R., Nishimura,N., and Ikeda,S. (2002). Studies on scavenger receptor inhibitors. Part 1: synthesis and structure-activity relationships of novel derivatives of sulfatides. Bioorg. Med. Chem. *10*, 2445-2460.

Yoshinaga,K. and Toshimori,K. (2003). Organization and modifications of sperm acrosomal molecules during spermatogenesis and epididymal maturation. Microsc. Res. Tech. *61*, 39-45.

Yu,S., Kojima,N., Hakomori,S.I., Kudo,S., Inoue,S., and Inoue,Y. (2002). Binding of rainbow trout sperm to egg is mediated by strong carbohydrate-to-carbohydrate interaction between (KDN)GM3 (deaminated neuraminyl ganglioside) and Gg3-like epitope. Proceedings of the National Academy of Science USA *99*, 2854-2859.

Yuan,Y.Y., Chen,W.Y., Shi,Q.X., Mao,L.Z., Yu,S.Q., Fang,X., and Roldan,E.R. (2003). Zona pellucida induces activation of phospholipase a(2) during acrosomal exocytosis in Guinea pig spermatozoa. Biol. Reprod. *68*, 904-913.

Yurewicz,E.C., Pack,B.A., Armant,D.R., and Sacco,A.G. (1993). Porcine zona pellucida ZP3 à glycoprotein mediates binding of the biotin-labeled M{-r} 55,000 family (ZP3) to boar sperm membrane vesicles. Molecular Reproduction and Development *36*, 382-389.

Zanetti,S.R., Maldonado,E.N., and Aveldano,M.I. (2007). Doxorubicin affects testicular lipids with long-chain (C18-C22) and very long-chain (C24-C32) polyunsaturated fatty acids. Cancer Res. *67*, 6973-6980.

Zeng,Y., Cheng,H., Jiang,X., and Han,X. (2008). Endosomes and lysosomes play distinct roles in sulfatide-induced neuroblastoma apoptosis: potential mechanisms contributing to abnormal sulfatide metabolism in related neuronal diseases. Biochem. J. *410*, 81-92.

Zhang,H. and Martin-Deleon,P.A. (2003). Mouse epididymal Spam1 (pH-20) is released in the luminal fluid with its lipid anchor. J. Androl *24*, 51-58.

Zhang,Y., Hayashi,Y., Cheng,X., Watanabe,T., Wang,X., Taniguchi,N., and Honke,K. (2005). Testis-specific sulfoglycolipid, seminolipid, is essential for germ cell function in spermatogenesis. Glycobiology *15*, 649-654.

Zhao,M., Shirley,C.R., Hayashi,S., Marcon,L., Mohapatra,B., Suganuma,R., Behringer,R.R., Boissonneault,G., Yanagimachi,R., and Meistrich,M.L. (2004). Transition nuclear proteins are required for normal chromatin condensation and functional sperm development. Genesis. *38*, 200-213.

Zheng,M. and Hakomori,S. (2000). Soluble fibronectin interaction with cell surface and extracellular matrix is mediated by carbohydrate-to-carbohydrate interaction. Archives of Biochemistry and Biophysics *374*, 93-99.

Zhou,C.X., Zhang,Y.L., Xiao,L., Zheng,M., Leung,K.M., Chan,M.Y., Lo,P.S., Tsang,L.L., Wong,H.Y., Ho,L.S., Chung,Y.W., and Chan,H.C. (2004). An epididymis-specific beta-defensin is important for the initiation of sperm maturation. Nat. Cell Biol. *6*, 458-464.

Zhou,Y., Zheng,M., Shi,Q., Zhang,L., Zhen,W., Chen,W., and Zhang,Y. (2008). An epididymis-specific secretory protein HongrES1 critically regulates sperm capacitation and male fertility. PLoS. ONE. *3*, e4106.

Zhu,G.Z., Myles,D.G., and Primakoff,P. (2001). Testase 1({IADAM 24}) a plasma membrane-anchored sperm protease implicated in sperm function during epididymal maturation or fertilization. Journal of Cell Science *114*, 1787-1794.

Zirkin,B.R., Santulli,R., Awoniyi,C.A., and Ewing,L.L. (1989). Maintenance of advanced spermatogenic cells in the adult rat testis: quantitative relationship to testosterone concentration within the testis. Endocrinology *124*, 3043-3049.

Zitta,K., Wertheimer,E.V., and Miranda,P.V. (2006). Sperm N-acetylglucosaminidase is involved in primary binding to the zona pellucida. Mol. Hum. Reprod. *12*, 557-563.

Zoller,I., Bussow,H., Gieselmann,V., and Eckhardt,M. (2005). Oligodendrocyte-specific ceramide galactosyltransferase (CGT) expression phenotypically rescues CGT-deficient mice and demonstrates that CGT activity does not limit brain galactosylceramide level 1. Glia *52*, 190-198.

APPENDIX ONE

Table 4.1. Reproductive phenotype of gene-manipulated mice

Name	Location in the male reproductive system	Molecular mass (kda)	Functions	Phenotypes of KO male mice	References
I. GENE KNOCKOUTS AFFECTING SPERMATOGENESIS					
UDP-galactose:ceramide galactosyltransferase (CGT)	spermatogenic cells	~61	Synthesize galactosylalkylacylglycerol (GalEAG), galactosylceramide (GalCer), galactosylsphingosine (psychosine), and galactosyldiacylglycerol (GalAAG)	*Cgt*$^{-/-}$ male mice are infertile due to spermatogenesis arrest at the late pachytene stage. These mice lack both GG and its sulfated derivative SGG.	Fujimoto et al., 2000; Morell and Radin,1969; van der Bijl et al., 1996; Coetzee et al., 1996; Bosio et al., 1996, 1998; Ezoe et al., 2000
cerebroside sulfotransferase (CST)	spermatogenic cells	54	Synthesize SGG and SGC	*Cst* $^{-/-}$ males were infertile due to spermatogenesis arrest at the end of the meiotic prophase. These mice lack SGG in the testis, while the precursor GG is accumulated.	Honke et al., 2002; Honke et al., 1996
Basigin	Plasma membrane overlying the acrosome	26	May be involved in the primary binding of sperm to the ZP and sperm-cumulus interaction.	KO male mice are sterile due to spermatogenesis arrest.	Saxena et al., 2002; Chen et al., 2004
GBA2 (β-Glucosidase 2)	ER of Sertoli cells	105	β-Glucosidase 2 (GBA2) is a resident enzyme of the endoplasmic reticulum thought to play a role in the metabolism of bile acid–glucose conjugates.	Glucosylceramides are accumulated in multiple tissues including testis. Accumulation in the testes leads to decreased fertility and the formation of abnormal sperm.	Yildiz et al., 2006
NPC1 (Niemann-Pick C1)	Multiple membrane spanning protein	180	Regulate trafficking of LDL-mediated endocytosed cholesterol.	Npc1$^{-/-}$ mice are infertile. There is partial arrest of spermatogenesis, impaired binding to ZP, and high frequency of sperm abnormalities.	Fan et al., 2006; Patterson et al., 2001; Maxfield and Wustner, 2002; Roff et al., 1993;
II. GENE KNOCKOUTS AFFECTING FERTILIZATION					

APPENDIX ONE

SED1	Expressed in spermatogenic cells and secreted by the initial segment of the caput epididymis, resulting in the localization on the plasma membrane overlying the acrosome.	~58	ZP-binding protein	SED1 null males are subfertile and their sperm are unable to bind to the ZP in vitro.	Ensslin and Shur, 2003
Beta 1,4-galactosyltransferase (GalT)	Expressed in pachytene spermatocytes and redistributed to the sperm plasma membrane overlying the acrosome.	~60	ZP3-binding protein	GalT null male mice are subfertile. Their sperm were unable to bind to ZP3 and unable to undergo ZP-induced AR.	Shur and Hall, 1982; Lopez et al., 1985; Shur and Neely, 1988; Scully et al., 1987; Pratt et al., 1993; Asano et al., 1997, Lu and Shur, 1997
PH-20	Sperm plasma membrane & in the acrosome	52	a GPI-linked bifunctional protein containing a hyaluronidase activity important for cumulus cells dispersion, and ZP-binding domain	KO males are fertile, but with reduced ability to disperse cumulus cells.	Primakoff et al., 1985; Lin et al., 1994; Hunnicutt et al., 1996; Baba et al., 2002
Acrosin/proacrosin	Acrosome & inner acrosomal membrane	39/~41-42	A serine protease, involved in dispersing acrosomal content and maybe activating other proteases. Proacorosin is involved in the secondary sperm-ZP binding.	KO males are fertile, but their sperm penetrate the ZP less efficiently. The KO sperm are also disadvantageous to fertilize eggs in vitro when in competition with WT sperm.	Adham et al., 1997;Howes et al., 2001; Baba et al., 1994; De los and Barros, 2000Yamagata et al., 1998

sAC (soluble adenylyl cyclase)	Spermatogenic cells and sperm	186	Produce cAMP, second messenger in various signal transduction pathways.	KO males are sterile and produce sperm with deficits in progressive motility and are unable to fertilize zona-intact eggs in vitro.	Xie et al., 2006; Esposito et al., 2004
CatSper1	Localized to principal piece of sperm tail	79	Ca2+ channel controlling Ca2+ concentrations in the sperm tail	CatSper$^{-/-}$ sperm motility is decreased markedly and the sperm are unable to fertilize ZP-intact eggs. The cyclic-AMP-induced Ca2+ influx is abolished in the sperm of mutant mice.	Ren et al., 2001; Carlson et al., 2003
CatSper2	Localized to principal piece of sperm tail	69	Ca2+ channel controlling Ca2+ concentrations in the sperm tail	CatSper2$^{-/-}$ males are infertile. Their sperm fail to acquire hyperactivated motility. CatSper2-null spermatozoa lost the ability to swim forward in viscos medium.	Quill et al., 2001, 2003;
ADAM1a	Endoplasmic reticulum (ER) of testicular germ cells	100	Forms ADAM1a/ADAM2 (fertilin) complexes, which may be implicated in the selective transport of specific sperm proteins including ADAM3 from the ER of testicular germ cells onto the cell surface.	KO males are infertile due to severely impaired ability of sperm to migrate from the uterus into the oviduct through the uterotubal junction. Epididymal sperm of the mutant mice are capable of fertilizing cumulus-enclosed, ZP-intact eggs *in vitro* despite the delayed dispersal of cumulus cells and the reduced adhesion/binding to the zona pellucida.	Nishimura et al., 2001, 2004; Cho et al., 1998
ADAM1b	Testicular germ cells & on the plasma membrane of epididymal sperm	120 (testis)/60 (sperm)	Forms a heterodimeric protein complex (fertilin) with ADAM2, present on the sperm surface, that has been believed to mediate adhesion and fusion between the sperm and egg plasma membranes.	Mutant male mice lacking ADAM1b are fertile, and no significant sperm defects are observed.	Kim et al., 2003, 2006; Nishimura et al., 2002; Yamaguchi et al., 2006
ADAM2 (fertilin β)	Testicular germ cells & on the plasma membrane of epididymal sperm	100 & 80 (testis)/42 or 45 (epididymal sperm)	Forms a heterodimeric protein complex (fertilin) with ADAMib, present on the sperm surface, which has been believed to mediate adhesion and fusion between the sperm and egg plasma membranes.	Fertilin β null male mice are sterile. Their sperm are deficient in binding to the egg zona pellucida, migration from the uterus into the oviduct, sperm-egg membrane adhesion, and sperm-egg fusion	Cho et al., 1998; Stein et al., 2005
ADAM3 (Cyritestin)	Testicular germ cells & on the plasma	110 (testis)/~41	Involved in cell-cell adhesion through binding to integrins. A major candidate involved in sperm-	ADAM3-null males are infertile. Their sperm are deficient in adhesion to the ZP.	Nishimura et al., 2001; Shamsadin et al., 1999; Stein et

APPENDIX ONE

	membrane of epididymal sperm	(epididymal sperm)	egg interaction.		al., 2005; Kim et al., 2006; Yuan et al., 1997; Linder and Heinlein, 1997
Calmegin	ER of testicular germ cells	93	Chaperone protein	Calmegin-null males are nearly sterile, and their sperm are defective in ZP binding.	Yoshinaga et al., 1999
Testicular angiotesin-converting enzyme (tACE)	Spermatogenic cells & epididymal sperm	70	Exact substrates of tACE are uncertain. It has been shown to be involved in distributing ADAM3 to a location where it participates in sperm-ZP binding. It may also be involved in GPI-anchored proteins (e.g., TESP5 & PH-20) from sperm surface.	ACE-null males show reduced fertility. Their sperm are defective in transport within the oviducts and in binding to the ZP.	Hagaman et al., 1998; Yamaguchi et al., 2006; Kessler et al., 2000; Ramaraj et al., 1998; Kondoh et al., 2005
ZPB1 (Zona pellucida binding protein 1)	Acrosome of sperm & spermatids	38	Role in structural development during spermiogenesis	Males lacking ZPBP1 were sterile, with abnormal round-headed sperm morphology and no forward sperm motility. The absence of ZPBP1 prevents proper acrosome compaction, resulting in acrosome fragmentation and disruption of the Sertoli-spermatid junctions.	Lin et al., 2007
ZPB2	Acrosome of sperm & spermatids	29	Role in structural development during spermiogenesis	Males null for ZPBP2 were subfertile, demonstrated aberrant acrosomal membrane invaginations, and produced dysmorphic sperm with reduced ability to penetrate zona pellucida.	Lin et al., 2007
TESP5 (testicular serine protease 5)	Acrosome	42	May participate in limited proteolysis of ZP.	TESP5-null male mice are fertile, but the epididymal sperm are severely defective in the ability to fertilize the eggs in vitro. The reduced fertility of TESP5-null epididymal sperm can be rescued by exposure of the sperm to uterine microenvironment and by in vitro treatment of the sperm with uterine fluids.	Yamashita et al., 2008
Izumo	Acrosome	37.2	Sperm-egg plasma membrane	Izumo$^{-/-}$ male mice are sterile. Their sperm are	Inoue et al., 2005

			fusion.	incapable of fusing with eggs.	
TPST2 (Tyrosylprotein sulfonotransferase 2)	*trans*-Golgi network of almost all cells	54	Catalyze tyrosine *O*-sulfation.	*Tpst2*$^{-/-}$ males are infertile. *Tpst2*$^{-/-}$ sperm are severely defective in their motility in viscous media and in their ability to fertilize ZP-intact eggs.	Borghei et al., 2006

CONTRIBUTIONS OF COLLABORATORS

The following people have contributed to specific figure(s).

Dr. T. Rupar (University of Western Ontario) gave us the ASA knockout mice.

Dr. M. Wade (Health Canada) performed the flow cytometry analyses of sperm surface ASA (Figure 3.6).

Dr. W. Weerachatyanukul performed the Immunogold transmission electron microscopy of live sperm (Figure 3.9).

Dr. E. Carmona performed the Binding of Alexa-430 ASA to caudal epididymal sperm (Figure 3.11) and Table 3.1.

Drs. J. Tantibhedhyangkul and W Weerachatyanukul contributed to Figures 3.12 & 3.14.

Dr. J. Tantibhedhyangkul contributed to Figure 3.15.

Ms. F. Liu performed the work presented in Figure 3.20 (Protein profiles of purified recombinant ASAs) and Table 3.2.

All MS work was performed in Dr. K. Faull's lab (UCLA). Ms K. Kongmanas (Ph.D. student in our lab) helped him operating the instrument and data recording.

Quantitative analyses of light micrographs of testes and epididymis of 8-month old WT and ASA null mice and Ultrastructure of Leydig cells were performed by Dr. L. Hermo and his student Mr. P. Turmel (University of McGill).

Serum testosterone levels of 8-month-old WT and *ASA* null mice (Figure 3.32) were done in Thailand by Dr. P. Sretarugsa.